Well-to-Wheels Analysis of Advanced Fuel/Vehicle Systems — A North American Study of Energy Use, Greenhouse Gas Emissions, and Criteria Pollutant Emissions

May 2005

Well-to-Wheels Analysis of Advanced Fuel/Vehicle Systems — A North American Study of Energy Use, Greenhouse Gas Emissions, and Criteria Pollutant Emissions

Norman Brinkman, General Motors Corporation
Michael Wang, Argonne National Laboratory
Trudy Weber, General Motors Corporation
Thomas Darlington, Air Improvement Resource, Inc.

May 2005

Contents

Contents (Cont.)

Figures

Figures (Cont.)

Figures (Cont.)

Figures (Cont.)

Figures (Cont.)

Figures (Cont.)

Tables

Tables (Cont.)

Notation

Acronyms and Abbreviations

AA	attainment areas
AIR	Air Improvement Resource, Inc.
ANL	Argonne National Laboratory
ATR	autothermal reforming
CaNAA	nonattainment areas in California
CC	combined cycle
CD	conventional drive
CEM	continuous emissions monitoring
CFR	Code of Federal Regulations
CH_4	methane
CI	compression-ignition
CNG	compressed natural gas
CO	carbon monoxide
CO_2	carbon dioxide
CS	charge sustaining
CTR	Center for Transportation Research
CY	calendar year
DI	direct-injection
DOD	displacement on demand
DOE	U.S. Department of Energy
E85	85% ethanol with 15% gasoline by volume
EIA	Energy Information Administration
EPA	U.S. Environmental Protection Agency
ERG	Eastern Research Group
EtOH	ethanol
EV	electric vehicle
FCV	fuel cell vehicle
FE	fossil energy
FT	Fischer-Tropsch
GH_2	gaseous hydrogen
GHG	greenhouse gas
GM	General Motors Corporation
GREET	Greenhouse gases, Regulated Emissions, and Energy use in Transportation
GVW	gross vehicle weight
GWP	global warming potential
H_2	hydrogen
HCHO	formaldehyde
HEV	hybrid electric vehicle

HHV	higher heating value
HPSP	Hybrid Powertrain Simulation Program
I&M	inspection and maintenance
IAQR	Interstate Air Quality Rule
ICE	internal combustion engine
IPCC	Intergovernmental Panel on Climate Change
IPM	Integrated Planning Model
LDT	light-duty truck
LEV	low-emission vehicle
LH_2	liquid hydrogen
LHV	lower heating value
LNG	liquefied natural gas
LPG	liquefied petroleum gas
LS	low-sulfur
MeOH	methanol
MIT	Massachusetts Institute of Technology
MY	model year
N	nitrogen
N_2O	nitrous oxide
NA	North American
NEI	National Emissions Inventory
NG	natural gas
NGCC	natural-gas-powered combined cycle
NH	non-hybrid
NiMH	nickel metal hydride
NMOG	non-methane organic gas
NNA	non-North American
NonCaNAA	nonattainment areas outside California
NO_x	nitrogen oxides
NSPS	New Source Performance Standards
NSR	New Source Review
OBD	onboard diagnostic
ORVR	onboard refueling vapor recovery
PE	petroleum energy
PM_{10}	particulate matter with a diameter of 10 microns or less
PNGV	Partnership for a New Generation of Vehicles
PTW	pump-to-wheels
R&D	research and development
RACT	Reasonably Available Control Technology
RFG	reformulated gasoline
RVP	Reid vapor pressure

S	sulfur
SCC	Source Classification Code
SI	spark-ignition
SIC	standard industrial classification
SIP	State Implementation Plan
SMR	steam methane reforming
SO_2	sulfur dioxide
SOC	state-of-charge
SO_x	sulfur oxides
SULEV	super-ultra-low emission vehicle
SUV	sport utility vehicle
TE	total energy
TTW	tank-to-wheels
UAM	urban airshed model
ULEV	ultra-low emission vehicle
VMT	vehicle miles traveled
VOC	volatile organic compound
WOT	wide open throttle
WTP	well-to-pump
WTT	well-to-tank
WTW	well-to-wheels
ZEV	zero emission vehicle

Units of Measure

Btu	British thermal unit(s)
ft	foot (feet)
ft^3	cubic foot (feet)
g	gram(s)
GWh	gigawatt hour(s)
gal	gallon(s)
kWh	kilowatt hour(s)
lb	pound(s)
mi	mile(s)
mmBtu	million British thermal unit(s)
mpg	mile(s) per gallon
mph	mile(s) per hour
MW	megawatt(s)
psi	pound(s) per square inch
s	second(s)
SCF	standard cubic foot (feet)
yr	year(s)

EXECUTIVE SUMMARY

ES.1 Background

An accurate assessment of future fuel/propulsion system options requires a complete vehicle fuel-cycle analysis, commonly called a well-to-wheels (WTW) analysis. In this WTW study, we analyzed energy use and emissions associated with fuel production (or well-to-tank [WTT]) activities and energy use and emissions associated with vehicle operation (or tank-to-wheels [TTW]) activities. Energy resources, such as petroleum, natural gas (NG), coal, and biomass, as well as the energy carrier, electricity, are considered as feedstocks to produce various transportation fuels, including gasoline, diesel fuel, hydrogen (H_2), ethanol (EtOH), compressed natural gas (CNG), methanol (MeOH), and Fischer-Tropsch (FT) diesel. The propulsion systems evaluated were spark-ignition (SI) engines, compression-ignition (CI) engines, hydrogen fuel cells, and fuel processor fuel cells, all in non-hybrid and hybrid electric configurations.

This study updates and supplements a previous (2001) North American study, conducted by GM and others (General Motors [GM] et al. 2001), of energy consumption and greenhouse gas (GHG) emissions associated with advanced vehicle/fuel systems (GM Phase 1 North American study). The primary purpose of this Phase 2 study is to address criteria pollutant emissions, including volatile organic compounds (VOCs), carbon monoxide (CO), nitrogen oxides (NO_x), particulate matter with a diameter smaller than 10 microns (PM_{10}), and sulfur oxide emissions (SO_x). We also updated the vehicle modeling for energy consumption with the latest powertrain maps and added some additional propulsion systems, such as hydrogen internal combustion engines (ICEs).

As in the previous study, the vehicle modeled was a 2010-model-year, full-sized GM pickup truck. The truck was selected because it is a high seller among light-duty vehicles (cars and trucks) in the U.S. market, and light-duty trucks account for a large proportion of the fuel used in the U.S. vehicle fleet. In our study, we attempted to estimate the energy use and emissions for the 2010-model-year truck fleet over its lifetime. To simplify this effort, we modeled the year 2016 — when the lifetime mileage midpoint for the truck will be reached.

ES.2 Methodology

Well-to-wheels calculations were based on a fuel-cycle model developed by Argonne National Laboratory (ANL) — the Greenhouse gases, Regulated Emissions, and Energy use in Transportation (GREET) model. Probability-based distribution functions were developed to describe energy use and emissions for individual operations in fuel production and transportation processes, as well as vehicle operations. With the developed distribution functions and a commercial software (Crystal Ball™), GREET employs the Monte Carlo simulation method to address uncertainties in the input parameters and deliver results in the form of a statistical distribution.

Well-to-tank fuel economy and GHG emissions estimates were based on the same assumptions used in the 2001 study (GM et al. 2001), so the WTT emphasis in this study was on developing input assumptions for the criteria pollutants. The starting point for this effort was the U.S. Environmental Protection Agency's (EPA's) National Emissions Inventory (NEI) database. Representative data for each major WTT process were extracted from the inventory and combined with process throughput data to provide emissions factors. Then, on the basis of the inventory data and an assessment of future stationary source emissions controls, we developed distributions to represent expected emissions in 2016.

For the vehicle modeling effort, we characterized the emissions associated with each propulsion system in terms of meeting an emission standard target — an assumed emission certification level for 2010. On the basis of the certification level, we modeled vehicle in-use criteria pollutants by using both EPA's MOBILE and California's EMFAC models. Results for the two models were significantly different, so we established distributions based on the assumption that 80% of the vehicles would have emissions between the EMFAC and MOBILE estimates.

The vehicle fuel economy analysis used a GM proprietary modeling tool to estimate fuel consumption on the U.S. urban and highway driving cycles. The fuel economies generated for the two cycles were then combined together as a 55/45 combined cycle to derive the composite fuel economy for use in WTW simulations in GREET. Input to the model included maps of powertrain efficiency as a function of speed, load, and vehicle mass for each propulsion system. Powertrains and components for each propulsion system were sized to provide equivalent vehicle performance.

ES.3 Results

The GREET WTW simulations completed for this study show that, in general, fuel production and vehicle operation are two key WTW stages in determining WTW energy use and emissions results. The fuel production stage usually has the largest energy-efficiency losses of all WTT stages. This is true for production of gasoline, diesel, hydrogen, FT diesel, ethanol, methanol, and electricity.

For the vehicle operation stage, the most significant factor in determining WTW results is the fuel consumption of the vehicle technologies. Fuel efficiency (or fuel energy consumption per distance driven) directly determines GHG emissions per mile during operation of vehicles fueled with carbon-containing fuels. Furthermore, fuel consumption directly affects the allocation of WTT emissions (in grams per million Btu [g/mmBtu]) to WTW emissions (in grams per mile [g/mi]). Thus, simulations to determine the fuel consumption values for vehicle technologies are key activities for WTW analyses.

The best estimate of composite fuel economy for the baseline SI vehicle with displacement on demand (DOD) technology was 21.3 mpg, or 4.7 gal/100 mi. Figure ES-1 shows the reduction in fuel consumption, based on gasoline-gallon-equivalent energy, for several advanced propulsion systems. Without hybridization, the diesel direct-injection, compression-ignition (Diesel DI CI) engine with conventional drive and the hydrogen internal combustion engine (H_2 DOD SI) each reduced fuel consumption by 17%. The E85 (85% denatured ethanol with 15% gasoline by volume) flexible-fueled vehicle (E85 DOD SI) had fuel consumption equal to that of gasoline, and the non-hybrid hydrogen fuel cell vehicle (H_2 FCV) reduced gasoline-equivalent fuel consumption by 58%. Hybridization of the gasoline or E85 propulsion systems reduced fuel consumption by 20%. The fuel consumption benefits of hybridization were somewhat smaller for the more-efficient diesel and hydrogen engines (14% and 16%, respectively). The lowest fuel consumption benefit of hybridization (4%) was seen with the hydrogen fuel cell vehicle.

These fuel consumption reductions contribute directly to reductions in WTW energy use and emissions by these advanced vehicle technologies. In the cases in which hydrogen is used to power vehicles, the large reductions in fuel consumption by fuel cell technologies far offset energy-efficiency losses during hydrogen production (except for electrolysis hydrogen production, for which fuel consumption reductions are not enough to offset the large energy losses of electricity generation and hydrogen production together).

Vehicle fuel consumption has a smaller impact on WTW emissions of criteria pollutants (except for SO_x emissions) for ICE-based technologies. This is because vehicular criteria pollutant emissions are regulated on a per-mile basis, and after-combustion emission control technologies are designed to reduce per-mile emissions, resulting in a disconnection between the amount of fuel consumed and the amount of per-mile criteria pollutant emissions generated. For vehicle technologies that do not generate tailpipe emissions (such as direct-hydrogen FCVs and battery-powered electric vehicles [EVs]), fuel economy directly affects WTW criteria pollutant emissions.

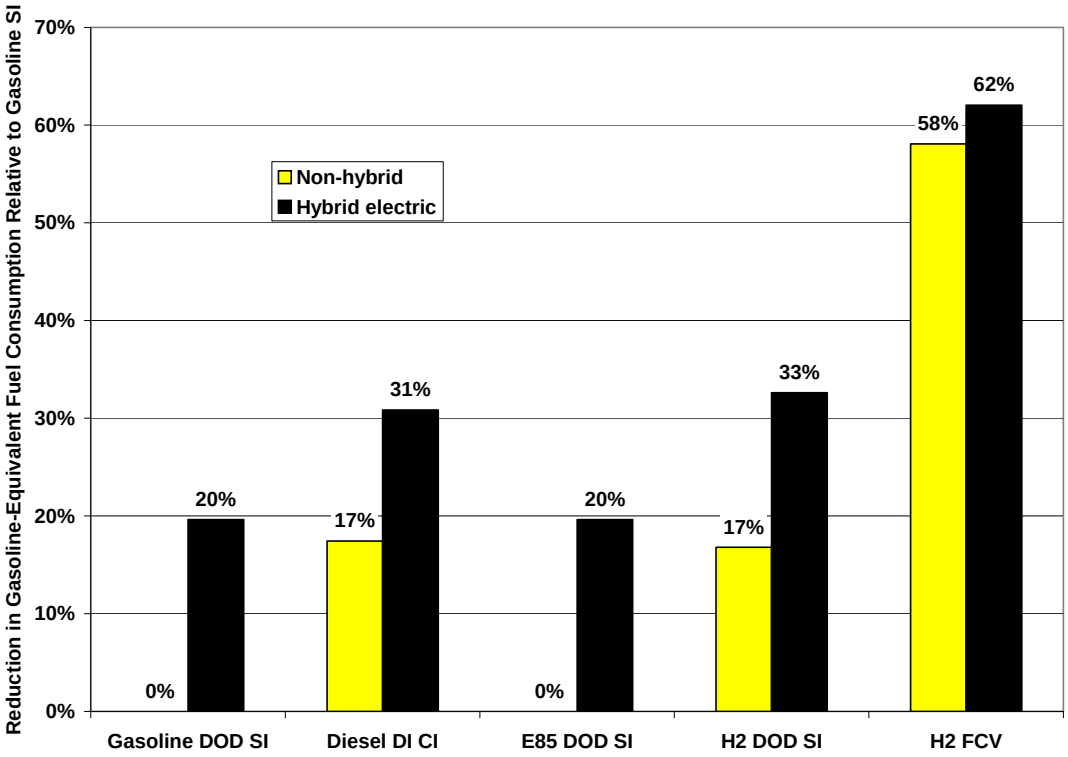

Figure ES-1 Change in Tank-to-Wheels Gasoline-Equivalent Fuel Consumption for Selected Propulsion Systems Relative to Gasoline Spark-Ignition Conventional Drive

By using GREET, our research team calculated WTW energy use and emissions for 124 pathways. Figure ES-2 compares WTW energy use and emissions for eight key pathways with those for the gasoline SI baseline. The chart shows total energy use, petroleum energy use, total GHG emissions, and total emissions of three criteria pollutants (NO_x, VOC, and PM_{10}). The first two sets of bars represent advanced petroleum-based vehicles: reformulated gasoline hybrid (RFG DOD SI HEV) and low-sulfur-diesel conventional drive (LS Diesel DI CI CD). The next three sets of bars show results for three vehicles fueled by hydrogen manufactured in central plants from North American natural gas: the gaseous hydrogen internal combustion engine (NA NG Central GH_2 ICE), gaseous hydrogen fuel cell (NA NG Central GH_2 FCV), and liquid hydrogen fuel cell (NA NG Central LH_2 FCV). The next set of bars (Cell. E85 DOD SI CD) shows the effects of using cellulosic (cellulose-derived) ethanol to make E85 for use in a spark-ignition, conventional drive vehicle. Finally, the last two sets of bars (Electro. GH_2 FCV: U.S. kWh and Electro. GH_2 FCV: Renew. kWh) are fuel cell vehicles with electrolysis-derived gaseous hydrogen from U.S. average electricity and from renewable electricity sources.

As shown in Figure ES-2, the advanced petroleum-based ICE vehicles provided moderate reductions in all of the displayed WTW parameters. In general, the effects for gasoline hybrid and diesel were similar,

about a 10–20% reduction compared with the baseline gasoline SI vehicle. An exception was diesel engine VOC emissions, which were low because of diesel's low volatility.

The hydrogen ICE vehicle modeling results revealed large reductions in petroleum use and VOC emissions compared with the baseline gasoline engine. However, we found increases in total energy use, NO_x emissions, and PM_{10} emissions. Although the hydrogen internal combustion engine was more efficient than the gasoline engine, WTW energy use was high because of the relatively low efficiency of making and transporting hydrogen, compared with that for gasoline. The relatively low efficiency of producing and transporting hydrogen and the operation of steam methane reformers were responsible for part of the increase in NO_x emissions for the hydrogen internal combustion engine. The NO_x emissions associated with generating the electricity (U.S. mix) required to compress hydrogen was also significant, accounting for about 20% of the WTW NO_x emissions. Electricity generation accounted for almost 50% of the WTW PM_{10} emissions for the hydrogen engine.

The FCV, shown in the fourth set of bars in Figure ES-2, achieved reductions in all energy and emissions categories except PM_{10}. Total energy use, GHG emissions, and NO_x emissions were all about 50% below the corresponding gasoline values. The PM_{10} emissions increase resulted primarily from the emissions associated with generating electricity for hydrogen compression. Comparing the third and fourth sets of bars in Figure ES-2 shows the impact of a fuel-cell-based versus a combustion-engine-based propulsion system operating on the same source of fuel. The FCV's results were more favorable than those of the combustion engine for all parameters because of two benefits. The most obvious is on the vehicle (TTW) side: fuel cells provide low fuel consumption and generate zero vehicle emissions. However, the low fuel consumption also benefits the WTT energy use and emissions. Reduced fuel consumption per mile results in reduced per-mile energy losses and emissions associated with fuel production and distribution.

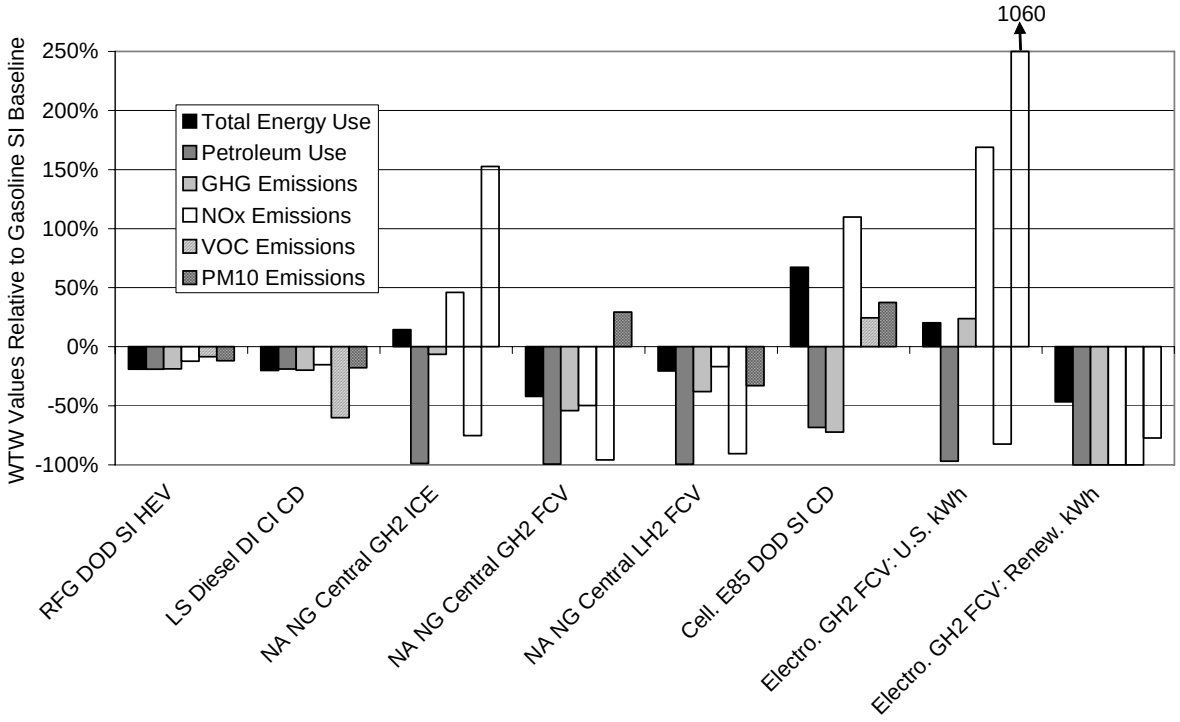

Figure ES-2 Summary of Well-to-Wheels Energy Use and Emissions for Selected Pathways

The liquid hydrogen fuel cell pathway (fifth set of bars in Figure ES-2) showed reductions in all parameters relative to gasoline. However, for all except PM_{10}, the relative benefits of liquid hydrogen are smaller than those of gaseous hydrogen. Benefits are reduced because energy losses for liquefying hydrogen are greater than those for compressing hydrogen. PM_{10} emissions are lower for the liquid hydrogen because the assumed electricity source is different. Because we assumed that hydrogen compression would take place at the refueling station, the U.S. electricity mix was used. Because liquid hydrogen is easier to transport, we assumed that the hydrogen would be liquefied at a central hydrogen production plant using electricity made at the plant site from NG. So the lower PM_{10} emissions for liquid hydrogen result from the use of NG as the fuel source instead of coal, which is a primary source for the U.S. electricity mix that is used for gaseous hydrogen compression.

The final three sets of bars show results for cellulosic ethanol and electricity-based pathways. Both corn-based and cellulosic ethanol were analyzed in this study, but we selected cellulosic E85 for this summary chart to show the potential of renewable fuels. The combustion engine operating on E85 provided about a 70% reduction in petroleum use and GHG emissions compared with gasoline. However, total energy use and NO_x, VOC, and PM_{10} emissions were higher than those for gasoline. These increases all resulted from fuel production (farming operations and ethanol manufacture). Total energy losses and emissions associated with ethanol manufacture are higher than those associated with gasoline refining.

As shown in the last two sets of bars in Figure ES-2, the impacts of FCVs operating on electrolysis-produced hydrogen depend heavily on the source of electricity. Producing hydrogen by means of the U.S. electricity mix is not an attractive option from a WTW perspective. Petroleum use and total VOC emissions decrease substantially compared with gasoline, but GHG, NO_x, and PM_{10} emissions are the highest of any of the pathways because of the relatively low efficiency and high emissions associated with the coal-based power plants that dominate electricity generation in the United States.

The most favorable WTW results were found for the fuel cell operating on hydrogen produced from renewable energy (last set of bars in Figure ES-2). This pathway resulted in zero petroleum use and zero GHG, NO_x, and VOC emissions. Combustion-based PM_{10} emissions were also zero. The remaining vehicle PM_{10} emissions resulted from tire and brake wear.

The criteria emissions results illustrated in Figure ES-2 do not take into account the location of the emissions source. GREET can be used to estimate emissions occurring in urban areas. For all pathways, per-mile urban emissions are substantially lower than total emissions. Changes in urban criteria pollutant emissions for the same WTW pathways are shown in Figure ES-3. Considering urban emissions only, reductions make the non-petroleum pathways more attractive. The only increases seen relative to the baseline gasoline system are NO_x and PM_{10} emissions for the hydrogen internal combustion engine and the FCV fueled by hydrogen produced from the U.S. electricity mix.

Because this report addresses energy use and emissions associated with a variety of fuel/propulsion system options, it provides a good starting point in deciding which are the best options for the future. However, our study does not address resource availability, economics, and infrastructure issues — all of which must be considered in selecting the best mix of future propulsion system and fuel options.

Our WTW results show that some advanced vehicle technologies offer great potential for reducing petroleum use, GHG emissions, and criteria pollutant emissions. Modest reductions in petroleum use are attributable to vehicle fuel consumption reductions by advanced vehicle technologies. On the other hand, the switch from petroleum to non-petroleum energy feedstocks, in the case of hydrogen, electricity, CNG, FT diesel, methanol, and ethanol, essentially eliminates the use of petroleum.

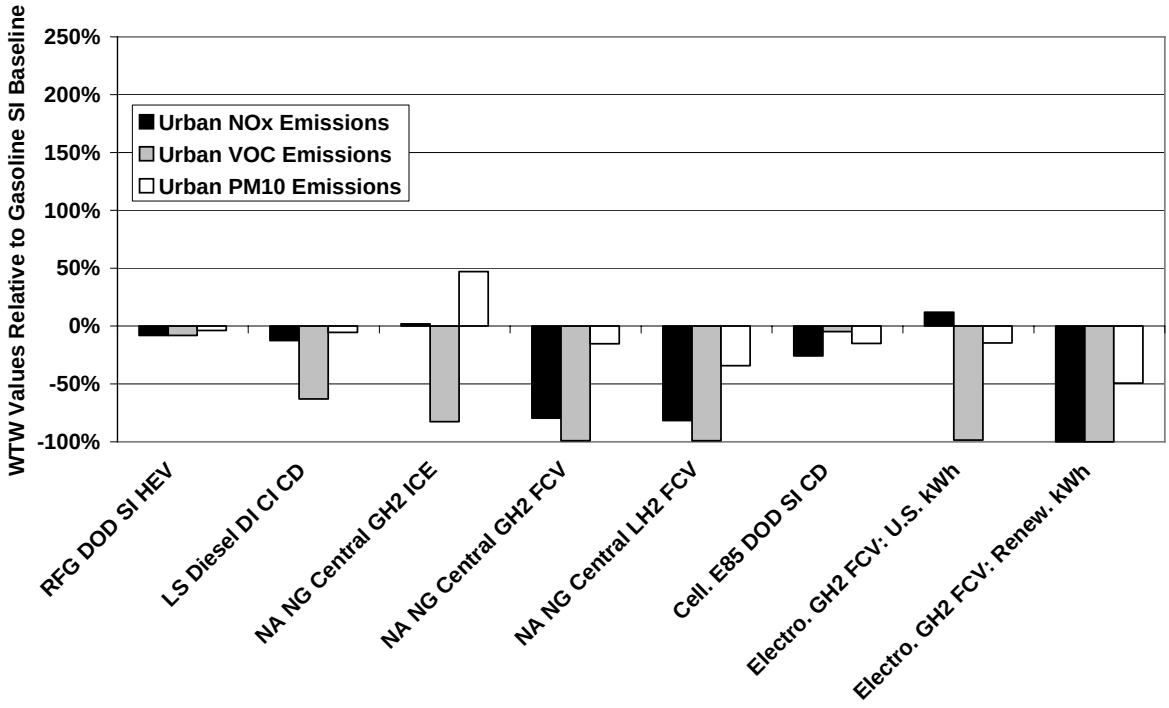

Figure ES-3 Summary of WTW Emissions in Urban Areas for Selected Pathways

The WTW GHG emissions associated with advanced vehicle technologies are determined by the WTT energy efficiencies of the fuel pathways, the vehicle fuel consumption, the carbon content of energy feedstocks used for fuel production, and the renewable nature of those feedstocks. The use of renewable feedstocks (such as renewable electricity and cellulosic ethanol) helps eliminate (or almost eliminate) GHG emissions. Even vehicle technologies with high fuel consumption can still eliminate GHG emissions, because the fuel and its feedstock do not have carbon burdens. For example, the use of renewable hydrogen in hydrogen ICE and fuel cell technologies achieves 100% reductions in GHG emissions. On the other hand, use of cellulosic E85 in ICE technologies achieves reductions of about 70% (the benefits are reduced because E85 contains 26% gasoline by energy content).

The GHG reduction results for advanced vehicles powered by carbon-containing fuels or fuels derived from carbon-containing feedstocks depend on WTT efficiencies and vehicle fuel consumption. For example, FCVs powered by NG-derived hydrogen achieve GHG reductions of about 50% because of the low fuel consumption of direct-hydrogen FCVs. If NG-derived hydrogen is used in hydrogen ICE technologies that are less efficient than hydrogen fuel cell technologies, there may be no GHG reduction benefits. In hydrogen plants, all of the carbon in NG ends up as CO_2. If CO_2 is captured and stored, this hydrogen production pathway essentially becomes a zero-carbon pathway. Any vehicle technologies using hydrogen produced this way will eliminate GHG emissions. In our analysis, we did not assume carbon capture and storage for central hydrogen plants fueled with NG.

Some of the vehicle technologies and fuels evaluated in this study offer moderate reductions in GHG emissions: corn-based E85 in flexible-fuel vehicles, HEVs powered by hydrocarbon fuels, and diesel-fueled vehicles. In general, these vehicle/fuel systems achieve 20–30% reductions in GHG emissions. The reduction achieved by using corn-based E85 is only moderate because (1) significant amounts of GHG emissions are generated during corn farming and in corn ethanol production plants; (2) diesel fuel, liquefied petroleum gas, and other fossil fuels are consumed during corn farming; (3) a large amount of

nitrogen fertilizer is used for corn farming, and production of nitrogen fertilizer and its nitrification and denitrification in cornfields produce a large amount of GHG emissions; and (4) usually, NG or coal is used in corn ethanol plants to generate steam. If a renewable energy source, such as corn stover or cellulosic biomass, is used in corn ethanol production plants, use of corn-based E85 could result in larger GHG emission reductions.

Hybrids fueled with CNG achieve larger GHG reductions than their fuel consumption reductions, because NG is 21% less carbon-intensive (defined as carbon content per energy unit of fuel) than gasoline (our baseline fuel). On the other hand, diesel ICEs and hybrids achieve smaller GHG reductions than their fuel consumption reductions, because diesel fuel contains 7% more carbon per unit energy than gasoline.

GHG results for hydrogen generated by means of electrolysis may be the most dramatic WTW results in this study. Two major efficiency losses occur during electricity generation and hydrogen production via electrolysis. Consequently, this pathway is subject to the largest WTT energy-efficiency losses. Using hydrogen (itself a non-carbon fuel) produced this way could result in dramatic increases in WTW GHG emissions. For example, if hydrogen is produced with U.S. average electricity (more than 50% of which is generated by coal-fired power plants), its use, even in efficient FCVs, can still result in increased GHG emissions; its use in less-efficient hydrogen ICEs results in far greater increases in GHG emissions. On the other hand, if a clean electricity generation mix, such as the California generation mix, is used, the use of electrolysis hydrogen in FCVs could result in moderate reductions in GHG emissions. Furthermore, if renewable electricity, such as wind power, is used for hydrogen production, the use of hydrogen in any vehicle technology will result in elimination of GHG emissions. This case demonstrates the importance of careful examination of potential hydrogen production pathways so that the intended GHG emission reduction benefits by hydrogen-powered vehicle technologies can truly be achieved.

Ours is the first comprehensive study to address WTW emissions of criteria pollutants. The results reveal that advanced vehicle technologies help reduce WTW criteria pollutant emissions. We assumed in our study that ICE vehicle technologies will, at minimum, meet EPA's Tier 2 Bin 5 emission standards. Improvements in fuel consumption by advanced vehicle technologies will help reduce per-mile WTT criteria pollutant emissions. For example, gasoline or diesel HEVs with low fuel consumption will reduce WTW criteria pollutant emissions by 10–20%, exclusively because of reduced WTT emissions.

Probably the most revealing results are the differences in WTW criteria pollutant emissions between ICE and fuel cell technologies. Although tailpipe criteria pollutant emissions generated by ICE technologies will be reduced significantly in the future, they will continue to be subject to on-road emissions deterioration (although to a much smaller extent than past ICE technologies, thanks to onboard diagnostic systems). On the other hand, FCVs, especially direct-hydrogen FCVs, generate no tailpipe emissions. Except for electrolysis hydrogen generated with U.S. average electricity, hydrogen FCVs reduce WTW emissions of criteria pollutants. For example, NG-derived hydrogen FCVs reduce WTW NO_X emissions by about 50%. FCVs also reduce the uncertainty range of criteria pollutant emissions, because they do not experience on-road deterioration of criteria pollutant emissions during the lifetime of motor vehicles.

Vehicle technologies fueled with hydrogen generated via electrolysis usually result in increased criteria pollutant emissions. Power plant emissions, together with the low efficiency of electrolysis hydrogen production, cause the increases. In order to mitigate these increases, power plant emissions will have to be reduced drastically or clean power sources will have to be used for hydrogen production.

Ethanol-based technology options also result in increased total emissions for criteria pollutants, because large amounts of emissions occur during biomass farming and ethanol production. Our study estimates

total and urban emissions of criteria pollutants separately. Although total emissions are increased by the use of ethanol, a significant amount of the total emissions occurs outside of urban areas (on farms and in ethanol plants that will be located near biomass feedstock farms). While total emission results show the importance of controlling ethanol plant emissions, urban emission estimates show that the negative effects of biofuels (such as ethanol) on criteria pollutant emissions are not as severe as total emission results imply. These emissions are likely to be controlled in the future along with other stationary source emissions.

Examination of GHG and criteria pollutant emissions reveals tradeoffs for some vehicle/fuel technologies. For example, while diesel vehicle technologies offer the potential to reduce fuel use and, consequently, to reduce GHG emissions, they may face challenges in reducing NO_x and PM_{10} emissions. Our assumption that diesel vehicles will meet Tier 2 Bin 5 standards by no means understates the technical challenges that automakers face in achieving this goal. On the other hand, FCVs can achieve emission reductions for both GHGs and criteria pollutants — thus offering a long-term solution to emissions of both GHGs and criteria pollutants from the transportation sector.

ES.4 Conclusions

The results of our WTW analysis of criteria pollutant emissions show that, as tailpipe emissions from motor vehicles continue to decline, WTT activities could represent an increased share of WTW emissions, especially for hydrogen, electricity, ethanol, and FT diesel. Thus, in order to achieve reductions in criteria pollutant emissions by advanced vehicle technologies, close attention should be paid to emissions from WTT, as well as TTW, activities.

Our study analyzed advanced vehicle technologies together with new transportation fuels, because vehicle technologies and fuels together have become increasingly important in seeking solutions to transportation energy and environmental problems. High-quality fuels are necessary to allow introduction of advanced vehicle technologies. For example, low-sulfur gasoline and diesel are needed for gasoline lean-burn and clean-diesel engines. The energy and environmental benefits of FCVs can be guaranteed only by using hydrogen from clean feedstocks and efficient production pathways. In a way, the recent popularization of WTW analyses reflects the new reality — that vehicles and fuels must be considered together in addressing transportation energy and environmental issues.

Our study separates energy use into total energy, fossil energy, and petroleum energy. Separate results for each of the three energy types shed light on the true energy benefits offered by various transportation fuels. For example, some other studies that developed estimates for total energy use showed large increases in energy use for biofuels. But those studies failed to differentiate among the different types of energy sources. An energy pathway that offers a significant reduction in petroleum use may help U.S. domestic energy supply and energy security concerns. In Section 4, we demonstrate that total energy calculations can sometimes be arbitrary. For these reasons, we maintain that the type of energy sources, as well as the amount of energy use, should be considered in evaluating the energy benefits of vehicle/fuel systems.

ES.5 Study Limitations

Our intent was to evaluate the energy and emission effects of the vehicle/fuel systems included in this study, with the premise that they could be introduced around 2010. Like many other WTW studies, ours did not address the economics and market constraints of the vehicle/fuel systems considered. Costs and commercial readiness may eventually determine which vehicle/fuel systems will be able to penetrate the

vehicle market. The results of this study provide guidance to help ensure that R&D efforts are focused on the vehicle/fuel systems that will provide true energy and emission benefits. Because WTW studies do not usually address economics, consumer acceptance, and many other factors, they cannot determine the marketability of vehicle/fuel systems.

The fuel consumption of vehicle/fuel systems is one of the most important factors in determining WTW results for energy use and emissions, especially GHG emissions. Our analysis based vehicle fuel consumption simulations on the full-size Silverado pickup truck. Compared with a typical passenger car, the pickup truck has higher fuel consumption and higher tailpipe emissions, resulting in higher WTW energy use and emissions per mile. Most other WTW studies were based on passenger cars. Absolute results per mile driven between this study and other completed studies cannot be compared. However, the relative changes that can be derived from per-mile results in this study and other studies can be compared to understand the differences in potential energy and emission benefits of different vehicle and fuel technologies.

Several major WTW studies have been completed in the past several years. For example, the Massachusetts Institute of Technology (MIT) conducted a WTW study in 2000 and updated the study in 2003 (Weiss et al. 2000; 2003). The MIT study was based on a mid-size passenger car. The GM-sponsored European WTW study (L-B-Systemtechnik GmbH et al. 2002) was based on an Opel Zafira minivan with an engine displacement of 1.8 L. A WTW study sponsored by the Joint Research Centre of the European Commission, Concawe, and European Council for Automotive R&D (2003) was based on a typical European compact car similar to the Volkswagen Golf. Comparison of absolute results from these studies and our study are less meaningful, mainly because different vehicle sizes were used in these studies. However, comparison of the relative change results among these studies should improve our understanding of the range of energy and emission benefits of advanced vehicle technologies and new transportation fuels, although such comparisons are beyond the scope of this study.

The fuel consumption improvements of HEVs directly affect their WTW energy and emission benefits. The extent of HEV fuel consumption improvements depends largely on the degree of hybridization and on designed tradeoffs between fuel consumption and vehicle performance. The HEV design simulated in this study was intended to fully meet the performance goals of the conventional Silverado truck. Furthermore, engine downsizing was not assumed here for the best-estimate HEV design. This design decision resulted in smaller fuel consumption reductions by HEVs in this study than could be achieved with downsized engines. Downsized engines were considered in the best-case HEV scenario.

Although we included many hydrogen production pathways in this study, we certainly did not cover every potential hydrogen production pathway. For instance, we included neither hydrogen production via gasification from coal and cellulosic biomass nor hydrogen production via high-temperature, gas-cooled nuclear reactors. R&D efforts are currently in progress for these hydrogen production pathways. For some of the hydrogen production pathways considered in this study (such as hydrogen from NG in central plants), we did not assume carbon capture and storage. Had we done so, those pathways might have been shown to result in huge GHG emission reductions.

Although we addressed uncertainties in our study with Monte Carlo simulations, the results of our simulations depend heavily on probability functions that we established for key WTW input parameters. Data limitations reduced the reliability of the distribution functions we built for some of the key input parameters, such as criteria pollutant emissions associated with key WTT and TTW stages. Nonetheless, systematic simulations of uncertainties in WTW studies could become the norm for future WTW studies.

1. INTRODUCTION

Since the 1980s, various transportation fuel-cycle analyses have been conducted to evaluate the energy and environmental impacts associated with fuel/vehicle systems. Earlier transportation fuel-cycle analyses were driven mainly by the introduction of battery-powered electric vehicles (EVs). Current transportation fuel-cycle analyses stem primarily from interest in fuel-cell vehicles (FCVs). While these vehicles could generate zero emissions from the point of view of vehicle operation, there are emissions associated with production and distribution of the fuels (i.e., electricity and hydrogen [H_2]). An accurate evaluation of the energy and environmental effects associated with these vehicles in relation to those associated with conventional internal combustion engine (ICE) technologies requires a full fuel-cycle analysis. In consumer products research, such analyses are often called "life-cycle" or "cradle-to-grave" analyses. In the transportation field, the fuel-cycle analysis is also referred to as a "well-to-wheels" (WTW) analysis. However, unlike life-cycle analyses, WTW analyses usually do not take into account the energy and emissions required to construct fuel production infrastructure or those required to produce the vehicles.

Figure 1-1 shows the scope of a typical transportation WTW analysis. To allow comparison with conventional analyses covering only vehicle operations, results of a WTW analysis are often separated into two groups: well-to-tank (WTT) and tank-to-wheels (TTW). WTT stages start with fuel feedstock recovery and end with fuels available in vehicle tanks. TTW stages cover vehicle operation activities. Because regulatory agencies have included evaporative emissions of volatile organic compounds (VOCs) that occur during vehicle refueling in calculating emissions for vehicle operation activities, a precise separation of WTW stages for criteria pollutant emissions estimation is more appropriate at the fuel pumps of refueling stations, in order to be consistent with vehicle emissions estimates. Thus, WTW stages are divided into well-to-pump (WTP) and pump-to-wheels (PTW) stages. Although our analysis has been conducted with the WTP and PTW separation, we use the terms WTT and TTW in this report (instead of WTP and PTW) to be consistent with the terms used in the Phase 1 report prepared by General Motors Corporation (GM) and others.

There are a variety of fuel production pathways (or WTT options) from different energy feedstocks to different transportation fuels. Energy feedstocks for transportation fuel production could include crude oil, natural gas (NG), coal, biomass (grains such as corn and cellulosic biomass), and different energy sources for electricity generation. Transportation fuels for evaluation could include gasoline, diesel, methanol (MeOH), ethanol (EtOH), compressed natural gas (CNG), Fischer-Tropsch (FT) diesel, hydrogen, and electricity. These combinations, plus different production technology options, can result in

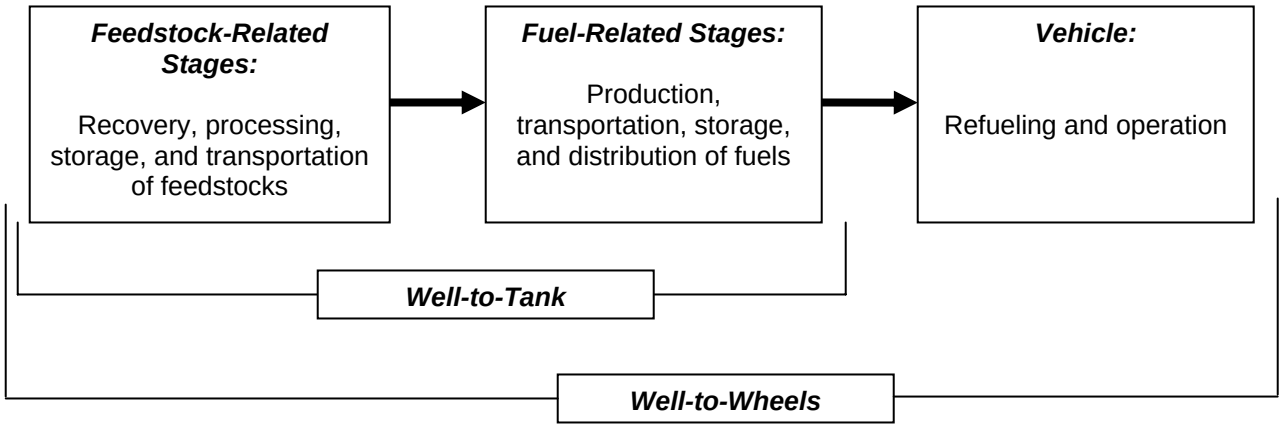

Figure 1-1 Scope of a Well-to-Wheels Analysis for Fuel/Vehicle Systems

many fuel pathways for WTW evaluation. Recent interest has been primarily in NG-based fuels, renewable fuels, and hydrogen.

On the other hand, various vehicle propulsion technologies (TTW technologies) have been promoted for improving vehicle efficiencies, reducing vehicle emissions, and diversifying vehicle fuels. Vehicle propulsion technologies of interest include spark-ignition (SI) engines, direct-injection (DI) compression-ignition (CI) engines, hybrid electric vehicles (HEVs) with SI and CI engines, FCVs, and battery-powered electric vehicles (EVs). These technologies, together with the different fuels used to power them, result in many vehicle/fuel combinations for WTW evaluations.

To provide a systematic basis for comparing advanced propulsion technologies, GM sponsored a series of WTW analyses. The first of these, a North American analysis of energy consumption and greenhouse gas (GHG) emissions associated with a light-duty truck (LDT), was published in 2001 (GM et al. 2001). In this report, we refer to the 2001 study as the GM Phase 1 North American study. Because vehicle type, driving cycle, and fuels infrastructure can impact the results of WTW studies, a similar energy and GHG emissions study was conducted for Europe (GM Phase 1 European study), and the results were published in 2002 (L-B-Systemtechnik GmbH et al. 2002).

Neither of these published studies included the WTW impacts of advanced vehicles and new fuel systems on criteria pollutant emissions. This study, which we refer to as the GM Phase 2 North American study, extends the Phase 1 North American study (GM et al. 2001) to include analysis of criteria pollutants including volatile organic compounds (VOCs), nitrogen oxides (NO_x), carbon monoxide (CO), particulate matter with a diameter smaller than 10 microns (PM_{10}), and sulfur oxides (SO_x). In addition, the vehicle modeling was updated with the latest performance data, and a few additional vehicle propulsion systems were included in the analysis.

Chapter 2 of this report describes the methodologies used in the Phase 2 study, presents fuel production pathways and vehicle propulsion systems, and provides data sources and processing. Chapter 3 presents vehicle fuel consumption results. Chapter 4 presents WTW energy and emission results and discusses key issues identified from the WTW results. Chapter 5 presents conclusions. Chapters 6 and 7 provide acknowledgments and a list of references cited in this report. Appendix A describes our analysis of the national emission inventory (NEI) database. Appendix B presents specific methods used to generate individual distribution functions for emissions associated with WTT activities. Appendices C and D provide tables listing WTT and WTW energy and emission results.

2. METHODOLOGIES AND FUEL/VEHICLE SYSTEM OPTIONS

As part of our study, we analyzed 124 different WTW pathways. A pathway is a complete set of assumptions about the resource used, transportation, fuel production, and characteristics of the vehicle using the fuel. These 124 WTW pathways were constructed from 29 WTT fuel production pathways and 22 TTW propulsion systems. Section 2.1 addresses fuel (WTT) production methodologies and pathways; Section 2.2 describes vehicle technology (TTW) methodologies and vehicle propulsion systems; and Section 2.3 presents the fuel/vehicle systems examined in our study.

2.1 Fuel Production Simulation Methodologies and Pathways

2.1.1 The GREET Model

In 1995, with funding from the U.S. Department of Energy (DOE), the Center for Transportation Research (CTR) of Argonne National Laboratory (ANL) began to develop a spreadsheet-based model for estimating the full fuel-cycle energy and emissions impacts of alternative transportation fuels and advanced vehicle technologies (Wang 1996). The intent was to provide an analytical tool to allow researchers to readily analyze various parametric assumptions that affect fuel-cycle energy use and emissions associated with various fuels and vehicle technologies. The model, called GREET (Greenhouse gases, Regulated Emissions, and Energy use in Transportation), calculates fuel-cycle energy use in Btu/mi and emissions in g/mi for various transportation fuels and vehicle technologies. For energy use, GREET includes total energy use (all energy sources), fossil energy use (petroleum, natural gas [NG], and coal), and petroleum use (each energy item is a part of the preceding energy item). For emissions, the model includes three major GHGs (carbon dioxide [CO_2], methane [CH_4], and nitrous oxide [N_2O]) and five criteria pollutants (VOCs, CO, NO_x, PM_{10}, and SO_x).

In the GREET model, the three GHGs are combined together with their global warming potentials (GWPs) to calculate CO_2-equivalent GHG emissions. The default GWPs in the latest GREET version — 1 for CO_2, 23 for CH_4, and 296 for N_2O — are recommended by the Intergovernmental Panel on Climate Change (IPCC 2001) for the 100-year time horizon. On the other hand, because the location, as well as the amount, of criteria pollutant emissions is important, emissions of the five criteria pollutants are further separated into total and urban emissions. Total emissions are emissions occurring everywhere. Urban emissions, which are a subset of total emissions, are those occurring within urban areas. Urban areas in GREET are metropolitan areas with populations above 125,000, as defined by the U.S. Bureau of the Census. The separation of criteria pollutant emissions is a crude step to provide some information about potential human exposure to criteria pollutant emissions. The separation is based on information regarding facility locations.

Since the release of the first version of GREET, CTR/ANL continues to update and upgrade the model. Development and use of earlier GREET model versions were documented in Wang (1999a, b) and in Wang and Huang (1999). In 2000, CTR/ANL began to work with GM and three energy companies to analyze WTW energy and GHG emission effects associated with advanced fuel/vehicle systems (GM et al. 2001). During this Phase 1 study, stochastic simulation based on the Monte Carlo method was introduced into the GREET model. Because of that effort and other ANL efforts, a new version — GREET 1.6 — was developed (Wang 2001).

The GREET model is in the public domain, and any party can use it free of charge. The model and its associated documents are posted at Argonne's GREET website: http://www.transportation.anl.gov/software/greet/index.html.

A WTW analysis includes many WTT activities related to production and transportation of feedstocks and fuels. Figure 2-1 is a simplified diagram showing calculation logic for energy use and emissions associated with WTT production activities. For a given type of fuel production, total energy use is derived from the energy efficiency of each production activity. Then, energy use by each fuel type (e.g., NG, diesel, electricity) is estimated from the estimated total energy use and shares of fuel types. We calculate emissions by using energy use by fuel type, emission factors by fuel type, and combustion technology shares. Finally, urban emissions are estimated from total emissions and a split of facility locations between urban and non-urban locations. For CO_2 emissions, GREET takes a carbon-balance approach. That is, the carbon in CO_2 emissions is equal to the carbon contained in the fuel burned minus the carbon contained in combustion emissions of VOC, CO, and CH_4. For details on calculation methodologies, see Wang (1999a, b).

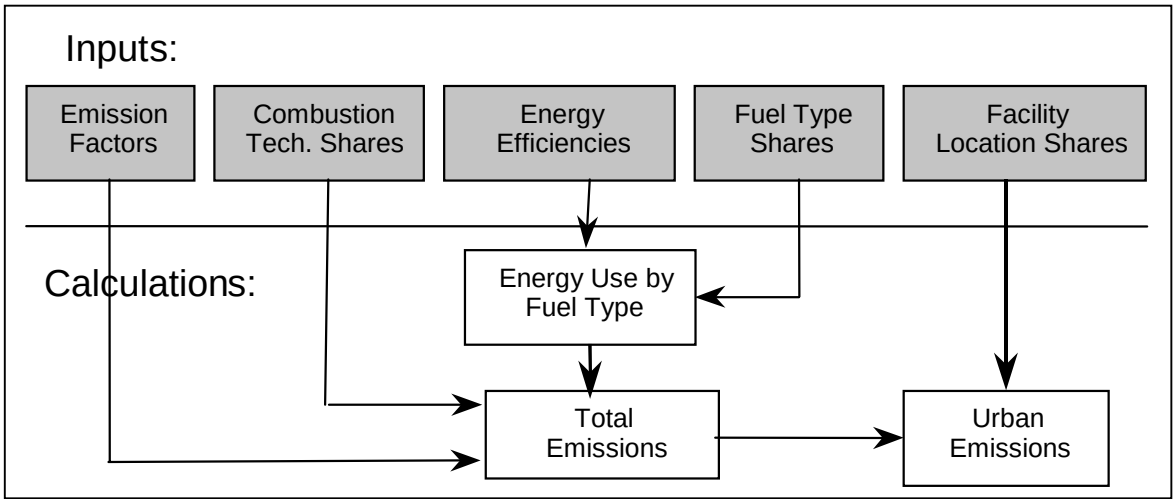

Figure 2-1 Calculation Logic for Well-to-Tank Energy Use and Emissions for Activities Related to Production of Feedstocks and Fuels

The GREET model includes detailed simulations for activities related to transportation of feedstocks and fuels. Figure 2-2 schematically shows GREET simulation logic for transportation-related activities. For a given transportation mode (e.g., ocean tanker for crude transportation), input assumptions of energy intensity of the mode, transportation distance, energy use by fuel type, and emission factors by fuel type are specified. GREET then calculates energy use and emissions for the given mode of transporting a product. Transportation of a given product usually involves multiple transportation modes (for example, ocean tankers and pipelines are used for crude transportation). Thus, energy use and emissions for transporting a given product equal the share-weighted average of all the transportation modes for the product.

Detailed assumptions regarding transportation activities, as shown in Figure 2-2, are presented in the GM Phase 1 report (GM et al. 2001). Simulations of transportation-related activities require specification of transportation logistics for energy feedstocks and fuels. Transportation logistics flowcharts for key feedstocks and fuels are presented in the GM Phase 1 report. Simulations of transportation activities in the

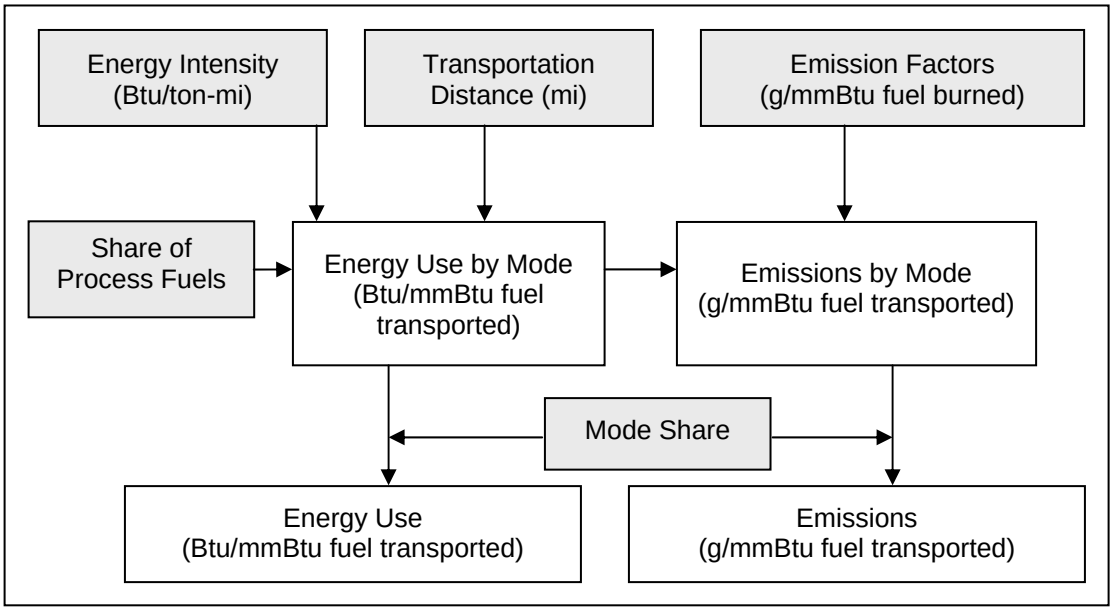

Figure 2-2 Calculation Logic for Well-to-Tank Energy Use and Emissions for Activities Related to Transportation of Feedstocks and Fuels

Phase 2 study relied on Phase 1 study logistics specifications. In addition, readers can obtain detailed information regarding simulations of the transportation-related activities addressed in this study from the GREET model.

As Figures 2-1 and 2-2 show, energy use associated with the WTT stages is determined mainly by energy efficiencies (for production-related activities) and energy intensities (for transportation-related activities). Carbon dioxide emissions are then determined by the energy use and the carbon contents of the fuels used. In the Phase 1 GM study, significant efforts were made to determine the energy efficiencies and intensities for key WTT stages. The Phase 2 study relies on the efficiency and intensity results from the Phase 1 study.

For estimation of criteria pollutant emissions, emission factors (in g/mmBtu of process fuel burned) are a key determinant. That is, emissions of criteria pollutants for a given activity are determined by the amount of process fuels used during the activity and the emission factors of the process fuels used. Because criteria pollutant emissions are subject to stringent emission controls, there are no theoretical means of calculating emission factors for the criteria pollutants, except for SO_x, for which the emission factor, in most cases, can be calculated from the sulfur content of a given process fuel. The majority of the effort in the Phase 2 study has been in establishing emission factors for the various steps involved in the WTT processes. Details regarding these efforts are presented in later sections of this report.

The new GREET version is capable of applying Monte Carlo simulations to address the uncertainties involved in key input parameters. The Phase 2 study, as well as the completed Phase 1 study, uses this GREET feature to generate results with uncertainty ranges. For Monte Carlo simulations, probability distribution functions need to be established for key input parameters. In particular, on the basis of published data for given fuel-cycle stages, ANL established subjective probability distribution functions for each stage. These distribution functions are incorporated into the GREET model. In the Phase 1 study, distribution functions were established for energy efficiencies and GHG emissions of key WTW stages. In the Phase 2 study, distribution functions were established for emission factors (in g/mmBtu of fuel

burned for different combustion technologies used in WTT stages). For the TTW stage, the Phase 1 study established distribution functions for fuel economy associated with various vehicle/fuel systems. For the Phase 2 study, we established distribution functions for vehicular criteria pollutant emissions and revised the distribution functions for fuel economy values from the Phase 1 study.

A commercial software, Crystal Ball™, is used in GREET to design and conduct Monte Carlo simulations. Distribution functions established for the Phase 1 and Phase 2 studies are embedded in the new GREET version. In order to use the new Monte Carlo simulation feature in GREET, users need to have both Excel and Crystal Ball™ software. However, if Crystal Ball™ software is not available, users can still conduct point estimates with the new GREET version in Excel.

2.1.2 Fuel Production Pathways

Figure 2-3 illustrates the WTT energy feedstocks and fuels considered this study. Key feedstocks analyzed include oil, NG, and biomass. We also considered the feedstocks currently used to make electricity (including coal, NG, nuclear, and renewables). Starting with these feedstocks, we analyzed various pathways used to make the following fuels: gasoline, diesel, crude naphtha, CNG, methanol, FT naphtha, FT diesel, gaseous hydrogen (GH_2), liquid hydrogen (LH_2), ethanol, and E85 (85% denatured ethanol with 15% gasoline by volume).

Figure 2-3 illustrates the overall coverage from feedstocks to fuels of the Phase 2 study, but does not completely describe detailed production options for a given feedstock-to-fuel selection. Important factors for a specific fuel production pathway include the source of NG (North American [NA] or non-North American [NNA] sources) and whether the NG is converted to hydrogen at the fueling station or remotely

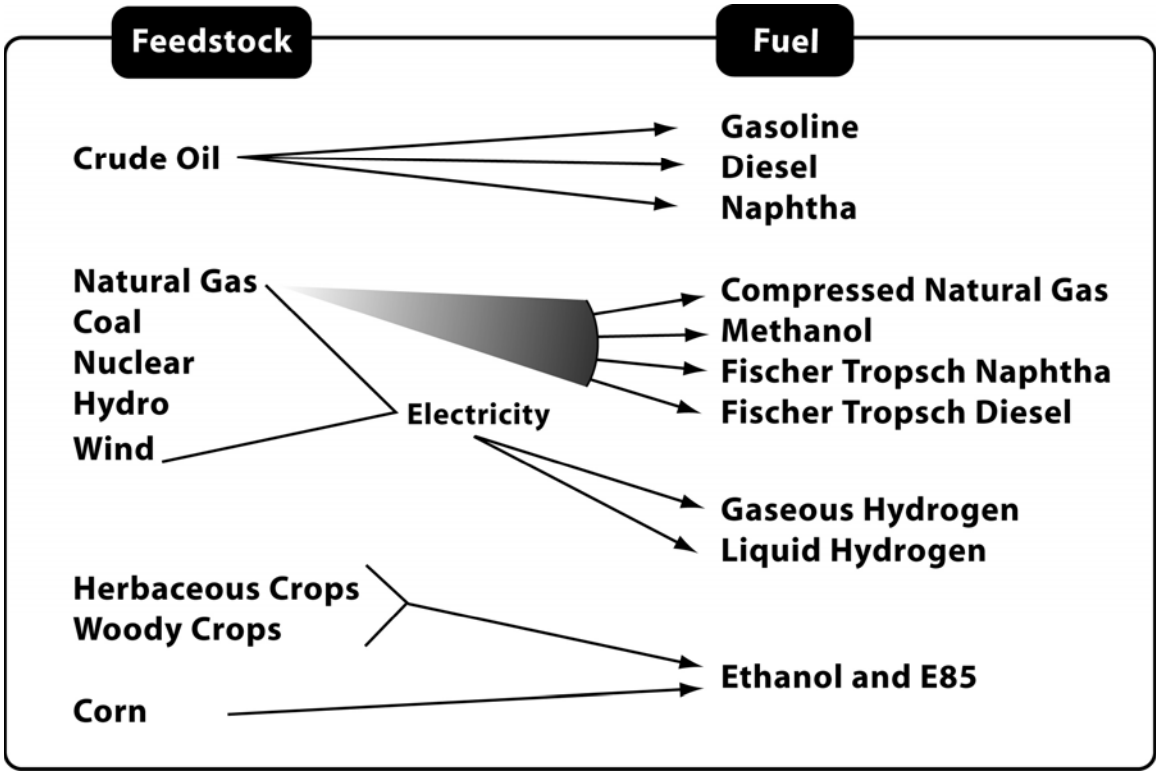

Figure 2-3 Energy Feedstocks and Fuels Examined in this Study

in large central plants. In total, 29 different fuel production pathways were analyzed in this study. These are listed in Table 2-1.

The WTT portion of the Phase 1 study included 75 WTT pathways. However, not all of these WTT pathways were used in the WTW integration. In fact, the 75 original WTT pathways were reduced to 13 for integration into the WTW analysis. In the Phase 2 study, on the other hand, all 27 WTT pathways were integrated into the WTW analyses. Pathways for which WTW integration analyses were added in the Phase 2 study include NG combined-cycle (CC) electricity to hydrogen via electrolysis and NA NG to CNG and hydrogen. During the Phase 1 study, WTW integration was not conducted on pathways involving NA NG because our analysis revealed that insufficient NA gas would be available to fuel a large share of the transportation fleet. Although we still recognize the resource limitations of NA NG, we included it in the Phase 2 WTW analysis to show the sensitivity of WTW results to the assumed location of the NG resource. In the GM Phase 1 report (GM et al. 2001), flowcharts for these fuel production

Table 2-1 WTT Fuel Pathway Options Analyzed in Phase 2 Study

Feedstock	Fuel
Petroleum	(1) 30-ppm-sulfur (S) reformulated gasoline (RFG) without oxygenate (for conventional spark-ignition [SI] engine)
	(2) 10-ppm-S RFG without oxygenate (for direct-injection SI engine)
	(3) 5-ppm-S gasoline (for gasoline-powered FCVs)
	(4) 15-ppm-S (low-sulfur [LS]) diesel
	(5) Crude naphtha
NA and NNA NG	(6) NA NG to CNG[a]
	(7) NNA NG to CNG via liquefied NG (LNG)
	(8) NNA NG to methanol
	(9) NNA NG to FT diesel
	(10) NNA NG to FT naphtha
	(11) NA NG to GH_2 in central plants[a]
	(12) NNA NG to GH_2 in central plants via LNG
	(13) NA NG to GH_2 in refueling stations[a]
	(14) NNA NG to GH_2 in refueling stations via LNG
	(15) NA NG to LH_2 in central plants[a]
	(16) NNA NG to LH_2 in central plants
	(17) NA NG to LH_2 in refueling stations[a]
	(18) NNA NG to LH_2 in refueling stations via LNG
Biomass	(19) Corn to ethanol for E85 blend (for ICEs)
	(20) Cellulosic biomass to ethanol for E85 blend (for ICEs)
	(21) Corn to ethanol (for FCVs)
	(22) Cellulosic biomass to ethanol (for FCVs)
Electricity to H_2	(23) U.S. average electricity to GH_2 in refueling stations
	(24) U.S. average electricity to LH_2 in refueling stations
	(25) Calif. average electricity to GH_2 in refueling stations
	(26) Calif. average electricity to LH_2 in refueling stations
	(27) NG CC electricity to GH_2 in refueling stations[a]
	(28) NG CC electricity to LH_2 in refueling stations[a]
	(29) Renewable electricity to GH_2 in refueling stations[a]

[a] WTT analysis, but not WTW analysis, was conducted for these pathways in the GM North American Phase 1 study (GM et al. 2001).

pathways were presented. Key issues for each of the pathways covered in the Phase 2 study are presented below. Fuel properties assumed for this study are listed in Table 2-2.

2.1.2.1 Petroleum to Gasoline, Diesel, and Naphtha

The United States currently imports about 60% of its crude oil. Production of both domestic and foreign crude was taken into account in our study to determine petroleum recovery efficiencies, transportation modes, and distances from oil fields to U.S. refineries.

In the Phase 2 study, we include 30-ppm-sulfur (S) reformulated gasoline (RFG), 10-ppm-S RFG, 5-ppm-S gasoline, 15-ppm-S diesel, and naphtha. The three types of gasoline are assumed to contain no oxygenates. Requirements for 30-ppm-S gasoline began to be implemented nationwide in 2004. The 10-ppm-S RFG would probably be required if direct-injection spark-ignition (DI SI) engines are to be introduced in the U.S. so that they could meet the U.S. Environmental Protection Agency's (EPA's) Tier 2 NO_X emission standards for light-duty vehicles. The 5-ppm-S gasoline is for FCVs to produce hydrogen from gasoline via onboard fuel processors. Even with 5-ppm-S gasoline, onboard desulfurization may be required for FCVs.

The 15-ppm-S diesel will be introduced in 2006 in the U.S. market to help heavy-duty diesel vehicles meet upcoming 2007 emissions standards. Naphtha is currently produced in petroleum refineries and used as a gasoline blending component. Because of its low octane number, pure naphtha can not be used for ICEs, However, naphtha could be used as an FCV fuel to produce hydrogen via onboard fuel processors. For that purpose, we assume a sulfur content below 10 ppm for naphtha.

Table 2-2 Properties of Fuels Included in this Study

Fuel	Lower Heating Value (Btu/gal)	Density (g/gal)	Carbon mass fraction (%)	Sulfur Content (ppm)	Carbon Content (g/mmBtu)
30-ppm-S gasoline	115,500	2,791	85.5	30	20,661
10-ppm-S gasoline	115,500	2,791	85.5	10	20,661
5-ppm-S gasoline	115,500	2,791	85.5	5	20,661
LS diesel	128,000	3,240	87.0	15	22,022
Petroleum naphtha	118,760	2,861	85.3	1	20,549
NG-based FT naphtha	111,780	2,651	84.2	0	19,969
FT diesel	118,800	2,915	86.0	0	21,102
Methanol	57,000	2,996	37.5	0	19,711
Ethanol	76,000	2,996	52.2	5	20,578
E85 (81% ethanol/19% gasoline by volume[a])	83,505	2,957	58.2	10	20,609
Liquid hydrogen	30,900	268.7	00.0	0	0
Gaseous hydrogen[b]	288[c]	2.545[d]	00.0	0	0
Natural gas[b]	928[c]	20.5[d]	74.0	7	16,347

[a] Ethanol contains about 5% of gasoline as a denaturant. Thus, E85 actually contains 81% ethanol and 19% gasoline by volume.

[b] At normal atmospheric pressure.

[c] Btu per standard cubic foot.

[d] Grams per standard cubic foot.

Petroleum refining is the most important of the petroleum-based WTT stages. Past efforts at Argonne and during the GM North American Phase 1 study addressed the energy efficiencies associated with producing different petroleum products in great detail (see GM et al. 2001 and Wang et al. 2004). Because refineries produce multiple products (e.g., gasoline, diesel, naphtha), WTT analysis of a specific fuel requires the allocation of the overall refining efficiency among individual petroleum products. The Phase 1 report documented our approach to determining product efficiencies for each product (GM et al. 2001). Subsequently, we addressed allocation of petroleum refinery energy use among products at the level of individual refining processes (Wang et al. 2004). Our detailed allocation analysis showed that allocation at the aggregate refinery level, as was done in the Phase 1 study, is a good approximation of the detailed allocation. We retained the Phase 1 allocation results for use in the Phase 2 study.

2.1.2.2 Natural Gas to Compressed Natural Gas

For the CNG production pathway, we include two potential NG sources: North American and non-North American natural gas. In the Phase 1 report, we summarized the trend of NG production and consumption in the United States and concluded that the NG reserve in North America may not be able to support a large-scale transportation market in addition to expanding conventional NG markets (GM et al. 2001). For large-scale transportation fuel production from NG to be feasible, the United States may have to rely on NNA NG. Thus, in our Phase 1 and 2 analyses, we consider both NNA and NA NG. In order to ship it to the United States for CNG production at refueling stations, NNA NG needs to be liquefied. Liquefaction of NG introduces an energy efficiency loss of about 10%.

We assumed that NG would be compressed to 4,000 psi for storage at 3,600 psi aboard CNG vehicles. Energy requirements for CNG compression were calculated by using a formula discussed in the Phase 1 report (GM et al. 2001). We did not consider CNG at pressures higher than 3,600 psi because the increase in NG density as pressure increases beyond 3,600 psi diminished due to the nonlinear compressibility of NG. We assumed electric compressors would be used at CNG refueling stations, because of their high reliability relative to gas compressors. Electric compressors are more efficient than gas compressors if one considers only the energy in electricity (vs. energy in NG for gas compressors). However, because GREET takes into account the energy loss for electricity generation, the overall efficiency of electric compressors, with consideration of electric power plant efficiency losses, could be lower than that of gas compressors.

2.1.2.3 Natural Gas to Methanol

Methanol is produced primarily from NG via steam methane reforming (SMR) or autothermal reforming (ATR). As of 2001, worldwide methanol production capacity was 11.8 billion gal/yr; of that total, South America accounts for 22%, the Middle East and Africa 22%, the Asian Pacific 21%, Europe 19%, and North America 16% (American Methanol Institute 2003). Mega-size methanol plants, especially newly built ones, are located in non-North American countries that have a plentiful (and therefore inexpensive) supply of natural gas. If a significant amount of methanol is to be used to power FCVs in the United States, it is likely that the methanol will be produced outside of North America. So only imported methanol was considered in the Phase 2 study. The Phase 1 study included methanol produced both in and outside of North America.

We assumed that methanol would be produced in South America, the Middle East, and Africa and shipped to North America via ocean tankers. Once imported, we assumed that methanol would be distributed to bulk terminals and refueling stations via rail, barge, and truck.

2.1.2.4 Natural Gas to Fischer-Tropsch Diesel and Fischer-Tropsch Naphtha

Although FT diesel can be produced from a variety of feedstocks, including NG, coal, and biomass, the current commercial interest involves FT diesel production from NG. Shell has announced plans for large-size NG-based FT plants in Australia, South Africa, and the Middle East. SasolChevron has announced plans for these types of plants in Nigeria and Qatar. Diesel fuel produced from NG via the FT process has low aromatics, extremely low sulfur content, and a high cetane number. It is a premium fuel for CI engines. We included FT diesel for CI engine technologies.

In FT plants, naphtha is produced together with FT diesel. The volumetric share of FT naphtha could be 20–30% of FT plant production. FT naphtha, with almost zero sulfur content and relatively high hydrogen content, could be a source for hydrogen production (via fuel processors) onboard FCVs.

Natural gas feedstock cost is a major cost component of FT plant economics. Because of this, all the NG-based FT plants announced for construction are to be located in countries where NG is abundant and cheap. In the Phase 2 study, we assumed that FT diesel and naphtha would be produced in the Middle East and North Africa, and shipped to North America via ocean tankers.

2.1.2.5 Natural Gas to Gaseous and Liquid Hydrogen

Hydrogen is currently produced primarily from NG via SMR. For the purpose of completeness, we included both NA and NNA NG for hydrogen production, even though NA NG could be limited for large-scale hydrogen production. We included both GH_2 and LH_2 in our evaluation. Although other hydrogen storage technologies, such as metal hydrides, are being researched and developed, we do not include these because insufficient data were available to characterize system mass and energy required to release hydrogen. We assumed that GH_2 would be compressed to 6,000 psi at refueling stations for onboard storage at 5,000 psi. For LH_2, we assumed that the hydrogen would be liquefied at the site where it is produced. While hydrogen is currently produced from NG at central production facilities, we included both central plant production and refueling station production. The latter can avoid or reduce the need for building an expensive hydrogen transportation and distribution infrastructure.

2.1.2.5.1 Gaseous Hydrogen

For GH_2 production, we included four pathways: central plants with NA NG, refueling stations with NA NG, central plants with NNA NG, and refueling stations with NNA NG. Although tanks for storage of hydrogen at 10,000 psi are being developed, we did not include this option in our analysis. Increasing compression pressure from 5,000 to 10,000 psi would result in the following increases in total energy use for GH_2-powered FCVs: a 17% increase in energy use for compressing hydrogen; a 5% increase in WTT energy use, and a 2% increase in WTW energy use. Thus, the effect of 10,000 psi vs. 5,000 psi on energy use and resultant emissions is small on a WTW basis. For the first pathway, GH_2 production in central plants with NA NG, the NG is transmitted via pipelines from NG processing plants to hydrogen plants. GH_2 is then transmitted via pipelines from hydrogen plants to refueling stations, where GH_2 is compressed for refueling hydrogen ICE and FC vehicles. For the pathway of hydrogen production at refueling stations from NA NG, the NG is transmitted from NG processing plants to refueling stations via pipeline.

The third and fourth pathways, producing GH_2 in both central plants and refueling stations with NNA NG, the NNA NG is liquefied offshore near NG fields. LNG is then transported via ocean tankers to U.S. LNG terminals, where it is gasified. In the case of central plant production, NG is transmitted to central

hydrogen plants via pipelines. The produced GH_2 is then transported via pipelines to refueling stations, where it is compressed to 6,000 psi. For GH_2 production from NNA NG at refueling stations, NG is transported via pipelines to refueling stations. Although both NG and electric compressors can be used for compressing GH_2, we assumed in our study that electric compressors would be used. Energy requirements for compressing GH_2 are estimated with a formula presented in the Phase 1 report (GM et al. 2001).

2.1.2.5.2 Liquid Hydrogen

For LH_2, we included four production pathways: central plants with NA NG, refueling stations with NA NG, central plants with NNA NG, and refueling stations with NNA NG. For the first pathway, central plant LH_2 production with NA NG, the NG is transported from NG processing plants to hydrogen plants, where hydrogen is produced and liquefied. The LH_2 is then transported to refueling stations primarily via rail and trucks. For the second pathway, station LH_2 produced with NA NG, the NG is transmitted from NG processing plants to refueling stations via pipelines, where hydrogen is produced and liquefied.

The third pathway, central plant LH_2 production with NNA NG, involves production of LH_2 offshore and transportation to U.S. ports via ocean tankers. The LH_2 is then transported to refueling stations via rail and trucks. For the last pathway, refueling station LH_2 production with NNA NG, the NG is liquefied offshore and transported to U.S. LNG terminals via ocean tankers. The LNG is then gasified and transmitted to refueling stations via pipelines. Hydrogen is produced and liquefied in refueling stations.

NG-based hydrogen plants convert the carbon in NG into CO_2. The generated CO_2 in hydrogen plants could be captured and sequestered for further CO_2 reductions by hydrogen ICE vehicles and FCVs, if there were incentives to do so. However, CO_2 capture and sequestration were not considered in our analysis.

2.1.2.6 Electricity to Gaseous and Liquid Hydrogen via Electrolysis of Water

Hydrogen can be produced from electricity by electrolyzing water. Because a large amount of electricity is required for hydrogen production, this production option is only economically feasible where electricity is cheap. On the other hand, the distribution and production infrastructure for hydrogen production via central SMR is expensive and could take a long time to establish. Because commercial electrolyzers and an extensive electricity distribution system are already available, electrolysis hydrogen was included in our analysis as an option during the early stage of hydrogen vehicle introduction into the marketplace.

Energy and emission impacts of electrolysis hydrogen depend very much on the energy source from which electricity is generated. Our analysis included hydrogen from U.S. average electricity, electricity from NG-powered combined-cycle (NGCC) turbines, and electricity from renewable sources such as hydro-power, wind, and other energy sources. In the past 20 years, most new fossil fuel power plants have been efficient, low-polluting NGCC turbines, although because of recent NG price spikes, construction of many coal-fired power plants is planned in the near future. Renewable electricity could provide large fossil energy and emissions benefits. These three sources for electricity generation provide a range of results that cover the effects of potential electricity supply sources for hydrogen production.

2.1.2.7 Biomass to Ethanol

Ethanol can be produced through fermentation of sugars derived from corn or cellulosic biomass. In 2003, the United States consumed nearly 3 billion gallons of fuel ethanol for transportation use. About 90% of

the ethanol is produced from corn. Although essentially no ethanol is currently produced from cellulose, research and development (R&D) is under way to develop and improve the technologies required to produce ethanol from cellulosic biomass. Because of the limited supply of corn, ethanol produced from corn cannot meet a large enough fraction of the transportation fuel demand. For example, the current 3 billion gallons of ethanol production in the United States already consumes about 11% of total U.S. corn production — 10.1 billion bushels in 2003 — accounting for only about 1.4% of the total U.S. gasoline demand of 142 billion gallons (on an energy basis). Corn-based ethanol is produced in both wet and dry milling ethanol plants. Wet milling plants are larger and require more capital investment to build than dry milling plants. Wet milling plants produce multiple co-products besides ethanol, while dry milling plants produce a single co-product — animal feed. In recent years, newly added U.S. ethanol production capacity has been in the form of dry milling plants because of their low capital requirements and short period of construction. As a result, in 2004, about 75% of total U.S. corn ethanol was produced from dry milling plants. In our simulations of corn ethanol for year 2016, we assume that 70% of corn ethanol is produced from dry milling plants and the remaining 30% from wet milling plants. That is, we assume that in the future, large-size wet milling ethanol plants will be added to the U.S. corn ethanol production capacity.

In the long run, cellulosic biomass, such as crop residues and managed biomass growth (e.g., switchgrass and fast-growing trees), can provide a large amount of feedstock for ethanol production. We included ethanol production from both corn and cellulosic biomass in our study. We assumed that cellulosic biomass for ethanol production was 50% from herbaceous (grasses) and 50% from woody sources.

Processes analyzed for ethanol production pathways included manufacture of fertilizers and pesticides, transportation of fertilizers and pesticides to farms, farming activities, transportation of corn (in the case of corn ethanol) and cellulosic biomass (in the case of cellulosic ethanol) to ethanol plants, ethanol production in corn or cellulosic ethanol plants, and ethanol transportation and distribution to refueling stations.

2.1.3 Fuel Production Assumptions

2.1.3.1 Assumptions Related to Energy and GHG Emissions

Table 2-3 lists the assumptions used for WTT energy efficiency and GHG emissions. These assumptions are discussed extensively in the Phase 1 study report (GM et al. 2001). For WTT stages, there are two major CO_2 emission sources: combustion of process fuels and direct emissions from production or conversion processes (such as the SMR process for hydrogen production). CO_2 emissions from process fuel combustion are calculated by using the carbon balance approach. That is, the carbon contained in a process fuel combusted minus the carbon in emissions of VOCs, CO, and CH_4 equals the carbon in CO_2 emissions of the combustion. Furthermore, in GREET, the CO_2 formation from oxidation of VOCs and CO is taken into account in CO_2 emissions from a given process, because VOCs and CO reside in the air for fewer than 10 days.

Emissions of CH_4 and N_2O from a combustion process are determined by emission factors, in g/mmBtu of fuel combusted, based primarily on EPA's AP-42 report (EPA 1995). During the Phase 2 study, detailed emissions data for VOCs, CO, NO_x, PM_{10}, and SO_x were obtained from EPA's emissions inventory data (as discussed in a later section) for developing the distribution functions of emission factors for these pollutants. Emissions factors for CH_4 and N_2O in Phase 2 simulations still rely on

Table 2-3 Key Parametric Assumptions for WTT Energy Efficiencies and GHG Emissions

Pathway	Distribution Function Type	P20[a]	P50[a]	P80[a]
Petroleum Pathways				
Petroleum recovery efficiency	Triangular[b]	96.0%	98.0%	99.0%
CH_4 emissions during crude recovery: g/mmBtu[c]			81.757	
Petroleum refining efficiency: 5- to 30-ppm-S gasoline without oxygenate	Normal	83.0%	84.5%	86.0%
Petroleum refining efficiency: 15-ppm-S diesel	Normal	85.0%	87.0%	89.0%
Petroleum refining efficiency: 5-ppm-S naphtha	Normal	89.0%	91.0%	93.0%
Gasoline production CO_2 emissions: g/mmBtu[d]			1,253	
NG Pathways				
NG recovery efficiency	Normal[e]	96.0%	97.5%	99.0%
NG processing efficiency	Normal[e]	96.0%	97.5%	99.0%
NG liquefaction efficiency (for NNA NG transported to North America)	Triangular[b]	87.0%	91.0%	93.0%
NG compression efficiency with electric compressors[f]	Triangular[b]	96.0%	97.0%	98.0%
Methanol plant efficiency[g]	Triangular[b]	65.0%	67.5%	71.0%
FT plant efficiency[g]: for FT diesel and naphtha production	Normal	61.0%	63.0%	65.0%
H_2 central plant efficiency[g]: GH_2 production	Normal	68.0%	71.5%	75.0%
H_2 station efficiency[g]: GH_2 production	Normal	62.0%	67.0%	72.0%
H_2 central plant efficiency: liquefaction of GH_2	Triangular[b]	65.0%	71.0%	77.0%
H_2 station efficiency: liquefaction of GH_2	Normal	60.0%	66.0%	72.0%
GH_2 compression efficiency[h]: sent via pipeline to stations from central plant	Triangular[b]	90.0%	92.5%	95.0%
GH_2 compression efficiency[h]: GH_2 produced at stations	Triangular[b]	91.5%	94.0%	96.5%
CH_4 emissions during NG recovery and processing: g/mmBtu			106.063	
CH_4 emissions during NG transmission to central plants: g/mmBtu			81.161	
CH_4 emissions during NG transmission to stations: g/mmBtu			122.581	
CH_4 emissions from LNG boil-off after recovery: g/mmBtu			48.0	
FT plant carbon conversion efficiency			80%	
Electricity to Hydrogen Pathways				
NG-fired boiler electric power plant efficiency[i]	Normal	32.0%	35.0%	38.0%
NG-fired CC electric power plant efficiency[j]	Triangular[b]	50.0%	55.0%	60.0%
Coal-fired boiler electric power plant efficiency[k]	Normal	33.0%	35.5%	38.0%
Coal-fired advanced boiler electric power plant efficiency[l]	Normal	38.0%	41.5%	45.0%
Electrolysis efficiency: GH_2 from electricity in station	Normal	67.0%	71.5%	76.0%
GH_2 compression efficiency[h]: GH_2 produced at stations	Triangular[b]	91.5%	94.0%	96.5%
H_2 station efficiency: liquefaction of GH_2	Normal	60.0%	66.0%	72.0%

Table 2-3 (Cont.)

Pathway	Distribution Function Type	P20[a]	P50[a]	P80[a]
Biomass to Ethanol Pathways				
Corn farm energy use: Btu/bushel of corn	Weibull	20,895	23,288	27,735
Woody biomass farm energy use: Btu/dry ton	Normal	176,080	234,770	293,460
Herbaceous biomass farm energy use: Btu/dry ton	Normal	162,920	217,230	271,540
Corn farm nitrogen (N) fertilizer use: g/bushel	Weibull	370	470	545
Woody biomass farm N fertilizer use: g/dry ton	Normal	532	709	886
Herbaceous biomass farm N fertilizer use: g/dry ton	Normal	7,980	10,635	13,290
N in N_2O from N in fertilizer: corn farms	Triangular[b]	1.0%	2.0%	3.0%
N in N_2O from N in fertilizer: cellulosic biomass farms	Triangular[b]	1.0%	1.5%	2.0%
Soil CO_2 emissions from cornfields: g/bushel of corn	Triangular[b]	0	195	390
Soil CO_2 sequestration of tree farms: g/dry ton of biomass	Triangular[b]	-225,000	-112,500	0
Soil CO_2 sequestration of grass farms: g/dry ton of biomass	Triangular[b]	-97,000	-48,500	0
Corn ethanol plant ethanol yield – dry mill: gal/bushel	Triangular[b]	2.5	2.65	2.8
Corn ethanol plant ethanol yield – wet mill: gal/bushel	Triangular[b]	2.4	2.55	2.7
Corn ethanol plant energy use – dry mill: Btu/gal	Normal	32,101	36,120	40,139
Corn ethanol plant energy use – wet mill: Btu/gal	Normal	42,043	45,950	49,857
Woody cellulosic ethanol plant ethanol yield: gal/dry ton	Normal	76	87	98
Herbaceous cellulosic ethanol plant ethanol yield: gal/dry ton	Normal	80	92	103
Woody cellulosic ethanol plant electricity production[m]: kWh/gal	Triangular[b]	-1.73	-1.145	-0.560
Herbaceous cellulosic ethanol plant electricity production[m]: kWh/gal	Triangular[b]	-0.865	-0.572	-0.280

[a] Here, P20 values mean that there is a probability of 20% that actual values would be equal to or below the P20 values; P50 values mean that there is a probability of 50% that actual values would be equal to or below the P50 values; and P80 values mean that there is a probability of 80% that actual values would be equal to or below the P80 values.

[b] These values are for the minimum, the most likely, and the maximum values for the triangular distribution function.

[c] CH_4 emissions from crude oil processing in oil fields and associated gas venting during crude recovery. No distribution function was established for this parameter.

[d] CO_2 emissions from processes other than fuel combustion in petroleum refineries. The value here is for gasoline production. Emissions generated during production of other fuels (such as diesel and naphtha) are estimated by using the gasoline value and relative refining intensity between gasoline and each of the other fuels.

[e] For these distributions, the maximum value was set at 100%.

[f] The efficiency for electric compressors is calculated based on Btu of input electricity. Energy loss for electricity generation is taken into account by GREET during electricity generation.

[g] Efficiencies here are for plant designs without steam or electricity co-generation.

[h] Electric compressors are assumed for GH_2 compression. Efficiencies, defined previously (GM et al. 2001), are calculated based on Btu of input electricity. Energy loss of electricity generation is taken into account by GREET during electricity generation.

[l] We assume that NG-fired boiler electric power plants generate 10.5% of total U.S. electricity.

[j] We assume that NG-fired CC electric power plants generate 4.5% of total U.S. electricity.

[k] We assume that coal-fired boiler electric power plants generate 43% of total U.S. electricity.

[l] We assume that coal-fired advanced boiler electric power plants generate 10.8 % of total U.S. electricity.

[m] The amount of electricity co-generated in cellulosic ethanol plants for export. The negative values here mean export of electricity from ethanol plants.

point-based emissions factors from AP-42. That is, the potential uncertainties in CH_4 and N_2O emissions from fuel combustion were not taken into account in either the Phase 1 or Phase 2 simulations because of data limitation.

This section presents key parametric assumptions for WTT energy efficiencies and GHG emissions used in the Phase 2 study. In many cases, energy efficiency and GHG emission assumptions are the same for both the Phase 1 and Phase 2 studies.

2.1.3.2 Assumptions Related to Criteria Pollutant Emissions

2.1.3.2.1 GREET Simulation Approach for Criteria Pollutant Emissions

This section discusses the general approach and issues in estimating WTT criteria pollutant emissions using GREET. To estimate WTT energy use and emissions for a given fuel production pathway, GREET first estimates energy use (in Btu) and emissions (in g) per million Btu of fuel throughput for a given WTT activity, such as petroleum refining and hydrogen production. The model then combines the energy use and emissions from all WTT activities associated with a fuel production pathway to estimate total WTT energy use and emissions for a million Btu of the fuel available at the pump of a refueling station.

For a given WTT activity, energy input per unit of energy product output is calculated in GREET from the energy efficiency of the activity. By definition, energy efficiency is the energy output divided by the energy input (including energy in both process fuels and energy feedstock). Thus, total energy input for a unit of energy output for a WTT activity is calculated by the following:

$$Energy_{in} = 1/efficiency,$$

where

$Energy_{in}$ = Energy input of a given stage (say, in Btu per Btu of energy product output from the activity), and
Efficiency = Energy efficiency for the given activity (defined as [energy output]/[energy input] for the activity).

Energy efficiencies of WTT activities for various fuel production pathways were addressed in the Phase 1 WTW report (GM et al. 2001). The energy efficiency results of these prior efforts, presented in Table 2-3, were used in the Phase 2 study.

The above equation calculates total energy input required for a given activity. The total energy input could comprise the Btus in energy feedstock and process fuels. In most cases, energy feedstock includes both a feed for production of a fuel and a process fuel involved in combustion during a given activity. To calculate emissions, total feedstock input needs to be separated into feed and fuel, as described in Wang (1999a). Converting feed to a given fuel (which, in most cases, is a chemical process) may produce emissions. Combustion of a feedstock as a fuel, as well as combustion of other process fuels, certainly produces emissions. The combustion emissions are estimated in GREET by using the amount of fuels burned and the combustion emission factors for given fuels with given combustion technologies.

Combustion of different process fuels can have very different emission profiles. GREET includes process fuels such as NG, residual oil, diesel, gasoline, crude oil, liquefied petroleum gas (LPG), coal, electricity, and biomass. Different activities could involve very different shares of these process fuels. For example,

corn ethanol plants are powered primarily by NG and coal; petroleum refineries by NG, refinery gas, and electricity; NG SMR hydrogen plants by NG. GREET specifies shares of process fuels for individual WTT activities based primarily on statistical data and data available from open literature.

Emissions of VOCs, CO, NO_x, PM_{10}, SO_x, CH_4, N_2O, and CO_2 for a particular WTT activity are calculated in g/10^6 (million) Btu of fuel throughput from that activity. Emissions occurring during an individual activity include those resulting from the combustion of process fuels and from non-combustion processes such as chemical reactions and fuel leakage and evaporation. The latter emission sources are fuel-specific and activity-specific; they are discussed later in this section. Emissions from combustion of process fuels for a particular activity are calculated by using the following formula:

$$EM_{cm,i} = \left(\sum_j \sum_k EF_{i,j,k} \times [FC_{j,k} \div 1{,}000{,}000] \right)$$

where

$EM_{cm,i}$ = Combustion emissions of pollutant i in g/10^6 Btu of *fuel throughput*,
$EF_{i,j,k}$ = Emission factor of pollutant i for process fuel j with combustion technology k (g/10^6 Btu of *fuel burned*), and
$FC_{j,k}$ = Consumption of process fuel j with combustion technology k (Btu/10^6 Btu of fuel throughput).

$FC_{j,k}$ for a given activity is, in turn, calculated by using the following formula:

$$FC_{j,k} = FC \times Share_{fuelj} \times Share_{techk,j} \ ,$$

where

FC = Total process fuel consumption for the given activity (in Btu/10^6 Btu of fuel throughput, calculated with energy efficiencies and separation between feeds and fuels for feedstocks, see above discussion),
$Share_{fuelj}$ = Share of process fuel j out of all process fuels consumed during the activity ($\sum_j fuel_j = 1$), and
$Share_{techk,j}$ = Share of combustion technology k out of all combustion technologies for fuel j ($\sum_k tech_{k,j} = 1$).

Emission factors ($EF_{i,j,k}$) are a key component in determining WTT criteria pollutant emissions. Stationary emission regulations by EPA and by state and local air regulatory agencies dictate emission factors for given combustion technologies and given emission sources. Emission factors for VOCs, CO, NO_x, PM_{10}, CH_4, and N_2O for different combustion technologies fueled by different process fuels in previous GREET versions were derived primarily from EPA's AP-42 document (EPA 1995). Through the Phase 2 study, a significant amount of effort was spent to update emission factors in GREET (these efforts are discussed in later sections).

In the GREET model, SO_x emission factors for combustion technologies fueled with all fuels except coal, crude oil, and residual oil are calculated by assuming that all sulfur contained in these process fuels is converted into sulfur dioxide (SO_2). The following formula is used to calculate the SO_x emissions for the combustion technologies:

$$SO_{x,j} = Density_j \div LHV_j \times 1{,}000{,}000 \times S\_ratio_j \times 64 \div 32,$$

where

$SO_{x,j}$	=	SO_x (in SO_2) emission factor for combustion of process fuel j (in g/10^6 Btu of fuel j burned),
$Density_j$	=	Density of process fuel j (in g/gal for liquid fuels, g/SCF [standard cubic foot] for gaseous fuels such as NG [density for solid fuels such as coal and biomass is not needed]),
LHV_j	=	Low heating value of process fuel j (in Btu/gal for liquid fuels, Btu/SCF for gaseous fuels, or Btu/ton for solid fuels),
S_ratio_j	=	Sulfur ratio by weight for process fuel j,
64	=	Molecular weight of SO_2, and
32	=	Molecular weight of elemental sulfur.

As this formula implies, SO_x emission factors for fuel combustion are determined by the sulfur content of the burned fuels and not by combustion technologies. However, uncontrolled SO_x emission factors associated with combustion of residual oil, crude oil, and coal are very high — they all exceed emission standards. Desulfurization measures have to be employed for combustion technologies powered by these fuels to reduce SO_x emissions to acceptable levels. For these cases, SO_x emission factors for various combustion technologies are derived by using a method similar to that used to identify the emission factors of other criteria pollutants.

There are some exceptions to using the formula provided above to calculate SO_x emissions. Some chemical conversions of feedstocks to fuels require catalysts; these conversions include production of methanol, hydrogen, and FT diesel from NG in plants and production of hydrogen from gasoline, methanol, and ethanol onboard FCVs by means of fuel processors. In these cases, sulfur contained in a feedstock can poison catalysts and must be removed from the feedstock before it enters the fuel production units. Desulfurization of feedstocks usually produces solid wastes that contain immobilized sulfur. In these cases, the sulfur contained in the feedstocks becomes solid waste; it is not released as air emissions. No SO_x air emissions are assigned for these cases.

In GREET, combustion CO_2 emission factors (in g/mmBtu of fuel throughput) are calculated by using a carbon balance approach, in which the carbon contained in a process fuel burned minus the carbon contained in combustion emissions of VOCs, CO, and CH_4 is assumed to convert to CO_2. The following formula is used to calculate CO_2 emissions:

$$CO_{2,j,k} = [Density_j \div LHV_j \times 1{,}000{,}000 \times C\_ratio_j - (VOC_{j,k} \times 0.85 + CO_{j,k} \times 0.43 + CH_{4,j,k} \times 0.75)] \times 44 \div 12,$$

where

$CO_{2,j,k}$	=	Combustion CO_2 emission factor for combustion technology k burning process fuel j (in g/mmBtu of fuel j burned),
$Density_j$	=	Density of process fuel j (in g/gal for liquid fuels, g/SCF for gaseous fuels [density for solid fuels is not needed]),
LHV_j	=	Low heating value of process fuel j (in Btu/gal for liquid fuels, Btu/SCF for gaseous, or Btu/ton for solid fuels),
C_ratio_j	=	Carbon ratio by weight for process fuel j,

$VOC_{j,k}$ = VOC emission factor for combustion technology k burning process fuel j (in g/mmBtu of fuel j burned),
0.85 = Estimated average carbon ratio by weight for VOC combustion emissions,
$CO_{j,k}$ = CO emission factor for combustion technology k burning process fuel j (in g/mmBtu of fuel j burned),
0.43 = Carbon ratio by weight for CO,
$CH_{4,j,k}$ = CH_4 emission factor for combustion technology k burning process fuel j (in g/mmBtu of fuel j burned),
0.75 = Carbon ratio by weight for CH_4,
44 = Molecular weight of CO_2, and
12 = Molecular weight of elemental carbon.

The above formula shows that combustion CO_2 emissions do not include carbon contained in VOCs, CO, and CH_4 emissions. On the other hand, VOCs and CO reside in the atmosphere for fewer than 10 days before they are oxidized into CO_2. In GREET, the indirect CO_2 emissions from VOC and CO oxidation in the atmosphere are considered in total CO_2 emission calculations.

Besides emissions from combustion of process fuels, emissions are also caused by non-combustion chemical and physical processes. GREET takes these non-combustion, or process-related, emission sources into account. Such emission sources include VOC evaporative emissions and emissions from fuel spillage during transportation and storage of volatile liquid fuels, fuel leakage of gaseous fuels, emissions from flaring and venting of associated gas in oil fields, refining-process-related emissions in petroleum refineries, and emissions from SMR in hydrogen and other chemical plants. These emission sources are considered for individual non-combustion processes as needed; they are discussed in later sections.

Energy use and consequent CO_2 emissions from WTT activities are not regulated in the United States. The performance of individual facilities with respect to these two factors may be determined primarily by economic tradeoffs between the costs of technologies and the benefits of their fuel savings. Emissions of criteria pollutants in major facilities — such as petroleum refineries and electric power plants — and by major combustion technologies, on the other hand, are strictly regulated. This is especially true for those facilities located in air quality standard non-attainment areas.

A major challenge we faced in completing the Phase 2 study was addressing the complexity of criteria pollutant emissions associated with WTT activities with respect to geographic locations and over time. This study was intended to analyze cases representing the United States as a whole. During our study, we investigated emissions from facilities located in attainment areas, California non-attainment areas, and non-attainment areas in the rest of the United States to cover geographic variations and uncertainties. Although some of the fuel pathways included in this study involve production facilities outside of North America (such as NNA NG-based LH_2 and NNA NG-based FT diesel), we assumed that these facilities would have emission profiles similar to those of the facilities located in North America. Although this assumption is crude, its effects on urban emissions of criteria pollutants are minimal (see discussion of urban emissions on the following page).

In order to better understand the trends and uncertainties associated with criteria pollutant emissions over time, we decided to investigate historical trends in criteria pollutant emissions between 1990 and 2000 to provide hints for future trends — from 2000 to 2016 (the latter is the target year for this analysis).

In this study, both spatial and temporal variations and uncertainties in criteria pollutant emissions were addressed through investigating, in great detail, the National Emissions Inventory (NEI) database maintained by EPA.

While the effects of GHG emissions are global, those of criteria pollutants are primarily focused on local populations. Thus, human exposure to criteria air pollution needs to be taken into account. This is especially important for WTW analyses of criteria pollutant emissions because such analyses usually add emissions in different locations together. To address this issue, GREET is designed to separate emissions of criteria pollutants into total emissions and urban emissions (the latter is a subset of the former). Total emissions are the sum of emissions occurring everywhere during a WTW chain. Urban emissions are those only occurring within U.S. urban areas. Urban areas here are defined by the U.S. Bureau of the Census as cities having populations greater than 125,000. Our estimates of urban emissions for individual facilities are based on their locations. For existing facilities — such as petroleum refineries and electric power plants — the share of urban and non-urban facilities (by capacity) is based on the locations of existing facilities, which we collected from the Energy Information Administration (EIA) and industry databases. For new facilities — such as plants constructed to produce hydrogen as a transportation fuel — the share is determined based on the specification of a given hydrogen production pathway (e.g., central plants vs. refueling stations), the split of urban vehicles and non-urban vehicles, and their vehicle miles traveled (VMT).

The separation of criteria pollutant emissions into total and urban emissions is an important first step to address potential human exposure, as well as the total amount of emissions from a particular fuel pathway. However, this approach is not a precise way to address the human health effects associated with these pollutants. To do so precisely, researchers need to estimate emissions by geographic location, conduct simulations of air quality and human exposure, and assess the human health effects of such exposure. These tasks are far beyond the scope of the WTW analysis conducted for this study.

2.1.3.2.2 Development of Criteria Pollutant Emission Factors

I. The National Emissions Inventory

Previous versions of the GREET model employed criteria pollutant emission factors primarily from EPA's AP-42 documents (EPA 1995). In addition to AP-42, however, EPA maintains the NEI database (EPA 1999), which consists of emissions inventory information for point sources collected from state and local air agencies. Data in this inventory are commonly used for air quality monitoring and human exposure modeling. Commercial enterprises are required to report emissions inventory information to these state and local agencies, and this information is then reported to EPA and input into the NEI. In many cases, the commercial enterprises may use emission factors from AP-42 to estimate emissions from their facilities. However, if they believe their emissions are different from those provided in AP-42, they report the actual emissions, particularly if they are subject to continuous emissions monitoring (CEM) requirements. Because the NEI appears to be the most complete listing of point source emissions, it was used to update the emission factors in GREET for all sources except utilities. As discussed in the section below, utility emission factors were based primarily on recent EPA analyses and projections in the EPA Interstate Air Quality Rule (EPA 2004a).

Air Improvement Resource, Inc. (AIR) contracted with Eastern Research Group (ERG) to analyze emissions inventory information in the NEI in order to derive emission factors for combustion processes and major facilities. Following ERG's analysis of the emission factors, AIR used these data to create distributions of point source emissions for GREET. ERG's analysis of the NEI database and other

databases necessary to estimate emission factors is discussed in the following sections. AIR's analyses of these data are also discussed in a later section.

The retrospective emissions data obtained in this analysis were not used directly in our study. Instead they were one of several inputs used to project emissions factor distributions for 2016.

The draft 1999 NEI database for criteria pollutants from point sources was used for this analysis. These NEI data files represent emissions and activity data from 1999. Some data elements, including process-level emissions and facility locations, are required when submitting data to the NEI. However, other data elements, like standard industrial classification (SIC), activity data (e.g., fuel throughput), and emission factors (in mass per fuel throughput), are not required. In order to estimate emission factors using data contained in the NEI, both process-level emissions and activity data were needed for each source. In some cases, the lack of activity data limited the amount of emissions data that could be used to estimate emission factors. In other cases, if possible, we used activity data for facilities of interest from other sources (journals and web sites) to supplement the NEI data.

II. Extraction and Refinement of Emissions Data in the NEI

Several steps were performed to extract emissions data from EPA's NEI. Figure 2-4 provides a generalized flowchart of these steps. As a first step, industries relating to transportation fuels were

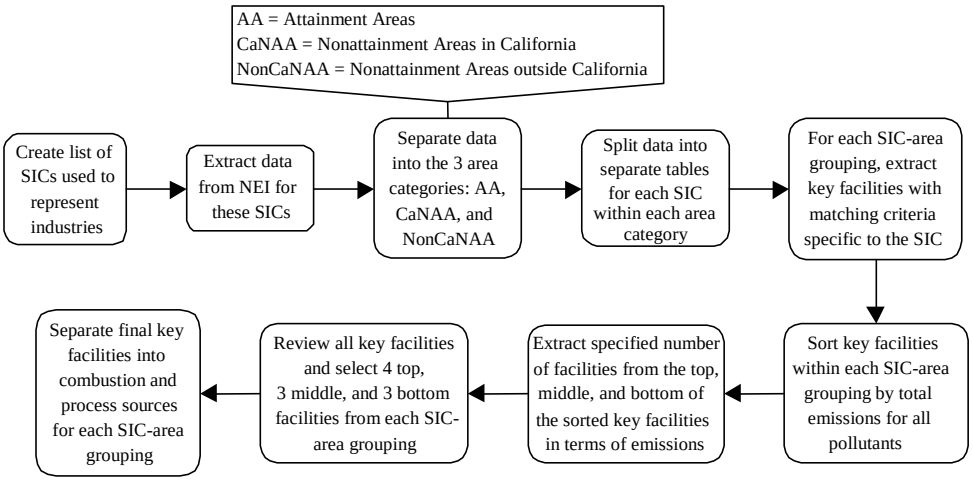

Figure 2-4 Steps Performed in the Extraction and Refinement of Emissions Data

assigned an SIC that represented the primary activities of the industry. We compiled a list of these assigned SICs. Facilities containing a primary SIC that matched one of the SICs in the list were extracted from the NEI database. Data from roughly 13,000 facilities were originally extracted from the NEI database, representing 40 SICs.

Data from the collection of SICs were then divided by area category. The three area categories are: attainment areas (AA), nonattainment areas in California (CaNAA), and nonattainment areas outside California (NonCaNAA). Once split by area category, the data were placed into separate tables according to SIC and area category. Criteria specific to each industry were constructed to refine the data extracted. Source classification codes (SCCs), which identify different types of emission sources, were used as the primary criteria for extracting key facilities from each SIC-area grouping. Each emission source reported

for each facility in the NEI database was assigned an SCC. Another criterion used to improve the quality of the data set was the requirement that all facilities extracted have throughput or capacity data reported for at least one source.

Within each group of the key facilities, selection of a smaller sample of facilities from each SIC-area grouping was "randomized" to ensure a representative, unbiased collection of emissions data by facility size. This "random" facility selection was done by sorting the facilities within each group by total emissions (in total mass, not emission factors in mass per throughput) for all pollutants. (Facilities with higher total emissions are generally larger facilities, not necessarily facilities that employ fewer emissions controls.) A specified number of facilities (between 3 and 12, depending on the industry) was extracted from the top, middle, and bottom of each sorted list. Every emission source from each of these groupings was then reviewed to choose the most representative facilities: four top-emitting, three middle-emitting, and three bottom-emitting facilities. The following questions were used as further checkpoints when reviewing and selecting given facilities:

- Does the facility represent a complete group of process and combustion sources for the industry?
- Does at least one process source within the facility contain throughput or capacity data that represents the entire facility?
- Do different types of combustion sources contain throughput or capacity data?
- Unless the industry is found only in particular regions of the United States, are multiple states represented?
- If there are both controlled and uncontrolled sources within an SIC-area grouping, or different types of controls within an SIC-area grouping, is there a representative mixture of controlled and uncontrolled sources?

Once the representative key facilities were selected, emission sources were divided according to combustion sources and process source for each SIC-area grouping. Table 2-4 provides the original SIC-area groupings for industries for which we calculated emission factors. Several SIC-area groupings were dropped at various stages of the extraction and refinement analysis for different reasons, including missing or invalid throughput data (unavailable elsewhere) and unrepresentative facilities for a particular industry.

III. Activity Data Used to Estimate Emission Factors

For combustion sources, excluding those for electric utilities (which were processed differently, as described later), activity data provided in the NEI were used in all cases. Emission factors were developed in terms of mass per million Btu (mmBtu) of fuel input. Fuel specific heating values from AP-42 were used to convert fuel input units reported in NEI to units of mmBtu. Table 2-5 lists input units and heating values used for the different fuel types. As the table shows, heating values of the fuels are higher heating values (HHVs). Thus, emission factors generated from NEI are HHV-based. On the other hand, GREET simulations are conducted with the low heating values (LHVs) of fuels. The NEI-based emission factors were eventually converted into LHV-based emission factors for GREET simulations.

For process sources, activity data were used when these data were available and representative of the overall process for each facility in an industry. Table A-1 in Appendix A provides a summary of sources used for process source activity data.

Table 2-4 Industries and Area Categories Originally Extracted for Calculation of Emission Factors

SIC	Industry Description	AA	CaNAA	NonCaNAA
1221	Bituminous coal and lignite surface mining and processing	X		
1222	Bituminous coal underground mining and processing	X		
1311	Oil and NG production/processing	X		
1321	NG liquids production	X	X	X
1381	Oil and NG wells	X		
2869	Ethanol production	X		
	Methanol production (from NG)	X	X	X
2873	Nitrogen fertilizer production	X	X	X
2874	Phosphate fertilizer production	X	X	X
2911	Petroleum refineries	X	X	X
4612	Crude petroleum pipelines	X		
4613	Refined petroleum product pipelines	X	X	X
4911	Electric utilities: bituminous/sub-bituminous coal-fired, lignite-fired, NG-fired boilers, NG turbines, oil-fired boilers	X	X	X
4922	NG transmission and storage	X		
5171	Petroleum bulk terminals: crude, gasoline, diesel	X	X	X
5541	Service stations: gasoline, diesel	X	X	X

Table 2-5 Fuel-Specific Data for Combustion Sources

Fuel Type	NEI Throughput Unit	Higher Heating Value
Residual oil and waste oil	10^3 gal/yr	150,000 Btu/gal
Distillate oil	10^3 gal/yr	140,000 Btu/gal
Gasoline	10^3 gal/yr	130,000 Btu/gal
Propane	10^3 gal/yr	94,000 Btu/gal
NG and process/refinery gas	10^6 ft^3/yr	1,050 Btu/SCF
Coke	ton/yr	13,300 Btu/lb
Bituminous/subbituminous coal	ton/yr	13,000 Btu/lb
Solid waste	ton/yr	4,500 Btu/lb

For electric utilities, fuel throughputs from all combustion units within each facility were summed, and heat rates from EPA's E-GRID2000 (EPA 2004b) were used to convert the total annual throughputs to total electricity generated annually from each facility.

IV. Calculation of Emission Factors from the NEI

In general, annual emissions data were divided by industry-specific activity data to produce emission rates in mass/mmBtu. In all of the calculations, emissions reported as zero tons/yr from the NEI were treated as missing data instead of zero values. This procedure was performed to reduce "false" zeros that were meant to represent missing data, not zero emissions. Removing zeros from approximately 3% of the total data analyzed resulted in more accurate average emission factors. Both arithmetic averages and volume-weighted averages were estimated for each set of emission factors.

We used several criteria to reduce the amount of erroneous data originating from the NEI or to eliminate unrepresentative outliers. First, we removed any individual combustion equipment for which emission factors for all pollutants appeared to be different from the mean of the same facility type by at least two orders of magnitude. Twenty-three pieces of combustion equipment were eliminated as potential "outliers" based on this criterion. Secondly, we eliminated some data that were obviously based on input of the wrong emission factors. One example was diesel fuel refueling stations for which gasoline emission factors were used. Finally, we eliminated some of the data that were more than an order of magnitude higher than the mean of the same facility type and in cases in which the facility was an unusually small one, such as a 100-MW electric utility plant, as shown in NEI.

For electric utilities, E-GRID2000 (EPA 2004b) was used to determine the primary fuel type to assign to each facility. The E-GRID2000 fuel mix for each power plant needed to have at least 93% of its fuel input from a particular fuel type to be included in the grouping. To then estimate emission factors, we separated combustion and process sources at electric utilities using SCC criteria and summed the emissions data independently. These total emissions for each facility were then divided by the total electricity generated, resulting in combustion emission factors and process emission factors for each power plant in g/kWh of electricity generated.

If E-GRID2000 indicated that a particular power plant was a cogeneration facility, we performed additional calculations on the emissions and activity data to adjust for only a portion of the fuel inputs being used to generate electricity. An electric allocation factor provided in E-GRID2000 for each of the cogeneration facilities was used to modify the data. This allocation factor was multiplied by the emissions data and the total energy (in kWh) generated for each cogeneration facility.

V. Results of Emission Factors

Analyses of the data by ERG (Burklin and Alexander 2002) showed that, for most cases, there were not significant differences in emission factors for sources among the different geographic regions. For this reason, the data from the three region types were combined to estimate nationwide average emission factors.

Mean and median emission factors for the various point sources, and various other statistics, are provided in Tables A-2 through A-4 in Appendix A. Table A-2 shows emission factors for non-utility combustion sources. Table A-3 shows emission factors for process sources. Table A-4 shows emission factors for electric utility sources. The following sections describe how we used the data in Tables A-2 through A-4

to project emissions distributions for 2016 for sources other than electric utilities. Electric utility emissions distributions are discussed in a later section.

VI. Creation of Emission Distributions for Base Year 1999

GREET utilizes probability-based distributions of emissions with Monte Carlo simulations to estimate emissions results with probability distributions. Therefore, it was necessary to fit emission data points from individual facilities with distribution functions. To accomplish this, the data from each source type were read into Crystal Ball™, a statistical software which, based on the number of data points and scatter of the data, attempts to fit a distribution about the data for that source type. In Crystal Ball™, a mathematical fit is performed to determine the set of parameters for each set of standard distribution functions that best describes the characteristics of the data. The quality or closeness of each fit is judged using a Chi-squared test. All distributions were also visually examined for reasonableness.

VII. Construction of Year 2016 Projected Distribution Functions

A. Distribution Functions for Non-Utility Combustion Sources

The previous section described distributions of emission factors based on the analysis of the 1999 NEI. These distributions provided a starting point for our estimate of the distribution of emission factors for the year 2016, the target year for our study. In this section, we describe the adjustment of these distributions to account for expected changes in emission factors attributable to (1) additional emissions controls that will be placed on newly constructed facilities, and (2) modifications to existing facilities. This section also describes the method used to establish estimates of emissions factor distributions for processes that were not included in the NEI.

For emissions sources that were included in the NEI, we evaluated — for each pollutant — the expected changes in emission distributions to account for additional controls expected to be in place by 2016. As part of this process, we examined some of the initiatives underway or being considered, including New Source Review Consent Decrees, New Source Performance Standards (NSPS), and the federal government's Clean Skies Initiative. None of these provided us with specific numbers we could use for estimating future emission factors. So we assembled a group of experts to make judgments concerning the impact of future regulations on the emission factor distributions in 2016. As part of this process, the group examined differences in emission factors between air quality attainment and nonattainment areas, past changes in emission factors (from EPA historical data), and lowest emission factors (from the NEI data). With all of these factors considered, we adjusted the distributions developed from the 1999 NEI to project distributions for 2016.

In making our adjustments, we did not apply one single methodology to all sources and pollutants. Instead, we examined each case individually and made appropriate judgments for each source by using several different methods. One frequent assumption we used was that controls would be instituted on the highest-emitting sources. Thus, we matched the maximum of our distribution to the second- or third-highest emission factors in the NEI data. In addition, for pollutants and sources for which additional controls were expected, we made sure the mean of the 2016 distribution was significantly below that of the current distribution. In some cases, the range of AP-42 factors was factored into the distribution decision.

Following are some examples to illustrate how we established the 2016 distributions for NO_x, PM_{10}, and VOC emissions. The examples were selected primarily on the basis of their importance in the overall WTT emissions results for the pathways in our WTW study. They also illustrate most of the

methodologies we used in developing the distributions. Appendix B provides a brief description of the methodologies used for each source and each pollutant. Tables 2-6 and 2-7 summarize distribution parameters for fuel combustion and noncombustion processes.

The first example, for NO_X emissions, illustrates one of the common methods we used to adjust the distribution to represent the impacts of new controls by 2016. Figure 2-5 shows a cumulative distribution plot of NO_X emissions for NG boiler combustion sources. The triangles show the NEI data with the percentile value of each, computed using Microsoft Excel's PERCENTRANK function. The line shows the distribution adjusted to represent 2016. Assuming that new controls will be implemented for the highest-emitting sources, we set the maximum to match that of the 98th percentile data point. The minimum was set to match the minimum value in *Power Magazine* (Schwieger et al. 2002), which summarized the emission factors for major U.S. electric power plants. The distribution did a good job of matching the remainder of the data and was consistent with the AP-42 range.

For industrial coal combustion sources, much fewer data were available in the NEI. In addition, as illustrated in Figure 2-6, five of the six data points had the same emission factor. These points, at 274 g/mmBtu, probably represent the use of standard factors rather than measured emissions data. We created a distribution with a minimum and a maximum value matching those from *Power Magazine* (Schwieger et al. 2002). In this distribution, the 10th percentile matches the minimum NEI data point, and the 90th percentile matches the upper AP-42 value.

Figure 2-7 shows the distribution we used for NO_X emissions from residual oil boiler combustion sources. In this case, we set the maximum to just below the highest NEI data point. There was a large group of data near the lower AP-42 value that probably represent emission factors rather than measured data. The selected distribution assumes reductions in the lower portion of the distribution.

In developing the distribution curve for PM_{10} emissions from combustion oil boilers, we compared the NEI data for residual oil boilers to that for diesel boilers. As shown in Table A-2 in Appendix A, the mean, minimum, and maximum for the residual oil boiler data were lower than those for diesel boilers. In our judgment, PM_{10} emissions for residual oil would be generally higher than those for diesel boilers. Therefore, to maintain the PM_{10} distribution higher than that of diesel boilers, we simply fit the distribution to the existing NEI data, as shown in Figure 2-8. The distribution was also consistent with the AP-42 range.

For NO_X emissions from NG-fueled gas turbines, we expected the highest emitters to be subject to stricter controls by 2016. As shown in Figure 2-9, we developed a distribution in which the maximum was about half of the NEI maximum. We set the minimum of the distribution to be below the controlled AP-42 factor, to match the lowest data values from the NEI. Compared to the NEI data, the major change was to eliminate the highest part of the distribution.

B. Example Distributions for Process Sources

In the case of NO_X emissions for petroleum refining, we also assumed that future reductions in NO_X emissions would occur in the refineries with the higher emission factors. Figure 2-10 compares our selected distribution with the NEI data. Note that the distribution we selected closely matches the NEI up to about the 40th percentile, but projects that significant controls will be applied to reduce the emissions in the upper half of the distribution. We cannot effectively compare this distribution to AP-42 because there are many different AP-42 factors for the different refinery processes.

Table 2-6 Parameters for Distribution Functions of Criteria Pollutant Emission Factors for Fuel Combustion (g/mmBtu of fuel burned)

Item	Type of Function	P10[a]	P50[a, b]	P90[a]
NG-fired utility/industrial boilers				
VOCs	Extreme value	0.431	1.557	2.825
CO	Extreme value	4.392	16.419	29.904
NO_x	Beta	18.519	52.890	102.063
PM_{10}	Gamma	1.004	2.776	5.973
NG-fired small industrial boilers				
VOCs	Lognormal	0.632	2.417	4.889
CO	Exponential	2.512	16.529	54.908
NO_x	Beta	8.889	33.284	74.706
PM_{10}	Logistic	0.697	2.960	5.091
NG-fired large gas turbines, combined-cycle gas turbines, and small gas turbines				
VOCs	Beta	1.111	3.173	6.124
CO	Beta	8.554	23.144	40.772
NO_x	Beta	36.043	106.924	197.651
PM_{10}	Beta	0.365	1.078	2.210
NG-fired reciprocating engines				
VOCs	Exponential	3.512	23.105	76.753
CO	Exponential	26.340	173.287	575.646
NO_x	Beta	178.320	491.442	892.459
PM_{10}	Extreme value	3.691	5.530	7.710
Oil-fired utility boilers, industrial boilers, and commercial boilers				
VOCs	Weibull	0.299	1.079	4.872
CO	Extreme value	13.063	15.764	18.966
NO_x	Normal	64.745	150.481	235.255
PM_{10}	Extreme value	24.747	44.436	67.779
SO_x	Beta	71.280	192.864	339.770
Diesel-fired industrial boilers and commercial boilers				
VOC	Extreme value	0.579	1.173	1.878
CO	Normal	12.684	16.686	20.688
NO_x	Beta	32.576	70.561	110.275
PM_{10}	Exponential	4.214	27.726	92.103
Diesel-fired reciprocating engines				
VOCs	Beta	21.609	76.737	155.460
CO	Beta	34.249	93.229	165.873
NO_x	Beta	178.320	491.442	892.459
PM_{10}	Beta	15.376	42.992	79.993
Gasoline-fired reciprocating engines				
VOCs	Beta	32.414	115.106	233.190
CO	Beta	51.374	139.844	248.810
NO_x	Beta	124.824	344.009	624.721
PM_{10}	Beta	6.150	17.197	31.997
LPG-fired industrial boilers[c]				
NO_x	Extreme value	43.211	71.619	105.299

Table 2-6 (Cont.)

Item	Type of Function	P10[a]	P50[a, b]	P90[a]
LPG-fired commercial boilers[c]				
NO_x	Extreme value	56.211	84.619	118.299
Coal-fired industrial boilers				
VOCs	Beta	0.241	1.540	4.730
CO	Beta	26.763	72.415	127.573
NO_x	Extreme value	106.515	155.249	191.953
PM_{10}	None	None	12.617	None
SO_x	Extreme value	87.707	98.355	110.981

[a] Here, P10 values mean that there is a probability of 10% that actual values would be equal to or below the P10 values; P50 values mean that there is a probability of 50% that actual values would be equal to or below the P50 values; and P90 values mean that there is a probability of 90% that actual values would be equal to or below the P90 values.

[b] For extreme value, lognormal, logistic, and normal distribution functions, the mean values, instead of the P50 values, are presented here.

[c] Distribution functions were established only for NO_x emissions of LPG-fired industrial and commercial boilers. Emissions for other pollutants were point estimates.

Table 2-7 Parameters for Distribution Functions of Criteria Pollutant Emission Factors for Non-Combustion Processes (g/mmBtu of fuel throughput)

Item	Type of Function	P10[a]	P50[a,b]	P90[a]
Petroleum-refinery process emissions for gasoline[c]				
VOC	Beta	0.542	2.022	4.500
CO	Beta	0.271	1.011	2.250
NO_x	Beta	0.285	1.120	2.781
PM_{10}	Beta	0.114	0.309	0.544
SO_x	Beta	0.989	3.769	8.771
Petroleum-refinery process emissions for LPG and residual oil[c]				
VOC	Beta	0.493	1.840	4.095
CO	Beta	0.247	0.920	2.048
NO_x	Beta	0.259	1.019	2.531
PM_{10}	Beta	0.104	0.281	0.495
SO_x	Beta	0.900	3.430	7.982
Petroleum-refinery process emissions for diesel fuel[c]				
VOC	Beta	0.526	1.961	4.365
CO	Beta	0.263	0.981	2.183
NO_x	Beta	0.276	1.086	2.698
PM_{10}	Beta	0.111	0.300	0.528
SO_x	Beta	0.959	3.626	8.508

Table 2-7 (Cont.)

Item	Type of Function	P10[a]	P50[a,b]	P90[a]
Petroleum-refinery process emissions for crude naphtha[c]				
VOC	Beta	0.509	1.901	4.230
CO	Beta	0.255	0.950	2.115
NO_x	Beta	0.268	1.053	2.614
PM_{10}	Beta	0.107	0.290	0.511
SO_x	Beta	0.930	3.543	8.245
VOC from gasoline bulk terminals	Beta	2.245	6.276	11.678
VOC from gasoline refueling stations	Gamma	2.000	10.000	40.000
VOC from LPG refueling stations	Gamma	0.200	1.000	4.000
VOC from diesel bulk terminals	Extreme value	0.031	0.207	0.316
VOC from diesel refueling stations	Beta	0.314	0.849	1.495
VOC from naphtha bulk terminals	Beta	2.245	6.276	11.678
VOC from naphtha refueling stations	Gamma	2.000	10.000	40.000
Process-related emissions of NG processing plants				
VOC	Beta	1.568	4.243	7.475
CO	Beta	0.428	1.157	2.039
NO_x	Beta	0.363	1.355	3.015
PM_{10}	Beta	0.006	0.019	0.0.36
SO_x	Beta	2.287	8.638	19.722
H_2 plant process emissions[d]				
VOC	Beta	0.861	1.903	2.729
CO	Beta	3.883	9.433	14.107
NO_x	Gamma	9.181	14.000	22.274
PM_{10}	Beta	8.011	11.836	14.716
MeOH plant process emissions[d]				
VOC	Beta	0.904	1.998	2.865
CO	Beta	4.077	9.905	14.812
NO_x	Gamma	9.640	14.700	23.387
PM_{10}	Beta	8.412	12.428	15.452
VOCs from MeOH refueling stations	Gamma	2.000	10.000	40.000
FT diesel plant process emissions[d]				
VOC	Beta	0.973	2.150	3.084
CO	Beta	4.388	1.066	15.941
NO_x	Gamma	10.375	15.820	25.170
PM_{10}	Beta	9.052	13.375	16.629
Corn EtOH plant process emissions				
VOC	Beta	18.579	26.724	33.671
PM_{10}	Beta	4.408	11.250	18.092
Cellulosic EtOH process emissions				
VOC	Beta	9.290	13.369	16.842
PM_{10}	Beta	4.408	11.250	18.092

Table 2-7 (Cont.)

Item	Type of Function	P10[a]	P50[a,b]	P90[a]
VOCs from EtOH bulk terminals	Beta	2.245	6.276	11.678
VOCs from EtOH refueling stations	Gamma	2.000	10.000	40.000
PM_{10} emissions of coal mining				
Underground mining	Beta	11.120	30.087	53.004
Surface mining	Beta	84.110	227.579	400.928

[a] Here, P10 values mean that there is a probability of 10% that actual values would be equal to or below the P10 values; P50 values mean that there is a probability of 50% that actual values would be equal to or below the P50 values; and P90 values mean that there is a probability of 90% that actual values would be equal to or below the P90 values.

[b] For extreme value, lognormal, and normal distribution functions, the mean values, instead of the P50 values, are presented here.

[c] Distribution functions of criteria pollutant emissions were established for gasoline production in refineries. Distribution functions for residual oil, LPG, diesel, and crude naphtha are derived from those for gasoline, with adjustment of relative refining energy efficiency between that of gasoline and that of each of the other fuels.

[d] Distribution functions of criteria pollutant emissions were established for hydrogen production in SMR plants. Distribution functions for methanol and FT diesel plants are derived from those for hydrogen plants, with adjustment of relative energy efficiency between that of hydrogen and those of methanol and FT diesel.

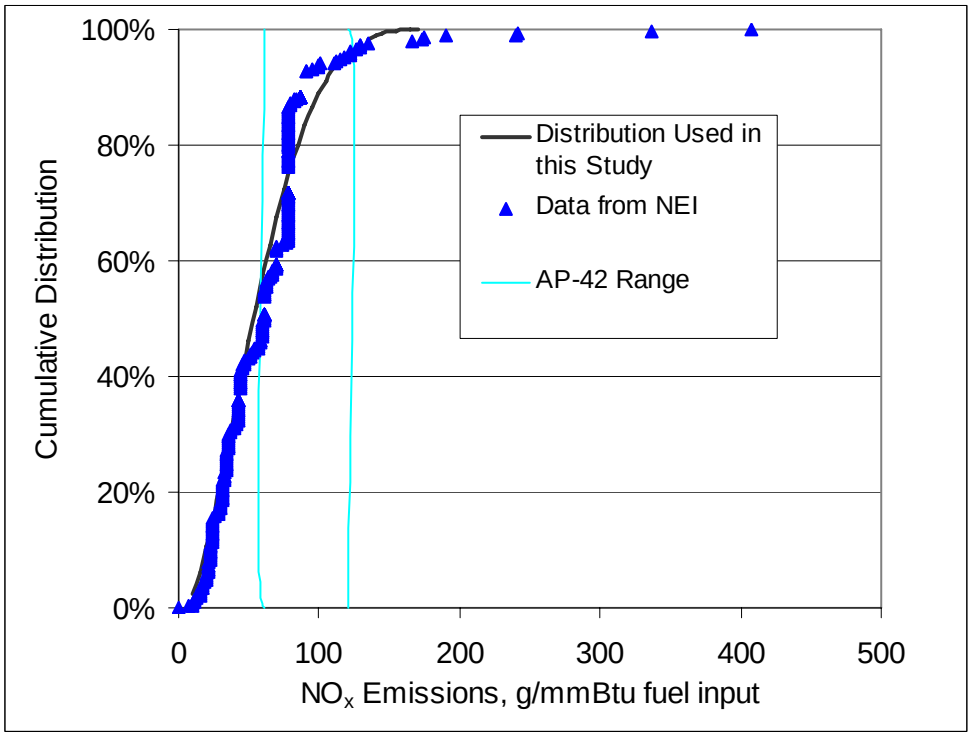

Figure 2-5 NO_x Emissions Distribution for NG Boiler Combustion Sources

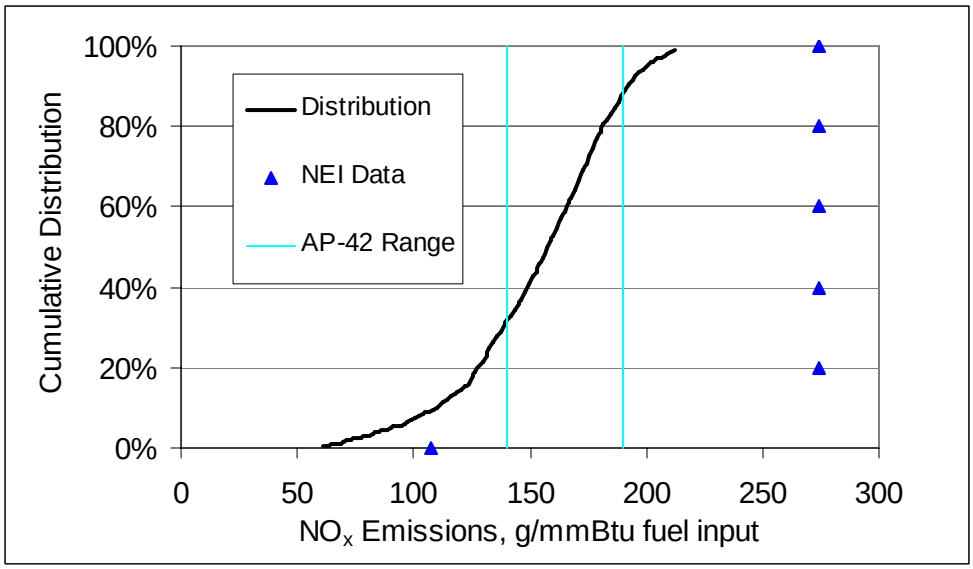

Figure 2-6 NO_x Emissions Distribution for Industrial Coal Boiler Combustion Sources

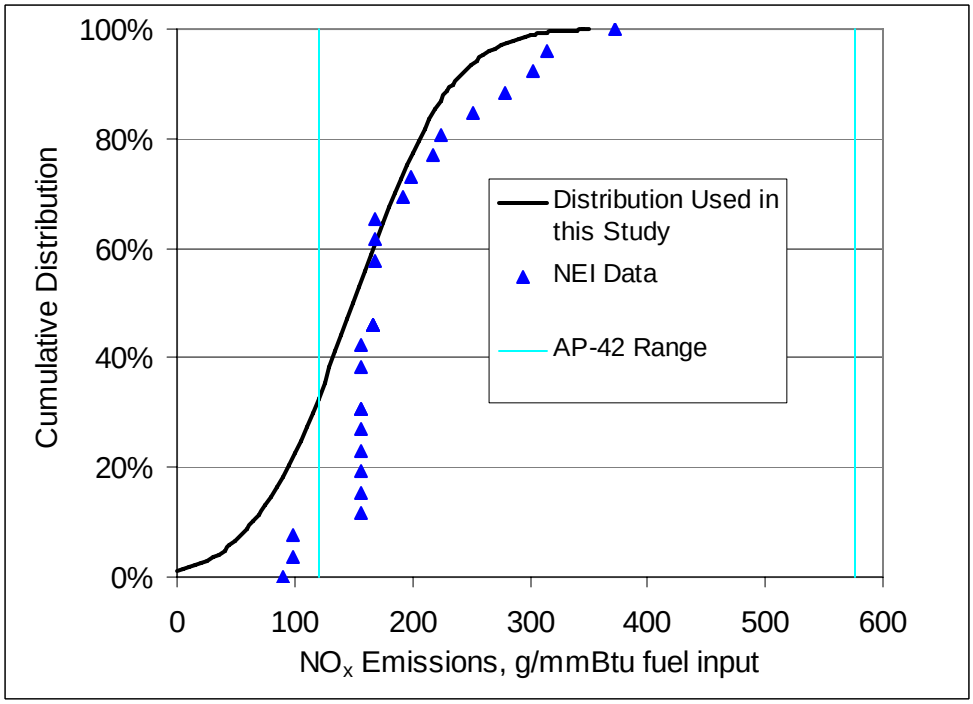

Figure 2-7 NO_x Emissions Distribution for Oil Boiler Combustion Sources

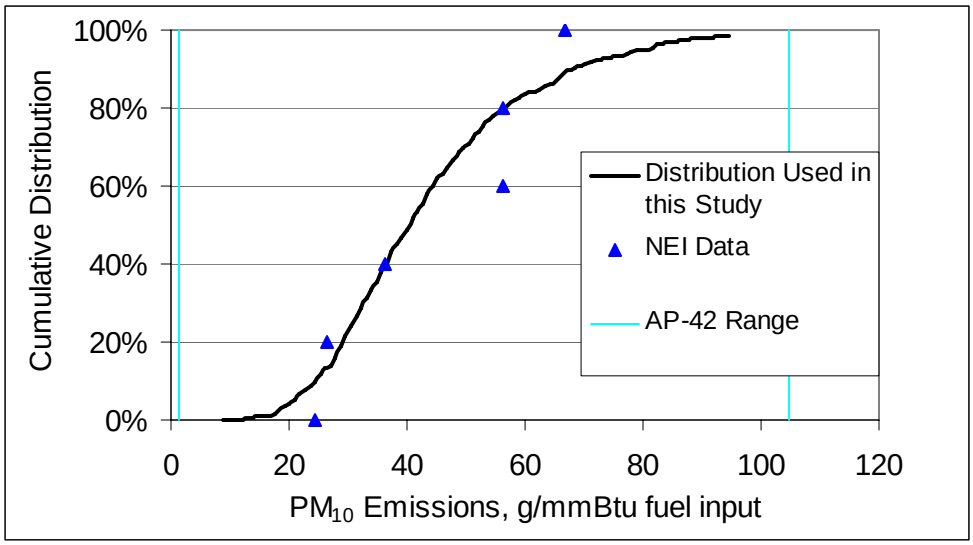

Figure 2-8 PM_{10} Emissions Distribution for Oil Boiler Combustion Sources

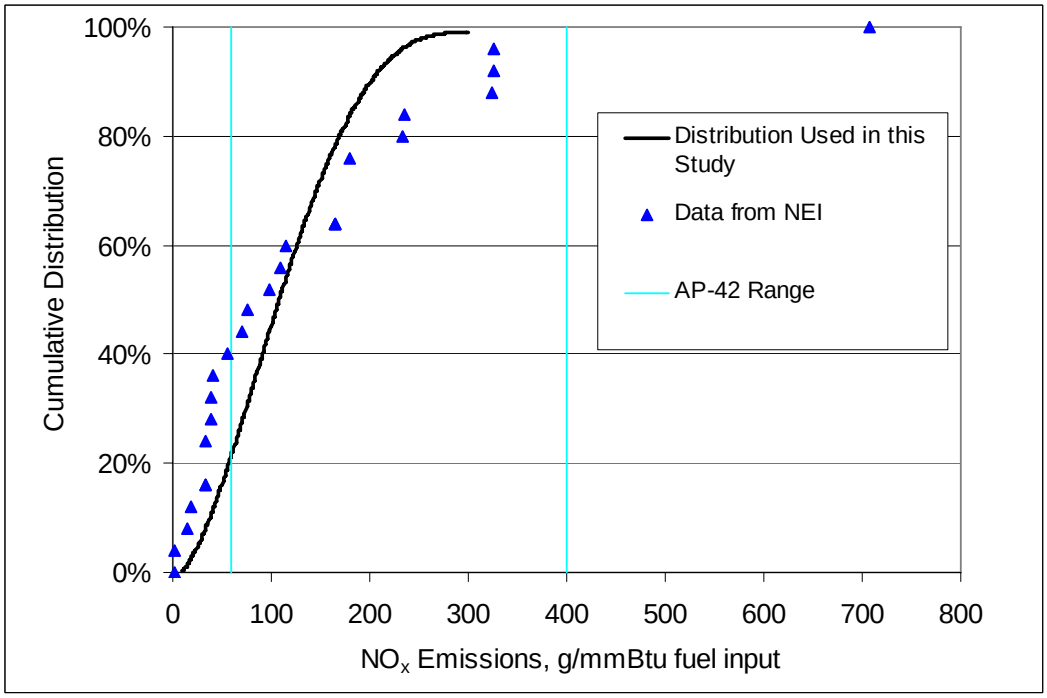

Figure 2-9 NO_x Emissions Distribution for NG Turbine Combustion Sources

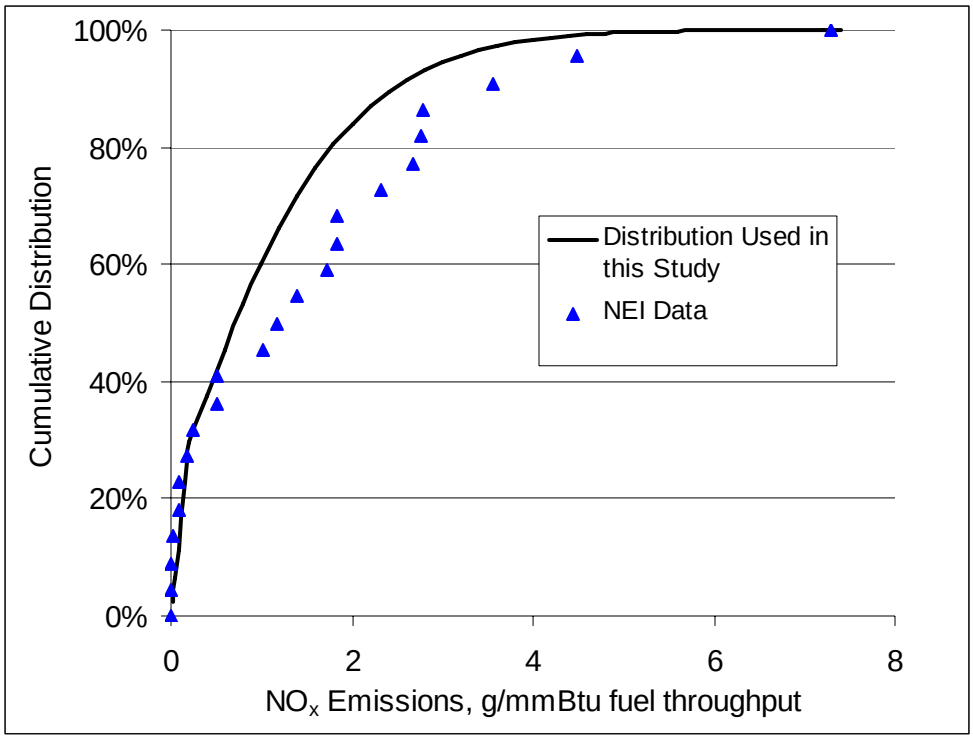

Figure 2-10 NO_x Emissions Distribution for Gasoline Refining Processes

Figure 2-11 shows PM_{10} emission factors for petroleum refinery process emissions. To construct this distribution, we set the maximum of our distribution to match that the second-highest data point from the NEI database. This approach, which reflects our assumption that the highest emitters will be subject to stricter controls by 2016, resulted in a distribution that had a 50th percentile of about 0.3, which was about the mode of the NEI database.

A similar technique was used for developing the 2016 distribution for VOC emissions associated with gasoline refining processes. As shown in Figure 2-12, we set the maximum of the distribution to 10 g/mmBtu fuel throughput, which was about the 90th percentile of the NEI data distribution.

In creating the distribution for VOC emissions from gasoline distribution bulk terminals, we assumed that the highest-emitting sources would be subject to stricter controls. The distribution and NEI data are shown in Figure 2-13.

An important source of VOCs for the gasoline WTT pathway is evaporative emissions that occur at gasoline refueling stations. As shown in Figure 2-14, the data from the NEI were bimodal. One set of data under 10 g/mmBtu probably represents stations at which evaporative emissions controls are in place. The remaining set of data, at just under 50 g/mmBtu, probably represents uncontrolled emissions. These data represent standard emission factors rather than measurements. The distribution we used for this study reflects the expectation that by 2016, a much larger fraction of gasoline refueling stations will have evaporative emissions controls in place.

Figure 2-15 shows VOC emission factors for production processes in ethanol plants. For this process, we assumed significant reductions from the current NEI data to 2016 production partly to account for a new

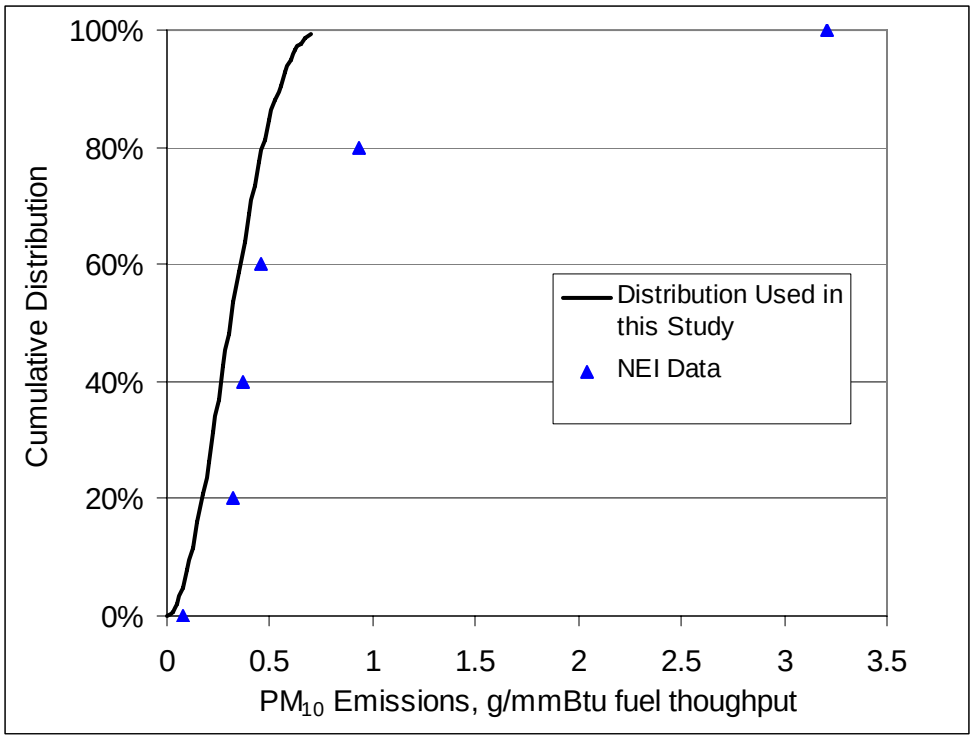

Figure 2-11 PM_{10} Emissions Distribution for Gasoline Refining Processes

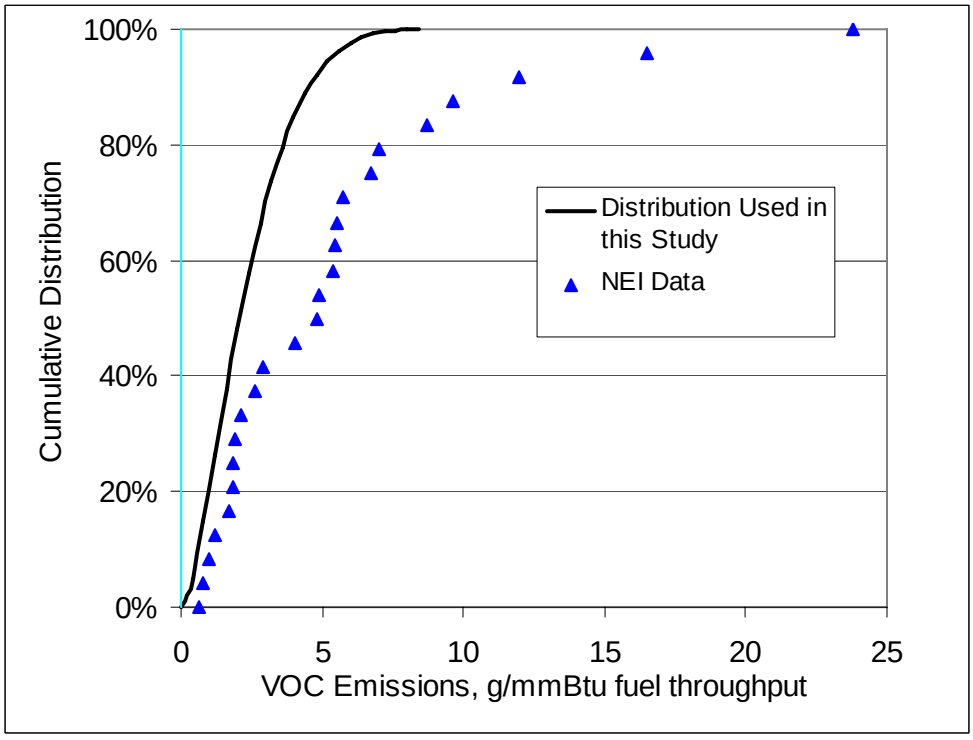

Figure 2-12 VOC Emissions Distribution for Gasoline Refining Processes

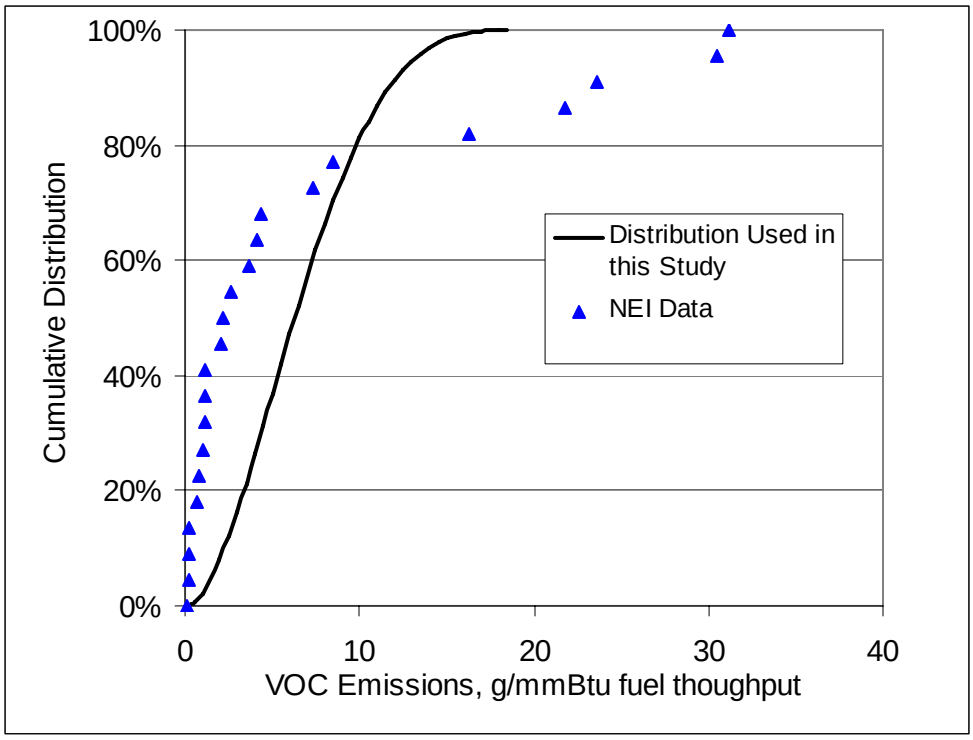

Figure 2-13 VOC Emissions Distribution for Gasoline Bulk Terminals

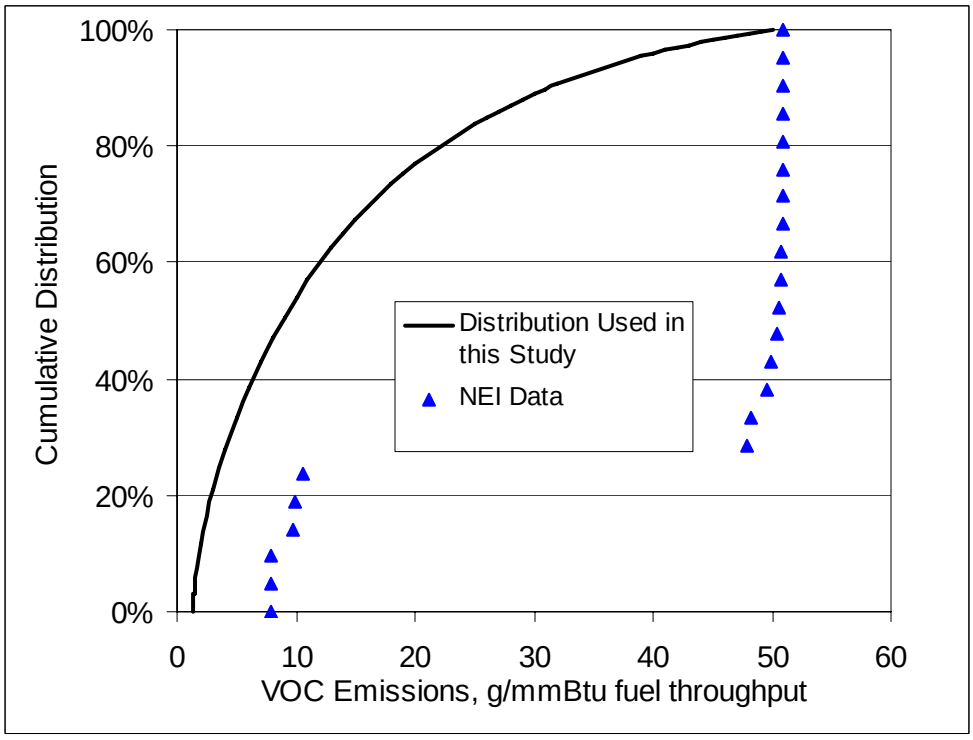

Figure 2-14 VOC Emissions Distribution for Gasoline Refueling Stations

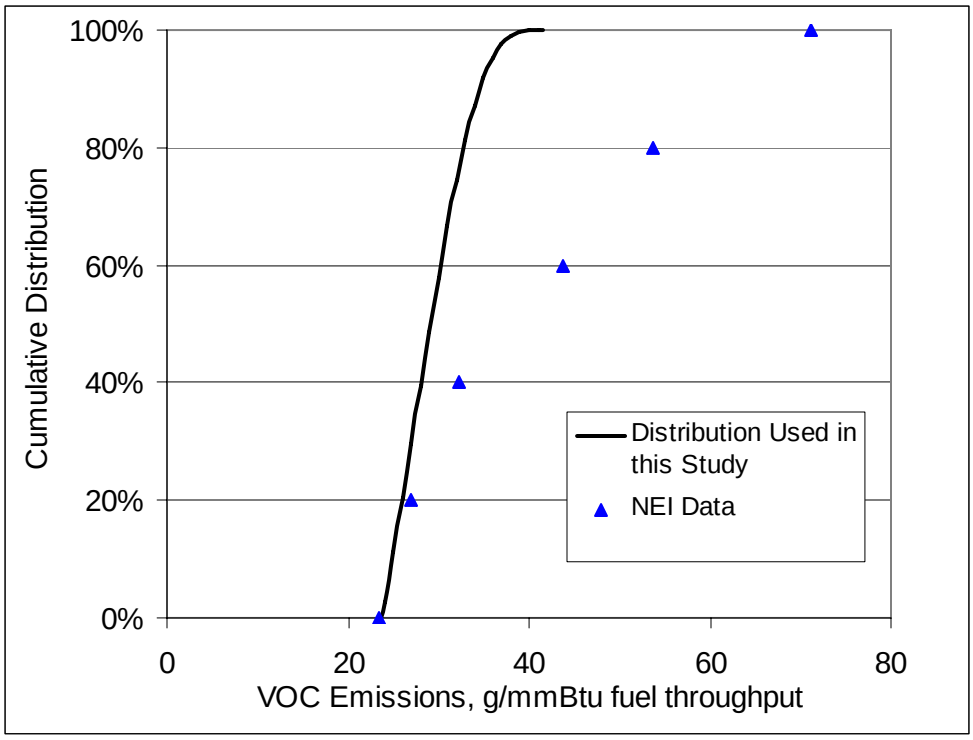

Figure 2-15 VOC Emissions Distribution for Ethanol Production Processes

effort, based on a 2002 agreement between EPA and ethanol plant operators, to control VOC emissions. Our distribution has a minimum equal to the minimum of the NEI data and a maximum near the three highest points of the NEI data. The 50th percentile of the distribution was about 30 g/mmBtu, which is near the 30th percentile of the NEI data.

Similarly, a significant reduction in emission factors was assumed by 2016 for PM_{10} emissions associated with the ethanol production process (see Figure 2-16). The maximum of the distribution was set to the second-highest point in the NEI data. The minimum was set to near zero. The mean of the 50th percentile of the distribution was just over half that of the NEI data.

The NEI did not include any data for the process of reforming NG into hydrogen. To fill in this gap, we solicited data from companies with experience in producing hydrogen from NG. The data we received reflected a range of emission factors for plants without controls, and one example emissions factor for a site with controls. These data are shown in Figure 2-17. We assumed a distribution with the controlled site source data representing about a 20th percentile and a maximum near the lower portion of the range of uncontrolled factors.

Figure 2-18 shows the projected distribution used for PM_{10} emissions for hydrogen production. The PM_{10} emissions factor data we obtained from manufacturers for hydrogen are relatively low compared to those for other processes. Therefore, in constructing the distribution for 2016, we did not project substantial additional controls over those reported by the manufacturers by 2016.

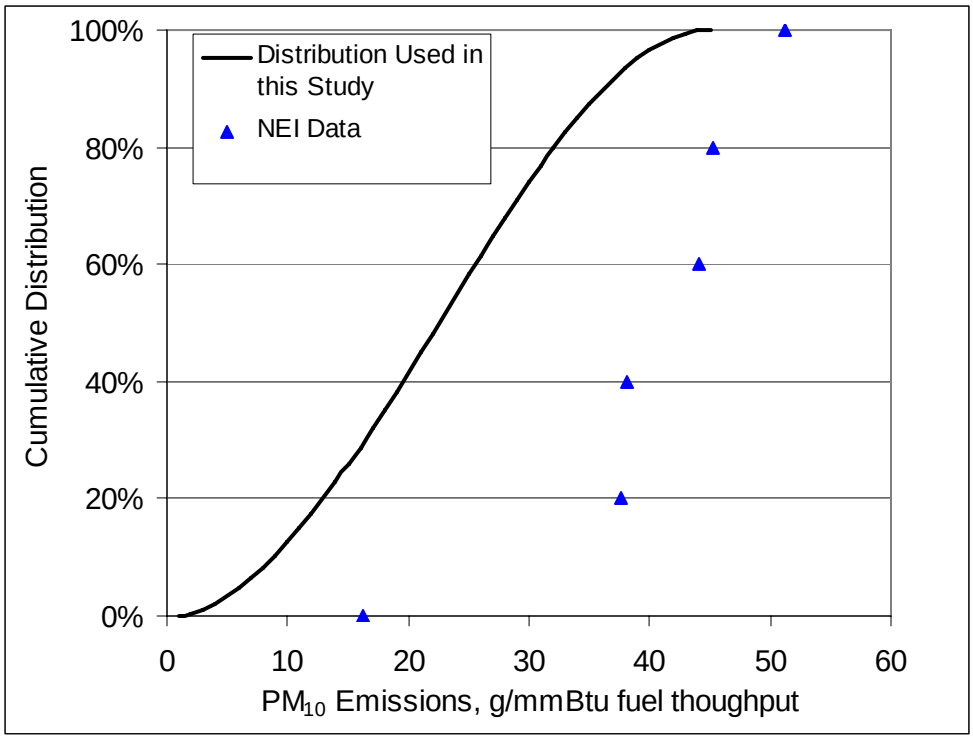

Figure 2-16 PM_{10} Emissions Distribution for Ethanol Production Processes

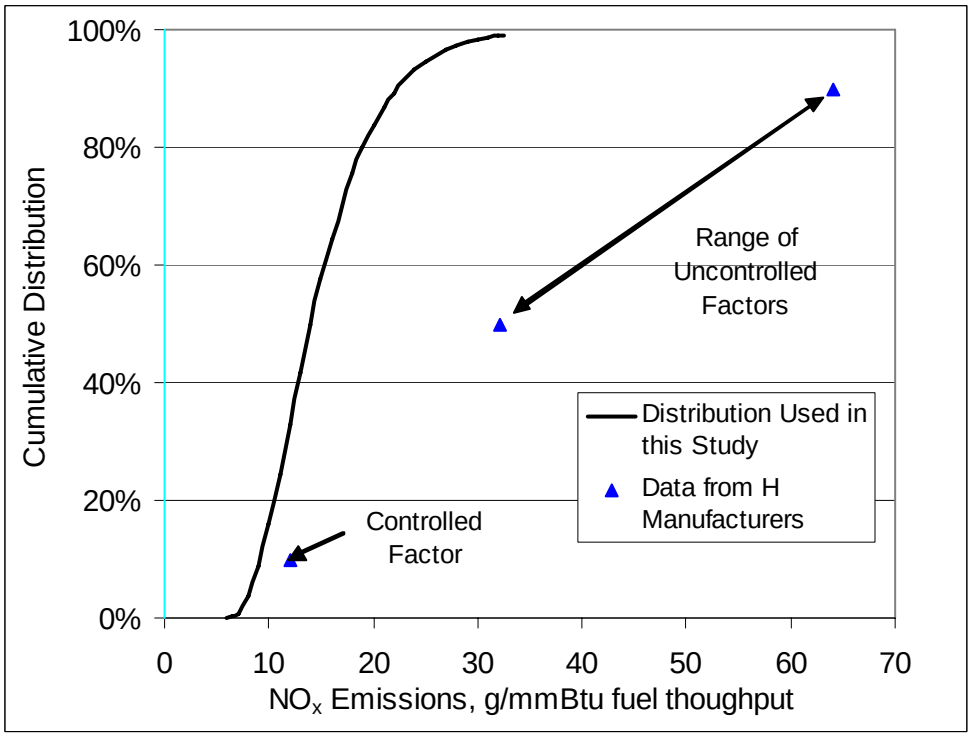

Figure 2-17 NO_x Emissions Distribution for Hydrogen Production by NG Steam Methane Reforming Process

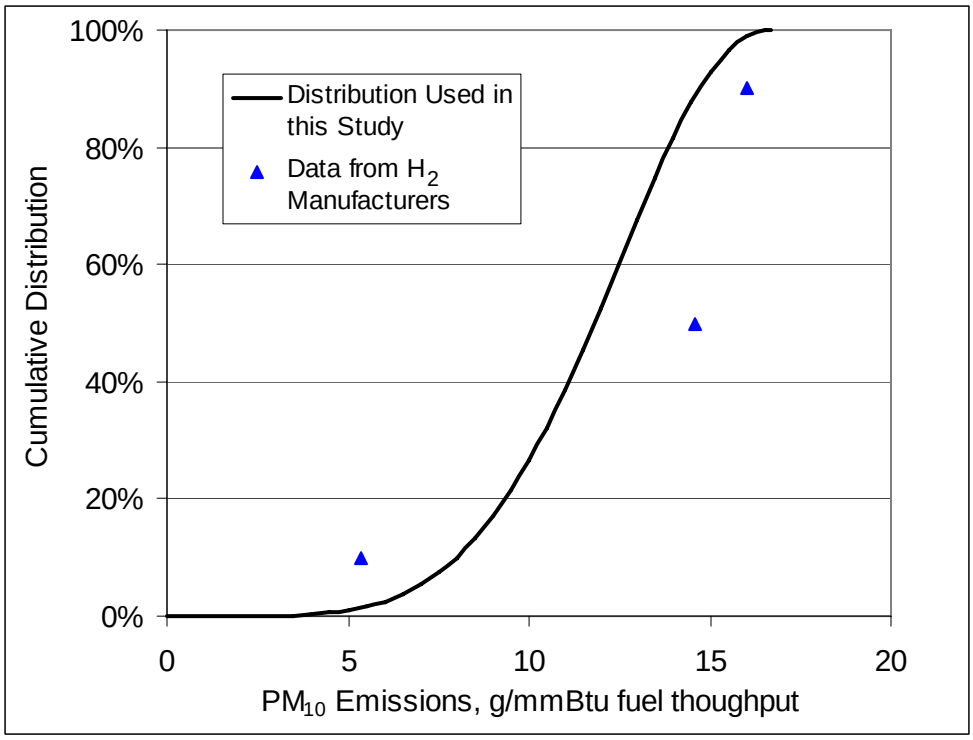

Figure 2-18 PM_{10} Emissions Distribution for Hydrogen Production by NG Steam Methane Reforming Process

PM_{10} process emissions from underground coal/lignite mining are shown in Figure 2-19. In developing the distribution for our study, we assumed that additional controls would be applied to the higher-emitting mine sources. Therefore, we matched the maximum of the distribution to the second-highest NEI data point and set the minimum to near zero.

C. Distribution Functions for Electric Utility Combustion/Process Sources

Although we did not examine electric vehicles or grid-powered hybrid vehicles in this study, many of the WTT processes in our study consume electricity. In addition, electricity is used for hydrogen production via electrolysis. In projecting emissions distributions for 2016 electric utility sources, we took a somewhat different approach than that taken for other sources in order to take advantage of a recent analysis of electric utility emissions by EPA to support its adopted Interstate Air Quality Rule (IAQR) (EPA 2004a; see http://www.epa.gov/interstateairquality/basic.html for all documents and data files related to the IAQR). According to EPA, the adopted IAQR would reduce emissions of SO_2 and NO_x in 29 eastern states and the District of Columbia in two phases. SO_2 emissions would be reduced by 3.6 million tons in 2010 (approximately 40% below 2002 levels) and by another 2 million tons per year when the rules are fully implemented (approximately 70% below 2002 levels). NO_x emissions would be cut by 1.5 million tons in 2010 and by 1.8 million tons annually in 2015 (about 65% below 2002 levels). Each affected state would be required to revise its state implementation plan to include control measures to meet specific statewide emission reduction requirements.

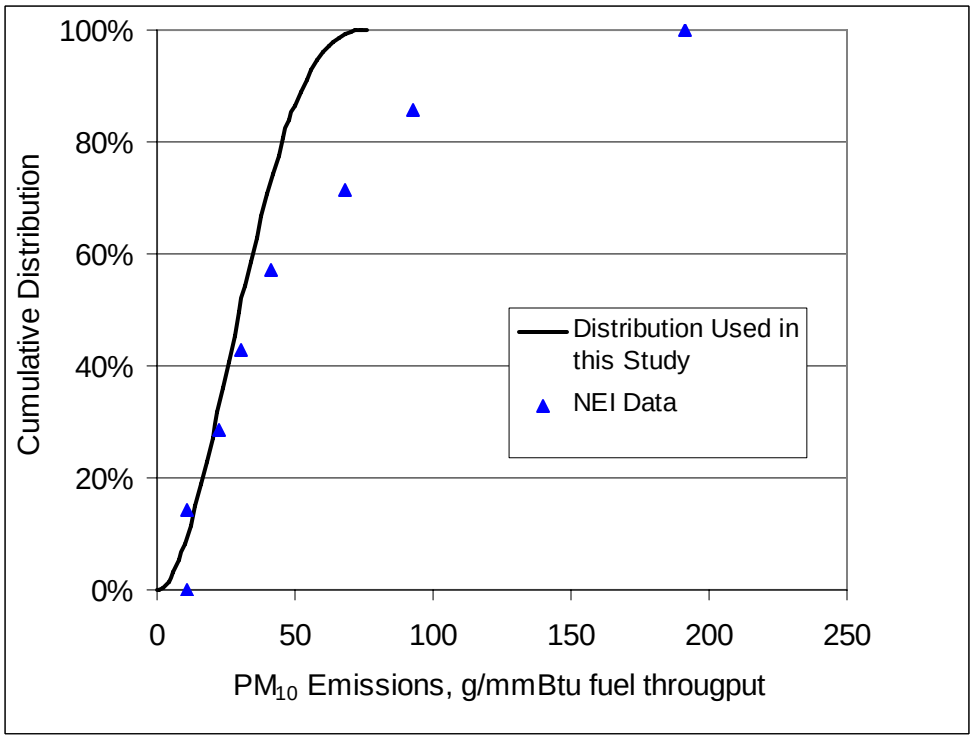

Figure 2-19 PM_{10} Emissions for Underground Coal/Lignite Mining Process

EPA's analysis supporting the rule (http://www.epa.gov/interstateairquality/rule.html) included current electric utility emissions, projected 2015 utility emissions, and projected 2015 utility emissions with implementation of the IAQR. EPA's projected emissions are summarized in Table 2-8.

In constructing the 2001 and 2015 baseline electric generation utility projections listed in Table 2-8, EPA started with 1996 gridded inventories for the Urban Airshed Model (UAM) air quality modeling from the NO_x State Implementation Plan (SIP) call. The 1996 inventories were converted to 2001 base-case emissions by using ratios of 2001 to 1996 emissions by state. The electric utility generation emissions were projected to 2010 and 2015 by using EPA's Integrated Planning Model (IPM), version 2.1.6. IPM included the following already-promulgated or state-adopted controls:

- NO_x SIP call, as remanded (excludes controls in Georgia and Missouri),
- NO_x Reasonably Available Control Technology (RACT) controls in 1-h ozone nonattainment areas,
- Incorporation of several state-mandated emission caps and New Source Review (NSR) settlements, and
- Updates to NG and coal supply curves.

To project the impact of the adopted IAQR, which applies to 28 eastern states and Washington, D.C., EPA estimated state-by-state emission reductions using the caps in the adopted rule. The resulting state-by-state percent reductions were applied to the detailed emissions of each electricity generation unit. The assumed total electric generation activity corresponding to the emissions listed in Table 2-8 was 2,583 billion kWh for 2001 and 3,350 billion kWh for 2015. On the basis of these activities and the total emissions listed in Table 2-8, we calculated projected emission factors, listed in Table 2-9.

Table 2-8 Projected Annual Emissions from U.S. Electricity Generation (in tons)[a]

Year	VOC	NO_x	CO	SO_2	PM_{10}
2001	57,485	4,824,967	451,932	10,714,558	224,044
2015 base case	34,332	4,008,241	700,418	9,222,097	223,265
2015 IAQR case	33,846	2,304,175	713,590	5,401,704	223,046

[a] Information processed from data files presented at http://www.epa.gov/interstateairquality/rule.html.

Table 2-9 Projected U.S. Electricity Generation Emission Factors (g/kWh)

Year	VOC	NO_x	CO	SO_2	PM_{10}
2001	0.0202	1.6984	0.1591	3.7715	0.0789
2015 base case	0.0093	1.0877	0.1901	2.5026	0.0606
2015 IAQR case	0.0092	0.6253	0.1937	1.4660	0.0605

For this study, 2016 electric utility emissions distributions were constructed so that U.S.-mix-weighted emission factors were consistent with the 2015 base emissions listed in Table 2-9. Furthermore, to evaluate the impact of the adopted IAQR on WTW emissions, we developed a set of distributions corresponding to the 2015 IAQR emission factors. Two different methodologies were used for constructing these distributions. For VOCs, CO, and PM_{10} emissions, we first constructed distributions based on the NEI study described previously. We compared the resulting U.S.-mix-weighted emission factors to those listed in Table 2-9 for the 2015 base case. EPA's 2015 baseline distributions were 38%, 25%, and 41% lower for VOCs, CO, and PM_{10}, respectively, than those derived from the latest NEI. Next, we adjusted the VOC, CO, and PM_{10} distribution scaling factors to reduce the means for each source type by 38%, 25%, and 41%, respectively. The resulting U.S.-mix-weighted emission factors matched those in Table 2-10. Properties of these distributions are given in Table 2.10.

More rigorous distributions were constructed for NO_x and SO_2, because in the documentation supporting the IAQR (EPA 2004a; see http://epa.gov/interstateairquality/rule.html for data files), EPA provided spreadsheets of projected NO_x and SO_2 emissions for each electricity generation unit in 2015. We used these projected emissions for each unit to construct NO_x and SO_2 distribution curves for each utility type in our study. The first step in our analysis was to classify each electricity generation unit according to the utility type used in GREET: coal or lignite boiler, oil boiler, NG boiler, NG turbine, NG combined cycle, or biofuel. We computed emission factors for each plant, based on the tons of emissions and annual electricity output from the EPA analysis, and we averaged these factors for each GREET utility type. To check this analysis, we also computed average emission factors for each GREET type by summing the tons of NO_x or SO_2 within each plant category and dividing by the total GWh for that GREET type. The NO_x emissions factor results are listed in Table 2-11.

Table 2-11 shows that NO_x emission factors are highest for coal boilers, intermediate for NG boilers as turbines, and lowest for NG combined cycle. The table also shows that the IAQR regulation primarily impacts plants powered by coal boilers.

Table 2-10 Parameters for Distribution Functions of Criteria Pollutant Emission Factors for Electric Power Plants (g/kWh of electricity generated)

Item	Type of Function	P10[a]	P50[a]	P90[a]
Oil-fired utility boilers				
VOC	Extreme value	0.0093	0.0416	0.0623
CO	Beta	0.0842	0.2150	0.3458
NO_x	Extreme value	0.7795	1.7158	2.8259
PM_{10}	Beta	0.0139	0.0397	0.0765
SO_x	Extreme value	0.7799	5.6602	10.6957
NG-fired utility boilers				
VOC	Beta	0.0066	0.0177	0.0313
CO	Beta	0.0766	0.2071	0.3649
NO_x	Extreme value	0.1692	0.7972	1.5417
PM_{10}	Beta	0.0084	0.0228	0.0401
SO_x	Extreme value	0.0000	0.2035	0.3842
NG-fired single-cycle and combined-cycle turbines				
VOC	Beta	0.0138	0.0386	0.0718
CO	Extreme value	0.0000	0.2838	0.5476
NO_x	Lognormal	0.0576	0.6126	1.3914
PM_{10}	Extreme value	0.0000	0.0266	0.0513
SO_x	Beta	0.0139	0.0397	0.0765
Coal-fired utility boilers				
VOC	Beta	0.0050	0.0135	0.0238
CO	Beta	0.0979	0.2500	0.4021
NO_x	Extreme value	1.0197	1.8387	2.8097
PM_{10}	Beta	0.0408	0.1205	0.2081
SO_x	Gamma	0.8059	3.0213	8.0293

[a] Here, P10 values mean that there is a probability of 10% that actual values would be equal to or below the P10 values; P50 values mean that there is a probability of 50% that actual values would be equal to or below the P50 values; and P90 values mean that there is a probability of 90% that actual values would be equal to or below the P90 values.

Table 2-11 Comparison of Two Methods for Calculating Utility NO_x Emission Factors (g/kWh of electricity generated)

	Mean of Individual Plant Emission factors		Based on Total NO_x and Total Amount of Electricity	
	Baseline	**IAQR**	**Baseline**	**IAQR**
Coal boiler	1.91	1.40	1.56	0.88
NG boiler	0.57	0.56	0.43	0.41
NG turbine	0.53	0.53	0.42	0.42
NG combined cycle	0.29	0.29	0.09	0.09

Another observation from Table 2-11 is that emission factors computed by averaging the emission factors for each plant were higher than those computed by summing the mass of emissions from all plants and dividing by the total amount of electric energy generated. The cause for the discrepancy was that smaller-capacity plants tended to have higher emission factors than larger plants.

Based on this analysis, it was clear that electric utility plant generation capacity had to be taken into account when creating emission factor distributions. Unfortunately, Crystal Ball™ did not have a procedure for weighting individual points, so we developed a method to approximate fitting a weighted distribution. For each GREET type and for both the baseline and IAQR cases, histograms of emission factors were created by using preselected bins. Then, total GWh was computed for each "bin." This method resulted in a histogram table of the total GWh of electricity generated at each emission factor bin value. Next, we developed a set of numbers in which each bin value was replicated a number of times proportional to the total GWh for each bin. From this set of numbers, we created a GWh-weighted distribution consisting of 100–1,000 total points. Finally, Crystal Ball™ was used to fit distributions to the total GWh-weighted emission factor data, and the best fit was selected by using the Anderson-Darling method. If necessary, the minimum value of the distribution was to set zero to avoid negative emission factor predictions The means of these distributions match the means derived by total NO_x/total GWh in Table 2-11.

This section provides several examples of electric utility distributions to demonstrate the methodology. The first example, Figure 2-20, shows NO_x emissions for utility coal boilers for the baseline and IAQR assumptions. Each graph in this section has three different curves. The first curve, indicated by diamonds, shows a cumulative distribution of emission factors computed on the basis of equal weighting for each individual plant. The second curve, indicated by triangles, shows the GWh-weighted distribution for each bin, computed as described in the previous section. Finally, the third curve, indicated by a solid line, shows the continuous distribution resulting from the Crystal Ball™ fit of the GWh-weighted points.

As is shown in the left side of Figure 2-20, a distribution created on the basis of individual plants results in a higher distribution of emission factors than that based on the GWh-weighted analysis. The left side of Figure 2-20 also shows that the distribution used in this study was a good fit of the cumulative distribution of weighted emission factors. Both distributions show a long tail of significantly high emission factors above the 90th percentile.

The adopted IAQR rule permits emissions trading among utility sources, so it is not possible to predict precisely the utility distributions under the IAQR. Comparing the IAQR to the baseline portion of Figure 2-20 illustrates the results of EPA's analysis. The main reduction in emissions was projected to take place in the generating plants with low emission factors. As indicated earlier, these are also the largest plants. This results in a discontinuity in the individual-plant distribution that is also seen in the weighted distribution. This discontinuity is smoothed out in the Crystal Ball™ fit, as shown by the solid line. Comparing the right to the left side of Figure 2-20 shows that the IAQR distribution estimated significantly lower NO_x emission factors for utility coal boilers. The 50th percentile NO_x emissions factor was about 1.5 g/kWh for the baseline and about 0.6 g/kWh for the IAQR.

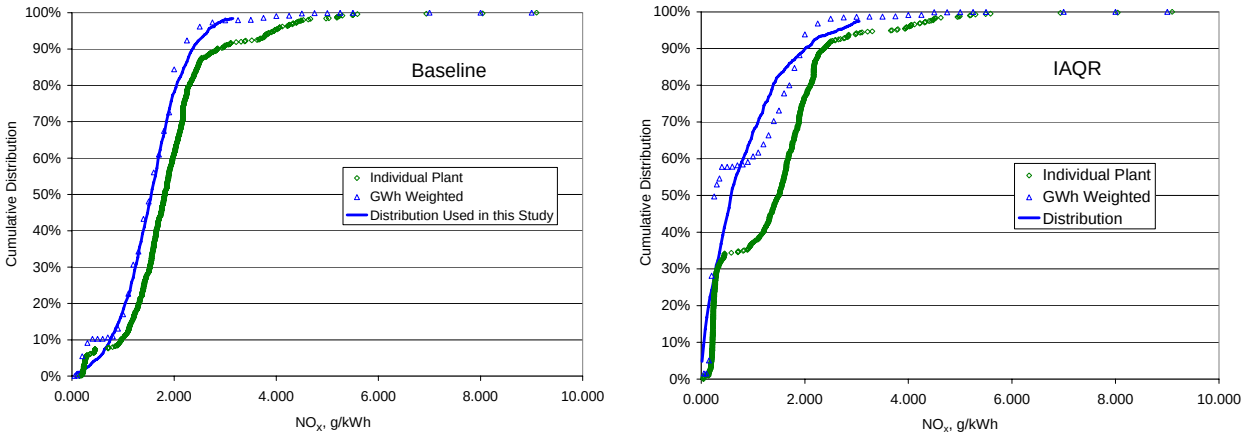

Figure 2-20 NO_x Emissions for Utility Coal Boilers

Figure 2-21 shows baseline and IAQR distributions for SO_2 from utility coal boilers. As with NO_x, the results show a small number (~2%) of plants with high SO_2 emission factors. For both the baseline and IAQR cases, the distributions used in this study matched up well with the discrete GWh-weighted emission factor distributions. The 50th percentile for the baseline was about 3.1 g/kWh, compared to about 1.8 g/kWh for the IAQR case. From the 10th to the 90th percentile, the IAQR distribution for SO_2 emission factors was significantly lower than that for the baseline.

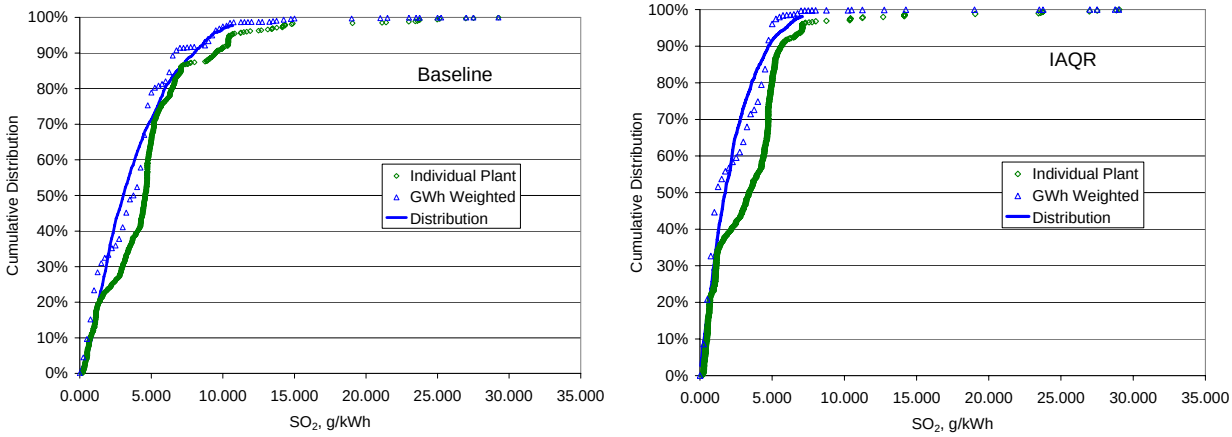

Figure 2-21 SO_2 Emissions for Utility Coal Boilers

Figure 2-22 shows distributions for NO_x emission factors from utility NG boilers. Again, the importance of weighting the distributions according to power generation is shown. EPA's analysis does not predict substantial changes in NO_x emissions from NG boilers for the IAQR. The right and left sides of Figure 2-22 are nearly identical. Compared to coal boilers, the NG boiler distributions have lower NO_x emissions across the distribution range.

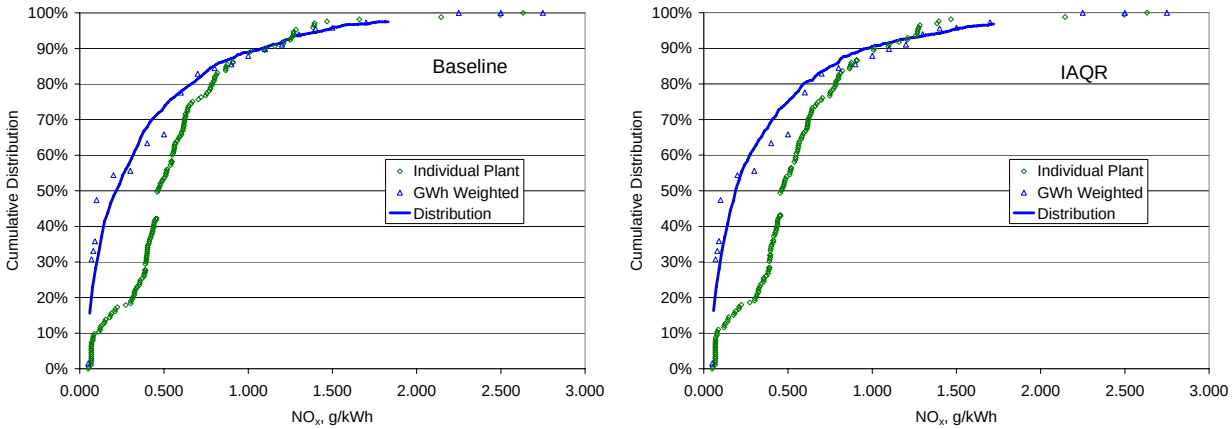

Figure 2-22 NO_X Emissions for Utility NG Boilers

Figure 2-23 shows NO_X emission factors distributions for utility NG combined-cycle plants. Of all of the examples shown, this figure best illustrates the importance of using the GWh-weighted distributions. The IAQR is projected to have little effect on NO_X emissions from NG combined cycle. NO_X emissions are significantly lower than those for NG or coal combustion.

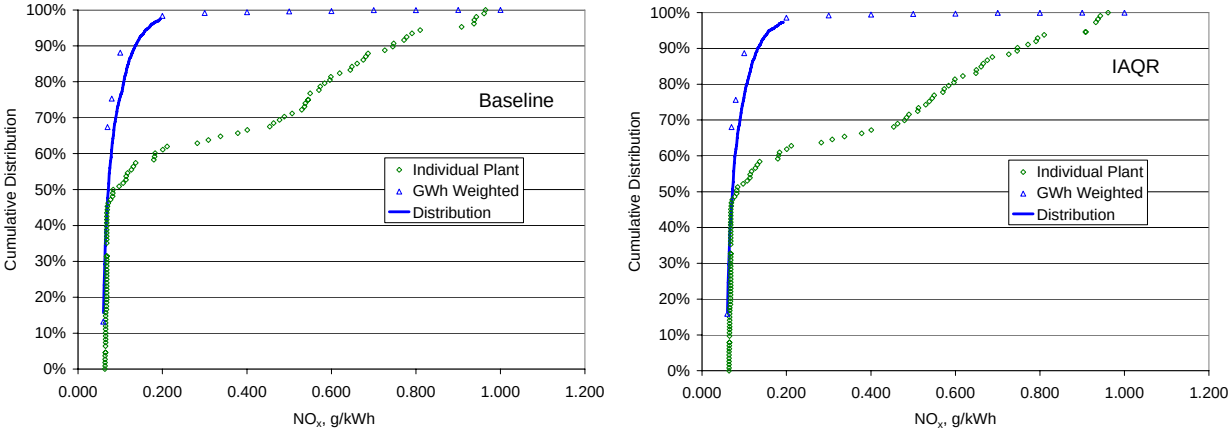

Figure 2-23 NO_X Emissions for Utility NG Combined Cycle Turbines

2.2 Tank-to-Wheels Technology Options and Simulation Methodologies

2.2.1 Tank-to-Wheels Vehicle Propulsion Options

As in the Phase 1 study, the vehicle modeled in this study was a full-sized pickup truck. We selected a truck for two reasons: (1) it is one of GM's highest-selling vehicle platforms, and (2) because light duty trucks are a high-fuel-consumption vehicle platform, any reduction in energy consumption and GHG emissions will have a large impact.

The TTW propulsion systems analyzed in this study are summarized in Table 2-12. All powertrains were modeled in both non-hybrid and hybrid architecture. The baseline engine was a port-fuel-injected,

Table 2-12 TTW Propulsion Systems and Notation Used in this Report

Propulsion System	TTW Notation Used in Report	
	Non-Hybrid	Hybrid Electric
Gasoline displacement-on-demand spark-ignition	Gasoline DOD SI CD	Gasoline DOD SI HEV
Gasoline direct-injection spark-ignition	Gasoline DI SI CD	Gasoline DI SI HEV
Diesel direct-injection compression-ignition	Diesel DI CI CD	Diesel DI CI HEV
E85 flexible-fuel displacement-on-demand spark-ignition	E85 DOD SI CD	E85 DOD SI HEV
CNG displacement-on-demand spark-ignition	CNG DOD SI CD	CNG DOD SI HEV[a]
Hydrogen displacement-on-demand spark-ignition (Bin 5 or 2 NO_x)	H_2 DOD SI CD[a]	H_2 DOD SI HEV[a]
Gasoline/naphtha fuel processor fuel cell	Gasoline FP FCV	Gasoline FP FC HEV
Methanol fuel processor fuel cell	MeOH FP FCV	MeOH FP FC HEV
Ethanol fuel processor fuel cell	EtOH FP FCV	EtOH FP FC HEV
Gaseous/liquid hydrogen fuel cell	H_2 FCV	H_2 FC HEV

[a] TTW pathway not included in the Phase 1 study.

gasoline SI engine with DOD technology. DOD is expected to be in common use in GM trucks in 2010. We also modeled this port-fuel-injected SI DOD technology for engines operating on fuel ethanol (E85), CNG, and hydrogen. To indicate the potential of advanced SI technology, we modeled a lean-burn DI SI engine fueled with gasoline. A DI CI engine was also modeled; performance on petroleum-derived and FT diesel fuels was assumed to be equal.

For fuel cell propulsion systems, we considered both direct-hydrogen and onboard fuel processing. Because the choice of fuel type impacts fuel-processing efficiency, we conducted separate analyses of hydrocarbon (gasoline/naphtha), methanol, and ethanol fuel processor FCVs.

All of the TTW propulsion systems examined in the Phase 1 study were included in the Phase 2 study. Propulsion systems added in the Phase 2 study were CNG hybrid, hydrogen ICE, and hydrogen ICE hybrid.

2.2.2 Tank-to-Wheels Vehicle Propulsion System Simulations

Phase 1 of the GM North American study (GM et al. 2001) encompassed powertrain technologies targeted for the 2010 timeframe. The study did not include a complete set of conventional powertrain technologies already being considered for production or others that are still in the R&D phase. During the Phase 2 study, the list of technologies and performance maps were updated for application to 2010 model-year (MY) production. As in the Phase 1 study, analysis of fuel economy and emissions was based on maintaining equal performance attributes for vehicles equipped with the various propulsion systems. Although cold-start conditions and criteria pollutants were not specifically modeled because of a lack of data for all technologies, the analysis approach assumed that these technologies would be compliant with EPA emission standards by including penalties for the aftertreatment systems.

Emissions targets for criteria pollutants for all vehicle concepts, which were based on EPA's Tier 2 standards, are discussed in detail in Section 2.2.2.4. Cost and packaging issues were not addressed because of the uncertainties surrounding the fuel cell and fuel reformer technologies. Further breakthroughs in the areas of fuel processor dynamics and start-/warm-up for the fuel processor system would be needed.

The analysis was based on high-integrity component characteristics data obtained from experts working on these advanced technologies throughout GM. The predictions based on these data were reviewed by their technology owners, ensuring agreement with corporate forecasts, market requirements, and customer expectations for performance and environmental friendliness. The tradeoffs among performance, fuel consumption, and emissions were treated in a consistent manner for all concepts to allow for robust fuel economy and energy consumption comparisons.

2.2.2.1 Vehicle Simulation Approach

The analysis was carried out by using a validated GM proprietary modeling tool, the Hybrid Powertrain Simulation Program (HPSP), which uses the reverse-driven simulation approach illustrated in Figure 2-24. Simulation was initiated by the instantaneous road-load requirement of vehicle speed and acceleration as a function of time, as specified by the driving cycle.

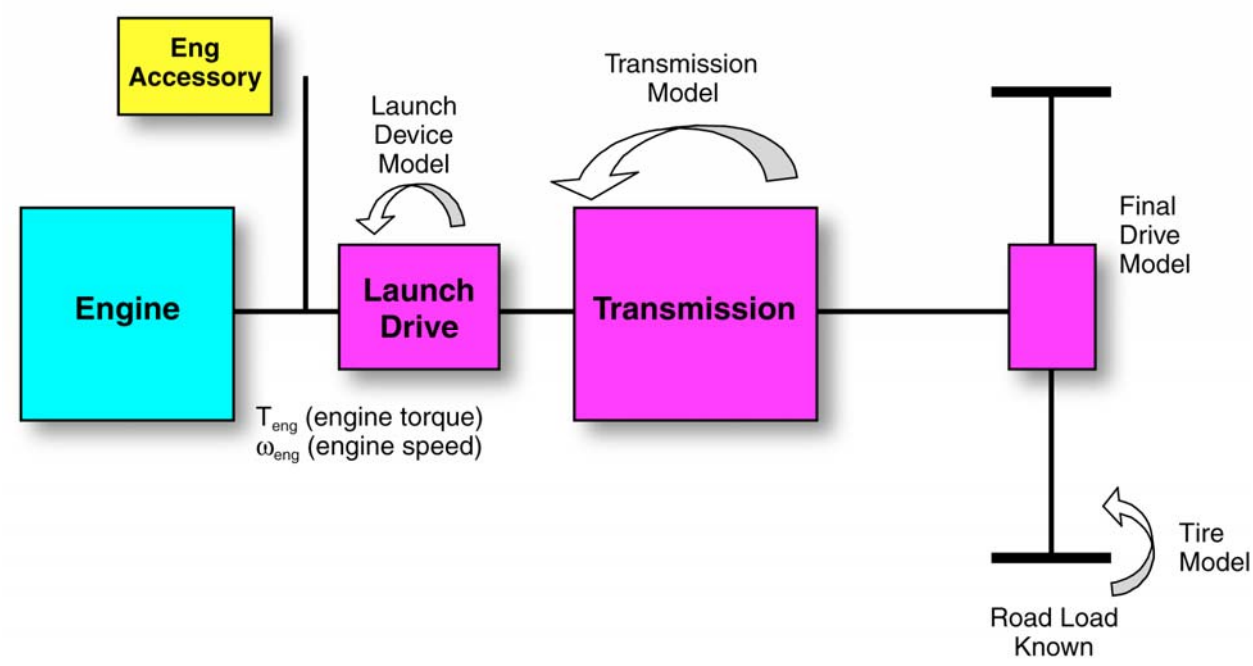

Figure 2-24 Reverse Analysis for Vehicle Duty-Cycle Simulation

All components and subsystems are represented by empirical, quasi-steady-state models and use efficiency maps, loss data, and system-specific parameters (e.g., inertias and ratios) as inputs. These torques and speeds are tracked backwards from the road-load requirement through all the driveline components, allowing researchers to eventually determine the engine torque and speed operating region requirements. The input torque and the speed of each component are calculated as a function of the given output torque and speed, and all torque, speed, and acceleration (inertia)-dependent losses within the component are accounted for in the process. In a similar manner, the electrical input current and voltage requirements are determined from the torque, speed, and acceleration requirements of the electrical components, including their electrical and mechanical losses. At the end of each time step, the torques and speeds are used to determine the energy consumed in each component. HPSP implements the torque and speed approach, rather than the power-requirement-based analysis. The torque and speed approach allows input of detailed component performance maps, providing more accurate predictions, especially at low-load and low-speed conditions.

This simulation approach is ideal for following a duty cycle to determine the engine operating regions under optimum controls of the powertrain or based on specified control and energy management strategies. It is also applicable for a maximum or wide open throttle (WOT) performance analysis to predict maximum vehicle acceleration. For this type of simulation, an iterative solution is required for the reverse-analysis approach, as shown in Figure 2-25.

In this case, the algorithm is driven by a seed value for the vehicle acceleration, *AccTrial*, to determine the road load and the same analysis tracking torque and power demands from component to component until the engine operating point is determined. If the engine can provide the torque required, this acceleration value is increased in an iterative procedure until the engine operating limits and the user-specified convergence criteria are met.

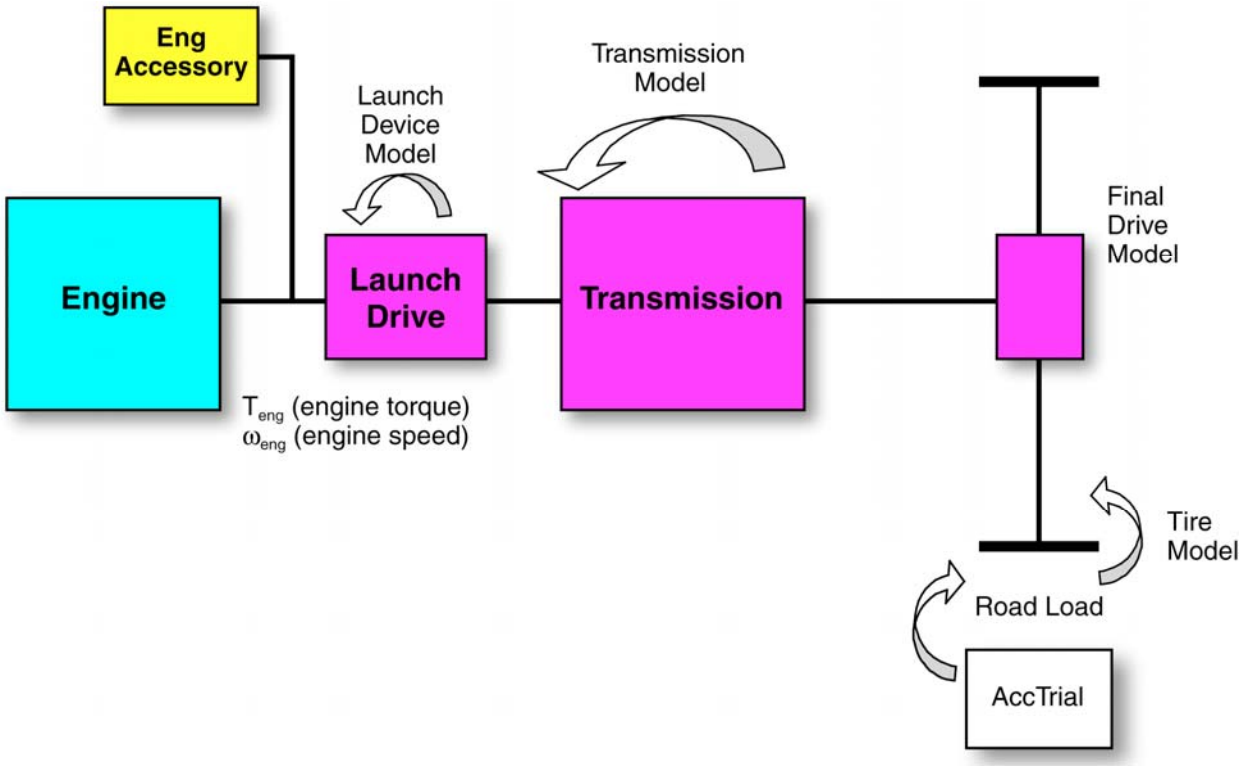

Figure 2-25 Reverse Analysis for Maximum Performance Simulation

In contrast to the reverse-driven approach, the forward-driven analysis performs the simulation from the engine throttle position input, following the energy and power flow through the driveline to the tire patch while calculating vehicle velocity and acceleration. With the forward-driven approach, a driving cycle is negotiated by a driver model, which adjusts the engine output to match the duty-cycle vehicle speed requirement. This approach is appropriate to simulate the dynamic behavior of the vehicle and driveline components, identify transients, and analyze responses to powertrain control systems.

In summary, the reverse-driven simulation approach is well suited for the following applications:

- Predicting fuel economy on a prescribed duty cycle,
- Predicting vehicle performance,
- Employing quasi-steady-state empirical models for the system components,
- Determining component sizes and energy management strategies, and

- Sizing components and designing energy management strategies within an optimization loop.

In order to implement an optimization methodology, as mentioned in the last bullet above (for the purpose of changing vehicle design parameters to maximize fuel economy while meeting performance requirements), a numerical algorithm had to be identified and tailored to the problems at hand. This algorithm had to provide a global solution, deal with nonlinear and discontinuous functions, use derivative-free methods, and converge in as few as possible function calls. A number of algorithms were evaluated (Fellini 1998; Fellini et al. 1999; Fellini et al. 2000; Sasena 1998; Weber 2003; Wurster et al. 2004), and the DIRECT method was found to be most appropriate for this application. This method was consistently used to size the components and determine the control system parameters for the hybrid vehicle systems.

In addition to fuel economy and performance, we calculated vehicle efficiency for each of the propulsion systems. The term "efficiency" is defined in Figure 2-26.

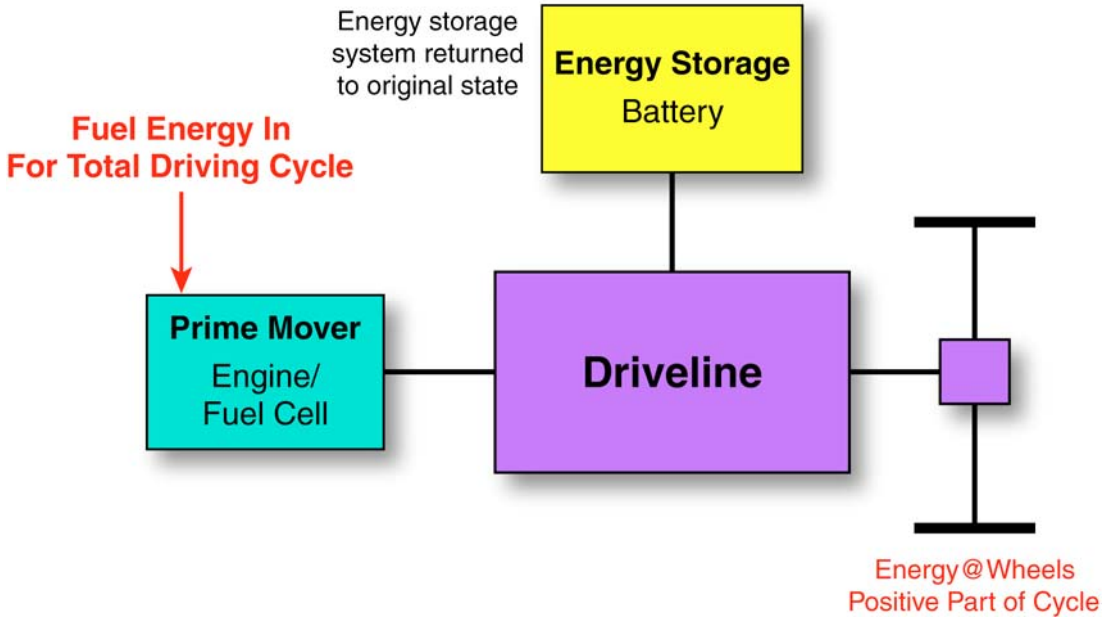

$$Vehicle\ Eff = \frac{\sum_{pos}(Rolling\ Resistance + Aero\ Load + Inertial\ Load) * V * \Delta t}{Fuel\ Energy\ In_{tot}} = \frac{Energy@Wheels_{pos}}{Fuel\ Energy\ In_{tot}}$$

where V is the vehicle velocity and the Fuel Energy In_{tot} includes all powertrain losses and the accessory loads on the engine.

Figure 2-26 Definition of Vehicle Efficiency

2.2.2.2 Vehicle Performance Criteria

The spider chart in Figure 2-27 presents the performance requirements imposed on each vehicle propulsion system designed and evaluated in this study. These requirements were based on current gasoline ICE-equipped vehicles and customer performance expectations for future powertrains. A 7.5-mi zero emission vehicle (ZEV) range (based on the urban driving cycle) was imposed on the hybrid vehicles, assuming that the vehicles could be driven in inner cities without using an engine.

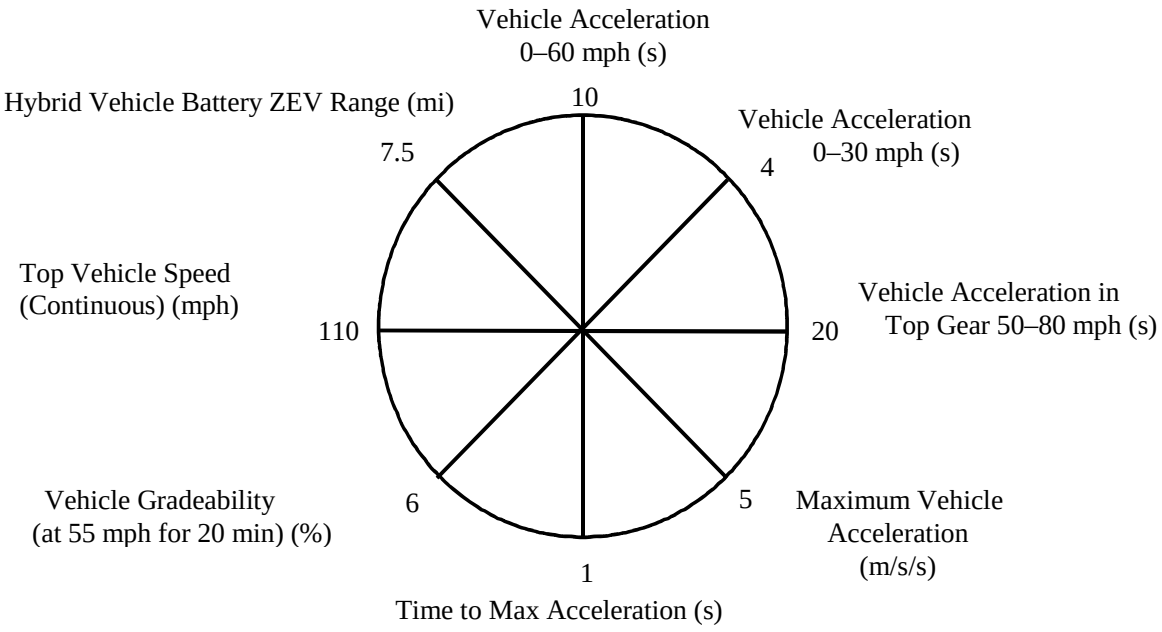

Figure 2-27 Minimum Vehicle Performance Requirements

The power sources for each propulsion system were sized in terms of their power, speed, and torque capacities to meet the performance criteria shown in Figure 2-27. The component characteristics also play a crucial role in meeting the criteria shown on the chart. For example, the maximum vehicle acceleration (5 m/s/s) to be reached within 1 s is a strong function of the torque delivered to the wheels, while the top vehicle speed and the acceleration time are dominated by the power capacity and mechanical gearing available in the driveline. Furthermore, the requirement for continuous performance at top vehicle speed precludes engine downsizing, which significantly impacts the fuel economy potential of hybrid vehicles.

The vehicle mass for each concept was adjusted to correct for added or eliminated components. In cases for which such data were not readily available, target component and subsystem mass data were used. The energy management and control strategies were subsequently developed to yield the lowest fuel consumption on the driving cycle and to take advantage of the inherent benefits of the particular powertrain architecture without compromising drive quality. These stringent performance requirements were imposed on the basis of our assumption of mass production of these vehicles rather than niche market applications.

In the absence of such a rigorous approach of including all the performance metrics, researchers could obtain significantly different results and large discrepancies in the quantified potential gains.

2.2.2.3 Propulsion System Architecture

The vehicle platform (full-sized truck) selected for the analysis and simulation of the propulsion systems remained unchanged from the Phase 1 study (GM et al. 2001) (see photo). The powertrain technology projected to the 2010 timeframe incorporated the displacement on demand (DOD) engine technology that is mature for high-volume application, as well as assumed improvements in driveline efficiency.

The DOD engine technology allows an eight-cylinder engine to run on four cylinders whenever the driver's power demands can be met using only four cylinders.

All powertrain technologies were characterized by means of component maps based on measured test data and/or realizable targets for efficiency and performance. The assumptions were geared toward maintaining consistency in the efficiency maps and mass when scaling the components for comparison of the technologies. Advanced control strategies with emission considerations such as engine-specific fuel shut-off strategies were implemented with appropriate constraints on vehicle driveability.

2.2.2.3.1 Conventional Drive or Non-Hybrid Vehicles

The non-hybrid (NH) or conventional drive (CD) powertrains shown in Figure 2-28 consist of an ICE with an automatic torque converter transmission and a standard accessory package, including devices such as power steering and an alternator load. The transmission was shifted to maintain engine response and avoid shift busyness, and the torque converter clutch was engaged at vehicle speeds to maintain drive quality.

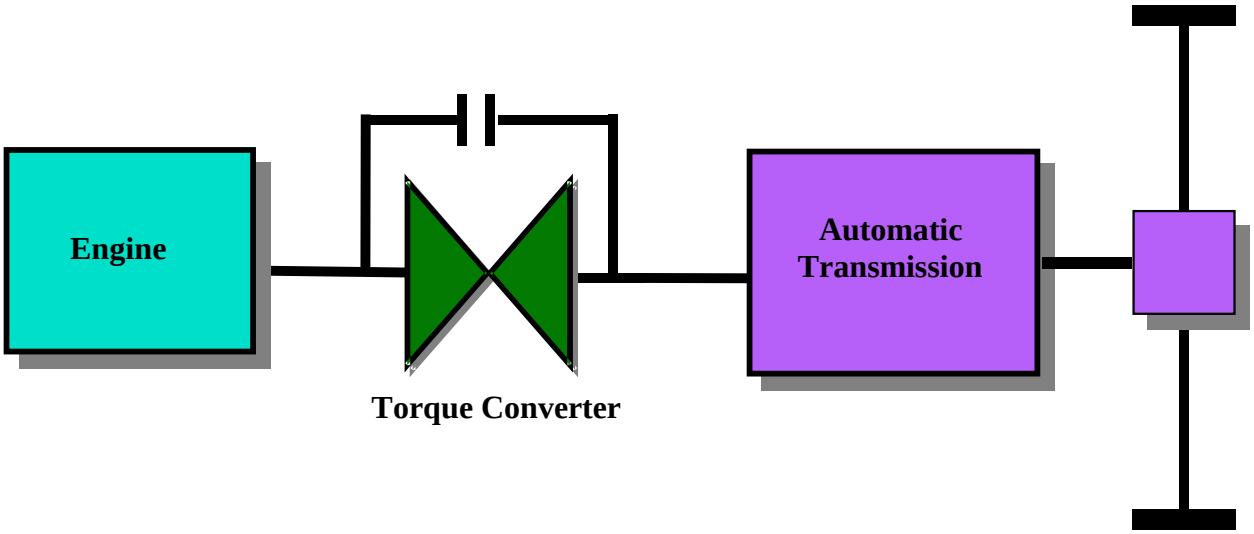

Figure 2-28 Conventional Drive or Non-Hybrid Powertrain Architecture

2.2.2.3.2 Hybrid Electric Vehicles

The hybrid concepts considered in the Phase 2 study were strong-parallel-type architectures that employ advanced electric drives and nickel metal hydride (NiMH) batteries. Strong HEVs, in contrast to mild HEVs, implement higher voltage and higher-power electric components, providing drivers with the ability to launch and drive in the electric mode at low to moderate vehicle speeds.

The Input Power Assist parallel HEV, shown in Figure 2-29 with the electric drive connected at the input to the transmission, was chosen for this study because it represents a hybrid option with the least deviation from the conventional powertrain. As indicated in Section 2.2.2.2, the battery was sized to meet

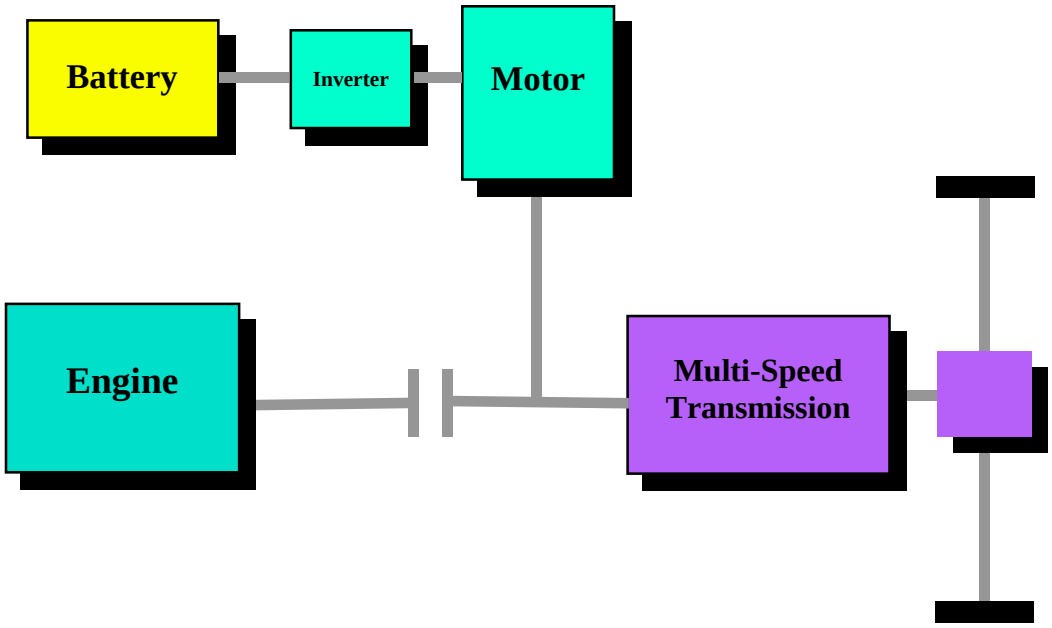

Figure 2-29 Parallel HEV Architecture

the 7.5-mi ZEV range, the electric motor was sized to follow the duty-cycle torque and power demands, and a full-size engine was incorporated to meet the sustained top vehicle speed of 110 mph.

The input data for the ICE and transmission were the same as those for the CD concepts. The electric motors and NiMH batteries represent the latest technology-level components, as used in the Precept vehicle that GM developed for the Partnership for a New Generation of Vehicles (PNGV).

The vehicle mass for each HEV concept was adjusted according to the component sizes. Other details, such as charging and discharging efficiency, engine restarting fuel penalty, and accessory loads, were also included to ensure accurate fuel consumption predictions.

Another significant impact on vehicle fuel consumption is the energy management strategy for controlling the powertrain while the vehicle negotiates the driving cycle. A charge-sustaining (CS) strategy, which assures that the battery state-of-charge (SOC) is returned to its initial state at the end of a driving cycle, was assumed for all HEVs. These control strategies also incorporate constraints on engine and motor operation, switching between operating modes, engine ramping rates, and hysteresis effects to avoid transmission shift and engine cycling busyness. The engine operating region was constrained to meet certain criteria for driveability, pleasability, performance, and emissions.

The engine was always turned off at standstill (idle), and the battery was used to launch the vehicle to about 20 mph. At high acceleration demands, the battery launch was cancelled, and the engine and battery were used together to drive the vehicle. To maximize engine efficiency, a load-following control strategy was implemented, and during deceleration or braking periods, the engine was shut off and disconnected from the transmission for maximum recovery of braking energy. At vehicle speeds above 44 mph, the engine remained connected to assure drive quality and performance response.

2.2.2.3.3 Fuel Cell and Fuel Processor Systems

The diagram shown in Figure 2-30 presents the model developed to simulate the fuel processor fuel cell systems. This model addresses the various fuel-based reformer systems, as well as the onboard hydrogen storage fuel cell systems with reformers, characterized by their efficiency and power delivery maps. A two-speed gearbox was incorporated between the motor and the final drive to meet the peak acceleration requirement.

The intention of the two-speed gearbox is to provide an underdrive ratio to be used only when maximum vehicle performance is required and in the direct-drive mode during normal duty-cycle operation for fuel economy prediction. This two-speed gearbox is characterized in a manner similar to that used for a conventional transmission in the simulation model.

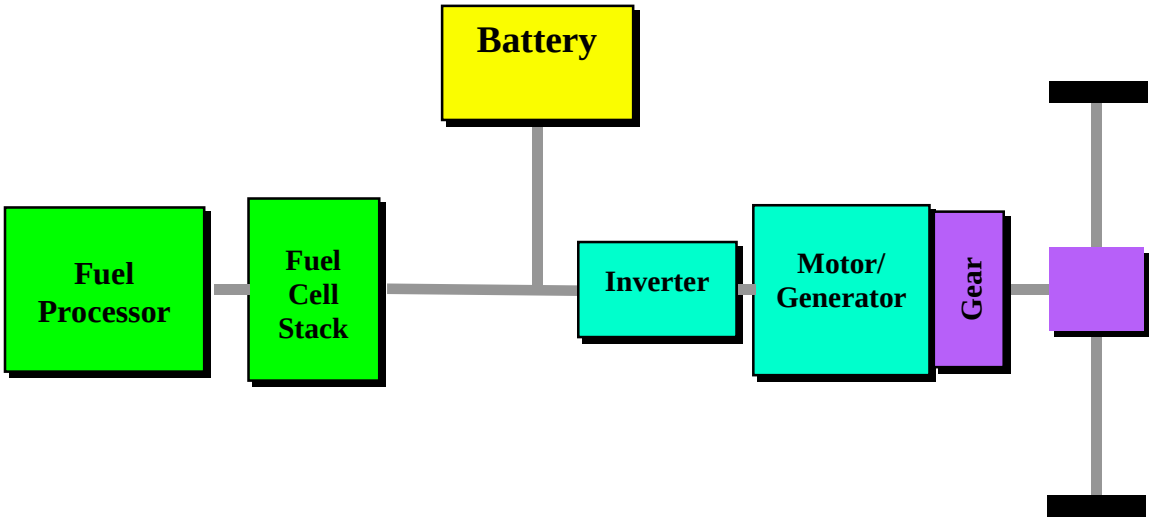

Figure 2-30 Fuel Cell/Fuel Processor Powertrain Architecture

Representative efficiency maps for all electric drive components were scaled to meet the vehicle performance requirements to maintain consistency with the other technologies.

2.2.2.3.4 Fuel Cell and Fuel Processor Hybrids

For completeness and in order to tap the potential regeneration capability of the electric drives in these concepts, we also assessed the hybridized architectures shown in Figure 2-31.

We determined that the best overall energy management strategy for these concepts was one that would minimize the use of the fuel cell to recharge the battery. Turning the fuel cell system off at standstill and at low power and transferring the accessory loads to the battery at high power allowed the fuel cell system to operate at near-optimum efficiency for most of the cycle without incurring excessive battery and motor losses.

In the case of the onboard hydrogen FCVs, the battery size criterion was not relevant because the FCV is already a ZEV. However, a system optimization in which the overall load is shared between the battery and the fuel cell system yielded further improvements in fuel economy.

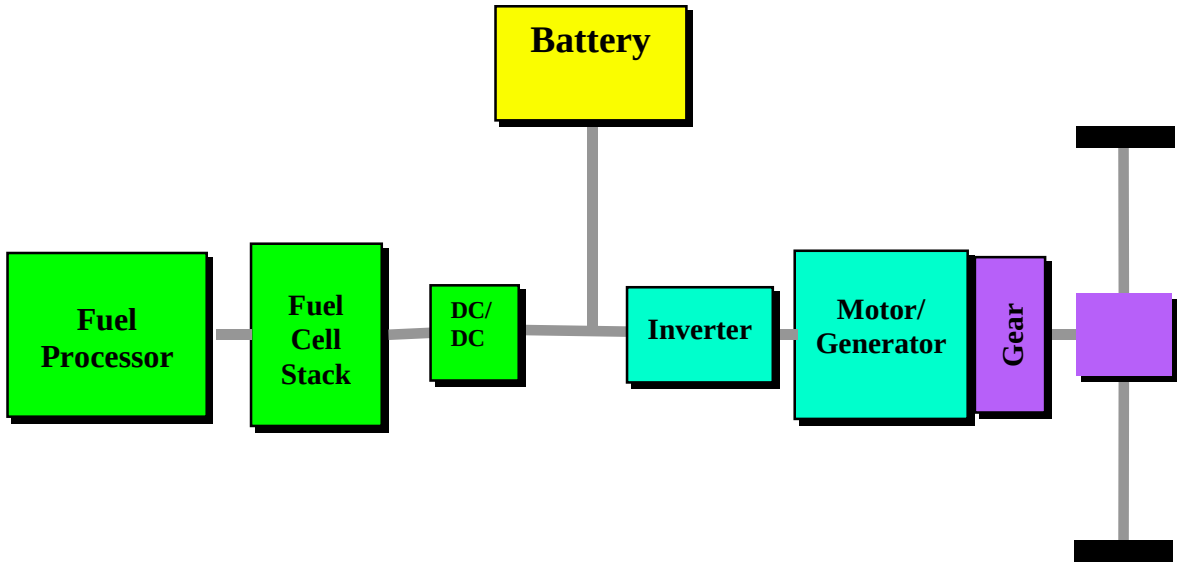

Figure 2-31 Fuel Cell/Fuel Processor HEV Architecture

2.2.2.4 Estimation of Vehicle Criteria Emissions Factors

Tier 2 standards for passenger cars and LDTs up to 8,500 lb GVW were adopted by EPA in 2001 (EPA 2000). These regulations phase in from 2004 through 2009. The Tier 2 standards established a number of "bins," with separate full-useful-life emission standards, as shown in Table 2-13. The regulations also established a fleet-average NO_x standard of 0.07 g/mi, which will gradually be phased in from 2004 to 2009. The fleet-average requirement allows manufacturers to design different vehicles to fit different emission standard bins, as long as the sales-weighted average NO_x emissions meet the average NO_x standards. The average NO_x level coincides with the "Bin 5" NO_x emission standard. EPA anticipated that, in the early years of the program, some heavier LDTs and sport utility vehicles (SUVs) would be certified to the higher emission bins, while lighter passenger cars would be certified to the lower bins. When the 0.07 NO_x average is fully phased in (2009), however, very few vehicle models (especially top-selling models) can be certified to the higher bins, because a fleet having a significant fraction of its vehicles in the higher bins would not meet the 0.07 g/mi. NO_x average standard. In implementing the Tier 2 emission standards, EPA also lowered the evaporative emission standards. The evaporative standard for a heavy light-duty truck (EPA's light-duty truck 3 class) under the Tier 2 requirements is 0.95 g/test, which includes a 3-day diurnal test and a hot soak test.

California also established stringent emissions standards for light-duty vehicles and trucks in its LEV II regulations (California Air Resources Board 1999). The various LEV categories are: low-emission vehicles (LEVs), ultra-low emission vehicles (ULEVs), and super ultra low emission vehicles (SULEVs). These emission categories overlap with the Tier 2 bins, as shown in Table 2-13.

2.2.2.4.1 Assumed Tier 2 Bin Standards for Vehicle Propulsion Systems

For the TTW portion of the study, emissions standards were selected for the various propulsion types to simulate the on-road emissions performance of different vehicle technologies, so that on-road emissions could be evaluated for WTW emission analysis. Table 2-14 shows the emission standards that were assumed for the various propulsion systems.

Table 2-13 Tier 2 Full-Useful-Life Exhaust Emission Standards (g/mi)

Bin	NO_x	NMOG[a]	CO	HCHO[a]	PM	Equivalent California LEV II NO_x Standard
8	0.20	0.125	4.2	0.018	0.02	None
7	0.15	0.090	4.2	0.018	0.02	None
6	0.10	0.090	4.2	0.018	0.01	None
5	0.07	0.090	4.2	0.018	0.01	LEV
4	0.04	0.070	2.1	0.011	0.01	ULEV
3	0.03	0.055	2.1	0.011	0.01	None
2	0.02	0.010	2.1	0.004	0.01	SULEV
1	0.00	0.000	0.0	0.000	0.00	ZEV

[a] NMOG = non-methane organic gas; HCHO = formaldehyde.

Table 2-14 Emission Standards Assumed for Hybrid and Non-Hybrid Propulsion Systems

Propulsion System	Tier 2 Exhaust Emissions Bin			Evaporative	Tire and Brake Wear
	VOC and CO	NO_x	PM	VOC	PM
Gasoline DOD SI engine	Bin 5	Bin 5	Bin 5	Tier 2 Evap	Bin 5/2/1
Gasoline DI SI engine	Bin 5	Bin 5	Bin 5	Tier 2 Evap	Bin 5/2/1
Diesel DI CI engine	Bin 5	Bin 5	Bin 5	Zero	Bin 5/2/1
E85 flexible-fuel DOD SI engine	Bin 5	Bin 5	Bin 5	Tier 2 Evap	Bin 5/2/1
CNG DOD SI engine	Bin 5	Bin 5	Bin 5	Zero	Bin 5/2/1
Hydrogen DOD SI engine	Bin 2	Bin 5/2	Bin 2	Zero	Bin 5/2/1
Gasoline/naphtha FP fuel cell	Bin 2	Bin 2	Bin 2	Tier 2 Evap	Bin 5/2/1
Methanol FP fuel cell	Bin 2	Bin 2	Bin 2	Tier 2 Evap	Bin 5/2/1
Ethanol FP fuel cell	Bin 2	Bin 2	Bin 2	Tier 2 Evap	Bin 5/2/1
Hydrogen fuel cell	Bin 1	Bin 1	Bin 1	Zero	Bin 5/2/1

Bin 5 (LEV) was selected for all exhaust emissions for the gasoline SI systems because Bin 5 matches the average Tier 2 NO_x emission standard. As indicated above, we maintained comparable vehicle performance requirements for all propulsion systems; therefore, standards for all of the propulsion systems were required to be at Bin 5 or lower. Meeting Bin 5 NO_x and PM standards will be most challenging for the diesel propulsion system. On the other hand, diesel vehicles have the advantage of not having evaporative VOC emissions.

Some propulsion systems have inherent emissions advantages compared with the baseline gasoline system. For example, the engine-out emissions of hybrid systems tend to be somewhat lower because engine-out emissions tend to scale with fuel consumption. However, this advantage is offset by the need for more frequent starts, so all hybrid systems were assumed to meet the same standards as their conventional drive counterparts. Besides generating zero evaporative VOC emissions, CNG may also have other inherent emissions advantages relative to gasoline, but we also assumed Bin 5 for CNG, reasoning that the advantage of CNG will be smaller at the very low Tier 2 standards and can be offset by using a less costly aftertreatment system.

The hydrogen SI engine will inherently have substantially lower VOC, CO, and PM emissions than the gasoline SI engine, because hydrogen fuel does not contain carbon. Because of lubricant combustion, however, VOC, CO, and PM emissions will not be zero, so we assumed Bin 2. For production of a full-size truck fleet, which is the basis of this study, it is appropriate to assume a less-costly Bin 5 NO_x emissions system for hydrogen SI vehicles. NO_x emissions can be quite low when hydrogen SI engines are operated under lean conditions and at low loads, but they are similar to gasoline NO_x emissions when the engine is operated near peak power (Natkin et al. 2003). Emission control systems are available to allow full certification of hydrogen SI engines at the Bin 2 level. Automobile makers might use this strategy to sell hydrogen SI engines in a niche application and to earn partial ZEV credits in California. For this reason, we established another case in which hydrogen SI engines meet the Bin 2 NO_x standard. Hydrogen internal combustion-engine-powered vehicles do not have evaporative VOC emissions.

The fuel processor fuel cell systems will produce emissions that are inherently lower than those of an ICE vehicle, but these emissions would not be zero. Bin 2 exhaust emissions were assumed for these fuel processor systems. The hydrogen fuel cell system will not emit any of the regulated pollutants, so Bin 1 (ZEV) exhaust emissions were assumed.

All of the propulsion systems using volatile liquid fuels (gasoline, methanol, and ethanol) were assumed to meet the Tier 2 evaporative standard. All other vehicles (hydrogen, CNG, and diesel) are assumed to have zero evaporative emissions.

Table 2-14 also lists assumptions for PM emissions caused by brake and tire wear. Such wear is independent of the certification emissions bin and of the propulsion system technology. We have shown this in Table 2-14 by indicating Bin 5/2/1 for tire and brake wear-related PM emissions for all vehicles. One could argue that PM emissions caused by brake wear could be reduced by using hybrid configurations because of braking energy recovery or that emissions caused by tire wear could be affected by changes in vehicle weight. However, we expect that such changes in PM emissions caused by brake and tire wear would be small.

2.2.2.4.2 On-Road Vehicle Emission Modeling

On-road emissions (VOC, CO, NO_x, and PM_{10}) for Bin 5 and Bin 2 vehicles were estimated by using both the MOBILE6.2 model (EPA 2003) and the EMFAC2002 model (CARB 2004). The modeling of emissions in this study could have been performed by using only one of the models, but the two available models produce quite different results for the same vehicle technology. Choosing only one of the models to make these estimates would have required an arbitrary decision. Further discussion of the models and methods used is provided below.

MOBILE6.2 allows the user to input Tier 2 bin phase-in fractions. The Tier 2 bin fractions were set to either 100% Bin 5 (LEVs) or 100% Bin 2 (SULEVs) for light-duty truck class 3 vehicles. Our WTW study is based on the lifetime emissions of a 2010-MY truck. The TTW emissions analysis was run assuming calendar year (CY) 2016 — the lifetime mileage midpoint of a 2010-MY truck. In 2016, the model indicates that 2010-MY LDTs will have accumulated about 85,000 mi. Exhaust PM_{10}, brake wear PM_{10}, and tire wear PM_{10} were also evaluated by using MOBILE6.2. The modeling effort assumed an onboard diagnostic (OBD) system, an inspection and maintenance (I&M) program, reformulated gasoline, a fuel Reid vapor pressure (RPV) of 6.8 psi, and diurnal temperatures of 72°F to 92°F.

For EMFAC, the technology fractions were again set to either 100% LEVs or 100% SULEVs, and the model was run in 2016 for the South Coast Air Basin to simulate the mid-point emissions performance of a 2010-MY vehicle.

Modeling results for VOCs, CO, and NO_x are listed in Table 2-15. Emission rates (in g/mi) generated by the MOBILE6.2 model for both Bin 5 and Bin 2 vehicles are much higher than those generated by EMFAC. EMFAC emission rates for exhaust VOCs, CO, and NO_x are typically less than 20% of the MOBILE6.2 emission rates. Evaporative VOC rates for EMFAC are about 50% of the MOBILE6 emission rates. Although there is a difference in CO standards between Bin 2 and SULEV (the Bin 2 CO standard is 2.1 g/mi; the SULEVII standard is 1.0 g/mi), we do not believe that this is the primary reason for the difference in the modeled CO emissions.

There are many differences between the two models that may cause the differences in simulated emissions:

- Mileage accumulation rates,
- Registration distributions,
- Speed correction factors and in-use speed distributions,
- Methods for calculating deterioration emission rates and the effects of I/M programs and OBD systems on in-use emissions, and
- Fuel correction factors.

While all of these factors would contribute to differences in the two models, it is our view that the major difference between the model predictions for these vehicles is attributable to different assumptions concerning the emission deterioration of these vehicles over the life of vehicles.

Table 2-16 shows PM_{10} emission factors from both models. In this comparison, the EMFAC PM_{10} exhaust emission rates are higher than those generated by MOBILE6.2, EMFAC brake wear emissions are lower, and tire wear emissions from the two models are about the same. Overall, EMFAC PM emission rates for both Bin 5 and Bin 2 vehicles are 75% higher than MOBILE6.2 rates. This is because the EMFAC model incorporates a modest amount of deterioration in exhaust PM, whereas the MOBILE6.2 model assumes that there is no deterioration in exhaust PM for gasoline vehicles. Although Bin 1 was not modeled, Table 2-16 shows our PM assumptions for Bin 1 — zero PM exhaust emissions but brake and tire PM emissions equal to those of Bin 5 and Bin 2.

Table 2-15 Emission Results of 2010-MY Bin 5 and Bin 2 Light-Duty Truck 3 Vehicles in CY 2016 Generated by MOBILE6.2 and EMFAC2002 (in g/mi)

Technology	Model	Exhaust VOC	Evaporative VOC	CO	NO_x
Bin 5	EMFAC (LEV)	0.0339	0.0590	1.278	0.068
	MOBILE6.2	0.2283	0.1187	9.226	0.353
Bin 2	EMFAC (SULEV)	0.0085	0.0590	0.474	0.034
	MOBILE6.2	0.1439	0.1187	6.168	0.294

Table 2-16 PM_{10} Emissions of 2010-MY Bin 5 and Bin 2 Gasoline Light-Duty Truck 3 Vehicles in CY 2016 Generated by MOBILE6.2 and EMFAC2002 (g/mi)

Technology	Model	Exhaust PM_{10}	Brake Wear PM_{10}	Tire Wear PM_{10}	Total PM_{10}
Bin 5 (LEV)	EMFAC	0.0254	0.0085	0.0085	0.0424
	MOBILE6.2	0.0037	0.0125	0.0080	0.0242
Bin 2 (SULEV)	EMFAC	0.0254	0.0085	0.0085	0.0424
	MOBILE6.2	0.0037	0.0125	0.0080	0.0242
Bin 1 (ZEV)	EMFAC	0.0000	0.0085	0.0085	0.0170
	MOBILE6.2	0.0000	0.0125	0.0080	0.0205

2.2.2.4.3 Establishment of Emission Distribution Functions with MOBILE and EMFAC Results

By using the on-road vehicular emissions generated by MOBILE6.2 and EMFAC, we developed probability distribution functions for each pollutant and vehicle technology. The distributions were based on emission levels estimated with MOBILE6.2 and EMFAC, future trends of on-road vehicle emission performance, the type of emission control systems installed, efforts to control on-road emissions (such as implementation of the I&M programs and the OBD II systems), and durability requirements for emission controls, among other factors.

We developed the distribution functions for TTW emissions using the gamma function and Crystal Ball™ software. In all cases, except for PM_{10} exhaust emissions, we used EMFAC-estimated emission values as P10 values (10% probability that emissions will be below this value) and MOBILE6.2-estimated values as P90 values (90% probability that emissions will be below this value). MOBILE6.2 estimates are based on an in-use deterioration rate that, in our judgment, is too high for the bulk of the population of future vehicles, which will all be equipped with sophisticated OBD systems. We believe that the emission performance of future vehicles will be closer to EMFAC-estimated values than to MOBILE-estimated values. Thus, we assigned P50 values (50% probability that emissions will be below this value) closer to P10 values. On the basis of these assumptions, we used the Crystal Ball™ software to develop probability distribution functions in Microsoft Excel. The functions we developed were eventually used in our WTW emissions simulations. An example distribution for TTW propulsion systems meeting Bin 5 NO_x emissions is shown in Figure 2-32.

Refueling emissions were also added to the evaporative emission rates. Refueling emissions are not estimated in EMFAC (they are considered part of the area source inventory), but they are estimated in MOBILE6.2. All vehicles would have onboard refueling vapor recovery (ORVR) systems; MOBILE6.2 estimates refueling emissions from vehicles equipped with ORVR systems at 0.02 g/mi. The refueling estimate of 0.02 g/mi was therefore added to the evaporative emissions. Table 2-17 shows the parameters for gamma distribution functions we established for vehicular emissions for all emission components.

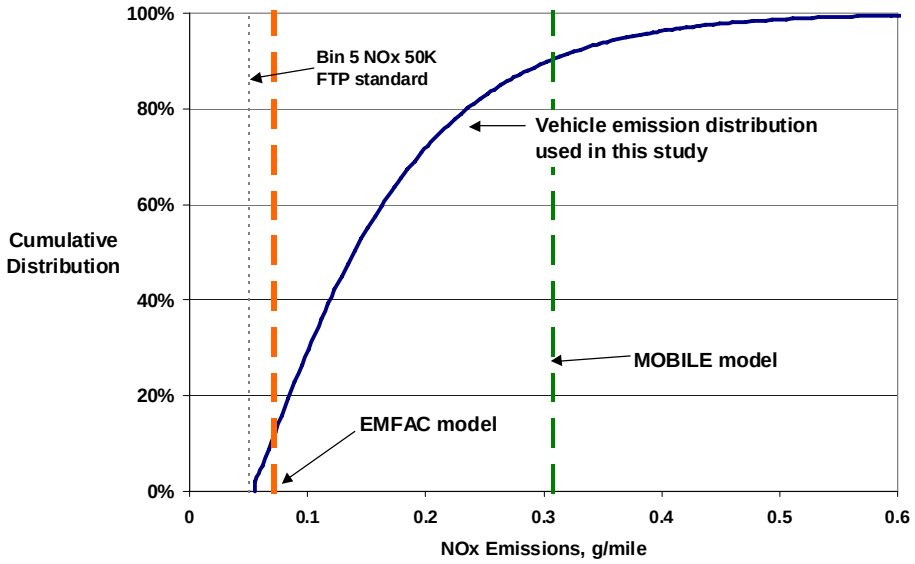

Figure 2-32 Emissions Distribution Function for Bin 5 Vehicle NO_x Emissions

Table 2-17 Parameters of Vehicular Emission Distributions Based on Gamma Distribution Function

Vehicle Type and Pollutant	Emissions (g/mi)		
	P10	**P50**	**P90**
Gasoline DOD SI CD, Gasoline SI DI CD, E85 DOD SI CD, Gasoline DOD SI HEV, Gasoline SI DI HEV, and E85 DOD SI HEV (Bin 5)			
Exhaust VOC	0.0339	0.0950	0.2283
Evaporative and refueling VOCs	0.0590	0.0790	0.1187
Exhaust CO	1.2778	3.9000	9.2262
Exhaust NO_x	0.0677	0.1540	0.3534
Exhaust PM_{10}	0.0037	0.0104	0.0254
Brake and tire wear PM_{10}[a]	Not available	0.0188	Not available
Diesel CI DI CD, CNG DOD SI CD, Diesel CI DI HEV, and CNG DOD SI HEV (Bin 5)			
Exhaust VOC	0.0339	0.0950	0.2283
Evaporative and refueling VOCs	Not needed	0.0000	Not needed
Exhaust CO	1.2778	3.9000	9.2262
Exhaust NO_x	0.0677	0.1540	0.3534
Exhaust PM_{10}	0.0037	0.0104	0.0254
Brake and tire wear PM_{10}[a]	Not available	0.0188	Not available

Table 2-17 (Cont.)

Vehicle Type and Pollutant	Emissions (g/mi)		
	P10	P50	P90
H_2 DOD SI CD and HEV (Bin 5/Bin2)[b]			
Exhaust VOC	0.0085	0.0654	0.1439
Evaporative and refueling VOCs	Not needed	0.0000	Not needed
Exhaust CO	0.4739	2.3000	6.1685
Exhaust NO_x	0.0677/0.0339	0.1540/0.1100	0.3534/0.2936
Exhaust PM_{10}	0.0037	0.0104	0.0254
Brake and tire wear PM_{10}[a]	Not available	0.0188	Not available
Gasoline, Methanol, and Ethanol FCV (Bin 2)			
Exhaust VOC	0.0085	0.0654	0.1439
Evaporative and refueling VOCs	0.0590	0.0790	0.1187
Exhaust CO	0.4739	2.3000	6.1685
Exhaust NO_x	0.0339	0.1100	0.2936
Exhaust PM_{10}	0.0037	0.0104	0.0254
Brake and tire wear PM_{10}[a]	Not available	0.0188	Not available
H_2 FCV (Bin 1)			
Exhaust VOC	Not needed	0.0000	Not needed
Evaporative and refueling VOCs	Not needed	0.0000	Not needed
Exhaust CO	Not needed	0.0000	Not needed
Exhaust NO_x	Not needed	0.0000	Not needed
Exhaust PM_{10}	Not needed	0.0000	Not needed
Brake and tire wear PM_{10}[a]	Not needed	0.0188	Not needed

[a] For brake and tire wear PM_{10} emissions, no distribution function was established. Instead, the P50 value (point estimate) was used in our simulations.

[b] For H_2 SI DOD CD and HEV, besides the case that they meet Bin 5 NO_x standard, another case that they meet Bin 2 NO_x standard was simulated in our study.

2.2.2.4.4 Non-CO_2 GHG Emissions Factors

The models used for TTW criteria pollutant emissions, MOBILE and EMFAC, do not include the non-CO_2 GHG emissions of CH_4 and N_2O. Therefore, we estimated these as point estimates based on available data. Table 2-18 lists the factors used in this study. The factors for CH_4 were based on available GM vehicle emissions testing data for gasoline, diesel, E85, and CNG. The N_2O factors were based on an EPA publication (Michaels 1998) and previous versions of GREET.

2.3 Well-to-Wheels Vehicle/Fuel Systems

One hundred twenty-four WTW pathways were analyzed in this study, representing nearly all potential combinations of WTT fuel pathways and TTW vehicle propulsion systems. These included 47 different fuel pathway/powertrain combinations, 45 of which were analyzed with both non-hybrid and hybrid architectures. Ten pathways use crude-oil-derived fuels in ICEs and fuel processor fuel cell propulsion systems. Twenty-six pathways involved NA NG; 32 were based on NNA NG. Eight pathways were based on biofuels and 49 on electrolysis-derived hydrogen. The pathways and notations used are listed in Table 2-19.

Table 2-18 Assumed Vehicular Emissions Factors for CH_4 and N_2O

Vehicle Type	Emissions, g/mi	
	CH_4	N_2O
Gasoline DOD SI CD and HEV	0.0068	0.0280
Gasoline DI SI CD and HEV	0.0068	0.0280
Diesel DI CI CD and HEV	0.0068	0.0280
E85 DOD SI CD and HEV	0.0068	0.0280
CNG DOD SI CD and HEV	0.3000	0.0140
H_2 DOD SI CD and HEV	0.0065	0.0280
Gasoline FP FCV and FC HEV	0.2000	0.0056
MeOH FP FCV and FC HEV	0.0020	0.0056
EtOH FP FCV and FC HEV	0.2000	0.0056
H_2 FCV and FC HEV	0.0000	0.0000

Table 2-19 WTW Vehicle/Fuel Systems and Notation Used in this Report

Pathways	Conventional Drive	Hybrid Electric
Petroleum-Based Pathways		
Reformulated gasoline (30-ppm-S) displacement-on-demand spark-ignition	RFG DOD SI CD	RFG DOD SI HEV
Reformulated gasoline (10-ppm-S) direct-injection spark-ignition	RFG DI SI CD	RFG DI SI HEV
Diesel (15-ppm-S) direct-injection compression-ignition	LS Diesel DI CI CD	LS Diesel DI CI HEV
Gasoline (5-ppm-S) fuel processor fuel cell	Gasoline FP FCV	Gasoline FP FC HEV
Crude oil naphtha fuel processor fuel cell	Crude Naph. FP FCV	Crude Naph. FP FC HEV
NA NG Pathways		
Compressed NG displacement-on-demand spark-ignition	NA NG CNG DOD SI CD	NA NG CNG DOD SI HEV
Gaseous hydrogen (central) displacement-on-demand spark-ignition Bin 5 and Bin 2 NO_x	NA NG Central GH_2 DOD SI CD: Bin 5 NO_x	NA NG Central GH_2 DOD SI HEV: Bin 5 NO_x
	NA NG Central GH_2 DOD SI CD: Bin 2 NO_x	NA NG Central GH_2 DOD SI HEV: Bin 2 NO_x
Gaseous hydrogen (station) displacement-on-demand spark-ignition Bin 5 and Bin 2 NO_x	NA NG Station GH_2 DOD SI CD: Bin 5 NO_x	NA NG Station GH_2 DOD SI HEV: Bin 5 NO_x
	NA NG Station GH_2 DOD SI CD: Bin 2 NO_x	NA NG Station GH_2 DOD SI HEV: Bin 2 NO_x
Liquid hydrogen (central) displacement-on-demand spark-ignition Bin 5 and Bin 2 NO_x	NA NG Central LH_2 DOD SI CD: Bin 5 NO_x	NA NG Central LH_2 DOD SI HEV: Bin 5 NO_x
	NA NG Central LH_2 DOD SI CD: Bin 2 NO_x	NA NG Central LH_2 DOD SI HEV: Bin 2 NO_x

Table 2-19 (Cont.)

Pathways	Conventional Drive	Hybrid Electric
NA NG Pathways (Cont.)		
Liquid hydrogen (station) displacement-on-demand spark-ignition Bin 5 and Bin 2 NO_x	NA NG Station LH_2 DOD SI CD: Bin 5 NO_x	NA NG Station LH_2 DOD SI HEV: Bin 5 NO_x
	NA NG Station LH_2 DOD SI CD: Bin 2 NO_x	NA NG Station LH_2 DOD SI HEV: Bin 2 NO_x
Gaseous hydrogen (central) fuel cell	NA NG Central GH_2 FCV	NA NG Central GH_2 FC HEV
Gaseous hydrogen (station) fuel cell	NA NG Station GH_2 FCV	NA NG Station GH_2 FC HEV
Liquid hydrogen (central) fuel cell	NA NG Central LH_2 FCV	NA NG Central LH_2 FC HEV
Liquid hydrogen (station) fuel cell	NA NG Station LH_2 FCV	NA NG Station LH_2 FC HEV
NNA NG Pathways		
Compressed NG displacement-on-demand spark-ignition	NNA NG CNG DOD SI CD	NNA NG CNG DOD SI HEV
Fischer-Tropsch diesel direct-injection compression-ignition	NNA NG FT Diesel DI CI CD	NNA NG FT Diesel DI CI HEV
Gaseous hydrogen (central) displacement-on-demand spark-ignition Bin 5 and Bin 2 NO_x	NNA NG Central GH_2 DOD SI CD: Bin 5 NO_x	NNA NG Central GH_2 DOD SI HEV: Bin 5 NO_x
	NNA NG Central GH_2 DOD SI CD: Bin 2 NO_x	NNA NG Central GH_2 DOD SI HEV: Bin 2 NO_x
Gaseous hydrogen (station) displacement-on-demand spark-ignition Bin 5 and Bin 2 NO_x	NNA NG Station GH_2 DOD SI CD: Bin 5 NO_x	NNA NG Station GH_2 DOD SI HEV: Bin 5 NO_x
	NNA NG Station GH_2 DOD SI CD: Bin 2 NO_x	NNA NG Station GH_2 DOD SI HEV: Bin 2 NO_x
Liquid hydrogen (central) displacement-on-demand spark-ignition Bin 5 and Bin 2 NO_x	NNA NG Central LH_2 DOD SI CD: Bin 5 NO_x	NNA NG Central LH_2 DOD SI HEV: Bin 5 NO_x
	NNA NG Central LH_2 DOD SI CD: Bin 2 NO_x	NNA NG Central LH_2 DOD SI HEV: Bin 2 NO_x
Liquid hydrogen (station) displacement-on-demand spark-ignition Bin 5 and Bin 2 NO_x	NNA NG Station LH_2 DOD SI CD: Bin 5 NO_x	NNA NG Station LH_2 DOD SI HEV: Bin 5 NO_x
	NNA NG Station LH_2 DOD SI CD: Bin 2 NO_x	NNA NG Station LH_2 DOD SI HEV: Bin 2 NO_x
Gaseous hydrogen (central) fuel cell	NNA NG Central GH_2 FCV	NNA NG Central GH_2 FC HEV
Gaseous hydrogen (station) fuel cell	NNA NG Station GH_2 FCV	NNA NG Station GH_2 FC HEV
Liquid hydrogen (central) fuel cell	NNA NG Central LH_2 FCV	NNA NG Central LH_2 FC HEV
Liquid hydrogen (station) fuel cell	NNA NG Station LH_2 FCV	NNA NG Station LH_2 FC HEV
Methanol fuel processor fuel cell	NNA NG MeOH FP FCV	NNA NG MeOH FC HEV
Fischer-Tropsch naphtha fuel processor fuel cell	NNA NG FT Naph. FP FCV	NNA NG FT Naph. FP FC HEV

Table 2-19 (Cont.)

Pathways	Conventional Drive	Hybrid Electric
Renewable and Electricity Pathways		
Corn 85% ethanol spark-ignition flexible-fuel displacement-on-demand	Corn E85 DOD SI CD	Not included
Cellulosic 85% ethanol spark-ignition flexible-fuel displacement-on-demand	Cell. E85 DOD SI CD	Cell. E85 DOD SI HEV
Corn ethanol fuel processor fuel cell	Corn EtOH FP FCV	Corn EtOH FP FC HEV
Cellulosic ethanol fuel processor fuel cell	Cell. EtOH FP FCV	Cell. EtOH FP FC HEV
U.S. mix electrolysis gaseous hydrogen spark-ignition Bin 5 and Bin 2 NO_x	Elecro. GH_2 DOD SI CD: U.S. kWh, Bin 5 NO_x	Elecro. GH_2 DOD SI HEV: U.S. kWh, Bin 5 NO_x
	Elecro. GH_2 DOD SI CD: U.S. kWh, Bin 2 NO_x	Elecro. GH_2 DOD SI HEV: U.S. kWh, Bin 2 NO_x
CA mix electrolysis gaseous hydrogen spark-ignition Bin 5 and Bin 2 NO_x	Elecro. GH_2 DOD SI CD: CA kWh, Bin 5 NO_x	Elecro. GH_2 DOD SI HEV: CA kWh, Bin 5 NO_x
	Elecro. GH_2 DOD SI CD: CA kWh, Bin 2 NO_x	Elecro. GH_2 DOD SI HEV: CA kWh, Bin 2 NO_x
NA NG combined-cycle electrolysis gaseous hydrogen spark-ignition Bin 5 and Bin 2 NO_x	Electro. GH_2 DOD SI CD: NA NG CC kWh, Bin 5 NO_x	Electro. GH_2 DOD SI HEV: NA NG CC kWh, Bin 5 NO_x
	Electro. GH_2 DOD SI CD: NA NG CC kWh, Bin 2 NO_x	Electro. GH_2 DOD SI HEV: NA NG CC kWh, Bin 2 NO_x
U.S. mix electrolysis liquid hydrogen spark-ignition Bin 5 and Bin 2 NO_x	Elecro. LH_2 DOD SI CD: U.S. kWh, Bin 5 NO_x	Elecro. LH_2 DOD SI HEV: U.S. kWh, Bin 5 NO_x
	Elecro. LH_2 DOD SI CD: U.S. kWh, Bin 2 NO_x	Elecro. LH_2 DOD SI HEV: U.S. kWh, Bin 2 NO_x
CA mix electrolysis liquid hydrogen spark-ignition Bin 5 and Bin 2 NO_x	Elecro. LH_2 DOD SI CD: CA kWh, Bin 5 NO_x	Elecro. LH_2 DOD SI HEV: CA kWh, Bin 5 NO_x
	Elecro. LH_2 DOD SI CD: CA kWh, Bin 2 NO_x	Elecro. LH_2 DOD SI HEV: CA kWh, Bin 2 NO_x
NA NG combined-cycle electrolysis liquid hydrogen spark-ignition Bin 5 and Bin 2 NO_x	Electro. LH_2 DOD SI CD: NA NG CC kWh, Bin 5 NO_x	Electro. LH_2 DOD SI HEV: NA NG CC kWh, Bin 5 NO_x
	Electro. LH_2 DOD SI CD: NA NG CC kWh, Bin 2 NO_x	Electro. LH_2 DOD SI HEV: NA NG CC kWh, Bin 2 NO_x
U.S. mix electrolysis gaseous hydrogen fuel cell	Electro. GH_2 FCV: U.S. kWh	Electro. GH_2 FC HEV: U.S. kWh
CA mix electrolysis gaseous hydrogen fuel cell	Electro. GH_2 FCV: CA kWh	Electro. GH_2 FC HEV: CA kWh
NG combined-cycle electrolysis gaseous hydrogen fuel cell	Electro GH_2 FCV: NA NG CC kWh	Electro GH_2 FC HEV: NA NG CC kWh
U.S. mix electrolysis liquid hydrogen fuel cell	Electro. LH_2 FCV: U.S. kWh	Electro. LH_2 FC HEV: U.S. kWh
CA mix electrolysis liquid hydrogen fuel cell	Electro. LH_2 FCV: CA kWh	Electro. LH_2 FC HEV: CA kWh

Table 2-19 (Cont.)

Pathways	Conventional Drive	Hybrid Electric
Renewable and Electricity Pathways (Cont.)		
NG combined-cycle electrolysis liquid hydrogen fuel cell	Electro LH_2 FCV: NA NG CC kWh	Electro LH_2 FC HEV: NA NG CC kWh
Electrolysis renewable electricity gaseous hydrogen FCV	Electro. GH_2 FCV: Renew. kWh	Not included
U.S. mix electrolysis gaseous hydrogen spark-ignition Bin 5 and Bin 2 NO_x adopted IAQR	Elecro. GH_2 DOD SI CD: U.S. kWh, Bin 5 NO_x, adopted IAQR	Elecro. GH_2 DOD SI HEV: U.S. kWh, Bin 5 NO_x, adopted IAQR
	Elecro. GH_2 DOD SI CD: U.S. kWh, Bin 2 NO_x, adopted IAQR	Elecro. GH_2 DOD SI HEV: U.S. kWh, Bin 2 NO_x, adopted IAQR
U.S. mix electrolysis gaseous hydrogen fuel cell adopted IAQR	Electro. GH_2 FCV: U.S. kWh, adopted IAQR	Electro. GH_2 FC HEV: U.S. kWh, adopted IAQR
U.S. mix electrolysis liquid hydrogen spark-ignition Bin 5 and Bin 2 NO_x adopted IAQR	Elecro. LH_2 DOD SI CD: U.S. kWh, Bin 5 NO_x, adopted IAQR	Elecro. LH_2 DOD SI HEV: U.S. kWh, Bin 5 NO_x, adopted IAQR
	Elecro. LH_2 DOD SI CD: U.S. kWh, Bin 2 NO_x, adopted IAQR	Elecro. LH_2 DOD SI HEV: U.S. kWh, Bin 2 NO_x, adopted IAQR
U.S. mix electrolysis liquid hydrogen fuel cell adopted IAQR	Electro. LH_2 FCV: U.S. kWh, adopted IAQR	Electro. LH_2 FC HEV: U.S. kWh, adopted IAQR

3. TANK-TO-WHEELS SIMULATED FUEL ECONOMY AND PERFORMANCE RESULTS

The methodology described in Section 2 was consistently implemented in designing each of the technologies using validated component models and input data and assumptions reflecting realistic vehicle operating constraints. Outputs of this study, summarized in the following tables, include vehicle fuel economy and acceleration performance predictions. The tables include the fuel economy in gasoline-equivalent mpg on the EPA urban and highway driving cycles, and the 0–60 mph acceleration performance time. Also included are urban/highway composite vehicle fuel economy and efficiencies, as defined in Figure 2-26, and the percent gain in fuel economy of each concept over the baseline vehicle.

The fuel economy predictions for the baseline vehicle on the urban and highway driving cycles are within the range of the EPA published ratings for a truck in the 4,750-lb test weight class.

The vehicle mass for each of the technologies was adjusted by the scale factors used for sizing the components. Thus, without disclosing specific proprietary component mass information, increases in test weight classes for the advanced technologies range (from the best- to the worst-case scenarios) from ~3% to 20% for the fuel cell systems with onboard hydrogen storage and between ~10% and 30% for the reformer vehicles. The hybrid powertrain systems increase mass from 0% and 10% for ICE parallel HEVs (0% meaning that the mass of an ICE HEV would not change relative to that of a conventional vehicle), from ~7% and 24% for fuel cell HEVs, and from ~16% and 34% for the reformer HEVs.

3.1 Fuel Economy and Performance Results

Tables 3-1 and 3-2 present the results for the conventional drive and the hybridized ICE propulsion systems. All fuel economies are reported as mpg of gasoline-equivalent energy (115,500 Btu/gal gasoline equivalent).

The baseline vehicle with a DOD engine demonstrated a composite fuel economy gain of ~ 5% over the 20.2-mpg fuel economy of the baseline technology estimated in the Phase 1 study. On the basis of GM data indicating that an ICE running on E85 operates at the same engine efficiency as its equivalent gasoline ICE, the E85 fuel economy (mpg gasoline equivalent) was equal to that for gasoline. A similar

Table 3-1 Best-Estimate Vehicle Fuel Economy Results for ICE CD Propulsion Systems

Propulsion System	Fuel Economy, mpg gasoline equivalent				0–60 mph Acceleration Time, s	Vehicle Efficiency, %
	Urban	Highway	Composite	Change, %		
Gasoline DOD SI CD Baseline[a]	18.5	26.2	21.3	—	7.9	17.7
Gasoline DI SI CD	21.5	28.7	24.2	14	7.9	20.6
Diesel DI CI CD	22.7	30.9	25.8	21	7.9	21.1
E85 DOD SI CD	18.5	26.2	21.3	0	7.9	17.7
CNG DOD SI CD	18.1	25.9	21.0	-1	8.2	17.9
H_2 DOD SI CD	22.5	31.5	25.6	21	7.9 s	21.3

[a] The fuel economy of the Phase 1 baseline technology (without DOD) was 20.2 mpg composite.

Table 3.2 Best-Estimate Vehicle Fuel Economy and Performance Results for ICE Parallel HEV Propulsion Systems with Charge-Sustaining Control Strategy

Propulsion System (see)	Fuel Economy, mpg gasoline equivalent				0–60 mph Acceleration Time, s	Vehicle Efficiency, %
	Urban	Highway	Composite	Change, %		
Gasoline DOD SI Baseline	18.5	26.2	21.3	—	7.9	18
Gasoline DOD SI HEV	25.9	27.2	26.5	24	6.2[a] – 8.0[b]	23
Gasoline DI SI HEV	29.2	29.3	29.2	37	6.2[a] – 8.0[b]	26
Diesel DI CI HEV	30.7	31.1	30.8	45	6.2[a] – 8.0[b]	26
E85 DOD SI HEV	25.9	27.2	26.5	24	6.2[a] – 8.0[b]	23
CNG DOD SI HEV	24.8	26.2	25.4	19	6.5[a] – 8.2[b]	23
H_2 DOD SI HEV	30.6	32.9	31.6	48	6.3[a] – 8.0[b]	27

[a] Fully charged battery.
[b] Fully discharged battery.

assumption regarding engine efficiency was also made for the dual-fuel CNG ICE. However, in order to maintain the same vehicle driving range as the baseline vehicle, the size of the fuel tank was increased, which imposed a penalty on vehicle mass and had a minor deleterious effect on fuel economy.

The DI SI gasoline engine was optimized over its stratified and homogeneous operating regions, while meeting emission requirements, resulting in a potential fuel economy gain of 14%. The DI diesel engine was scaled (4.7 L engine displacement) to meet the same top vehicle speed, resulting in a 21% gain in fuel economy on a gasoline-equivalent basis.

An efficiency map of the ICE running on hydrogen was not as readily available as maps for the other technologies and was thus created on the basis of information available in the literature. With the operating conditions optimized, increased compression ratio and the engine operating at steady state, theoretical thermal efficiency approaches 50% (Natkin et al. 2002; Eichlseder et al. 2003). However, when accounting for friction, heat, and pumping losses, as well as partial-load operation on the duty cycle, the brake thermal efficiency of our modeled engine yielded an estimated 5 percentage points higher efficiency than the same engine operating on gasoline. However, because of the low volumetric efficiency and combustion limitations, the maximum power of hydrogen engines is substantially lower than that of gasoline engines. Our simulation of hydrogen engine technology, based on estimated engine efficiency and scaling of engine power to meet the vehicle performance requirements, yielded about a 21% gain in gasoline-equivalent fuel economy.

The benefits attributable to hybridizing these engine technologies, under the control strategy assumption presented above, resulted in significant fuel economy gains while maintaining vehicle performance. These control strategies were tailored to each engine technology to take maximum advantage of the synergies between the hybrid architecture and the engine characteristics. The results show that, as the efficiency of the powertrain increases, the magnitude of the benefit attributable to hybridization decreases. In particular, benefits of hybridization are reduced for engine technologies with high efficiency at part load.

Table 3-2 also presents the performance (0–60 mph acceleration time) depending on availability of the battery to provide power assist. The lower acceleration time represents a fully charged battery, and the higher time represents no battery assist.

Table 3-3 shows results for FCV systems with onboard fuel processors and those with onboard liquid and gaseous hydrogen, all with both conventional drive and hybrid drive. Separate fuel processor efficiency maps were used for gasoline, methanol, and ethanol fuel processors. As noted previously, because of the efficiency characteristics of the fuel cell in contrast to those of an ICE, the relative gains these hybrids demonstrated were less than those for the ICE hybrids.

Table 3-3 Best-Estimate Vehicle Fuel Economy and Performance Results for Fuel Processor Fuel Cells and Hydrogen Fuel Cells with Conventional and Hybrid Electric Drives

Propulsion System	Fuel Economy, mpg gasoline equivalent				0–60 mph Acceleration Time, s	Vehicle Efficiency, %
	Urban	Highway	Composite	Change, %		
Gasoline DOD SI CD Baseline	18.5	26.2	21.3	—	7.9	18
Gasoline/naphtha FP FCV	29.9	35.4	32.2	51	9.9	28
Gasoline/naphtha FP FC HEV	38.5	36.4	37.5	76	9.2	34
MeOH FP FCV	32.7	38.7	35.2	65	9.9	31
MeOH FP FC HEV	41.8	39.6	40.8	92	9.1	37
EtOH FP FCV	29.9	35.4	32.2	51	9.9	28
EtOH FP FC HEV	38.5	36.4	37.5	76	9.2	34
H_2 FCV	49.4	52.6	50.8	139	9.6	43
H_2 FC HEV	58.5	53.3	56.1	163	8.4	48

The fuel economy results listed in Tables 3-1 through 3-3 represent the best-estimate scenarios; Table 3-4 also includes the best-case and worst-case scenario predictions. These predictions were also generated by using simulation models and are based on input data and assumptions that capture the uncertainties of the various technologies.

The worst-case scenarios for the conventional drive vehicles assumed that the current state-of-the-art technology levels (no DOD) for engines and transmissions are maintained without further improvements. For the hybrids and the fuel cell system vehicles, these scenarios incorporated more pessimistic assumptions about component masses and efficiencies. The worst-case hybrid scenarios also assumed a mild hybridization strategy in which the engines would be turned off only when the vehicle was stopped. Also included in this scenario for the fuel cell HEVs was the assumption that the fuel cell system could not be shut off throughout the duty cycle.

The best-case scenarios are based on assumptions that the technologies will exceed their targets in mass and efficiency for the 2010 timeframe. In the case of conventional drive vehicles, both vehicle level and powertrain improvements were assumed. Best-case vehicle-level assumptions include reductions in mass and aerodynamic losses. For powertrains, improvements in transmission design—such as the use of wider ratio spreads, providing additional overdrive ratios, and an additional gear to maintain customer shift pleasability— were included in the best-case scenarios. For the conventional hybrids and fuel cell system vehicles, best-case scenarios incorporated reductions in component mass and improvements in operating efficiencies. In addition, the best-case scenarios for the hybrid systems included downsized engines along with concepts often referred to as strong hybridization.

The data from Table 3-4 are plotted in Figure 3-1 with the best- and worst-case scenarios superimposed on the bars. The figure illustrates that the less-mature propulsion systems with larger uncertainties are strong hybrids and fuel processor FCVs.

Table 3-4 Composite Fuel Economy Results for Best-Estimate, Best-Case, and Worst-Case Scenarios

Propulsion System	Fuel Economy, mpg gasoline-equivalent		
	Worst Case	Best Estimate	Best Case
Gasoline DOD SI CD Baseline	20.2[a]	21.3	22.4
Gasoline DI SI CD	23.2	24.2	25.4
Diesel DI CI CD	25.2	25.8	27.1
E85 DOD SI CD	20.2[a]	21.3	22.4
CNG DOD SI CD	19.9[a]	21.0	22.1
H_2 DOD SI CD	24.3[a]	25.6	26.9
Gasoline DOD SI HEV	24.5	26.5	34.0
Gasoline DI SI HEV	27.0	29.2	33.6
Diesel DI CI HEV	28.5	30.8	39.4
E85 DOD SI HEV	24.5	26.5	34.0
CNG DOD SI HEV	23.5	25.4	32.5
H_2 DOD SI HEV	29.2	31.6	40.5
Gasoline/naphtha FP FCV	25.7	32.2	36.3
Gasoline/naphtha FP FC HEV	29.5	37.5	42.2
MeOH FP FCV	28.1	35.2	39.6
MeOH FP FC HEV	32.7	40.8	45.9
EtOH FP FCV	25.7	32.2	36.3
EtOH FP FC HEV	29.5	37.5	42.2
H_2 FCV	47.6	50.8	54.5
H_2 FC HEV	52.6	56.1	59.8

[a] Engine modeled without DOD for the worst-case scenario.

Distribution functions were developed for each TTW propulsion option to describe the variation in fuel economy for the Monte Carle WTW calculations. All of the ICE fuel economies were fit using a Gamma function. For each, the 0.1 percentile was set to the worst-case value and the 99.9 percentile was set to the best-case value. The Gamma function scale parameter was adjusted so that the mean of the distribution matched the best-estimate value. Figure 3-2 displays, as an example, the distribution used for the baseline gasoline engine.

For the fuel cell systems, we found that the Weibull distribution did the best job of fitting the vehicle fuel economy results. The 0.1 percentile was set to the worst-case value and the 95th percentile was set to the best-case value. The scale parameter was adjusted to match the mean of the distribution to the best-estimate value. A sample distribution for the hydrogen fuel cell conventional drive vehicle is shown in Figure 3-3.

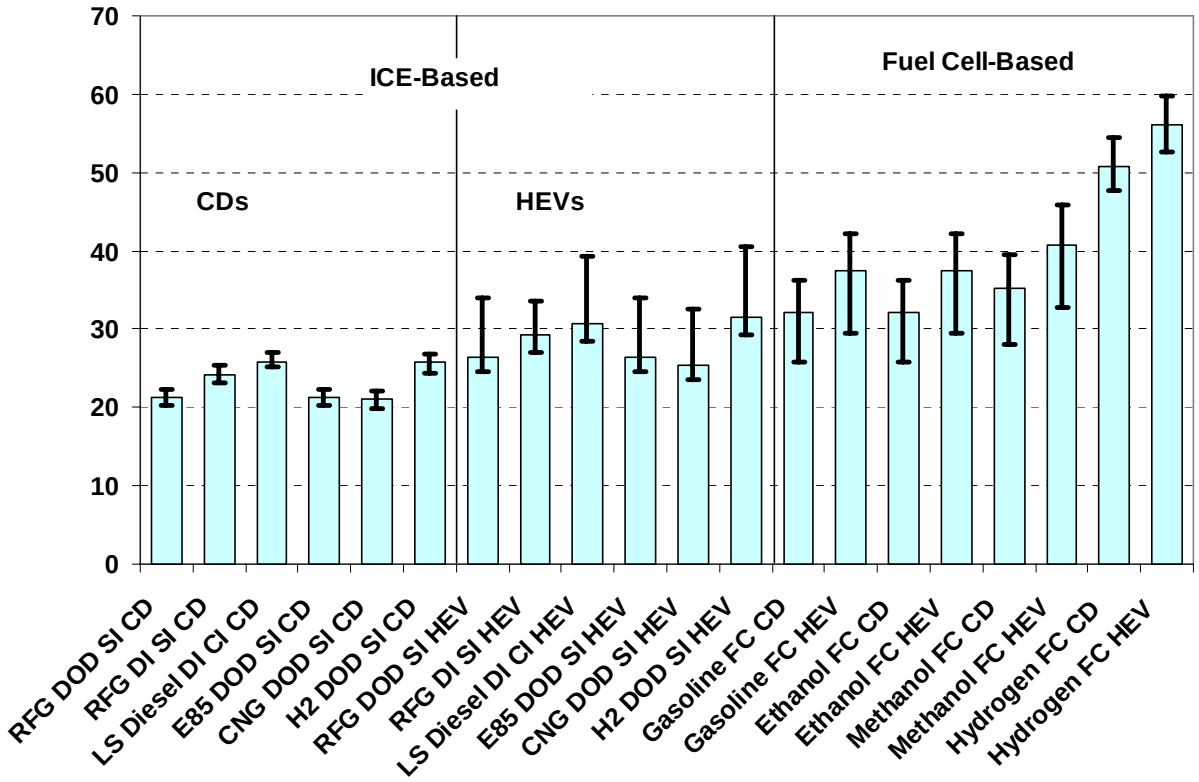

Figure 3-1 Fuel Economy Predictions with Superimposed Best-Case and Worst-Case Scenarios

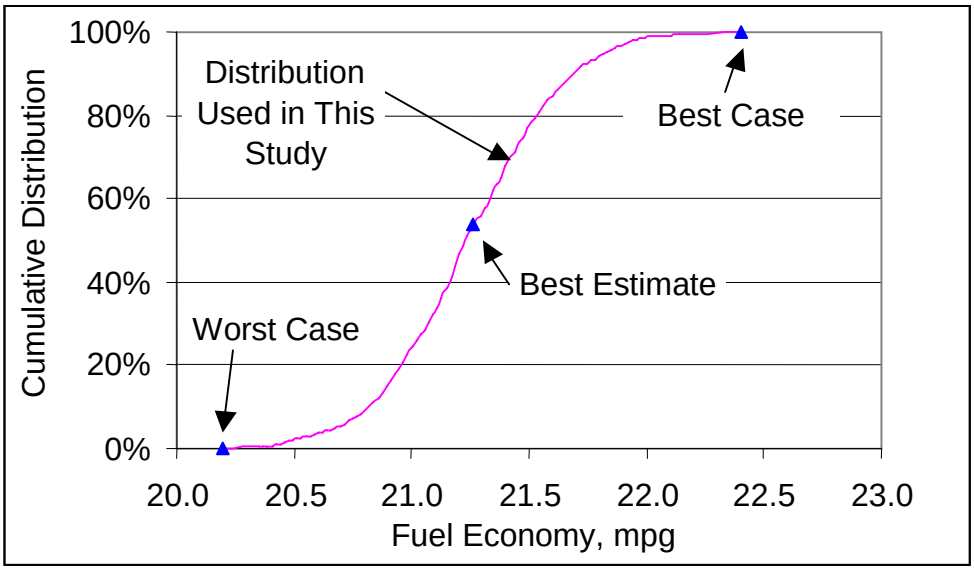

Figure 3-2 Fuel Economy Distribution for Baseline Gasoline Displacement on Demand Spark-Ignition Conventional Drive

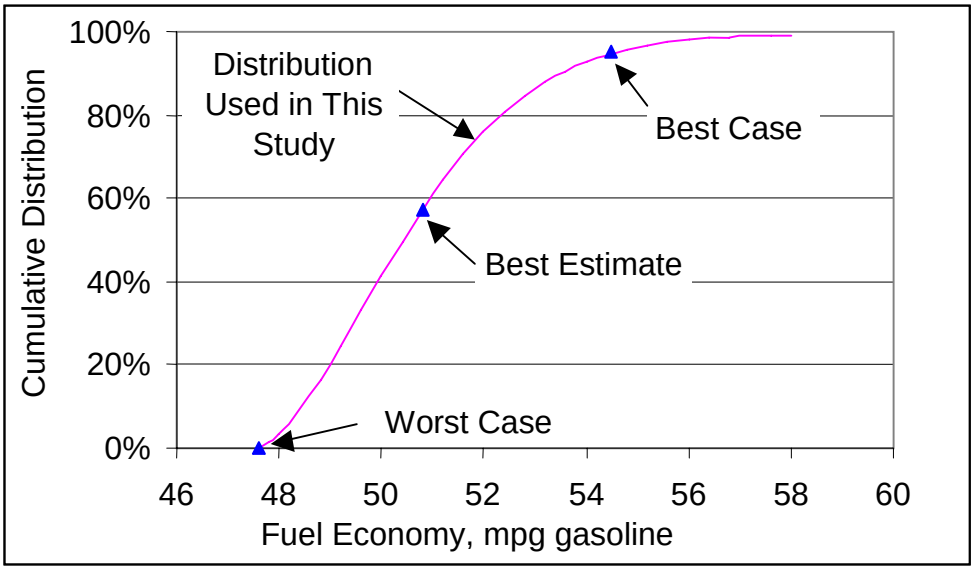

Figure 3-3 Fuel Economy Distribution for Hydrogen Fuel Cell Vehicle

3.2 Discussion of Tank-to-Wheel Fuel Economy Results

This analysis assesses the potential fuel economy benefits of numerous advanced engine technologies used in conjunction with alternative fuels and powertrain architectures. Our study included mature, production-ready technologies for improving fuel economy, such as DOD; more aggressive technologies such as DI SI, CNG, and DI diesel ICEs; and others, even more advanced technologies, such as fuel cell systems. Compliance with emission regulations was taken into account, and customer expectations of vehicle performance and drive quality were never compromised. Among the ICE technologies, the diesel engine offers the greatest benefit in fuel economy, hybridization provides additional gains for all technologies, and the onboard hydrogen fuel cell system yields the highest potential.

4. WELL-TO-WHEELS RESULTS

Section 2 described the methods we used to select and simulate fuel production pathways (WTT) and vehicle propulsion technologies (TTW). Section 3 presented fuel economy results. WTT energy and emission results for 27 fuel pathways and 2 electricity pathways with the IAQR are presented in Appendix C. In the Phase 2 study, the WTT and TTW simulations are integrated within the GREET model. Table 4-1 lists the subsections in this section where we present results for certain fuel/vehicle propulsion systems analyzed in the Phase 2 study. For each of the vehicle/fuel systems, we generated results for the 17 items listed in Table 4-2.

WTW simulations in the Phase 2 study included 84 vehicle/fuel systems with 17 items, 28 hydrogen ICE systems meeting the Bin 2 NO_X standard with 2 items (TNO_X and UNO_X); 8 systems meeting the IAQR power plant emissions with 17 items; and 4 hydrogen ICE systems meeting the IAQR power plant emissions and Bin 2 NO_X standards with 2 items. The 124 WTW options result in 1,628 individual items for which we generated probability-based output results by using GREET simulations. The results for the 1,628 items are presented in Appendix D. In this section, we present charts that illustrate the results for selected items associated with selected vehicle/fuel systems.

Section 4.1 presents results for 18 vehicle/fuel systems, selected to illustrate general trends in energy use and emissions changes that result from the use of advanced vehicle technologies and new transportation fuels. Section 4.2 explores specific issues of interest with results for selected fuel production pathway groups and for selected vehicle propulsion systems.

Table 4-1 Combinations of Fuel Production Pathways and Vehicle Propulsion Technologies Simulated in this Study

	Fuel Production Pathway	Vehicle Propulsion System	Included in Section 4.1?	Included in Section 4.2?										
				4.2.1	4.2.2	4.2.3	4.2.4	4.2.5	4.2.6	4.2.7	4.2.8	4.2.9	4.2.10	4.2.11
Oil-Based														
1	30-ppm-S RFG without oxygenate	DOD SI CD	Y	Y	Y	Y	Y	Y	Y	Y	Y	Y	Y	Y
2		DOD SI HEV	Y			Y				Y				
3	10-ppm-S RFG without oxygenate	DI SI CD	Y			Y								
4		DI SI hybrid		Y		Y	Y	Y						
5	5-ppm-S gasoline without oxygenate	FP FCV	Y			Y								
6		FP FC HEV		Y		Y		Y						
7	15-ppm-S diesel	DI CI CD	Y		Y	Y								
8		DI CI HEV	Y	Y		Y				Y				
9	Naphtha	FP FCV		Y										
10		FP FC HEV		Y			Y	Y						
NG-Based														
11	NA NG to CNG	DOD SI CD	Y		Y	Y					Y			
12		DOD SI HEV		Y		Y	Y	Y		Y	Y			
13	NNA NG to CNG via LNG	DOD SI CD									Y			
14		DOD SI HEV					Y				Y			
15	NNA NG to methanol	FP FCV	Y		Y						Y			
16		FP FC HEV		Y				Y		Y	Y			
17	NNA NG to FT diesel	DI CI CD	Y		Y	Y					Y			
18		DI CI HEV		Y		Y		Y		Y	Y			
19	NNA NG to FT naphtha	FP FCV									Y			
20		FP FC HEV						Y			Y			

Table 4-1 (Cont.)

	Fuel Production Pathway	Vehicle Propulsion System	Included in Section 4.1?	Included in Section 4.2?										
				4.2.1	4.2.2	4.2.3	4.2.4	4.2.5	4.2.6	4.2.7	4.2.8	4.2.9	4.2.10	4.2.11
NG-Based (cont.)														
21		DOD SI CD, Bin 5	Y			Y			Y		Y			Y
22		DOD SI HEV, Bin 5		Y		Y	Y	Y			Y			Y
23	NA NG to GH_2 produced in central plants	DOD SI CD, Bin 2	Y											
24		DOD SI HEV, Bin 2	Y											
25		FCV	Y		Y	Y					Y			
26		FC HEV		Y		Y	Y	Y		Y	Y			
27		DOD SI CD, Bin 5						Y	Y		Y			
28		DOD SI HEV, Bin 5					Y				Y			
29	NNA NG to GH_2 produced in central plants via LNG	DOD SI CD, Bin 2												
30		DOD SI HEV, Bin 2												
31		FCV									Y			
32		FC HEV					Y				Y			
33		DOD SI CD, Bin 5						Y	Y					Y
34		DOD SI HEV, Bin 5					Y							Y
35	NA NG to GH_2 produced in refueling stations	DOD SI CD, Bin 2												Y
36		DOD SI HEV, Bin 2												Y
37		FCV							Y					
38		FC HEV					Y							
39		DOD SI CD, Bin 5							Y					
40		DOD SI HEV, Bin 5					Y							
41	NNA NG to GH_2 produced in refueling stations via LNG	DOD SI CD, Bin 2												
42		DOD SI HEV, Bin 2												
43		FCV							Y					
44		FC HEV					Y							

Table 4-1 (Cont.)

	Fuel Production Pathway	Vehicle Propulsion System	Included in Section 4.1?	Included in Section 4.2?										
				4.2.1	4.2.2	4.2.3	4.2.4	4.2.5	4.2.6	4.2.7	4.2.8	4.2.9	4.2.10	4.2.11
NG-Based (cont.)														
45		DOD SI CD, Bin 5				Y			Y					Y
46		DOD SI HEV, Bin 5				Y	Y	Y						Y
47	NA NG to LH_2 produced in central plants	DOD SI CD, Bin 2												Y
48		DOD SI HEV, Bin 2												Y
49		FCV	Y			Y			Y					
50		FC HEV		Y		Y	Y	Y						
51		DOD SI CD, Bin 5							Y					
52		DOD SI HEV, Bin 5					Y							
53	NNA NG to LH_2 produced in central plants	DOD SI CD, Bin 2												
54		DOD SI HEV, Bin 2												
55		FCV							Y					
56		FC HEV					Y							
57		DOD SI CD, Bin 5							Y					
58		DOD SI HEV, Bin 5					Y							
59	NA NG to LH_2 produced in refueling stations	DOD SI CD, Bin 2												
60		DOD SI HEV, Bin 2												
61		FCV							Y					
62		FC HEV					Y							
63		DOD SI CD, Bin 5							Y					
64		DOD SI HEV, Bin 5					Y							
65	NNA NG to LH_2 produced in refueling stations via LNG	DOD SI CD, Bin 2												
66		DOD SI HEV, Bin 2												
67		FCV							Y					
68		FC HEV					Y							

Table 4-1 (Cont.)

	Fuel Production Pathway	Vehicle Propulsion System	Included in Section 4.1?	Included in Section 4.2?										
				4.2.1	4.2.2	4.2.3	4.2.4	4.2.5	4.2.6	4.2.7	4.2.8	4.2.9	4.2.10	4.2.11
Bioethanol														
69	Corn to ethanol	E85 DOD SI CD	Y		Y	Y				Y				
70		E85 DOD SI HEV		Y		Y		Y		Y				
71		E100 FP FCV								Y				
72	Cellulosic biomass to ethanol	E85 DOD SI CD	Y		Y	Y				Y				
73		E85 DOD SI HEV		Y		Y		Y		Y				
74		E100 FP FCV	Y							Y				
75		E100 FP FC HEV						Y		Y				
Electricity to Hydrogen via Electrolysis														
76	U.S. average electricity to GH_2 produced in refueling stations	DOD SI CD, Bin 5				Y			Y			Y	Y	Y
77		DOD SI HEV, Bin 5				Y		Y				Y	Y	Y
78		DOD SI CD, Bin 2												
79		DOD SI HEV, Bin 2												
80		FCV	Y		Y	Y							Y	Y
81		FC HEV		Y		Y				Y			Y	Y
82	CA average electricity to GH_2 produced in refueling stations	DOD SI CD, Bin 5						Y			Y	Y		Y
83		DOD SI HEV, Bin 5					Y				Y	Y		Y
84		DOD SI CD, Bin 2												Y
85		DOD SI HEV, Bin 2												Y
86		FCV										Y		
87		FC HEV										Y		

Table 4-1 (Cont.)

	Fuel Production Pathway	Vehicle Propulsion System	Included in Section 4.1?	Included in Section 4.2?										
				4.2.1	4.2.2	4.2.3	4.2.4	4.2.5	4.2.6	4.2.7	4.2.8	4.2.9	4.2.10	4.2.11
Electricity to Hydrogen via Electrolysis (Cont.)														
88	U.S. average electricity to LH_2 produced in refueling stations	DOD SI CD, Bin 5							Y			Y	Y	
89		DOD SI HEV, Bin 5						Y				Y	Y	
90		DOD SI CD, Bin 2												
91		DOD SI HEV, Bin 2												
92		FCV											Y	
93		FC HEV											Y	
94	CA average electricity to LH_2 produced in refueling stations	DOD SI CD, Bin 5						Y			Y	Y		
95		DOD SI HEV, Bin 5					Y				Y	Y		
96		DOD SI CD, Bin 2												
97		DOD SI HEV, Bin 2												
98		FCV										Y		
99		FC HEV										Y		
100	NA NG CC electricity to LH_2 produced in refueling stations	DOD SI CD, Bin 5							Y					
101		DOD SI HEV, Bin 5						Y						
102		DOD SI CD, Bin 2												
103		DOD SI HEV, Bin 2												
104		FCV	Y						Y					
105		FC HEV						Y						
106	NA NG CC electricity to LH_2 produced in refueling stations	DOD SI CD, Bin 5							Y					
107		DOD SI HEV, Bin 5						Y						
108		DOD SI CD, Bin 2												
109		DOD SI HEV, Bin 2												
110		FCV							Y					
111		FC HEV						Y						

Table 4-1 (Cont.)

	Fuel Production Pathway	Vehicle Propulsion System	Included in Section 4.1?	Included in Section 4.2?										
				4.2.1	4.2.2	4.2.3	4.2.4	4.2.5	4.2.6	4.2.7	4.2.8	4.2.9	4.2.10	4.2.11
Electricity to Hydrogen via Electrolysis (Cont.)														
112	Renewable electricity to GH_2 produced in refueling stations	FCV	Y						Y	Y				
113	U.S. average electricity to GH_2 produced in refueling stations, adopted IAQR	DOD SI CD, Bin 5											Y	
114		DOD SI HEV, Bin 5											Y	
115		DOD SI CD, Bin 2											Y	
116		DOD SI HEV, Bin 2											Y	
117		FCV											Y	
118		FC HEV											Y	
119	U.S. average electricity to LH_2 produced in refueling stations, adopted IAQR	DOD SI CD, Bin 5											Y	
120		DOD SI HEV, Bin 5											Y	
121		DOD SI CD, Bin 2												
122		DOD SI HEV, Bin 2												
123		FCV											Y	
124		FC HEV											Y	
	Total Number of Pathways	124	18	15	9	28	19	25	26	16	23	17	21	21

Table 4-2 Energy and Emission Items Analyzed in Phase 2 Study

Energy	Greenhouse Gases	Total Emissions	Urban Emissions
Total Energy (TE)	CO_2	Total VOC	Urban VOC
Fossil Energy (FE, subset of TE)	CH_4	Total CO	Urban CO
Petroleum Energy (subset of FE)	N_2O	Total NO_x	Urban NO_x
	Total CO_2-equivalent GHG	Total PM_{10}	Urban PM_{10}
		Total SO_x	Urban SO_x

4.1 Results for 18 Selected Propulsion Systems

Of the 124 vehicle/fuel systems simulated in this study, we selected 18 systems and present their WTW results for the 17 items analyzed (Table 4-2) to allow us to draw general conclusions about the energy and emission effects of advanced vehicle technologies and new transportation fuels. The WTW results for the 18 systems, for each of the 17 items, are discussed and illustrated in charts provided on the following pages.

Of the 18 systems we selected, six are petroleum-based, six are NG-based, and six are bioethanol- and electricity-based. The reformulated gasoline-fueled, spark-ignition engine with displacement on demand in conventional drive (RFG SI DOD CD) is the baseline to which other technology options are compared.

In all the charts presented in this section, for each vehicle/fuel system, the bottom section of the bar represents WTT per-mile results; the top section of the bar represents TTW per-mile results; the line superimposed on each bar represents the WTW uncertainty range for the P10 and P90 values (while the bar represents the P50 value). The pathways in the figures are grouped by energy resource: oil, NG, and bioethanol and electricity.

4.1.1 Total Energy Use

Of the six oil-based pathways shown in Figure 4-1, the reductions in WTW total energy use by the five advanced systems primarily result from the vehicle fuel consumption reductions provided by the advanced vehicle technologies, but the more efficient diesel WTT stage was a factor in the reduced WTW energy use for the diesel pathway. Direct injection gasoline, compression ignition diesel, and hybrids all reduce WTW total energy use. Our results show that gasoline fuel processor FCVs achieve energy savings equivalent to those of diesel hybrids. The uncertainty bands in Figure 4-1 indicate that, compared to conventional engine technologies, hybrid and fuel cell technologies are subject to greater WTW energy use uncertainties.

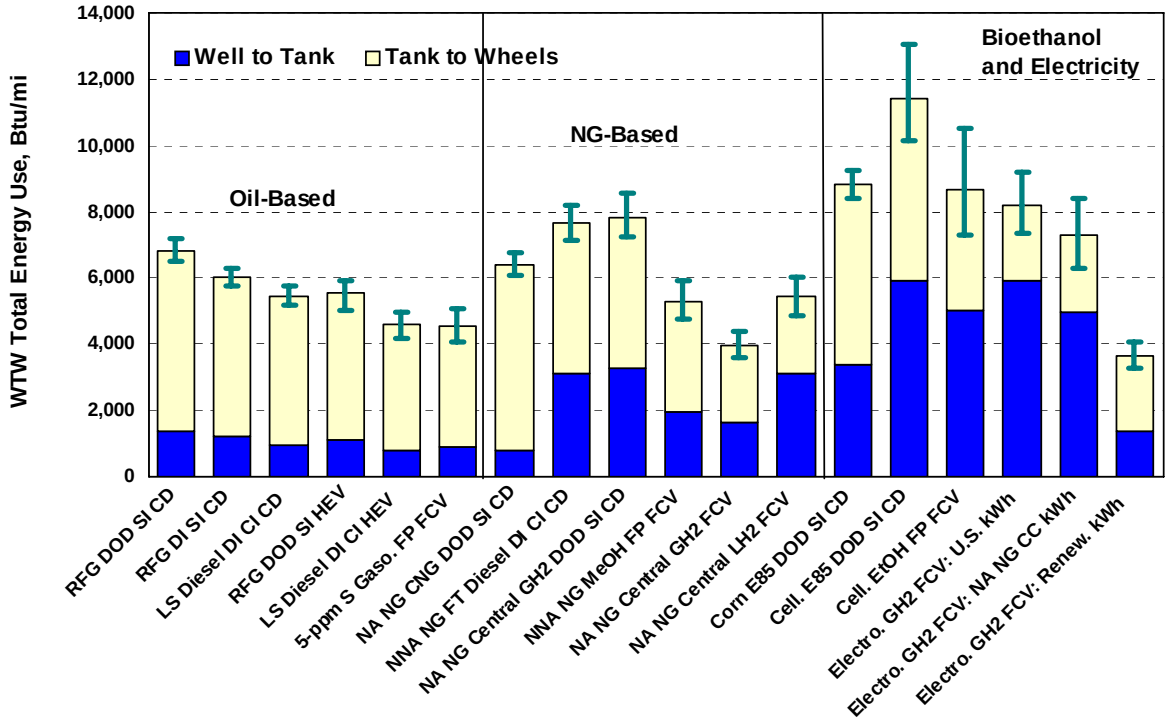

Figure 4-1 WTW Total Energy Use of 18 Vehicle/Fuel Systems (Btu/mi)

For the six NG-based systems, the CNG DOD SI engine achieves a small energy savings. Use of the CI diesel engine fueled with FT diesel and the DOD SI engine fueled with GH_2 result in increased WTW total energy use, relative to the energy use of the gasoline SI baseline. Figure 4-1 shows clearly that the energy use increases for these two technologies are attributable to the increased WTT energy use for production of FT diesel and GH_2. The moderate reductions in vehicle fuel consumption by these two engine technologies are not enough to offset the increased WTT energy use. On the other hand, the three FCVs fueled with methanol (via onboard fuel processors) and with GH_2 and LH_2 achieve WTW energy savings, even though WTT energy use for the three fuels is high. The fuel consumption reductions of these FC technologies more than offset their increased WTT energy use.

Of the six bioethanol- and electricity-based systems, all options, except renewable electricity for GH_2 FCVs, result in increased WTW energy use. For pathways involving renewable electricity (such as hydro-power, wind power, and solar power), only generated electricity (in Btu) was taken into account. If the primary energy for renewable electricity generation were included, the renewable electricity system would result in substantial WTW energy use. However, in our opinion, because renewable primary energy is not subject to energy resource depletion, inclusion of primary energy in renewable electricity is not meaningful. We will discuss this issue in detail later.

The largest increase in WTW total energy use is by SI engines powered with cellulosic ethanol. For cellulosic ethanol, our energy analysis is based on the energy (in Btu) in harvested biomass. Cellulosic ethanol processing plants consume a large amount of biomass energy for ethanol production. That consumption results in large amount of WTW total energy use for cellulosic ethanol systems. For corn ethanol, we account for the energy required for agriculture and processing corn into ethanol, not the energy in the corn kernels. This accounting decision results in less WTT energy use for corn ethanol than for cellulosic ethanol. For GH_2 from U.S. average electricity via electrolysis, the large WTT energy use is caused by energy losses during electricity generation, GH_2 production, and GH_2 compression.

The WTW total energy use results for bioethanol- and renewable electricity-based systems demonstrate a key issue concerning ways of accounting for Btu energy when very different primary energy sources are involved. The accounting system that researchers choose can significantly affect WTW total energy use results. We prefer a Btu accounting system that addresses energy resource depletion issues and emissions calculations (i.e., combustion emissions of an energy source). For that reason, we start to account for Btu energy use at different starting points for different fuels (see Figure 4-2). In particular, we begin to account for the energy in primary energy feedstocks for fossil energy-based fuels (i.e., Btu energy contained in crude oil, NG, and coal recovered from underground). For corn-based ethanol, the WTW analysis includes petroleum, fossil energy, and all emissions for agriculture, fertilizer manufacture, corn farming, corn transportation, ethanol manufacture, and ethanol transportation. For other renewable energy-based fuels, we begin to account for Btu energy in the fuels produced, because the Btus in primary *renewable* energy sources are not a concern. The exception is cellulosic ethanol, for which we begin to account for Btus in the biomass delivered to cellulosic plants. This starting point is influenced by the fact that we need to calculate the emissions associated with biomass combustion (as well as fermentation) in cellulosic ethanol plants. Some researchers may argue that accounting for Btus in primary renewable energy sources could be helpful in determining needs for other resources (such as land and water requirements). In this way, the Btus serve as a surrogate to depletion of resources other than energy resources. We argue that, in this case, depletion of other resources should be addressed directly instead of Btus serving as a surrogate.

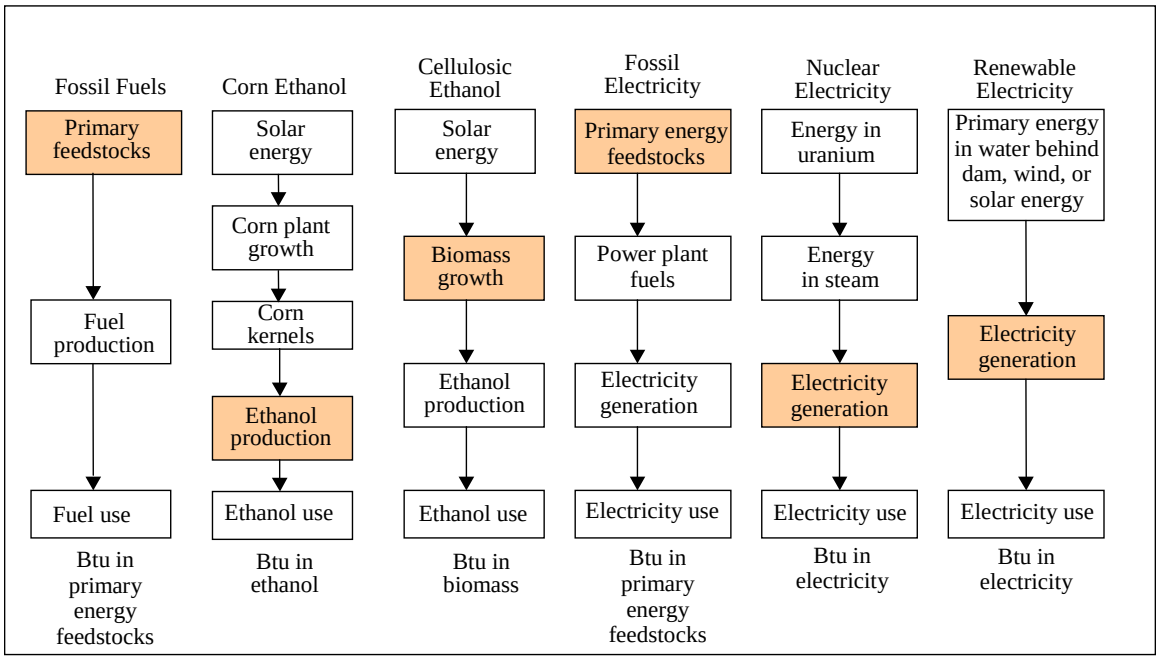

Figure 4-2 Energy Accounting System for Different Fuels in GREET

Btu accounting for nuclear electricity could be based either on the uranium resource or on the generated electricity. Although uranium is not renewable, the U.S. uranium resources will last for more than 150 years, based on current U.S. uranium consumption by domestic nuclear power plants, and the worldwide uranium resources are so large that uranium resource consumption may not be a concern. The estimated uranium reserve and resources in the United States are 1,418 and 8,330 million lb of U_3O_8 equivalent, respectively (EIA 2003). Between 1996 and 2003, the annual uranium consumption by U.S. nuclear power plants was about 55 million lb of U_3O_8 equivalent (EIA 2003). Thus, the U.S. uranium reserve and resources could potentially meet the U.S. uranium demand for about 177 years at the current

U.S. uranium consumption rate. U.S. uranium resources only account for a few percentage points of the total worldwide uranium supply. Worldwide uranium resources will last much longer to supply worldwide uranium demand.

Thus, uranium resources may not be a constraint for nuclear power generation. For this reason, we begin to account for Btus in electricity that is generated from nuclear power plants. In the GM-sponsored European WTW study (L-B-Systemtechnik GmbH et al. 2002), nuclear electricity energy was based on uranium. Also, we are aware that some engineering analyses for nuclear power plants account for Btus in the steam generated in nuclear plants. Although this accounting system could be helpful for nuclear power plant designs, it is not useful in addressing energy resource depletion issues.

Energy accounting systems involved in renewable energy resources obviously can be arbitrary. Total energy use results from such accounting systems could be misleading. We will demonstrate in our discussion of total fossil energy use results (below) that fossil energy use calculations are more meaningful when comparing fossil energy-based and renewable energy-based fuels.

4.1.2 Fossil Energy Use

Figure 4-3 presents WTW per-mile fossil energy use results for the 18 vehicle/fuel systems. Fossil energy use here includes petroleum, NG, and coal. Because all three resources are finite, estimates of fossil energy use can help understand how each vehicle/fuel system addresses fossil energy resource depletion issues.

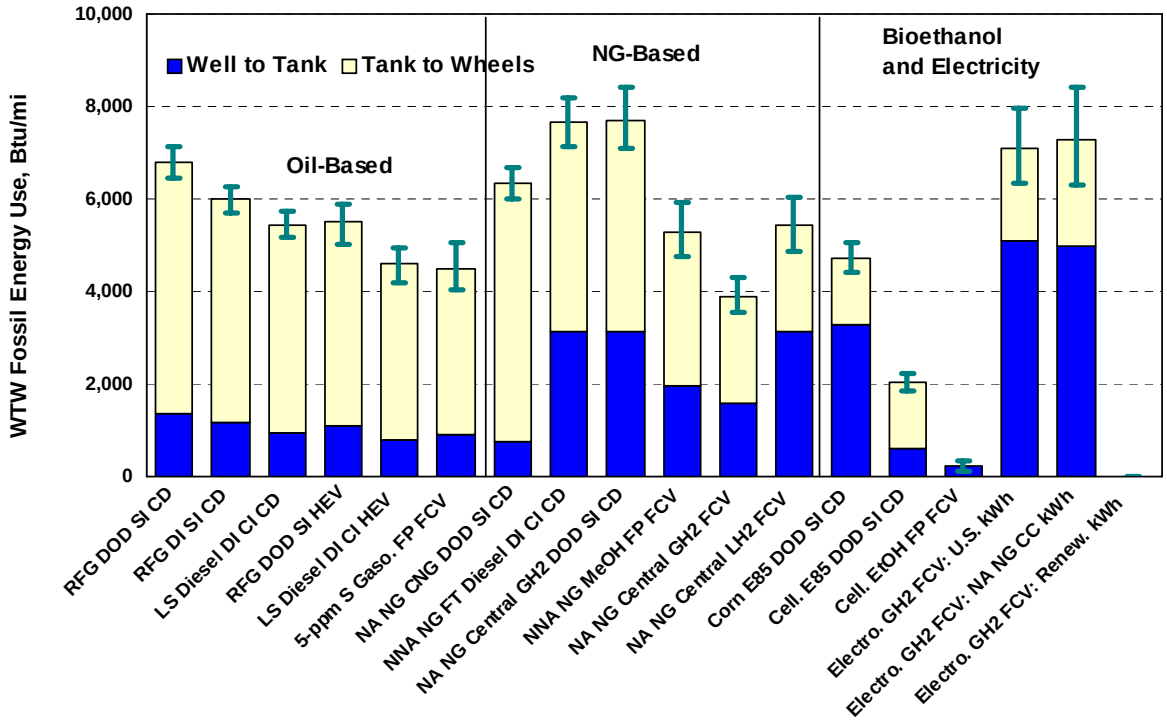

Figure 4-3 WTW Fossil Energy Use of 18 Vehicle/Fuel Systems (Btu/mi)

Among the 12 oil-based and NG-based systems, WTW fossil energy use patterns are similar to those for WTW total energy use. This is because the majority of the energy used for oil-based and NG-based systems is fossil energy. For these 12 systems, the reductions in fossil energy use primarily result from efficient vehicle technologies. CI engines, hybrids, and FCVs all achieve fossil energy reductions. Two systems, CI engines fueled with FT diesel and SI engines fueled with GH_2, consume more per-mile fossil energy than the baseline gasoline ICE technology, because of the high WTT fossil energy use for producing FT diesel and GH_2 from NG.

The distinct difference between total energy and fossil energy use lies in bioethanol- and renewable electricity-based systems. Because the Btus in corn, biomass, and renewable primary energy sources are not included, these systems show large reductions in fossil energy use. In fact, reduced fossil energy use is one of the major reasons for interest in renewable fuels. Contrary to the results for total energy, cellulosic ethanol and renewable electricity are the best fuel options to reduce WTW fossil energy consumption. The relatively high fossil energy use for E85 cellulosic ethanol ICE technology is attributable to the gasoline portion (19% by volume) of the E85 blend.

The fossil energy use for GH_2 production from U.S. average electricity is similar to that for NG CC electricity. On the one hand, NG CC efficiency is much greater than that of most fossil-fuel-fired electric power plants. On the other hand, about 30% of U.S. electricity is generated from non-fossil-fuel-powered power plants (e.g., nuclear power plants and hydroelectric power plants). This offsets the low efficiency of conventional fossil fuel power plants, causing the fossil energy use of GH_2 from U.S. average electricity to be close to that of GH_2 from NG CC electricity.

Figures 4-1 and 4-3 together demonstrate the importance of separating the types of Btus in WTW energy use estimates. When renewable energy sources are involved, it is fossil energy, not total energy, that should be used to compare different technologies. This is because renewable Btus are not subject to energy resource depletion issues. One may argue that total energy use results could provide some indication of the intensity of the use of resources such as land, wind power, and solar power. While use of total energy could be a first-order approximation of these other resources, we maintain that the requirement of these other resources should be analyzed directly.

In the U.S. context, energy resource depletion issues may need to be addressed with separation of coal from oil and NG because the U.S. has a large coal reserve but very small oil and gas reserves, relative to U.S. consumption of the three energy sources. If any vehicle/fuel systems can help to move energy use from oil and NG to coal, these technologies would have additional energy benefits for the United States. While this switch benefit is beyond the scope of this study, we caution that readers should use additional care in interpreting energy resource depletion implications for fossil energy.

4.1.3 Petroleum Use

Figure 4-4 shows WTW per-mile petroleum use. Reductions in petroleum use by these technologies are an important energy benefit because the U.S. now imports about 60% of its petroleum, adding to national energy security concerns and potential negative economic effects. Not surprisingly, NG-, bioethanol-, and electricity-based systems almost eliminate petroleum use, despite the fact that petroleum is used during WTT activities for these fuels. The moderate amount of petroleum use for E85 results from the 19% gasoline content of the E85 blend.

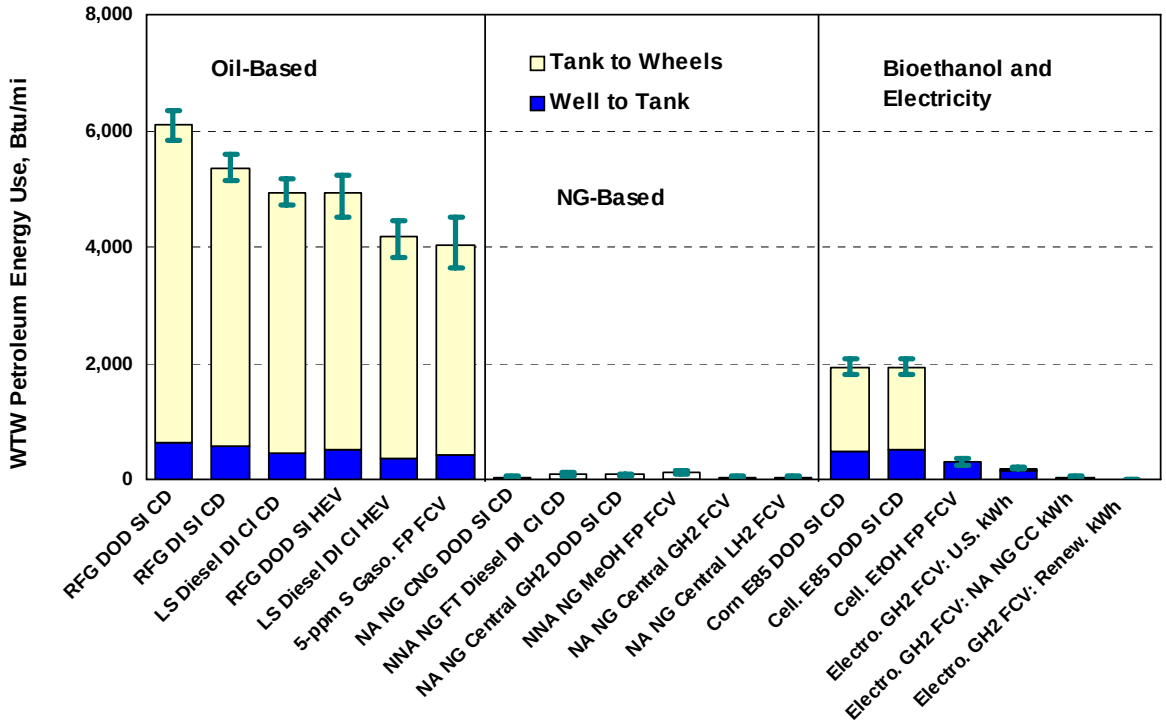

Figure 4-4 WTW Petroleum Use of 18 Vehicle/Fuel Systems (Btu/mi)

The reductions in petroleum use by the five oil-based systems, relative to the baseline gasoline ICE technology, result from vehicle efficiency gains (and efficient diesel production in the case of CI ICE technologies).

4.1.4 GHG Emissions

Figures 4-5 through 4-8 present WTW per-mile GHG emission results for the 18 vehicle/fuel systems. Figure 4-5 shows total GHG emissions as CO_2-equivalent emissions of CO_2, CH_4, and N_2O, the three major GHGs from motor vehicles. The three GHGs are combined with their IPCC-recommended GWPs over the 100-year horizon (1 for CO_2, 23 for CH_4, and 296 for N_2O).

Among the six oil-based systems, the reductions from the left to the right in the chart are caused primarily by vehicle efficiency gains. While *energy* reductions by the two diesel technologies (CI engine and CI engine hybrid) were large (see Figures 4-1 and 4-3), GHG emission reductions by the two technologies were relatively small, because diesel fuel has more carbon per unit of energy than gasoline. In particular, carbon intensity (grams of carbon per mmBtu) for diesel fuel is about 6% higher than that for gasoline. The high carbon intensity of diesel fuel offsets some of the GHG reduction benefits offered by efficient diesel engines.

Among the six NG-based systems, all result in GHG emission reductions relative to the GHG emissions of the baseline gasoline ICE. The GHG reductions by CI engines fueled with FT diesel and SI engines fueled with GH_2 are minimal because of the large amount of WTT GHG emissions. The small TTW GHG emissions for GH_2 ICE technology are N_2O emissions from hydrogen internal combustion. The three fuel-cell technologies achieve significant GHG emission reductions. The two hydrogen FCVs have zero TTW GHG emissions. GHG emissions of methanol-fueled and LH_2-fueled FCVs are comparable.

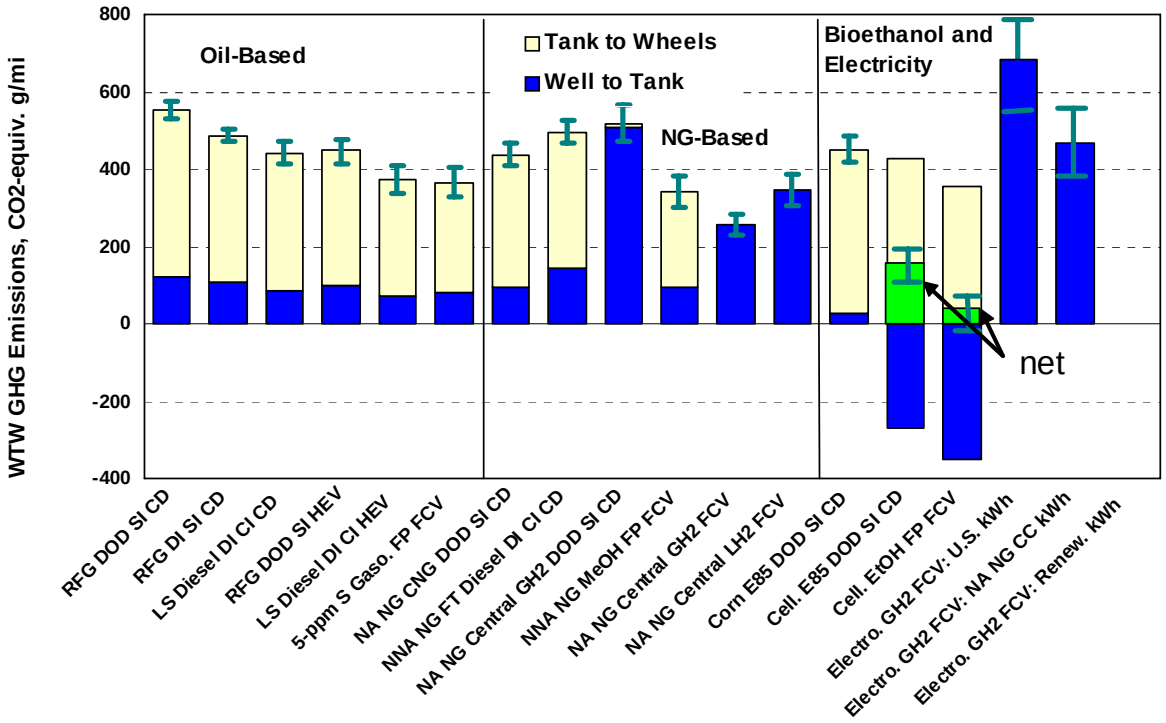

Figure 4-5 WTW GHG Emissions of 18 Vehicle/Fuel Systems (g/mi)

Among the six bioethanol- and electricity-based technologies, the renewable electricity-derived GH_2 system has zero GHG emissions. This is because our study includes the so-called operation-related emissions only. That is, emissions related to operational activities for the WTT stage are included. On the other hand, infrastructure-related GHG emissions (such as emissions associated with building roads, plants, and plant equipment) are not included for any of the pathways evaluated in this study.

The bars for cellulosic ethanol in Figure 4-5 require some additional explanation. The two cellulosic ethanol systems (for E85 SI and E100 FCVs) have negative WTT values because of carbon uptake during biomass growth, soil carbon sequestration in biomass farms, and GHG emission credits for electricity co-generated in cellulosic ethanol plants. The TTW emissions for E85 and E100 are similar to those for gasoline. Net emissions are shown by the positive or negative height of the light bars. For the cellulosic E85 in combustion engine case (Cell. E85 DOD SI CD), the best-estimate value for net GHGs was about 160 g/mi, a 70% reduction relative to the baseline. In the cellulosic ethanol-fueled FCV case (Cell. EtOH FP FCV), best-estimate GHG emissions were a little above zero because of soil carbon sequestration in biomass farms and GHG emission credits from co-generated electricity in cellulosic ethanol plants. The E85 SI ICE technology results in reduced GHG emission benefits because ICE technology is less efficient than FC technology and because E85 contains 19% gasoline. Corn ethanol E85-fueled SI ICE technology achieves only moderate GHG emission reductions, because WTT activities for corn ethanol consume a significant amount of fossil fuels (resulting in GHG emissions) and because cornfields produce a large amount of N_2O emissions from nitrogen nitrification and denitrification.

NG CC electricity-derived GH_2 achieves moderate GHG emission reductions, compared to those for the U.S. electricity generation mix, because of its efficient electricity generation. On the other hand, the U.S. average electricity-derived GH_2 results in increased GHG emissions relative to the baseline gasoline ICE technology because over 50% of U.S. electricity is produced in coal-fired power plants, which have high

GHG emissions, and because electrolysis hydrogen pathways are generally inefficient. Renewable electricity-derived GH_2 FCVs achieve zero WTW GHG emissions.

Results of the three electrolysis hydrogen pathways in Figure 4-5 demonstrate the importance of electricity sources for electrolysis hydrogen in WTW GHG emissions for hydrogen FCVs. Even though it is inefficient to produce hydrogen via electrolysis, electrolysis hydrogen could achieve GHG emission reductions where renewable or zero-carbon electricity is available for hydrogen production.

4.1.5 CO_2 Emissions

Figure 4-6 shows WTW per-mile CO_2 emissions. Except for the three bioethanol systems, the general trends between GHG and CO_2 emissions are similar, although emission reduction benefits for NG-based systems are a little larger for CO_2 emissions than for GHG emissions. This is because, in most cases, CO_2 emissions account for the majority of GHG emissions. For the three bioethanol systems, especially corn ethanol, N_2O emissions from farms are a significant emission source, accounting for about 1/5 of total WTW GHG emissions because N_2O emissions are amplified by the relatively high GWP of N_2O (296). Ignoring N_2O emissions would result in overly optimistic GHG emission reduction benefits for bioethanol.

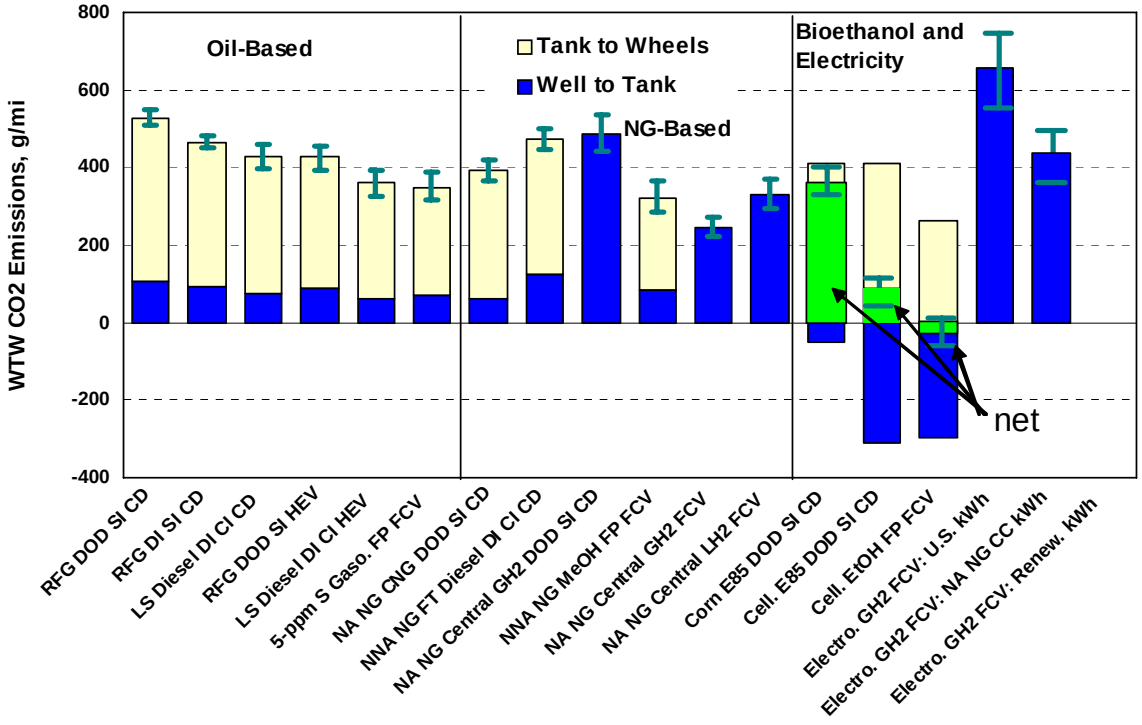

Figure 4-6 WTW CO_2 Emissions of 18 Vehicle/Fuel Systems (g/mi)

4.1.6 CH_4 Emissions

WTW CH_4 emissions, as shown in Figure 4-7, primarily result from WTT emissions. The CNG vehicle system has the largest CH_4 emissions because of it high WTT and TTW emissions. Electrolysis hydrogen generated by using the U.S. average electricity mix and NG CC electricity also have high CH_4 emissions. In the former case, a significant amount of CH_4 emissions are generated during coal mining and electricity generation. In the later case, a significant amount of CH_4 emissions are generated during NG recovery and transmission and during electricity generation. The high CH_4 emissions for NG-based GH_2 and corn-based ethanol are attributable to high WTT CH_4 emissions.

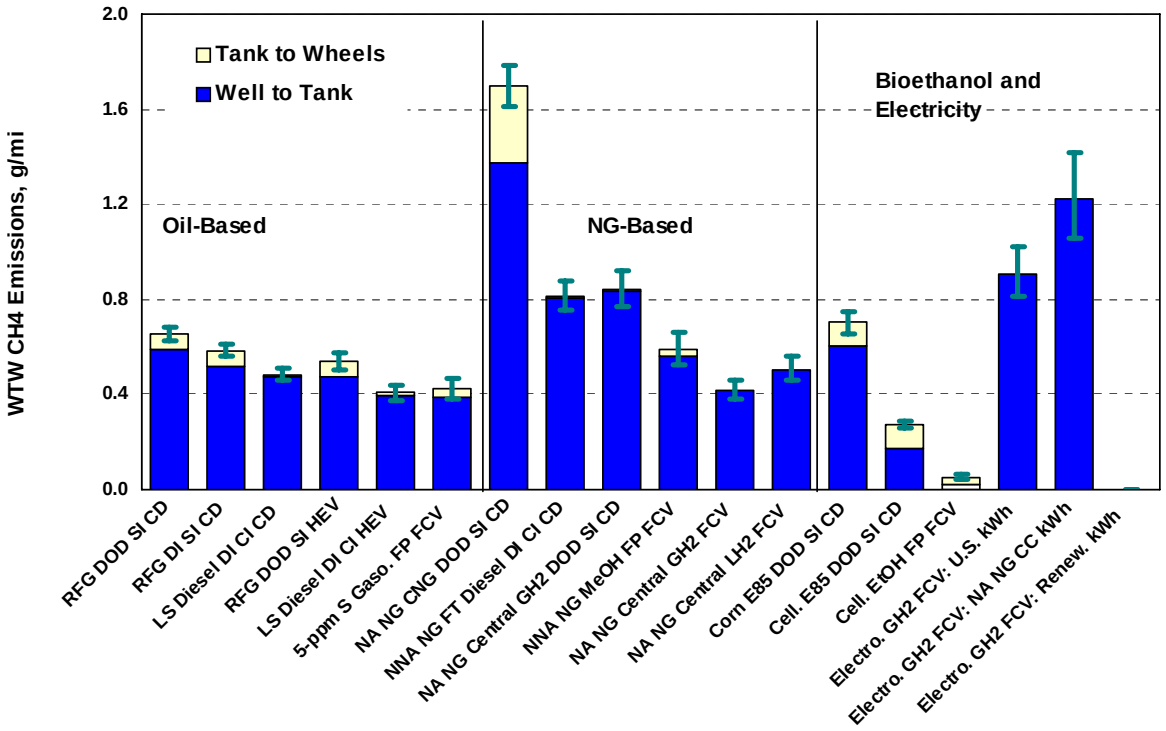

Figure 4-7 WTW CH_4 Emissions of 18 Vehicle/Fuel Systems (g/mi)

4.1.7 N_2O Emissions

Figure 4-8 presents WTW N_2O emissions for the 18 vehicle/fuel systems. On a per-mile basis, corn-ethanol's N_2O emissions are about ten times, and cellulosic ethanol's N_2O emissions are about five times, those for most non-bioethanol systems. These results demonstrate the large contribution of N_2O emissions from agriculture and the importance of including N_2O emissions in WTW GHG emission estimates when bioethanol is involved.

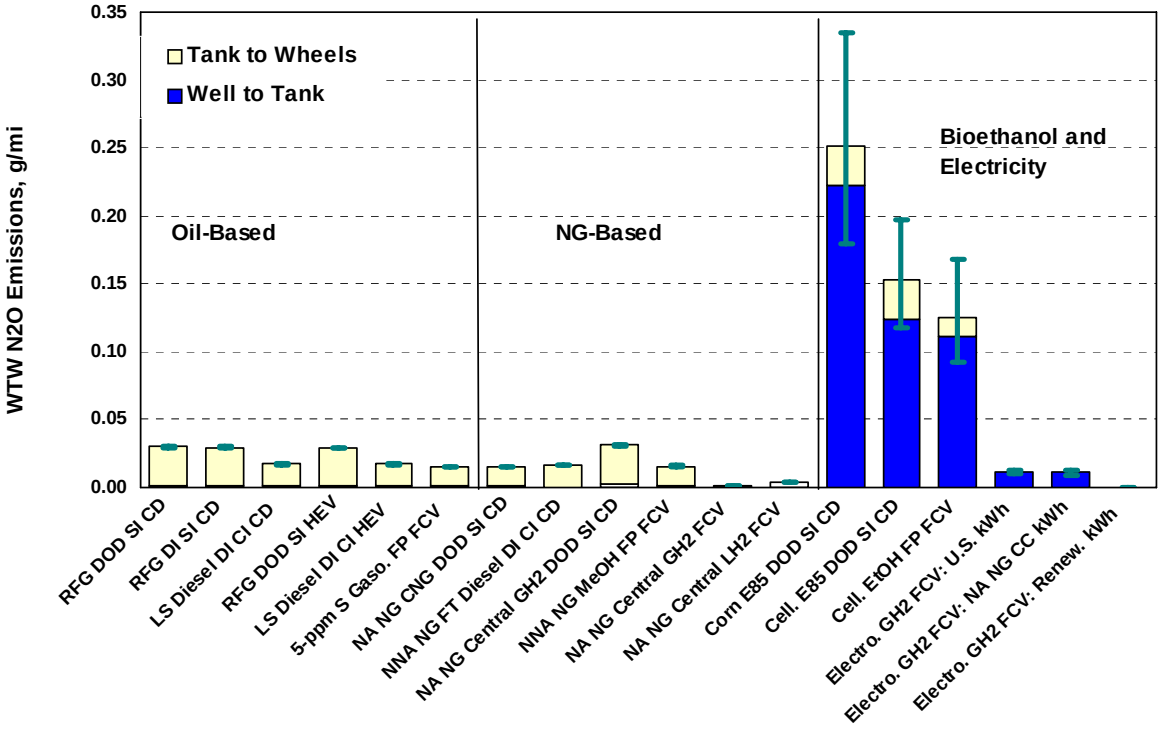

Figure 4-8 WTW N_2O Emissions of 18 Vehicle/Fuel Systems (g/mi)

4.1.8 Total/Urban VOC Emissions

Figures 4-9 and 4-10 present WTW total and urban VOC emissions. VOC emissions are a precursor for ozone formation. VOC emissions here include all hydrocarbon species. We do not address ozone-forming potentials, which could vary significantly among different vehicle/fuel systems for a given level of total VOC emissions.

In this study, total emissions of the five criteria pollutants include emissions occurring everywhere; urban emissions, a subset of total emissions, are those occurring within U.S. urban areas. For this study, total and urban emissions for the five criteria pollutants are determined by the locations of facilities. Urban areas here are consistent with the U.S. Bureau of the Census' definition of metropolitan areas, with a population of over 125,000 in 1990. In our simulations, urban WTT emissions in g/mmBtu were estimated on the basis of the share of urban facilities vs. all facilities for production of a given fuel. The urban WTT emissions in g/mmBtu were then converted into g/mi with vehicle energy use rate in Btu/mi. On the other hand, total TTW emissions in g/mi were estimated directly with MOBILE or EMFAC for a given vehicle technology. Urban TTW emissions in g/mi were then estimated by multiplying the total TTW emissions by the urban VMT share of a vehicle. Urban WTW emissions were the sum of urban WTT and urban TTW emissions. Consequently, the calculated urban WTW emissions in g/mi in our study represent the emissions share in urban areas for a mile driven by a vehicle in both urban and nonurban areas (that is, a composite mile instead of a urban mile). If one intends to use the urban g/mi emission results from this study to estimate aggregated urban emissions of a vehicle during its lifetime, the total VMT, not urban VMT, of the vehicle should be used.

Because population exposure is an important factor in assessing the health effects of criteria pollutants, the separation of emissions into total and urban emissions in the GREET model is intended to provide an

approximation of potential population exposure. A detailed health effects assessment of criteria pollutants requires separation of emissions by location (in finer resolutions than the total and urban emission separation used in this study), long-distance transport of emissions, residence time of pollutants in the air, simulations of atmospheric concentrations of pollutants (and formation of secondary pollutants such as ozone and acid rain), and population exposure of the atmospheric concentration of pollutants. The simple separation of urban emissions from total emissions here is the first step toward a full assessment of the human health effects of criteria pollutants. The separation is not intended to replace detailed health effects assessments of air pollution.

Figure 4-9 shows three general tiers of VOC emissions for the 18 vehicle/fuel systems. The first tier, which has the highest total VOC emissions, includes the three bioethanol systems. The high total VOC emissions for the bioethanol systems are caused by two factors. First, ethanol is a volatile fuel — use of ethanol during the TTW stage results in a more evaporative emissions than those for diesel or gaseous fuels. Second, the WTT stage, especially ethanol plants, generate a large amount of VOC emissions. The second tier for total VOC emissions includes other volatile fuels such as gasoline and methanol. These fuels have high WTT and TTW VOC emissions primarily because of their evaporative emissions. The third tier, which has the lowest total VOC emissions, includes non-volatile fuels such as petroleum diesel, FT diesel, CNG, and hydrogen. These fuels have low WTT and TTW VOC emissions. The five direct-hydrogen FC systems (NG-based GH_2 and LH_2 and GH_2 from three electricity sources) have the lowest VOC emissions. Furthermore, the uncertainty lines superimposed on the bars in Figure 4-9 show that direct-hydrogen FCVs reduce the uncertainty range of emissions, as well as the magnitude of emissions, relative to ICEs, ICE hybrids, and fuel-processor FCVs. The relatively large uncertainty ranges for ICE-based technologies are caused by their on-road emissions variations (see Section 2), while hydrogen FCVs will have zero emissions in any case.

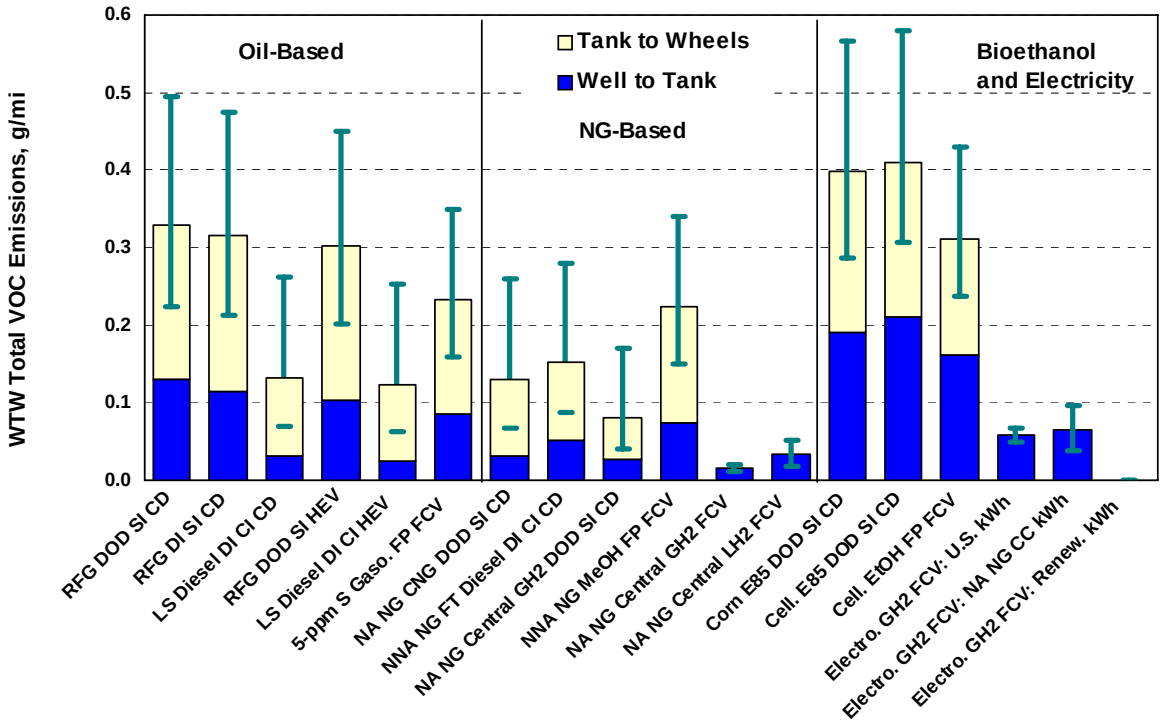

Figure 4-9 WTW Total VOC Emissions of 18 Vehicle/Fuel Systems (g/mi)

Figure 4-10 shows WTW urban VOC emissions. In contrast to the total VOC emission results, the three bioethanol systems have urban VOC emissions comparable to those of the four gasoline-powered systems. Urban VOC emissions for bioethanol systems are much lower than total VOC emissions because most ethanol plants are (or will be) located in rural areas, where corn and biomass feedstocks are produced. Diesel and CNG systems have lower urban VOC emissions. Direct-hydrogen FCVs have the lowest urban VOC emissions and the smallest uncertainty ranges.

Because VOC evaporative emissions represent a large share of total VOC emissions for volatile fuels including gasoline, ethanol, and methanol, differences in fuel characteristics, such as volatility, have a major impact on the total VOC emissions of the 18 systems.

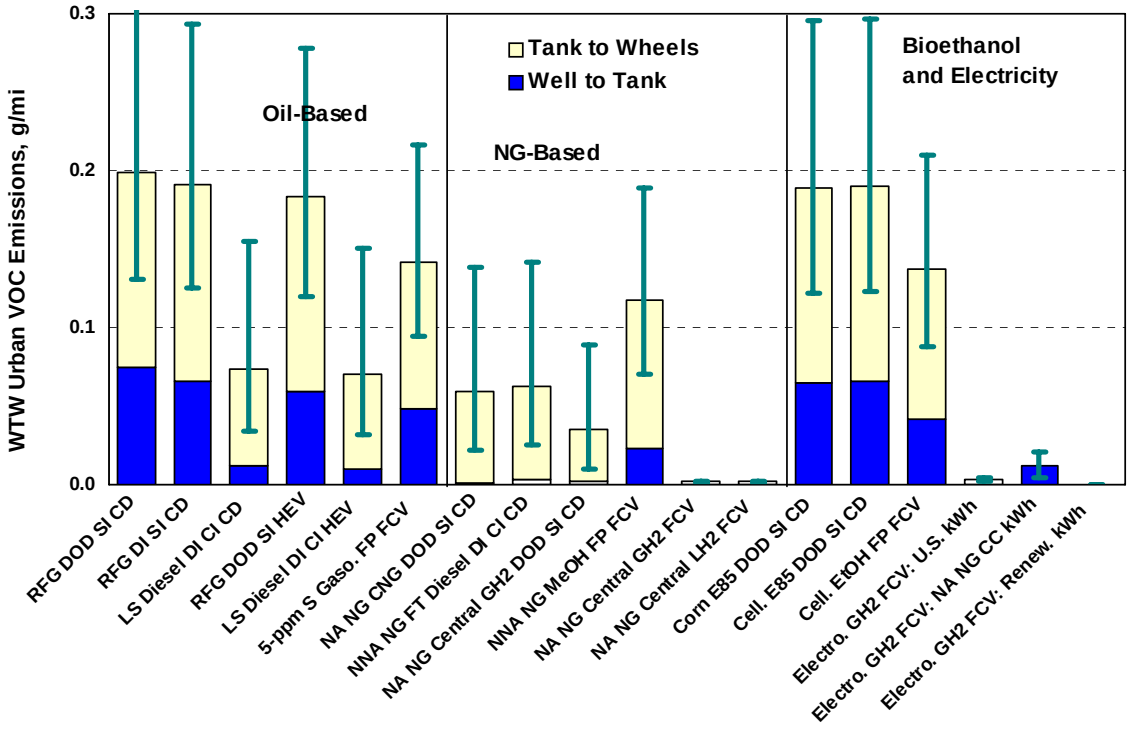

Figure 4-10 WTW Urban VOC Emissions of 18 Vehicle/Fuel Systems (g/mi)

4.1.9 Total/Urban CO Emissions

Figures 4-11 and 4-12 show WTW total and urban CO emissions. CO air pollution was a major urban air pollution concern until the middle of the 1990s. Since then, vehicular CO emissions have been reduced dramatically in U.S. cities, most of which have become CO attainment areas. As a result, the focus of U.S. motor vehicle emissions regulations has shifted to controlling other pollutants such as NO_x and PM_{10}.

ICE-based technologies, except for hydrogen-fueled ICEs, have the highest total CO emissions. Onboard fuel-processor FCVs have the next-highest total CO emissions. Direct-hydrogen FCVs have the lowest CO emissions.

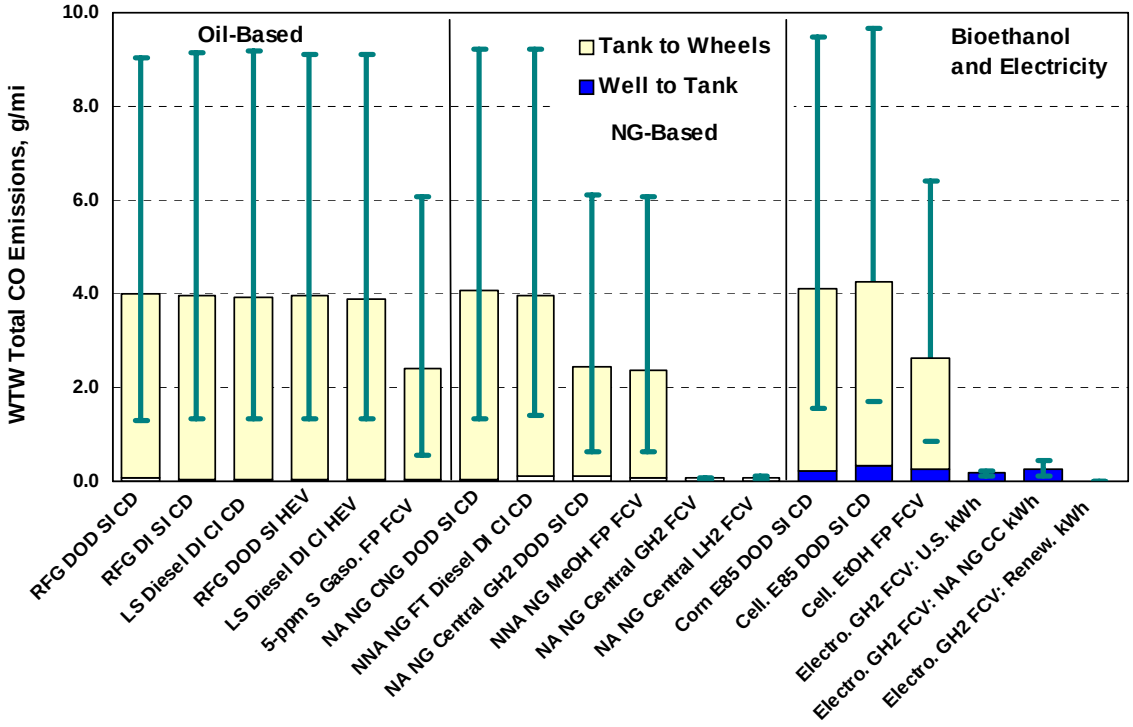

Figure 4-11 WTW Total CO Emissions of 18 Vehicle/Fuel Systems (g/mi)

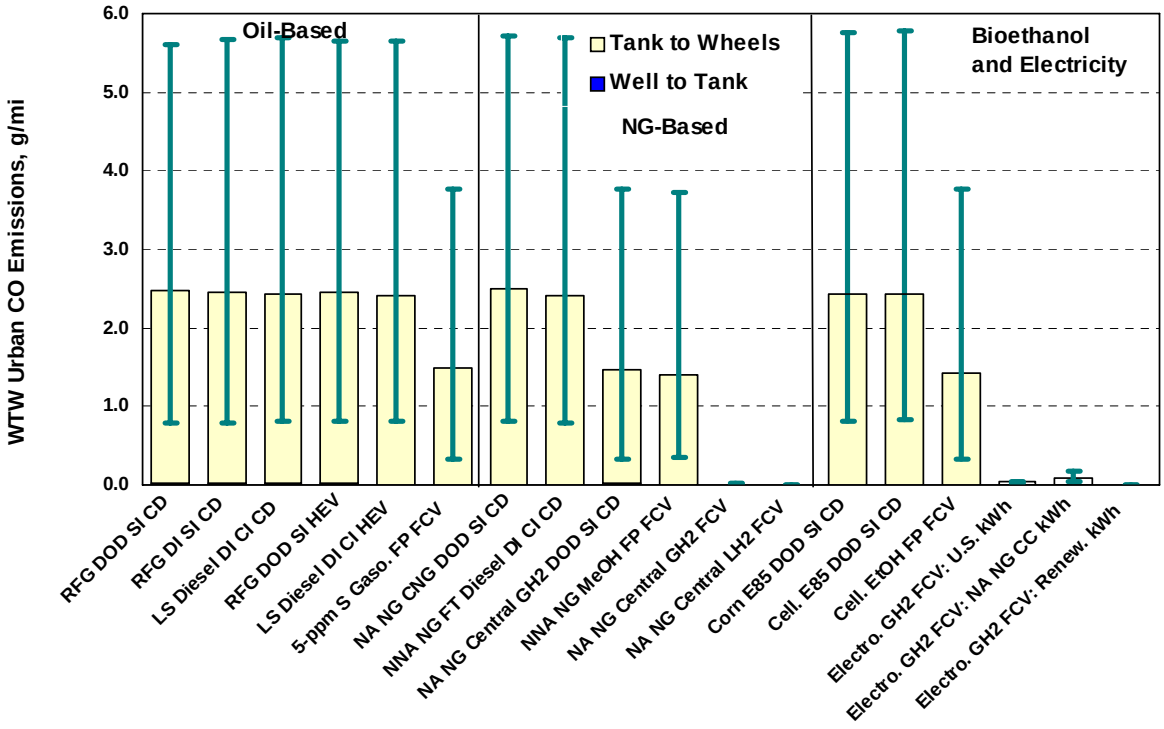

Figure 4-12 WTW Urban CO Emissions of 18 Vehicle/Fuel Systems (g/mi)

A distinct result, shown in Figure 4-11, is that almost all WTW CO emissions are produced during the TTW stage. Another noticeable result is that WTW CO emissions of ICE-based technologies and onboard fuel-processor FCVs are subject to great uncertainty because WTW CO emissions for these technologies are primarily from vehicle operations whose emissions are subject to great uncertainties (see Section 2).

Urban CO emissions are primarily driven by TTW vehicular CO emissions. Because of this, the patterns of urban CO emissions among the 18 vehicle/fuel systems are similar to those of total CO emissions. However, the amount of urban CO emissions is significantly lower than that of total CO emissions for a given technology because some of the total VMT (28%) by a given vehicle technology are in rural areas; consequently, some of the vehicular CO emissions are non-urban CO emissions.

Similar to VOC emissions results, direct-hydrogen FCVs are shown to have the lowest levels and the smallest uncertainty ranges for CO emissions.

4.1.10 Total/Urban NO_X Emissions

Figures 4-13 and 4-14 present WTW total and urban NO_x emissions for the 18 vehicle/fuel systems. Figure 4-13 shows that the six petroleum-based systems have similar total NO_x emission levels, with the exception that gasoline-fueled FCVs have fewer NO_x emissions than do the other five systems. The similar levels of total NO_x emissions are a result of similar WTT and TTW NO_x emissions, with the exception that gasoline-fueled FCVs generate fewer TTW NO_x emissions. The similar TTW NO_x emissions for the five ICE-based technologies are a result of our assumption that all ICE technologies will meet the NO_x emission standard for EPA's Tier 2 Bin 5 vehicle category.

Of the six NG-based systems, the NO_x emissions from CNG vehicles are lower than those of the baseline gasoline ICE technology because CNG WTT NO_x emissions are lower than gasoline and diesel WTT NO_x emissions. On the other hand, NO_x emissions from FT diesel CI ICE and hydrogen SI ICE (meeting Bin 5 NO_x standard) are higher than those of the baseline gasoline ICE technology because a significant amount of NO_x emissions are generated during production and transportation of FT diesel and production and compression of GH_2. Of the WTW total NO_x emissions for FT diesel CI ICE, TTW (vehicular) emissions account for 44%, cross-ocean transportation of FT diesel for 27%, and FT diesel production for 18%.

Table 4-3 lists the shares of total and urban NO_x emissions associated with hydrogen-fueled ICEs and FCVs. Depending on the production pathway selected, hydrogen production, compression, or liquefaction could account for a large amount of the WTW NO_x emissions.

Total NO_x emissions from methanol-powered FCVs are similar to those of baseline gasoline technology even though onboard methanol fuel processors have somewhat lower NO_x emissions than gasoline engines. This is because high NO_x emissions occur during methanol production. Both direct GH_2 and direct LH_2 FCVs have total NO_x emissions that are lower than those of the baseline gasoline technology because FCV operation generates zero emissions.

Of the six bioethanol- and electricity-based systems, the three bioethanol systems and GH_2 derived from U.S. average electricity result in much greater total NO_x emissions than the baseline gasoline technology. The increases are caused by dramatically high WTT total NO_x emissions for bioethanol and GH_2. For bioethanol pathways, increased WTT NO_x emissions are from farming activities, nitrification and denitrification of nitrogen fertilizer in agricultural fields, and from corn and cellulosic ethanol plants. The

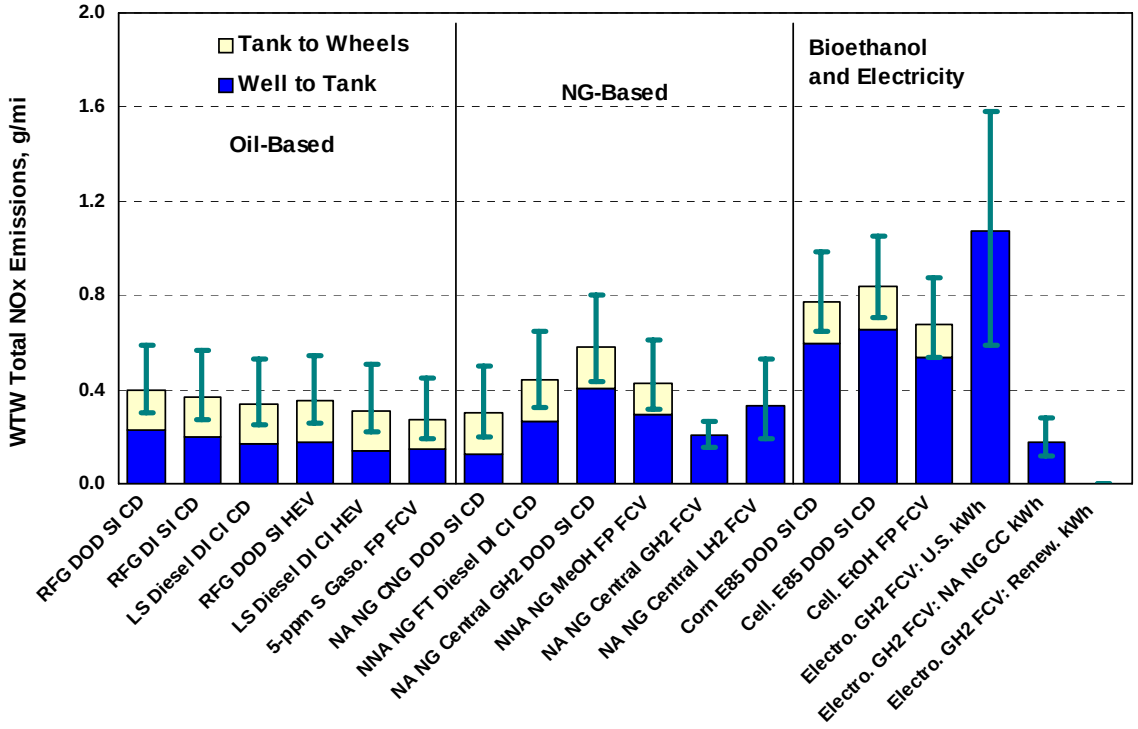

Figure 4-13 WTW Total NO_x Emissions of 18 Vehicle/Fuel Systems (g/mi)

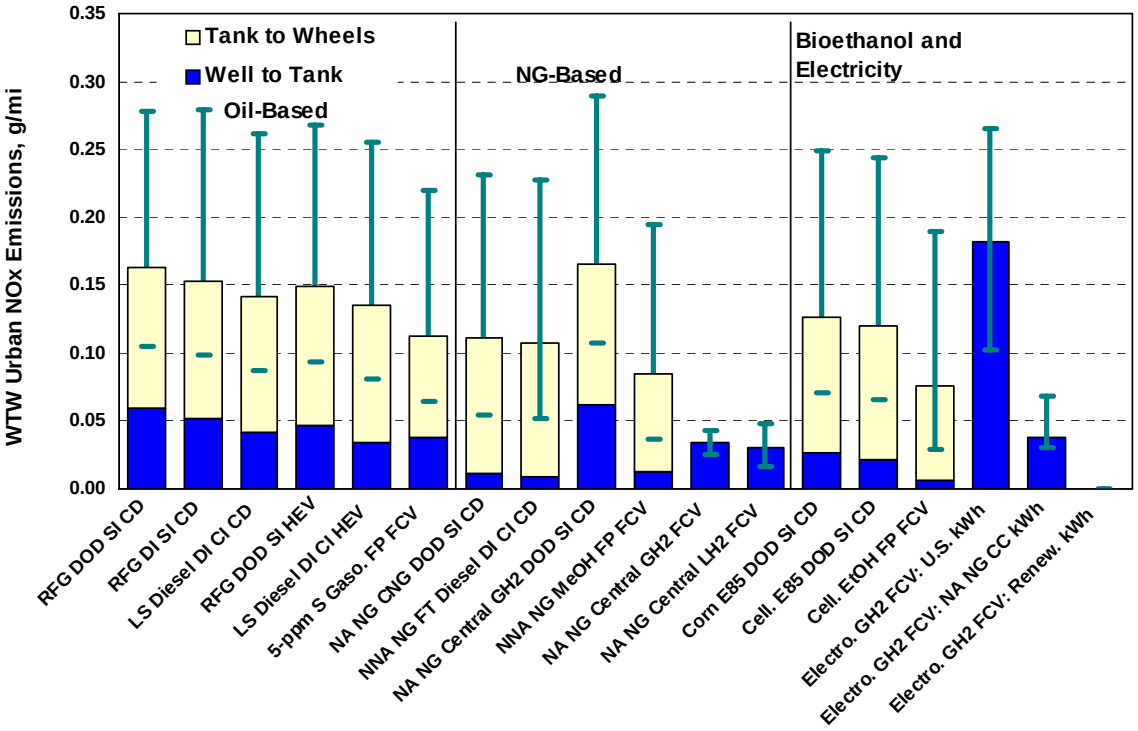

Figure 4-14 WTW Urban NO_x Emissions of 18 Vehicle/Fuel Systems (g/mi)

Table 4-3 Shares of NO_x Emissions by Hydrogen Production, Compression, and Liquefaction for Hydrogen-Fueled ICEs and FCVs[a]

	Total NO_x Emissions					Urban NO_x Emissions				
		Share, %					Share, %			
Production Method/ Propulsion Type	WTW, gpm	TTW	H_2 Production	H_2 Compression or Liquefaction	Other	WTW, gpm	TTW	H_2 Production	H_2 Compression or Liquefaction	Other
NA NG Central GH_2										
ICE	0.587	30.6	23.4	23.4	22.6	0.169	61.5	17.4	13.1	7.9
FCV	0.21	0.0	33.7	33.8	32.6	0.036	0.0	45.3	34.2	20.5
NA NG Central LH_2										
ICE	0.828	21.8	16.7	49.8	11.7	0.158	65.7	7.6	24.1	2.7
FCV	0.328	0.0	21.4	63.7	14.9	0.03	0.0	22.1	70.1	7.8
NA NG Station GH_2										
ICE	0.519	34.5	32.7	20.8	12.0	0.213	50.7	39.4	8.5	1.3
FCV	0.175	0.0	49.9	31.8	18.3	0.055	0.0	80.0	17.3	2.7
NA NG Station LH_2										
ICE	1.291	13.9	13.2	67.9	5.0	0.352	31.6	24.5	42.8	1.1
FCV	0.56	0.0	15.3	78.9	5.8	0.123	0.0	35.9	62.6	1.5
Electrolysis GH_2: U.S. Electricity Generation Mix										
ICE	2.616	6.7	89.2	4.1	0.0	0.538	20.6	75.9	3.5	0.0
FCV	1.228	0.0	95.7	4.4	0.0	0.211	0.0	95.7	4.4	0.0
Electrolysis LH_2: U.S. Electricity Generation Mix										
ICE	3.442	5.2	68.7	25.3	0.8	0.677	16.4	60.5	22.3	0.7
FCV	1.638	0.0	72.4	26.7	0.9	0.283	0.0	72.4	26.7	0.9

[a] Hydrogen ICEs here are to meet Bin 5 NO_x emission standard.

increased WTT NO_x emissions for the electrolysis GH_2 pathway are from NO_x emissions from fossil-fuel-powered electric power plants. Because NG CC electric power plants are efficient and clean, GH_2 derived from NG CC-based electricity actually results in reductions in total NO_x emissions, although a large uncertainty range is associated with NO_x emissions for this pathway. Renewable electricity-based GH_2 has zero total NO_x emissions. As mentioned earlier, this study includes operation-related emissions; infrastructure-related emissions are excluded.

The results of WTW total NO_x emissions for the 18 systems show that the WTT stage accounts for a larger share of WTW NO_x emissions than does the TTW stage, because future vehicle technologies will be designed to meet the stringent NO_x emission standards of EPA's motor vehicle Tier 2 standards. If total NO_x emissions are to be reduced, WTT NO_x emissions will need to be addressed.

Figure 4-14 shows WTW urban NO_x emissions of the 18 vehicle/fuel systems. Urban NO_x emissions are 60–80% lower than total NO_x emissions for most of the systems. Urban NO_x emissions for all the systems except for the five direct-hydrogen FCV technologies are dominated by WTT urban NO_x emissions. Of the five direct-hydrogen FCV systems, NG-based GH_2 and LH_2 and electrolysis hydrogen

derived from NG CC and renewable electricity help reduce urban NO_x emissions. Onboard fuel-processor-equipped FCVs achieve moderate urban NO_x emission reductions. ICE-based technologies generally have similar urban emissions. The U.S. average electricity-based GH_2 FCVs could result in increased urban NO_x emissions.

The significantly high urban WTT NO_x emissions for the six petroleum-based systems are attributable to the fact that a significant number of U.S. petroleum refineries are located within urban areas — in fact, we estimated that 67% of the U.S. refinery capacity is located within U.S. urban areas. NO_x emissions from these refineries are counted as urban NO_x emissions. On the other hand, plants for FT diesel, methanol, hydrogen, and ethanol production are generally located outside of urban areas. Nationwide, we estimated that 39% of oil-fired electric power plant capacity, 43% of NG-fired capacity, and 16% of coal-fired capacity are located within U.S. urban areas. NO_x emissions from these urban power plants contribute to the high WTT urban NO_x emissions from electricity-derived hydrogen pathways. To control urban NO_x emissions, consideration needs to be given to locating facilities in areas farther away from urban areas. In fact, this has been done in some of the major U.S. cities in the past in order to control urban emissions.

Although both total and urban WTW NO_x emissions are subject to uncertainties, the uncertainties with urban NO_x emissions are much greater than those with total NO_x emissions. This is primarily driven by the great uncertainty in TTW NO_x emissions during vehicle operations. That is, although future ICE technologies will meet stringent Tier 2 NO_x standards, MOBILE and EMFAC models predict that ICE technologies will continue to be subject to on-road emission deteriorations and malfunctioning. However, it is anticipated that the degree of uncertainties in emissions for future vehicles will be less than that for past and current vehicles because technologies such as OBD systems and others will be able to reduce the number of high emitting vehicles.

4.1.11 Total/Urban PM_{10} Emissions

Figures 4-15 and 4-16 present WTW total and urban PM_{10} emissions for the 18 vehicle/fuel systems. As Figure 4-15 shows, the U.S. average electricity-derived GH_2 FCVs increase total PM_{10} emissions by about ten times over the emissions of the baseline gasoline technology. This is because (1) more than 50% of U.S. electricity is generated in coal-fired power plants, which have high PM_{10} emissions; and (2) PM_{10} emissions associated with coal mining and cleaning are high. On the other hand, when NG CC or renewable electricity is used to produce GH_2, total PM_{10} emissions are actually reduced.

E85 vehicles fueled with ethanol from corn have the next-highest total PM_{10} emissions because farming equipment (such as diesel tractors) and ethanol plants produce a large amount of PM_{10} emissions. Note that PM_{10} emissions from agricultural field dusts are not included in estimates of ethanol PM_{10} emissions. The two cellulosic ethanol systems (ICE and fuel-cell technology) have relatively high PM_{10} emissions, again because of high PM_{10} emissions from farming equipment and cellulosic ethanol plants (although, in this case, the share of farming equipment's PM_{10} emissions is smaller because fewer farming activities are involved in biomass farming than in corn farming).

Table 4-4 presents shares of the PM_{10} emissions for hydrogen-fueled ICEs and FCVs. Similar to NO_x emissions, hydrogen production, compression, or liquefaction can account for a large amount of the WTW PM_{10} emissions, depending on the hydrogen production pathways.

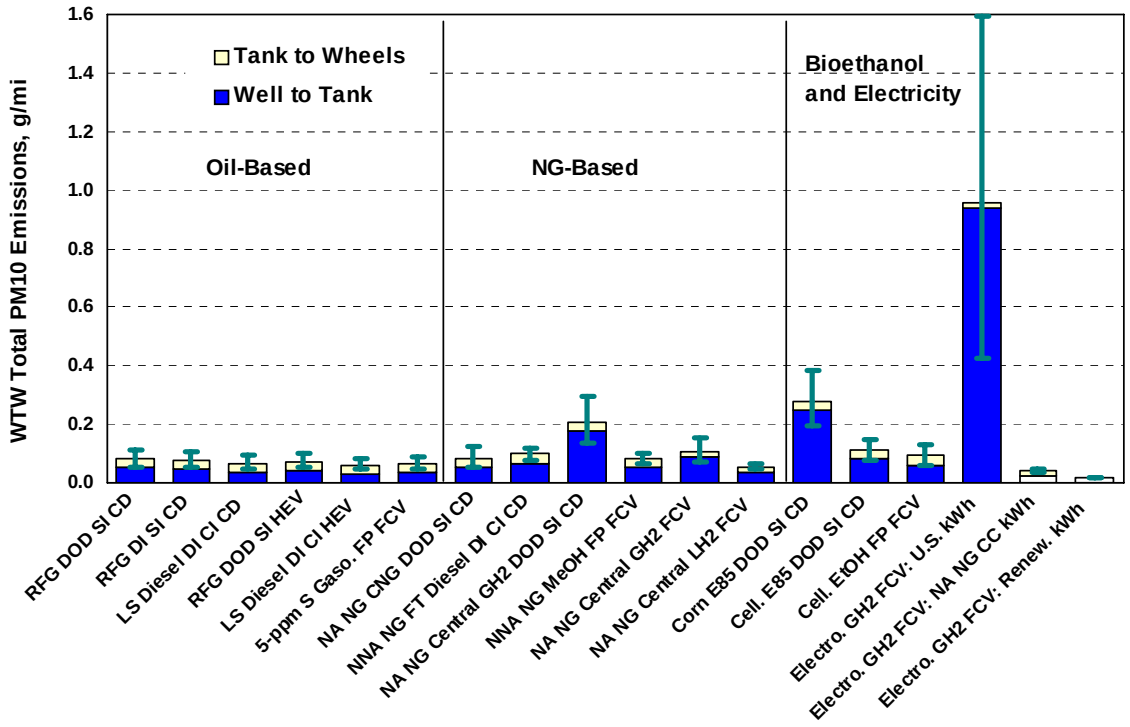

Figure 4-15 WTW Total PM_{10} Emissions of 18 Vehicle/Fuel Systems (g/mi)

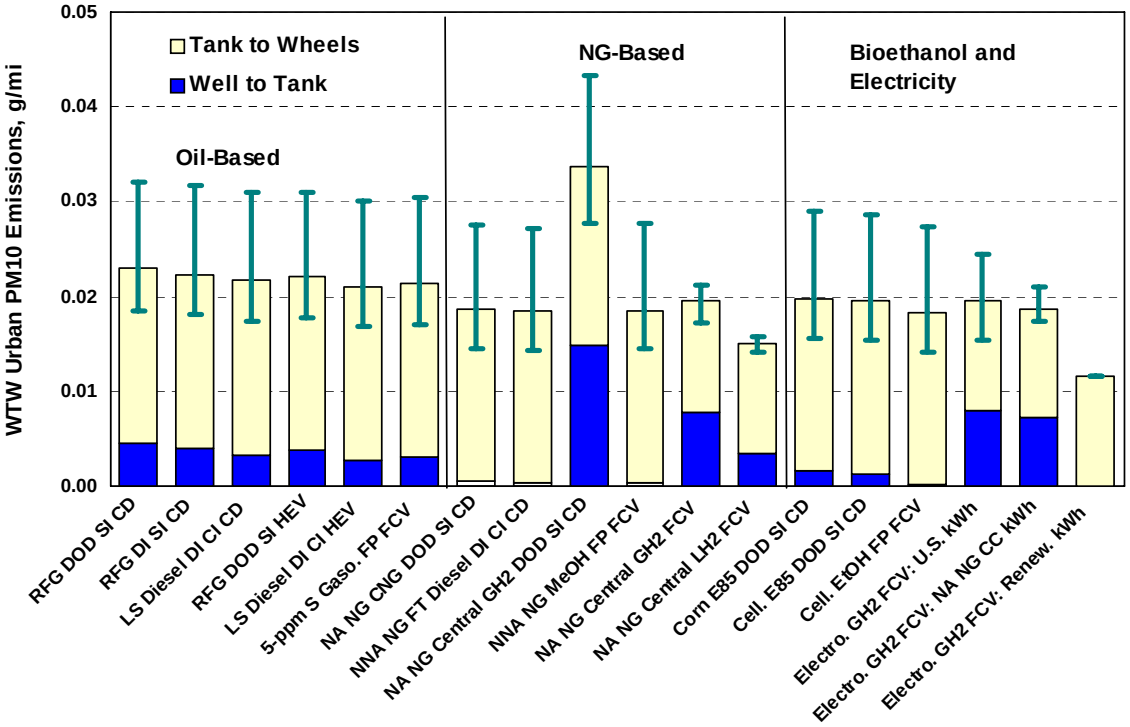

Figure 4-16 WTW Urban PM_{10} Emissions of 18 Vehicle/Fuel Systems (g/mi)

Table 4-4 Shares of PM_{10} Emissions by Hydrogen Production, Compression, and Liquefaction for Hydrogen-Fueled ICEs and FCVs

	Total PM_{10} Emissions					Urban PM_{10} Emissions				
		Share, %					Share, %			
Production Method/ Propulsion Type	WTW, gpm	PTW	H_2 Production	H_2 Compression or Liquefaction	Other	WTW, gpm	PTW	H_2 Production	H_2 Compression or Liquefaction	Other
NA NG Central GH_2										
ICE	0.186	16.7	30.2	46.5	6.7	0.035	55.3	39.4	4.2	1.0
FCV	0.097	19.1	29.3	45.1	6.5	0.02	59.4	35.8	3.8	0.9
NA NG Central LH_2										
ICE	0.102	31.1	56.5	6.4	6.0	0.025	74.8	21.4	2.5	1.4
FCV	0.055	34.9	53.4	6.1	5.6	0.015	77.8	18.8	2.2	1.2
NA NG Station GH_2										
ICE	0.188	16.5	45.5	36.3	1.7	0.063	31.2	66.7	1.9	0.1
FCV	0.098	19.0	44.1	35.3	1.6	0.034	35.0	63.1	1.8	0.1
NA NG Station LH_2										
ICE	0.655	4.6	12.7	82.1	0.6	0.071	27.4	58.6	13.4	0.7
FCV	0.333	5.4	12.6	81.4	0.6	0.038	30.9	55.8	12.7	0.6
Electrolysis GH_2: U.S. Electricity Generation Mix										
ICE	1.566	1.9	93.8	4.3	0.0	0.046	42.0	55.5	2.5	0.0
FCV	0.795	2.3	93.5	4.3	0.0	0.025	46.1	51.6	2.4	0.0
Electrolysis LH_2: U.S. Electricity Generation Mix										
ICE	2.078	1.5	71.4	26.3	0.9	0.055	35.4	46.8	17.2	0.6
FCV	1.052	1.7	71.2	26.2	0.9	0.029	39.3	44.0	16.2	0.5

Of the six NG-based systems, GH_2 ICEs result in increased PM_{10} emissions because of the high WTT total PM_{10} emissions, which are, in turn, caused primarily by electricity use for GH_2 compression (we assumed that U.S. average electricity would be used for hydrogen compression). On the other hand, the increase in PM_{10} emissions by GH_2 FCVs is smaller than that for GH_2 ICEs because efficient FCVs require less GH_2 per mile than ICEs. The increase in PM_{10} emissions by CNG vehicles is caused by electricity use for NG compression. The increase by FT diesel ICEs is attributable to PM_{10} emissions from production and across-ocean transportation of FT diesel (we assumed that FT diesel would be produced outside of North America with non-North American NG). The relatively small PM_{10} emissions for LH_2 FCVs are a result of NG being the sole energy source for hydrogen production and liquefaction. That is, U.S. average electricity was not used in the LH_2 pathway.

Figure 4-15 shows that all 18 systems have TTW PM_{10} emissions. This is because our estimates of TTW PM_{10} emissions include tailpipe exhaust emissions (zero for direct-hydrogen FCVs) and brake and tire wear PM_{10} emissions (see Section 2).

Among the six petroleum-based systems, total PM_{10} emissions are similar.

Figure 4-16 shows WTW urban PM_{10} emissions for the 18 systems, which are a small fraction of WTW total PM_{10} emissions. Because electricity is used to compress GH_2, use of GH_2 ICEs result in increased urban PM_{10} emissions. As noted in a previous section, a large percentage of U.S. electric power plants are located within urban areas. Similarly, FCVs with GH_2 from U.S. average electricity have high urban PM_{10} emissions. Except from GH_2-based systems, WTT emissions account for the majority of WTW urban PM_{10} emissions. Brake and tire wear are responsible for WTT urban PM_{10} emissions from direct-hydrogen FCVs. Inclusion of brake and tire wear PM_{10} emissions causes smaller variations in WTW PM_{10} emissions among the 18 systems.

4.1.12 Total/Urban SO_X Emissions

Figures 4-17 and 4-18 present WTW total and urban SO_x emissions, respectively, for the 18 systems. For total SO_x emissions, use of U.S. average electricity for GH_2 production via electrolysis results in huge increase in SO_x emissions. However, if NG CC or renewable electricity is used for hydrogen production, SO_x emissions could remain the same or decrease, relative to the emissions of the baseline gasoline ICE technology. Corn ethanol ICEs and NG-based GH_2 ICEs could result in increased total SO_x emissions. In the former case, the increase is caused by SO_x emissions from farming equipment and in ethanol plants. In the latter case, the increase is caused by the use of electricity for hydrogen compression. Other technologies have similar total SO_x emissions.

Figure 4-18 shows WTW urban SO_x emissions, which are dominated by WTT urban SO_x emissions. This is because, for our simulation target year of 2016, fuel sulfur content will be 30 and 15 ppm in gasoline and diesel, respectively. Consequently, TTW SO_x emissions, which are formed from sulfur in a fuel, will

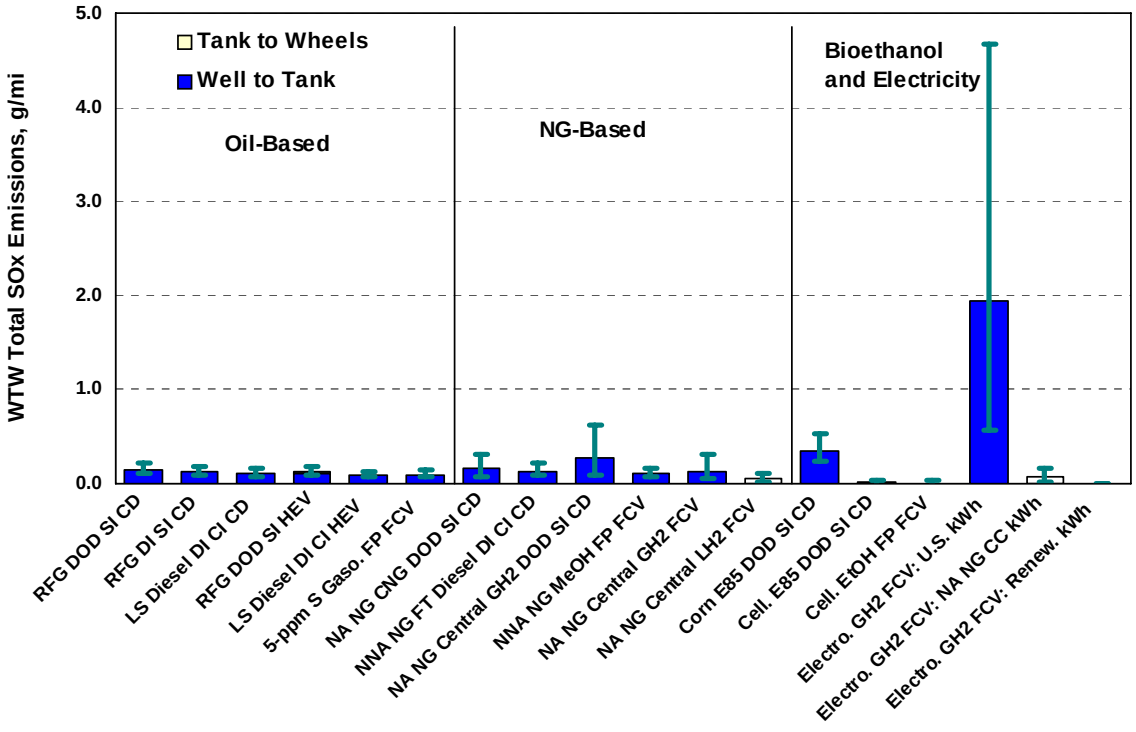

Figure 4-17 WTW Total SO_x Emissions of 18 Vehicle/Fuel Systems (g/mi)

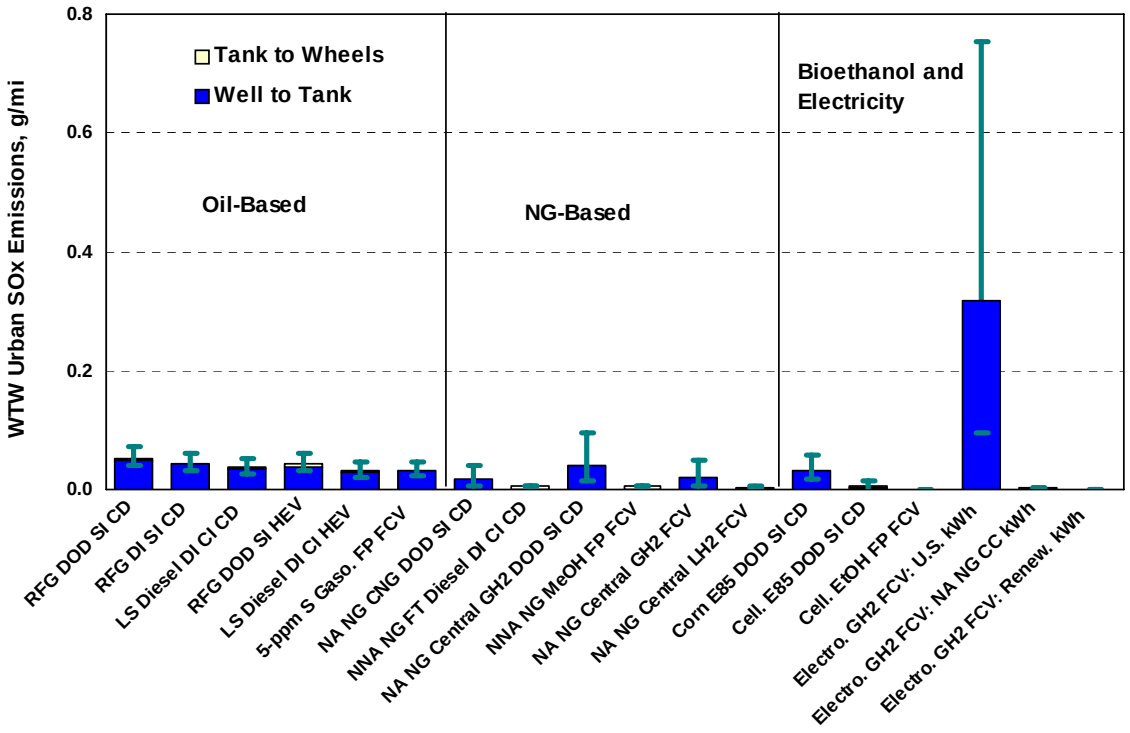

Figure 4-18 WTW Urban SO_x Emissions of 18 Vehicle/Fuel Systems (g/mi)

be minimal in the future. Again, use of U.S. average electricity for hydrogen production results in huge urban SO_x emissions (because a large percentage of U.S. electric generation capacity occurs within U.S. urban areas).

Of the six petroleum-based systems, WTW urban SO_x emissions (virtually WTT urban emissions) are about the same. Six systems (FT diesel ICEs, methanol FCVs, LH_2 FCVs, cellulosic ethanol ICEs, cellulosic FCVs, and renewable electricity-derived GH_2 FCVs) have almost zero WTW urban SO_x emissions. This is because (1) the WTT stage generates zero SO_x emissions (in the case of renewable electricity-derived GH_2) or (2) SO_x emissions occur outside of U.S. urban areas (in the case of the other five systems).

4.2 Specific Issues: Well-to-Wheels Results for Selected Vehicle/Fuel Systems

Section 4.1 presents results for all 17 items analyzed in this study for a set of 18 representative vehicle/fuel systems (of a total of 124 systems analyzed). The purpose of Section 4.1 was to provide general comparisons of advanced vehicle technologies and new transportation fuels. Many WTW studies have examined some specific issues. With the large amount of data generated from GREET simulations of the 124 vehicle/fuel systems, some specific issues of interest could be analyzed in detail. This section presents comparisons of the vehicle/fuel systems analyzed, with a focus on some specific issues: type of energy source; GHG, CO_2, CH_4, and N_2O emissions, vehicle hybridization benefits; use of NA and NNA NG for fuel production; benefits of hybridization of ICE and fuel cell technologies; and comparisons of hydrogen production pathways, renewable vs. nonrenewable fuels, and selected NG-based fuel pathways.

4.2.1 WTW Energy Use Results by Type of Energy Sources

In Section 4.1, we presented, for 18 vehicle/fuel systems, WTW total energy use, fossil energy use, and petroleum energy use separately in Figures 4-1, 4-3, and 4-4. We emphasized that, when renewable energy sources are involved, total energy use may not provide meaningful results when comparing the energy effects associated with different vehicle/fuel systems. To clearly demonstrate differences in energy use results by the three energy types (total energy [TE], fossil energy [FE], and petroleum energy [PE]), Figure 4-19 presents energy use by the three types of energy together for 15 selected vehicle/fuel systems.

Of the six selected petroleum-based systems, the patterns in energy use changes are similar for total energy use, fossil energy use, and petroleum use. Use of the results for any of the three energy types would lead to similar conclusions concerning the energy effects of the six petroleum-based technologies.

Of the six selected NG-based systems, the results for total energy use and fossil energy use are similar. This is because, for these pathways, the majority (if not all) of the energy consumption is derived from NG, which is accounted for in calculations of both total energy use and fossil energy use. However, if researchers are interested in the potential petroleum displacement by these six systems, they need to concentrate on the results of WTW petroleum energy use. Not surprisingly, all six NG-based systems almost eliminate petroleum energy use, even though some of the systems have total energy use and fossil energy use results similar to those for the baseline gasoline ICE.

The results for the two bioethanol systems and one electrolysis GH_2 system show the distortion of energy impacts if only total energy results are presented. Although bioethanol, especially cellulosic ethanol, has higher total energy use than the baseline gasoline ICE, bioethanol actually reduces fossil energy use and petroleum energy use significantly. If depletion of energy resources is a concern, we should focus on the fossil energy use results. If a reduction in petroleum use is a major U.S. goal, we should focus on the results of petroleum use. For GH_2 produced with U.S. average electricity, while the difference between total energy use and fossil energy use is small, the difference between the two on the one hand and petroleum use on the other hand is huge.

Some past WTW studies presented WTW energy efficiencies for various vehicle/fuel systems. The efficiencies in those studies were generally based on total energy use. In Section 4.1, we questioned the validity of including renewable energy in comparing renewable and non-renewable energy sources. Figure 4-2 showed the arbitrary nature of accounting for Btus when different primary energy sources are involved. WTW energy efficiencies based on total energy use for renewable energy (such as bioethanol) could be very low, but such efficiencies may be misleading about the true energy effects of renewable energy.

On the other hand, some researchers may suggest that energy efficiencies for vehicle/fuel systems could be calculated from fossil energy use. While the results based on fossil energy use may accurately reflect the advantage of the "renewable" nature of renewable energy, such efficiencies could exceed 100%. Without careful examination, readers could immediately question the seemingly counterintuitive results. But in fact, the over-100% efficiencies based on fossil energy use should be interpreted as the enhancement factor of renewable energy in terms of extending fossil energy use.

Researchers face another technical challenge in calculating WTW energy efficiency — comparing the TTW efficiencies of vehicles with different sizes and weights. Two vehicles could have the same TTW energy efficiency, but one could be much heavier than the other. A result showing the same efficiency for

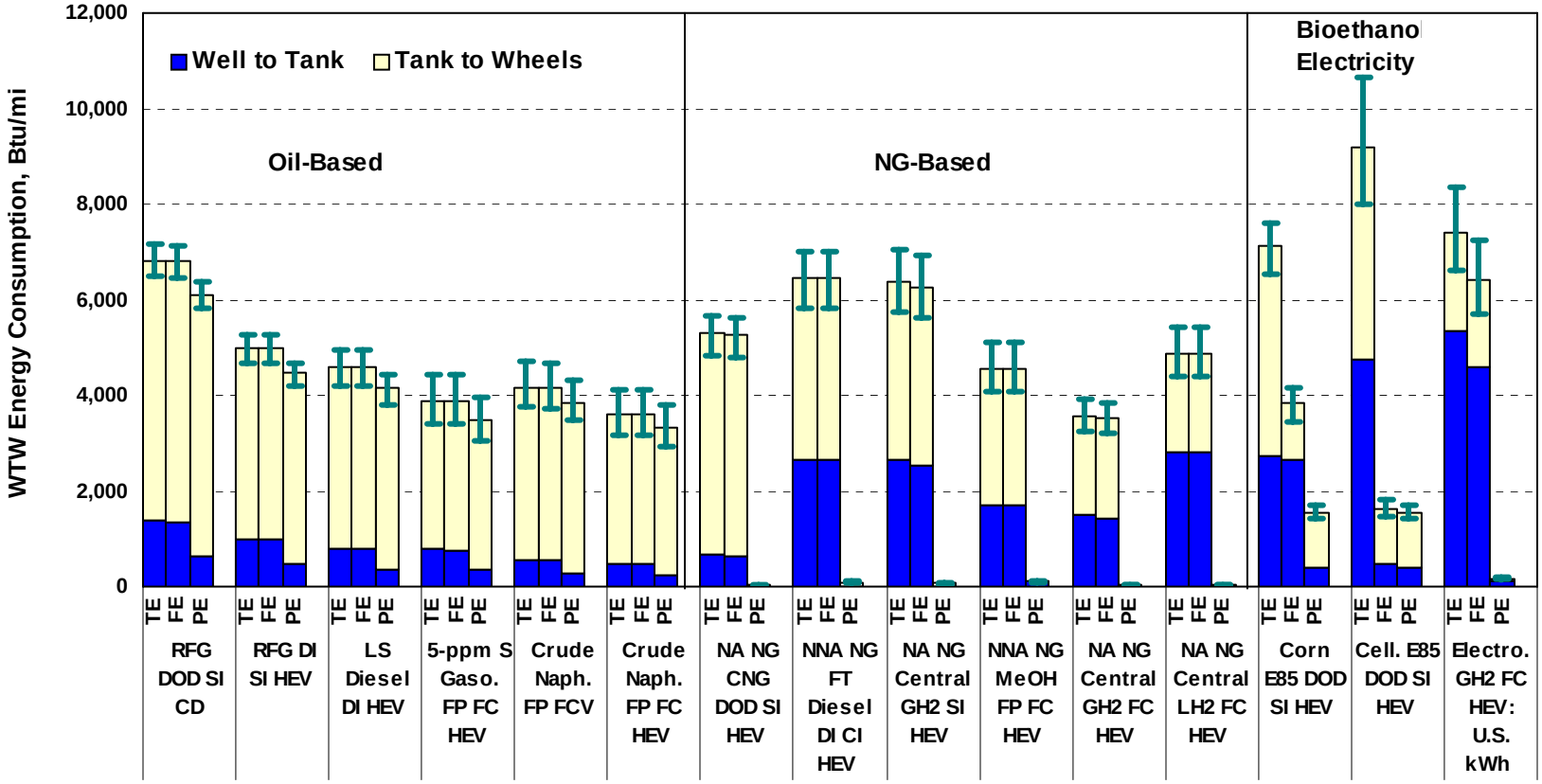

Figure 4-19 WTW Total Energy Use, Fossil Energy Use, and Petroleum Energy Use of Selected Vehicle/Fuel Systems (Btu/mi)

the two vehicles does not reveal the fact that the heavier vehicle could consume much more energy per mile driven than the lighter vehicle.

Because of these problems, we have not calculated WTW energy efficiencies (based on either total energy use or fossil energy use) for the vehicle/fuel systems that we evaluated in this study. Instead, we present per-mile energy use for the three energy types. We believe that this method provides readers with more meaningful results concerning the energy effects of advanced vehicle technologies and new transportation fuels. But we do present WTT efficiencies for fuel production pathways in Appendix D and TTW efficiencies for vehicle propulsion systems in Section 3 for information purposes. These efficiencies were calculated from total energy use results.

4.2.2 WTW Emissions of GHGs, CO_2, CH_4, and N_2O

Figures 4-5 through 4-8 in Section 4.1 present emissions of GHGs, CO_2, CH_4, and N_2O separately for the 18 vehicle/fuel systems. We demonstrated there that a complete assessment of GHG emission impacts of vehicle technologies fueled with different fuels requires inclusion of CO_2, CH_4, and N_2O emissions. To provide a clear comparison of the impacts of different GHGs, we present, for nine selected vehicle/fuel systems, emission results of GHGs (GWP-weighted CO_2, CH_4, and N_2O) and CO_2 together in Figure 4-20. Of the nine systems, the increases from CO_2 emissions to CO_2-equivalent GHG emissions are not proportional. In particular, the increases for corn ethanol, cellulosic ethanol, and CNG systems are higher than for the other six systems.

Figure 4-21 shows emissions of CH_4 and N_2O emissions for the nine selected systems. CH_4 emissions from CNG ICEs are significantly higher than those from other systems. The CH_4 emissions for CNG ICEs are generated during NG recovery, processing, and transmission. The U.S. average electricity-based GH_2 FCVs have relatively high CH_4 emissions because of CH_4 emissions that occur during coal mining.

The results for N_2O emissions show that the two bioethanol systems have dramatically higher N_2O emissions than the other seven systems. The N_2O emissions for bioethanol are from nitrification and denitrification of nitrogen fertilizer in agricultural fields.

Figures 4-20 and 4-21 show the need to include CH_4 and N_2O emissions in evaluating different transportation fuels, including CNG and ethanol. Some past studies included CO_2 emissions only in evaluating the climate change impacts associated with various vehicle/fuel systems. Exclusion of CH_4 and N_2O emissions gives CNG and ethanol additional benefits that are not warranted. Furthermore, because of the distortion by CH_4 and N_2O emissions among fuel types, patterns of relative GHG emission rankings of vehicle/fuel systems could be different from patterns of relative fossil fuel use rankings. Thus, GHG emissions and fossil fuel use need to be estimated separately in order to address both energy and GHG emission impacts of vehicle technologies and fuels. Fossil energy use results may not be a good surrogate for GHG emissions, especially when CNG and bioethanol are involved in the comparisons.

4.2.3 Benefits of Vehicle Hybridization

This study includes three vehicle power plant technologies: SI engine, CI engine, and fuel cell. For each technology, we simulated conventional drive and hybrid electric vehicle configurations. We presented the fuel economies for different vehicle technologies in Section 3. We showed that the shift from a CD configuration to an HEV configuration for the same power plant technology helps improve vehicle fuel consumption. In Figures 4-22 through 4-25, we present the impacts of the improved fuel consumption achieved via vehicle hybridization on WTW energy and emission results.

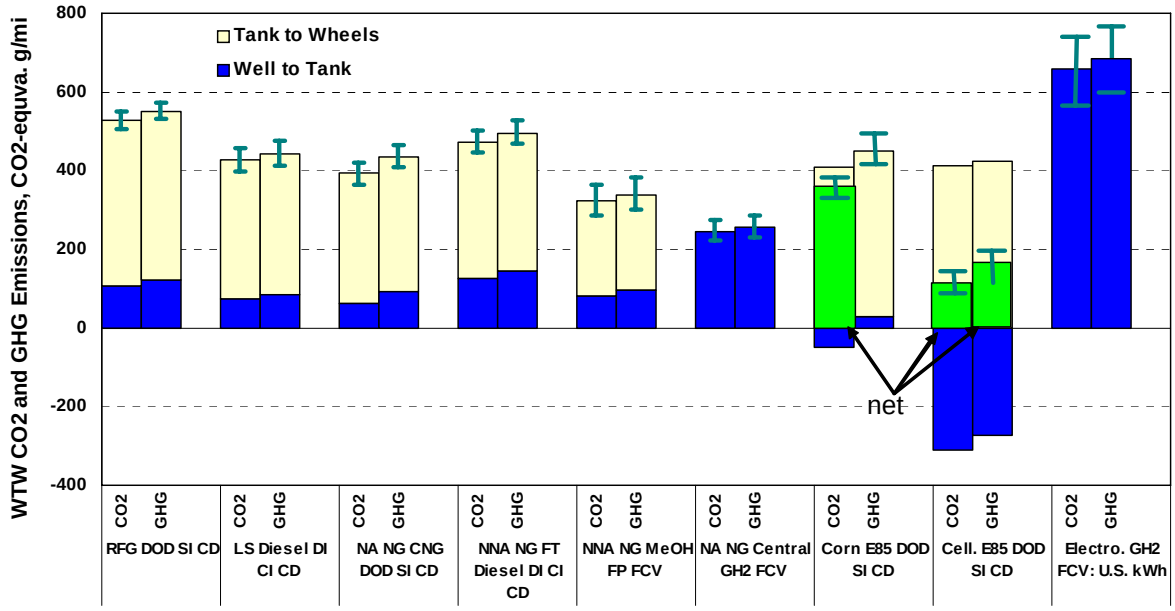

Figure 4-20 WTW GHG and CO_2 Emissions of Nine Vehicle/Fuel Systems (CO_2-equivalent g/mi)

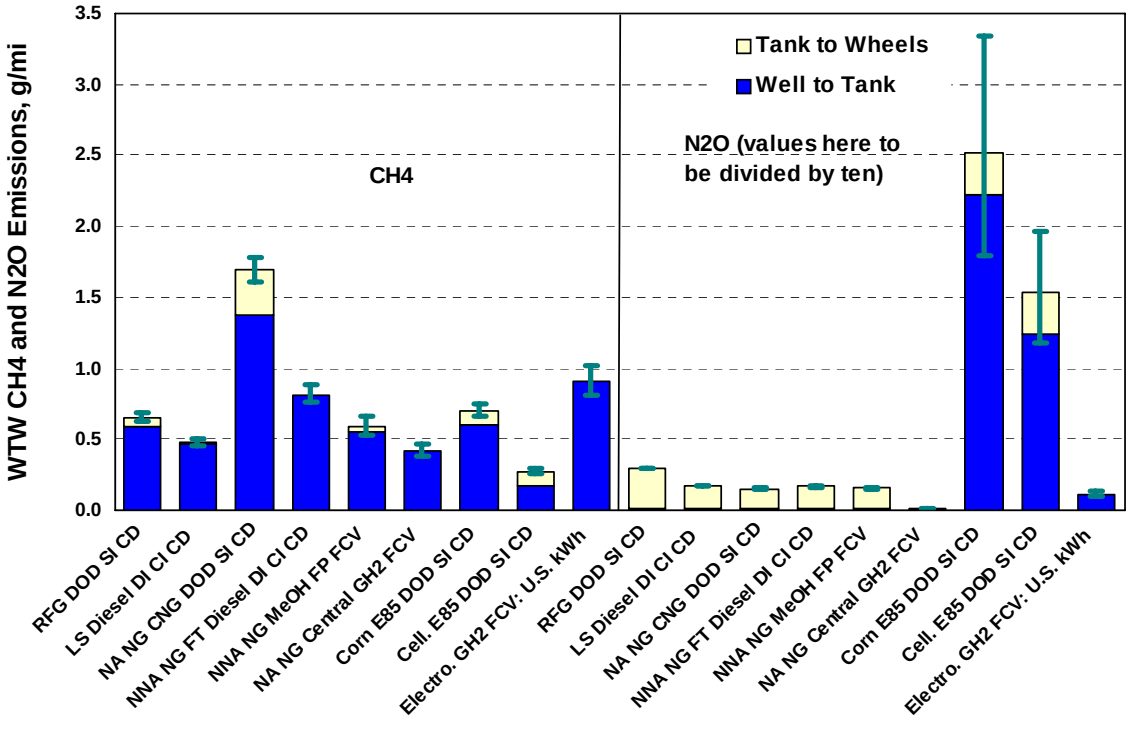

Figure 4-21 WTW CH_4 and N_2O Emissions of Nine Vehicle/Fuel Systems (g/mi)

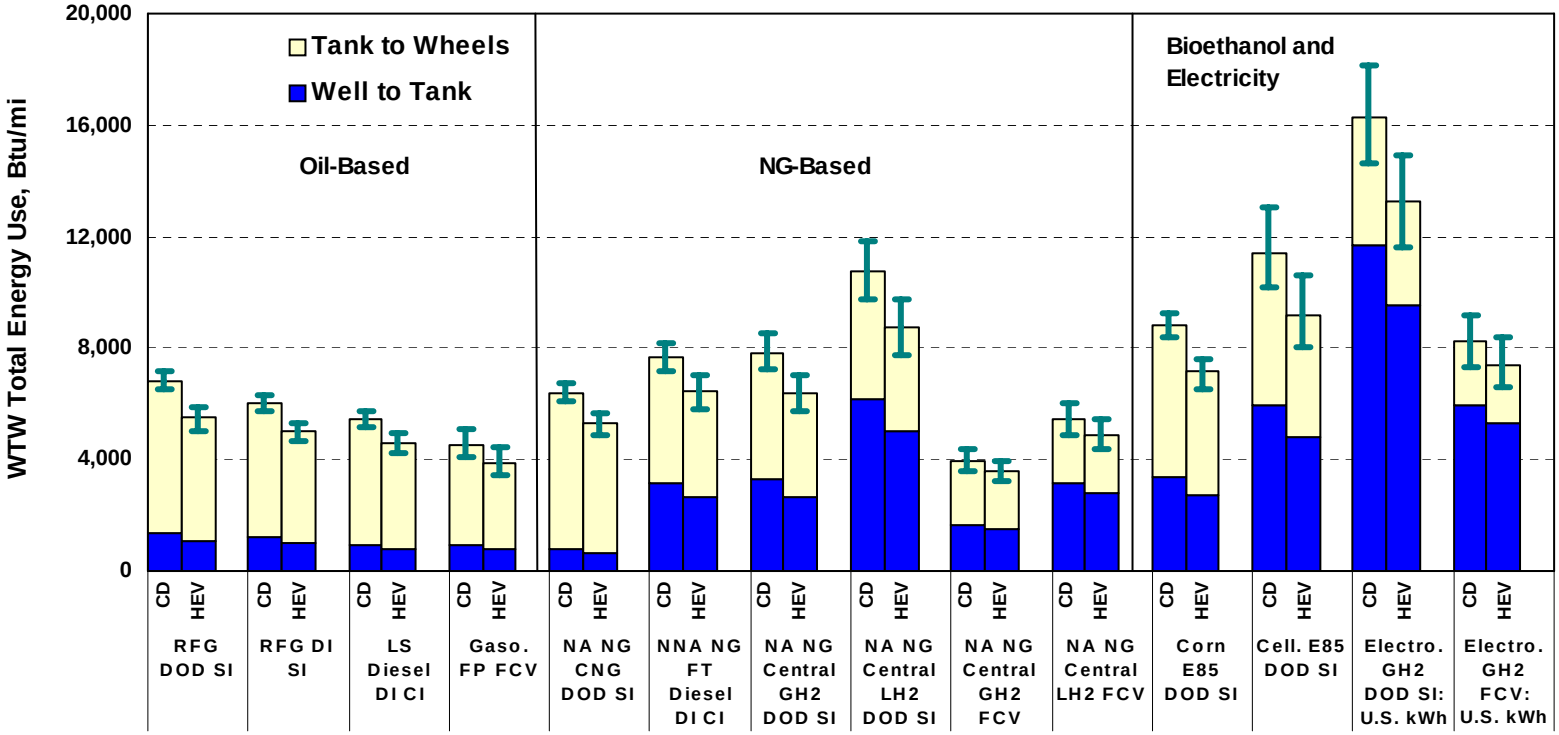

Figure 4-22 WTW Effects of Vehicle Hybridization: Total Energy Use (Btu/mi)

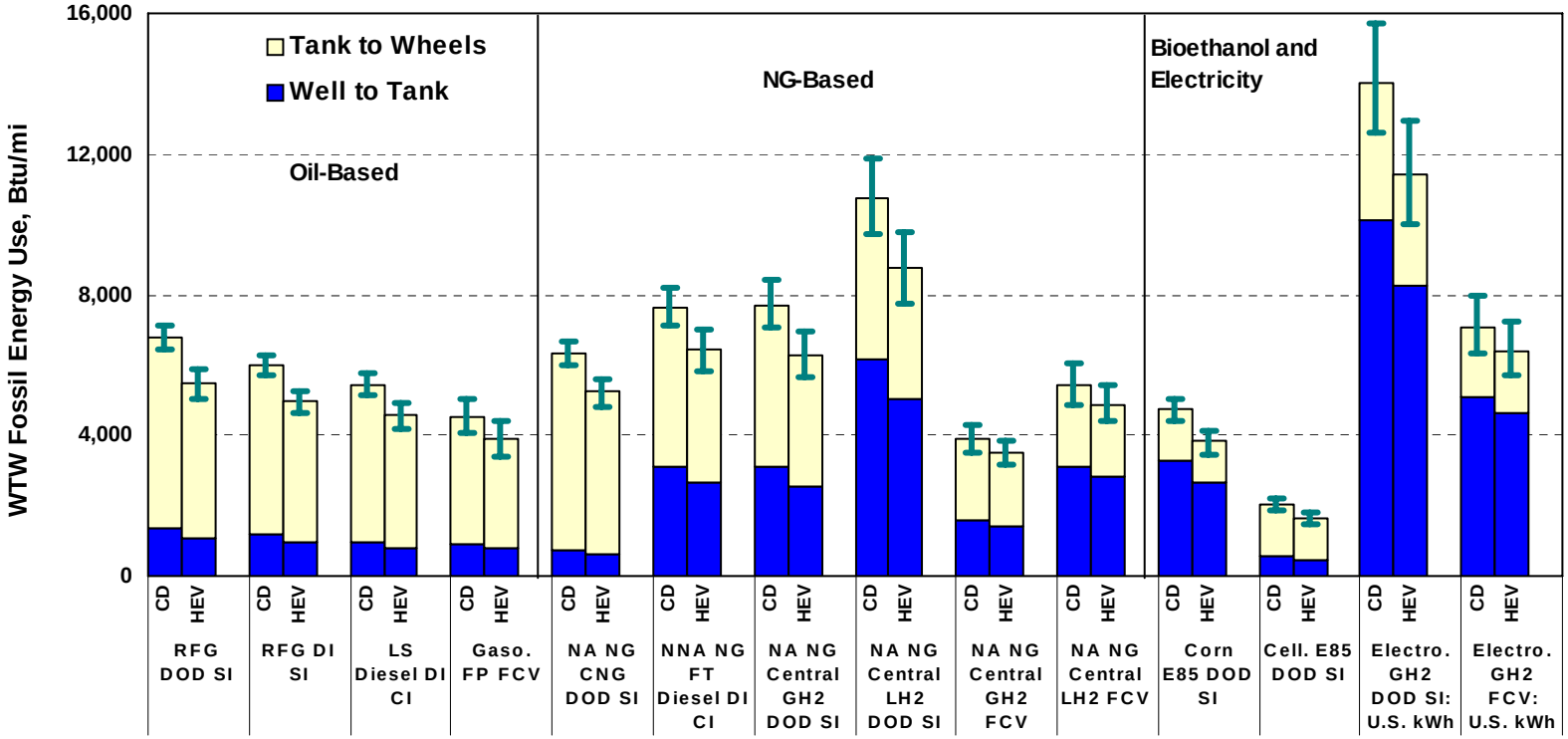

Figure 4-23 WTW Effects of Vehicle Hybridization: Fossil Energy Use (Btu/mi)

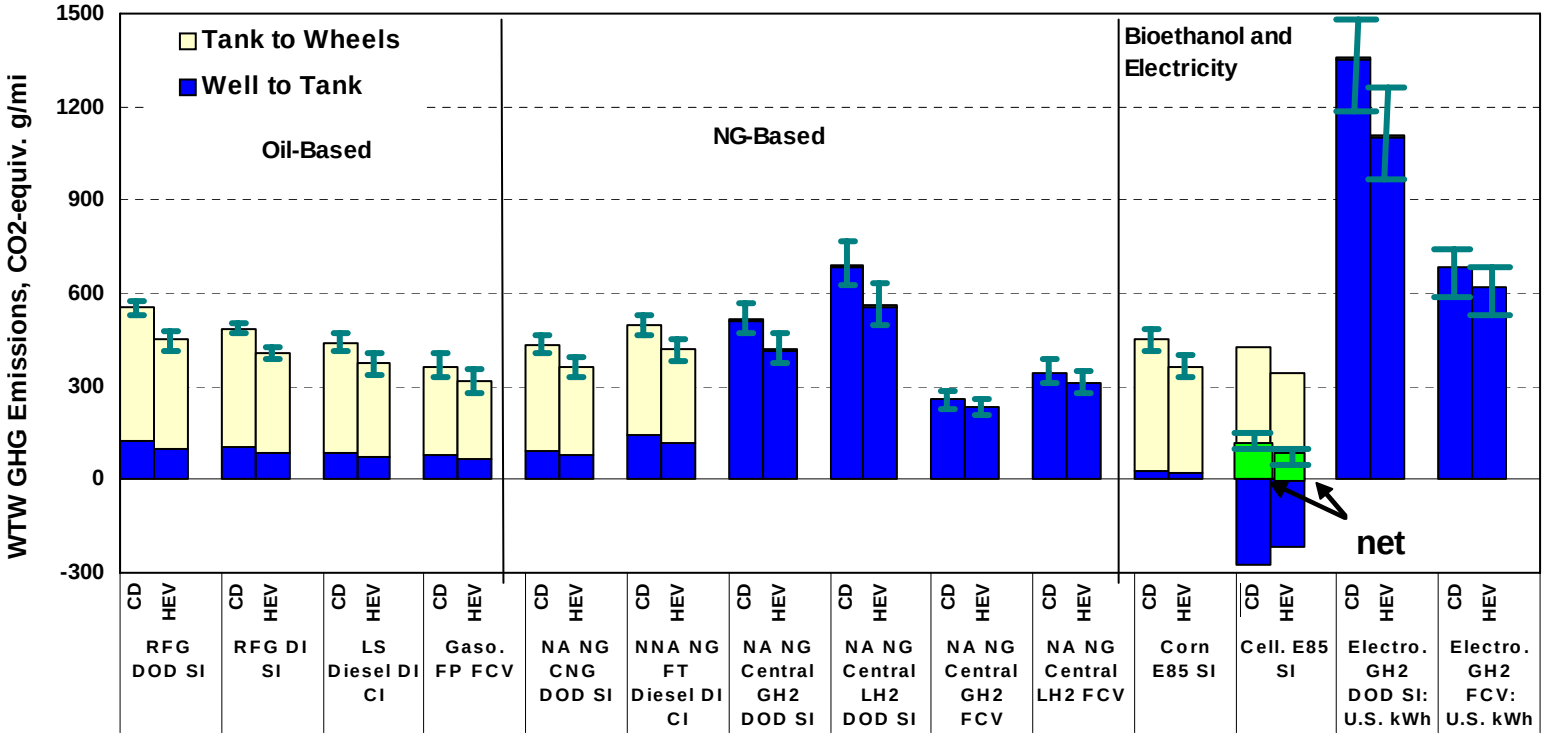

Figure 4-24 WTW Effects of Vehicle Hybridization: GHG Emissions (CO_2-equivalent g/mi)

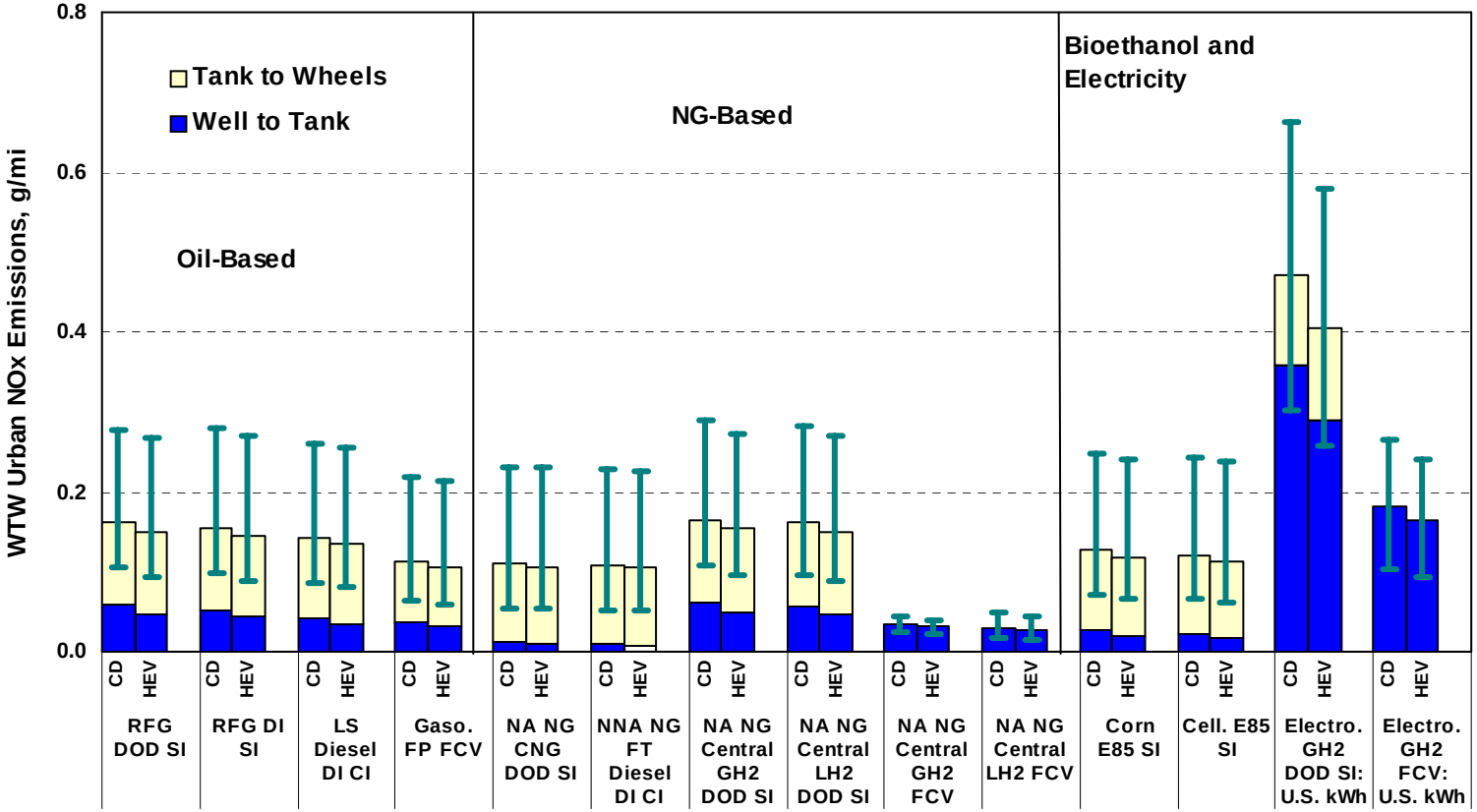

Figure 4-25 WTW Effects of Vehicle Hybridization: Urban NO_x Emissions (g/mi)

We selected 14 pairs of vehicle/fuel systems. Each pair consists of the CD and HEV configuration. Figure 4-22 presents WTW total energy results, Figure 4-23 fossil energy use, Figure 4-24 GHG emissions, and Figure 4-25 urban NO_x emissions.

The results show that vehicle hybridization helps reduce total and fossil energy use and GHG emissions. Figures 4-22 through 4-24 show that hybridization achieves larger reductions in per-mile energy use and GHG emissions for ICE technologies than it does for fuel cell systems. This is because, as discussed in Section 3, hybridization of ICEs achieves larger fuel consumption reductions than hybridization of FC systems. While WTW results here show that hybridization is more effective in reducing energy use and GHG emission with ICE systems, we realize that, in reality, the decision to hybridize FCVs will be made on the basis of costs, as well as energy and GHG emission benefits.

Figure 4-25 shows the impacts of hybridization on WTW urban NO_x emissions for the 14 selected systems. Except for GH_2 FCVs with U.S. average electricity, hybridization has little effect on urban NO_x emissions, primarily because WTW urban NO_x emissions are dominated by TTW NO_x emissions, which are regulated on a per-mile basis and are independent of the reductions in vehicle fuel consumption resulting from hybridization. For the electrolysis GH_2 system, reduction in energy use causes a reduction in per-mile NO_x emissions attributable to electric power plants.

4.2.4 Effects of Use of NA and NNA NG for Fuel Production

In the past 20 years, demand for NG in the United States has steadily increased. The NG supply in North America is already tight and will continue to be so in the future. If there is a large U.S. demand for NG-based transportation fuels (such as hydrogen, methanol, FT diesel, etc.), NG feedstocks could likely come from regions outside of North America. In this study, we analyzed WTW energy and emission impacts of producing transportation fuels from NA NG vs. from NNA NG.

Figures 4-26 through 4-30 present WTW energy and emission changes from NA NG to NNA NG for production of CNG, central GH_2, station GH_2, central LH_2, and station LH_2. The four hydrogen production options are applied to both SI engine-powered HEVs and FC-powered HEVs. In all cases, use of NNA NG in place of NA NG results in increased energy use and GHG emissions. But relative to fuel options and vehicle technologies, the increases attributable to the NG feedstock change are moderate. In addition, the five figures show the distinct energy use and GHG emissions reduction benefits of using fuel cell hybrid technologies relative to ICE hybrid technologies.

Figures 4-29 and 4-30 show WTW total and urban NO_x emissions for the pairs of vehicle/fuel systems with NA NG and NNA NG feedstocks. Total NO_x emissions are increased from NA NG to NNA NG when the same fuel is applied to a given technology. Total NO_x emissions from ICE technologies are significantly higher than those from fuel cell technologies. The uncertainty level of total NO_x emissions for hydrogen-fueled vehicle technologies is high, mainly because of the uncertainty surrounding NO_x emissions from hydrogen production and hydrogen combustion in ICEs. On the other hand, the level of WTW urban NO_x emissions is significantly lower than that of WTW total NO_x emissions. Figure 4-30 also shows that a switch from NA NG to NNA NG does not necessarily result in increased urban NO_x emissions because some of the NO_x emissions associated with NNA NG-based fuel production could occur outside of North America, and thus outside of U.S. urban areas.

The results for urban NO_x emissions in Figure 4-30 indicate two distinct trends. First, direct-hydrogen fuel cell technologies have much lower urban NO_x emissions than hydrogen ICE technologies because

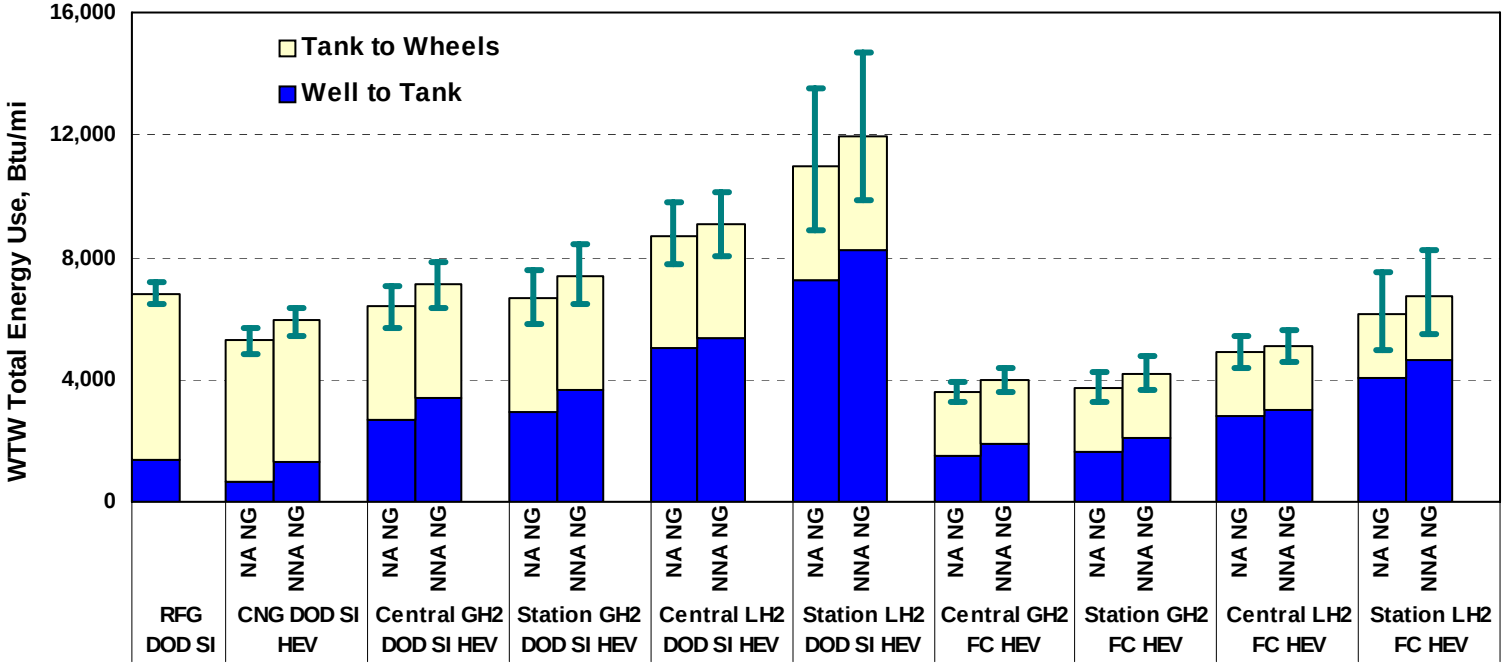

Figure 4-26 WTW Effects of North American NG vs. Non-North American NG: Total Energy Use (Btu/mi)

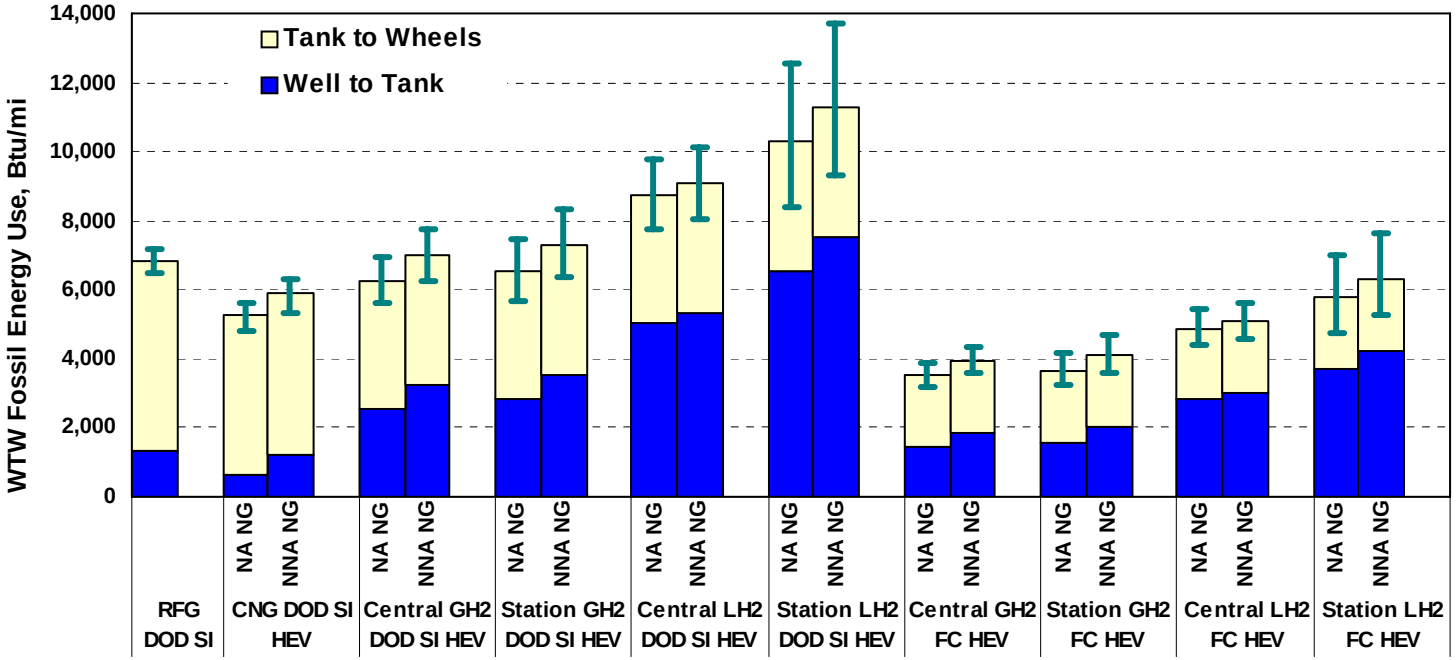

Figure 4-27 WTW Effects of North American NG vs. Non-North American NG: Fossil Energy Use (Btu/mi)

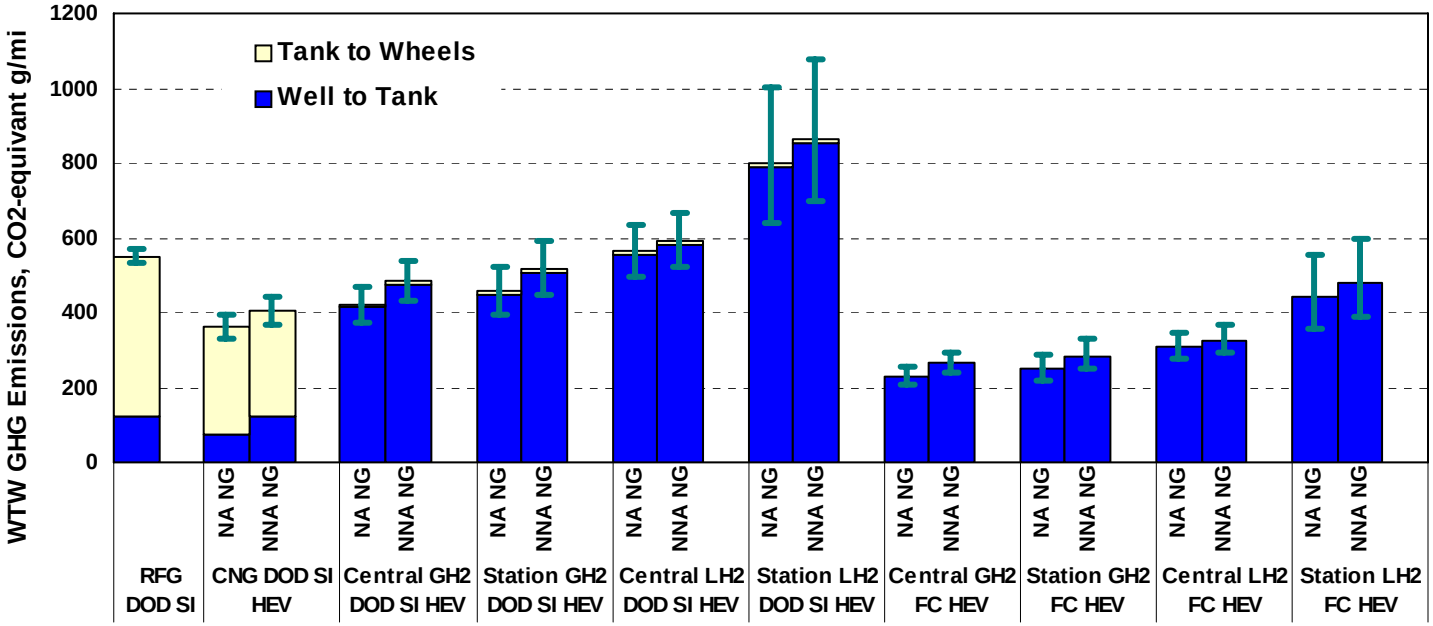

Figure 4-28 WTW Effects of North American NG vs. Non-North American NG: GHG Emissions (CO_2-equivalent g/mi)

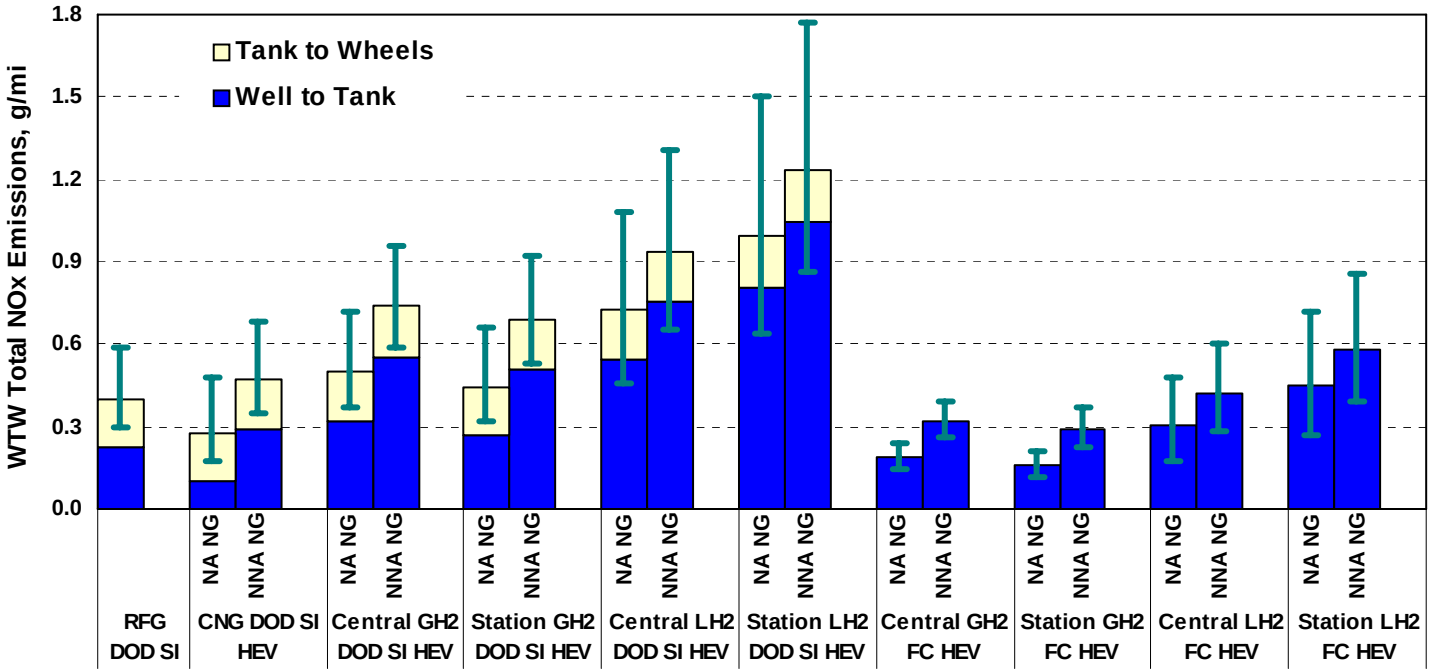

Figure 4-29 WTW Effects of North American NG vs. Non-North American NG: Total NO_x Emissions (g/mi)

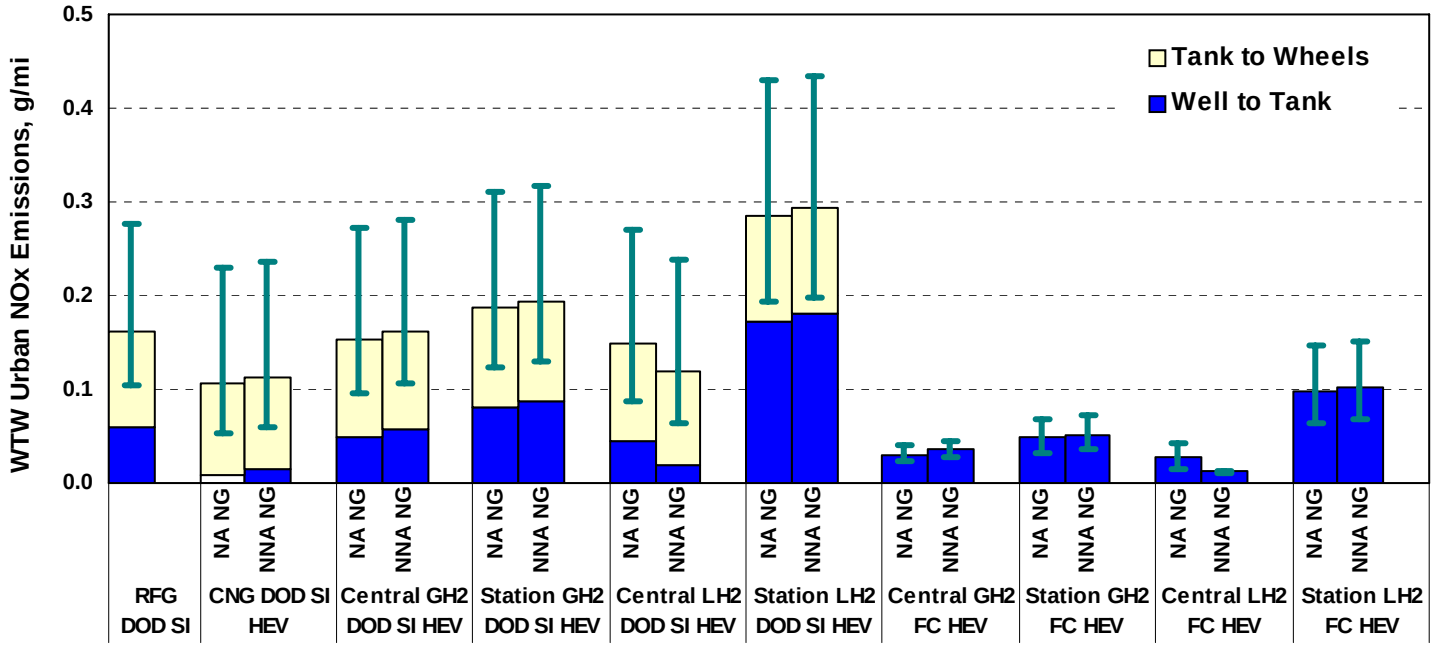

Figure 4-30 WTW Effects of North American NG vs. Non-North American NG: Urban NO_x Emissions (g/mi)

the former eliminates TTW NO_x emissions. Second, direct-hydrogen fuel cell technologies are subject to less uncertainty in WTW urban NO_x emissions than hydrogen ICE technologies, primarily because a great deal of uncertainty is involved in TTW NO_x emissions for hydrogen ICE technologies.

4.2.5 WTW Energy and Emission Reduction Benefits of ICE HEVs and Fuel Cell HEVs

Figures 4-31 through 4-36 present comparisons of WTW energy and emission results of ICE HEVs and fuel cell HEVs. We selected 25 vehicle/fuel systems for the comparison of ICE and fuel cell hybrid technologies. Of the 25 systems, there are nine pairs of ICE and fuel cell HEVs (gasoline, FT diesel and FT naphtha, NG-based GH_2, NG-based LH_2, cellulosic ethanol, electrolysis GH_2 produced with U.S. average electricity, electrolysis LH_2 produced with U.S. average electricity, electrolysis GH_2 produced with NG CC electricity, and electrolysis LH_2 produced with NG CC electricity). Within each pair, the fuel cell power plant shows reduced energy use and GHG emissions relative to the ICE power plant because the former is more efficient than the latter.

Researchers have debated in some completed WTW studies whether fuel cell technologies are more efficient than diesel HEVs. Our results, illustrated in Figures 4-31 and 4-32, show that fuel cell HEVs fueled with gasoline, methanol, and NG-based GH_2 require less WTW total energy and fossil energy than diesel HEVs. Cellulosic-ethanol-fueled fuel cell HEVs have higher WTW total energy use, but lower WTW fossil energy use, than diesel HEVs. However, if hydrogen is produced via electrolysis pathways, fuel cell HEVs could consume more energy than diesel HEVs. The relative differences in GHG emissions between diesel HEVs and FCVs, shown in Figure 4-33, are similar to energy use differences. A notable exception is the ethanol-fueled fuel cell HEV, which has lower GHG emissions, but higher energy consumption, than diesel HEVs.

Figures 4-34 through 4-36 present the WTW urban emissions of VOCs, NO_x, and PM_{10}. For each pair of ICE and fuel cell power plants, the fuel cell technology has consistently lower emissions of the three pollutants (except for VOC emissions of FT diesel and naphtha; naphtha is more volatile than diesel).

Between diesel HEVs and fuel cell HEVs, fuel cell HEVs fueled with volatile fuels such as gasoline, methanol, and ethanol have higher WTW VOC emissions than diesel HEVs, because of evaporative emissions from the volatile fuels. For WTW urban NO_x emissions, except for fuel cell HEVs fueled with U.S. average electricity-derived hydrogen, fuel cell HEVs have lower NO_x emissions than diesel HEVs. For WTW urban PM_{10} emissions, except for fuel cell HEVs fueled with electrolysis hydrogen, fuel cell HEVs have lower PM_{10} emissions than diesel HEVs. However, the differences in urban PM_{10} emissions between diesel HEVs and fuel cell HEVs are small because of the dilution effect of including brake and tire wear PM_{10} emissions, which were assumed to be the same for all vehicle/fuel systems.

Our results show that, in most cases, fuel cell HEVs consume less energy and generate fewer emissions than diesel HEVs. Furthermore, for the same fuel pathway, the fuel cell power plant is always more efficient and less polluting than the ICE power plant. Furthermore, FCVs, especially those powered with hydrogen, offer the opportunity for the U.S. transportation sector to switch from petroleum-based gasoline and diesel to different transportation fuels.

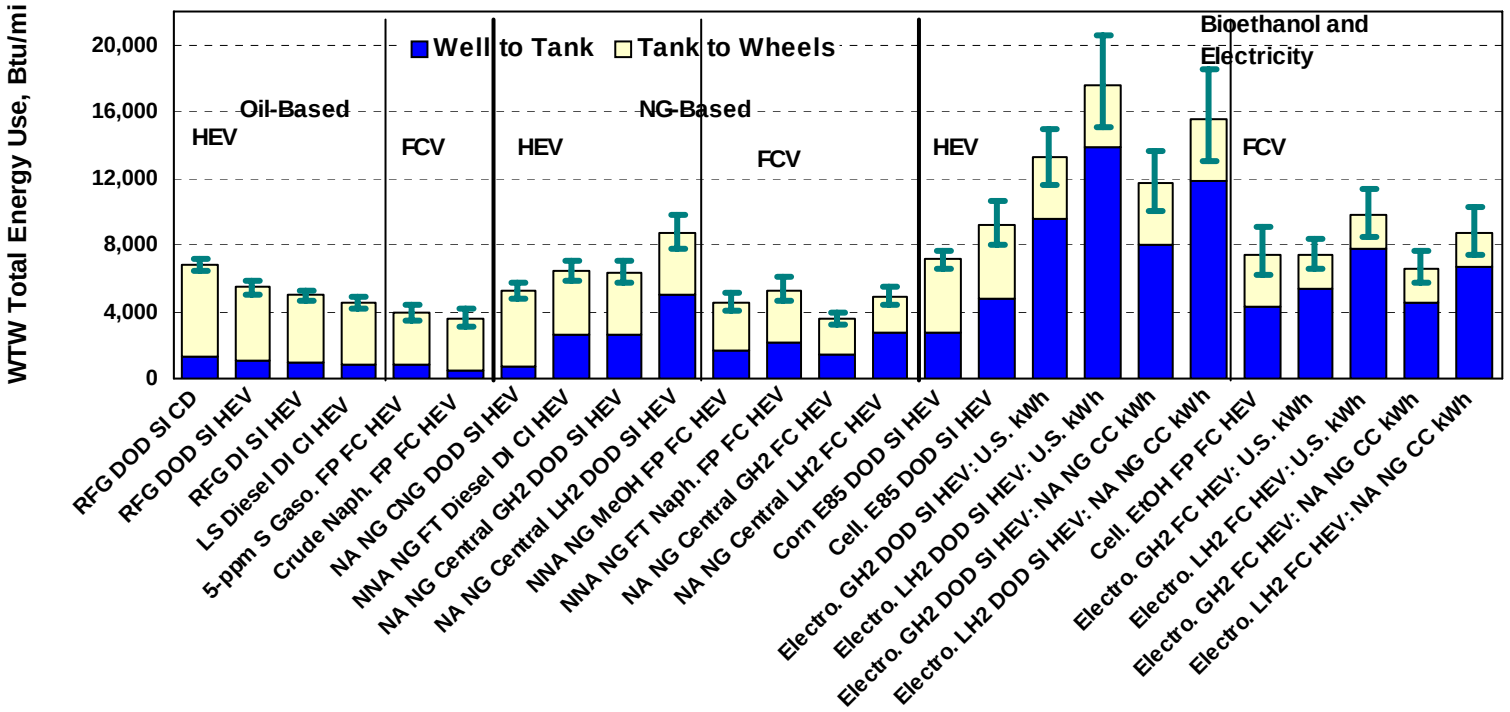

Figure 4-31 WTW Effects of ICE Hybrid and Fuel Cell Hybrid Technologies: Total Energy Use (Btu/mi)

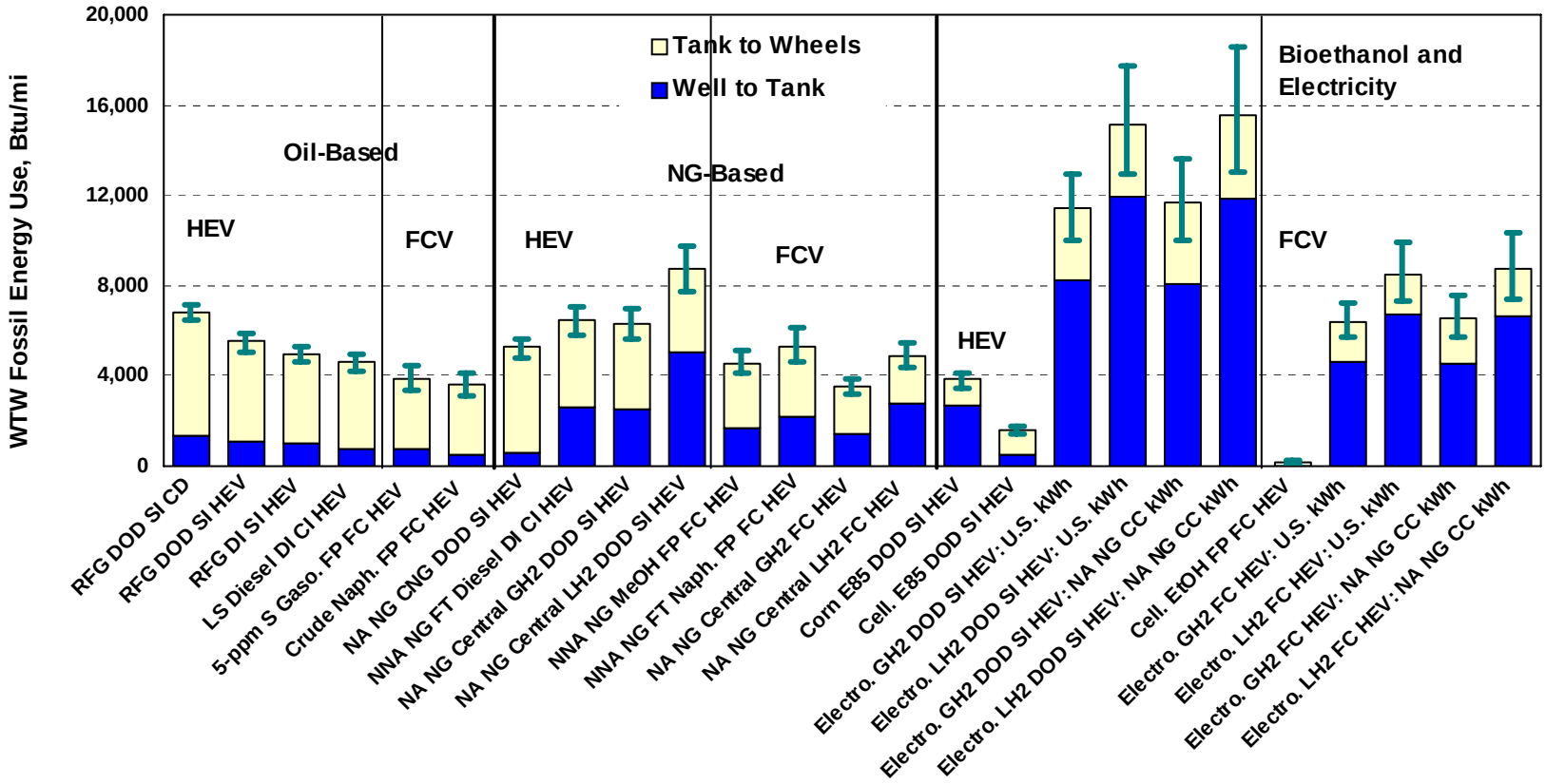

Figure 4-32 WTW Effects of ICE Hybrid and Fuel Cell Hybrid Technologies: Fossil Energy Use (Btu/mi)

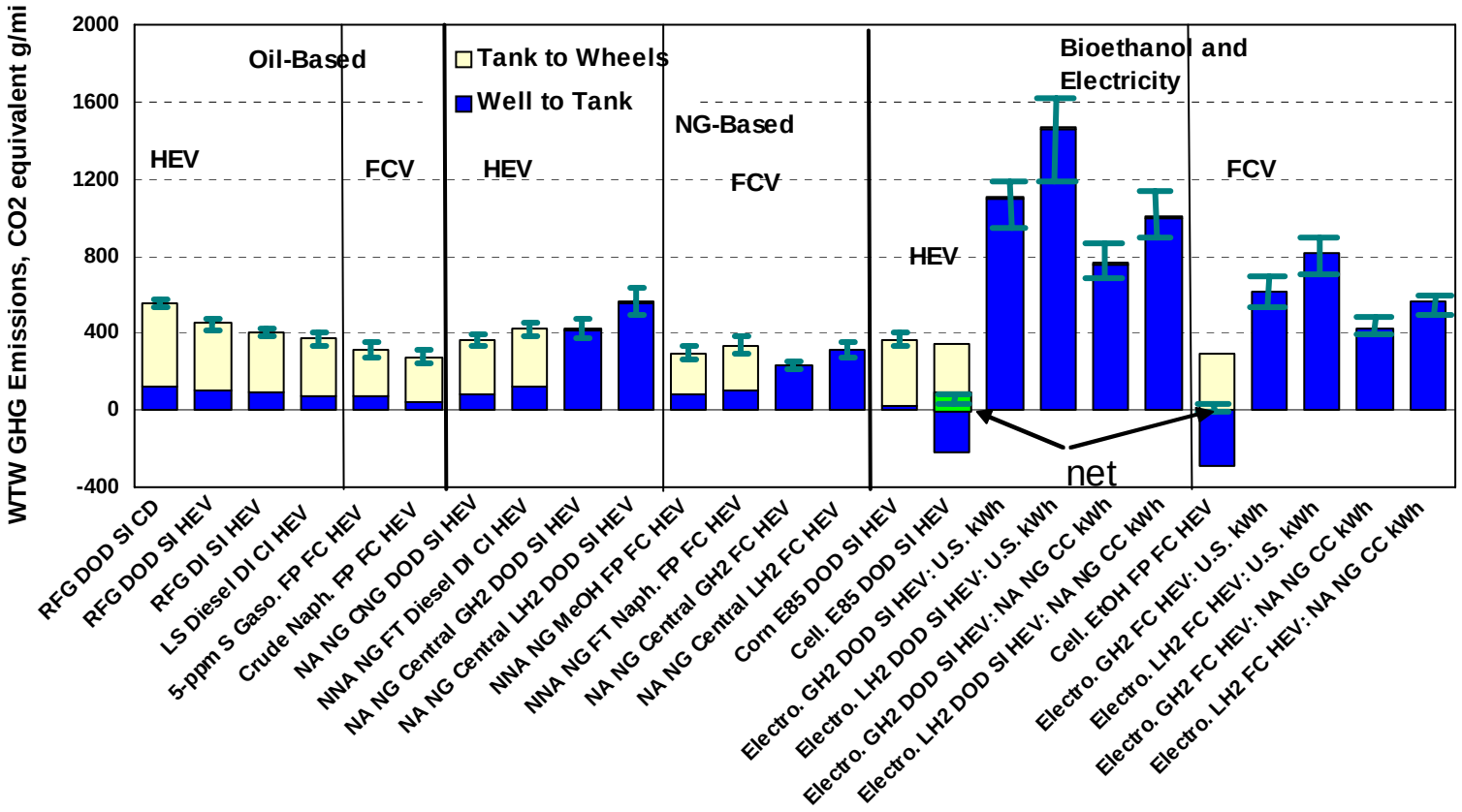

Figure 4-33 WTW Effects of ICE Hybrid and Fuel Cell Hybrid Technologies: GHG Emissions (CO_2-equivalent g/mi)

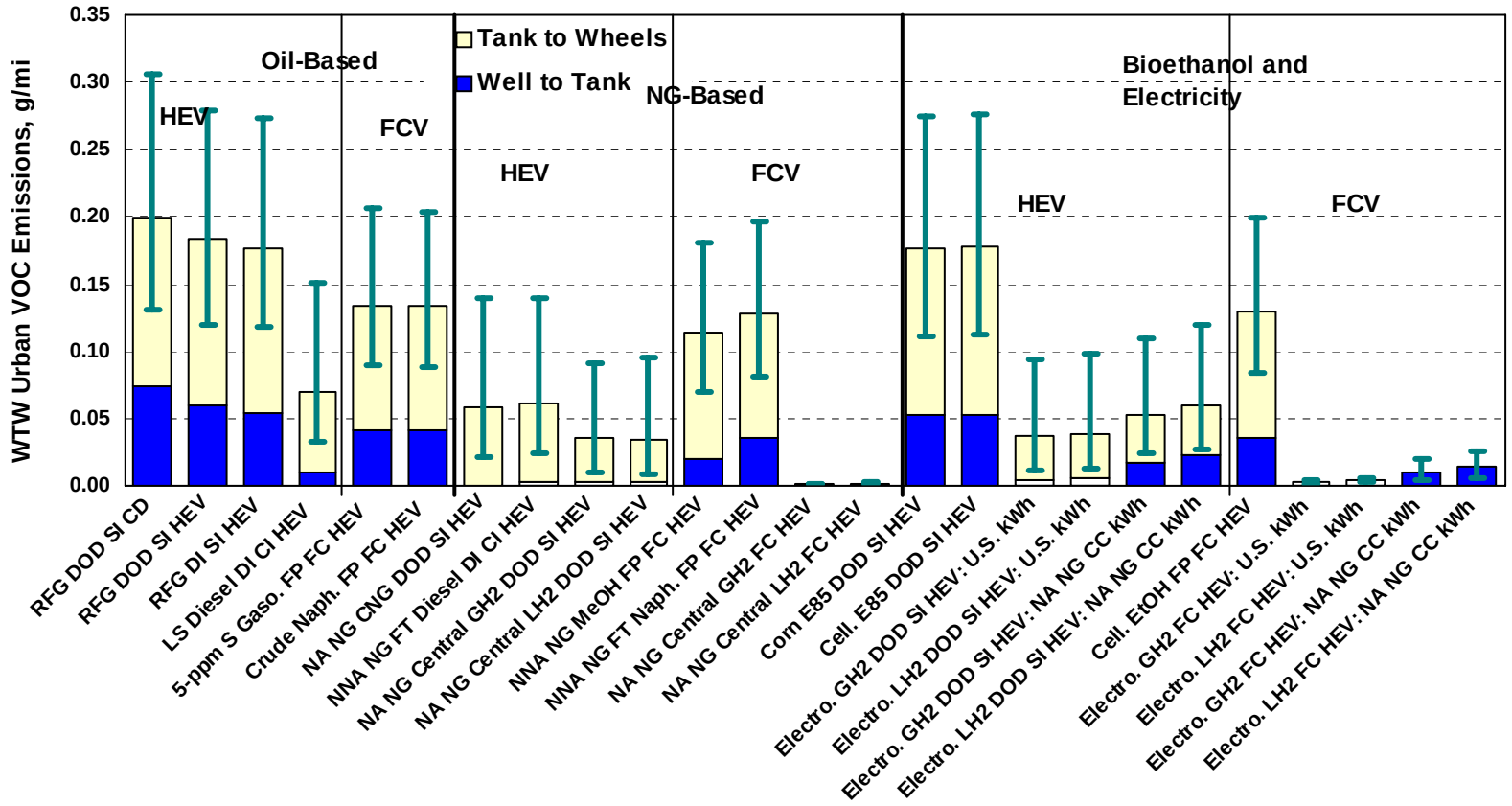

Figure 4-34 WTW Effects of ICE Hybrid and Fuel Cell Hybrid Technologies: Urban VOC Emissions (g/mi)

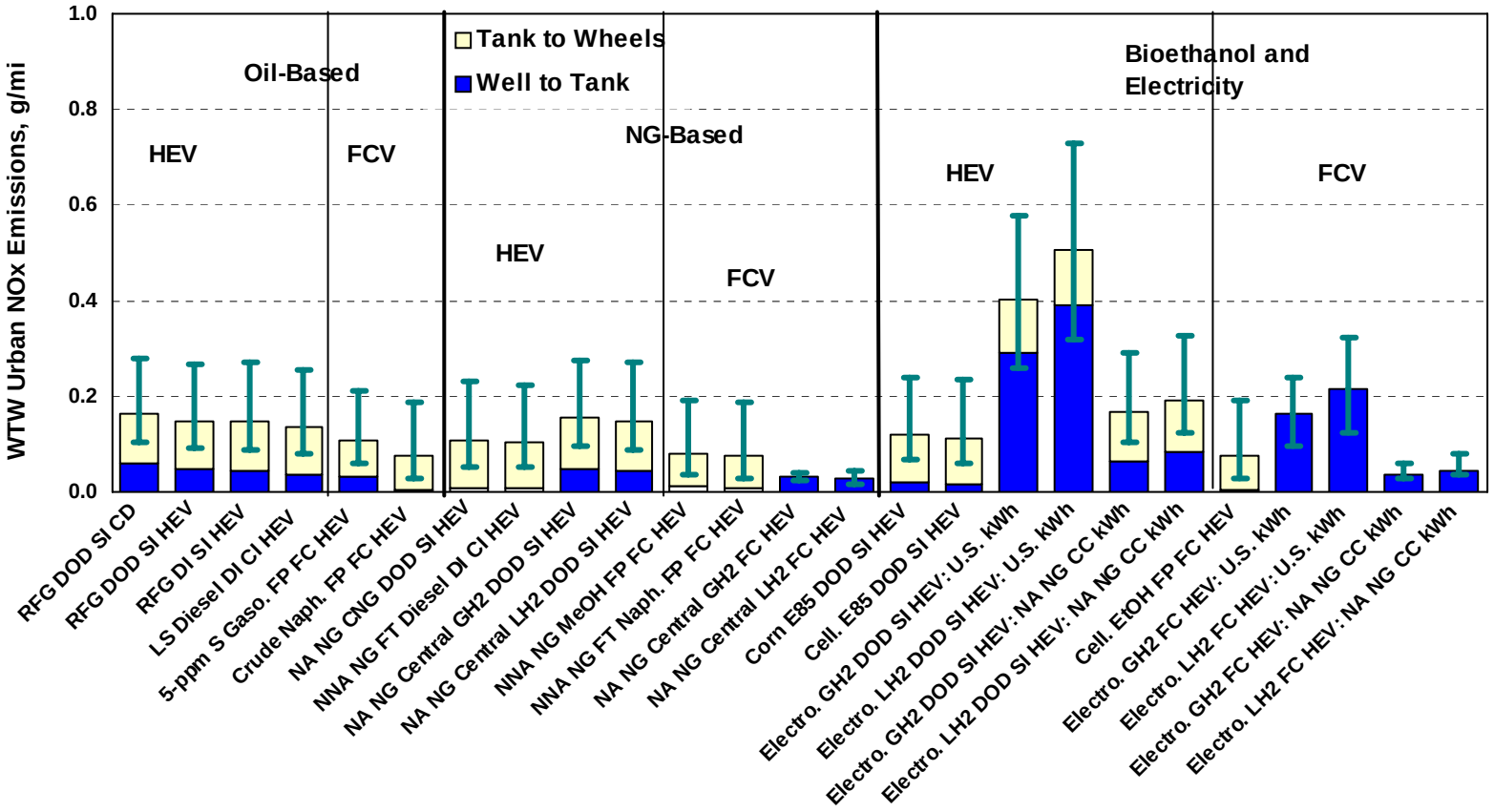

Figure 4-35 WTW Effects of ICE Hybrid and Fuel Cell Hybrid Technologies: Urban NO_{xE} missions (g/mi)

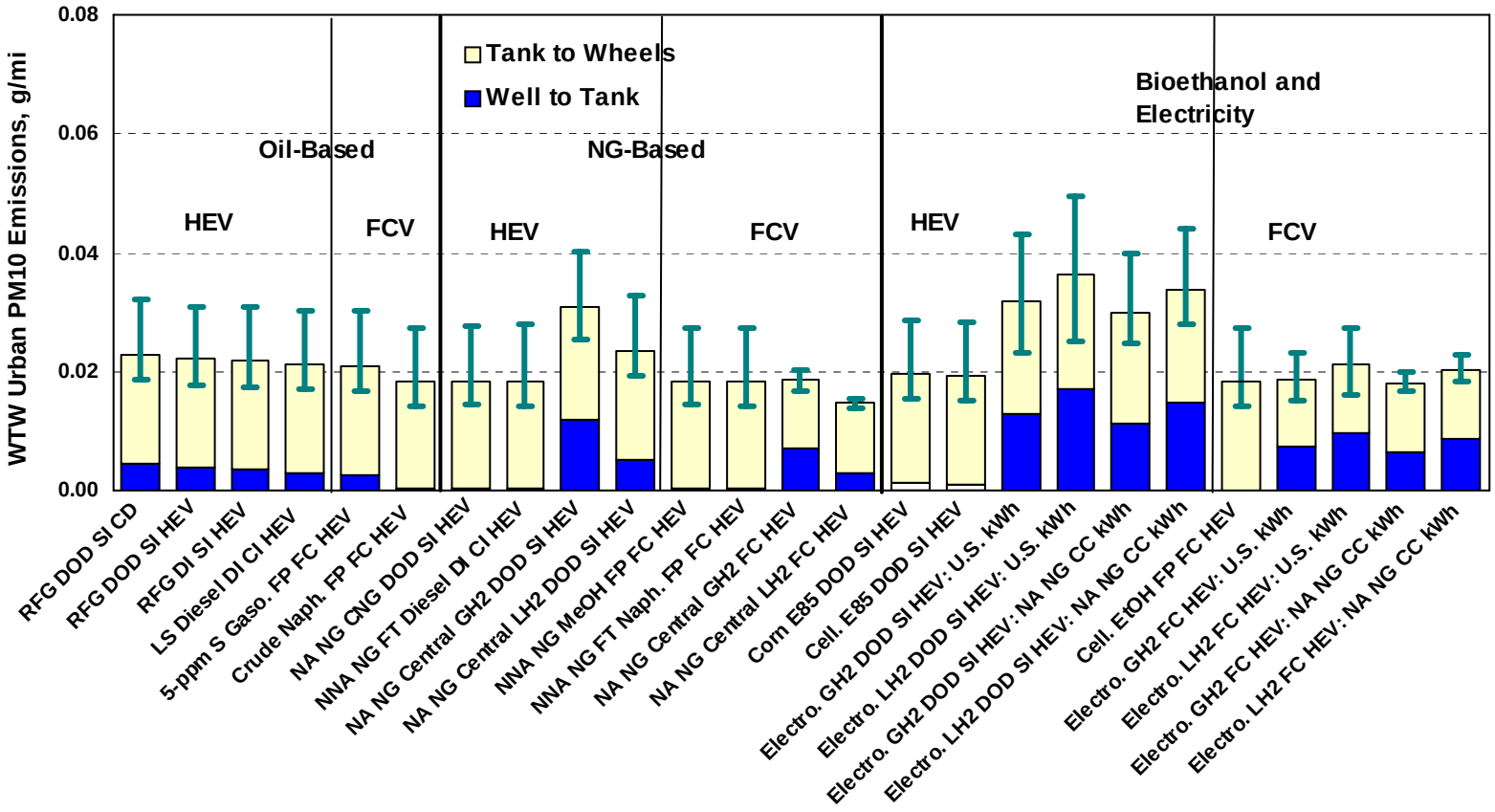

Figure 4-36 WTW Effects of ICE Hybrid and Fuel Cell Hybrid Technologies: Urban PM_{10} Emissions (g/mi)

4.2.6 Comparisons of Hydrogen Production Pathways

Among the 124 vehicle/fuel systems evaluated in this study, 97 are fueled with hydrogen. To demonstrate the WTW energy and emission effects of the different hydrogen production pathways, Figures 4-37 through 4-41 present WTW results for 25 hydrogen-fueled systems together with the results of the baseline gasoline ICE technology. Each figure is organized into four groups: central hydrogen production for ICE applications, refueling station hydrogen production for ICE applications, central hydrogen production for non-hybrid fuel cell applications, and refueling station hydrogen production for non-hybrid fuel cell applications.

Of the 25 hydrogen vehicle/fuel systems, there are 12 pairs of GH2- and LH_2-fueled systems for which the production pathways are the same (GH_2 and LH_2 in each pair are arranged next to each other in Figures 4-37 through 4-41). For each pair, Figures 4-37 through 4-39 show that the GH_2-fueled systems always have lower WTW energy use, GHG emissions, and total NO_x emissions than the LH_2-fueled systems. This is caused by the relatively large energy loss that occurs during hydrogen liquefaction with the LH_2 production options. However, Figures 4-40 and 4-41 show that levels of WTW urban emissions of NO_x and PM_{10} could be mixed between GH_2 and LH_2. For example, 4 out of the 12 pairs show that a GH_2-fueled system actually has higher urban NO_x and PM_{10} emissions than the comparable LH_2-fueled system. These pairs include central production of GH_2 and LH_2 with NA NG and NNA NG for ICE and fuel cell applications. In all these cases, while LH_2 is produced in central plants outside of urban areas, GH_2 is compressed at refueling stations with U.S. average electricity, which involves a significant amount of urban NO_x and PM_{10} emissions. If electricity generated in less-polluting electric power plants located outside of U.S. urban areas is used for GH_2 compression, a GH_2-fueled system would have fewer WTW urban NO_x and PM_{10} emissions than the comparable LH_2-fueled system.

If NG is the feedstock for hydrogen production, hydrogen could be produced in central plants and transported to refueling stations for vehicle use. Alternatively, hydrogen could be produced in refueling stations to avoid the need for inadequate, expensive hydrogen transportation and distribution infrastructure. For hydrogen production from electricity via electrolysis, we assumed that electricity is transmitted to refueling stations, where hydrogen is produced. In fact, avoiding the need for hydrogen transportation and distribution infrastructure by using electrolysis hydrogen production at refueling stations is a distinct advantage of electrolysis hydrogen production options. Between central and refueling station production of hydrogen from NG, Figures 4-37 through 4-39 show that central production of GH_2 has very small benefits in reducing WTW energy use and emissions. The differences in energy use and emissions between central and refueling station production for LH_2 are quite noticeable.

Section 4.2.4 described the energy and emission differences between using NA NG and NNA NG to produce transportation fuels. Figures 4-37 through 4-41 show again that NNA NG-based hydrogen production has somewhat larger WTW energy use and emissions than NA NG-based hydrogen production.

The results illustrated in Figures 4-37 through 4-41 show that, for refueling station hydrogen production, electrolysis hydrogen produced with U.S. average electricity has higher energy use and emissions than those associated with station SMR hydrogen production from NG. As emphasized in previous sections, electricity sources for electrolysis hydrogen are the key factor in determining its energy and emission effects. If clean, renewable electricity is used to generate hydrogen in refueling stations, electrolysis hydrogen will indeed achieve large energy and emission reduction benefits.

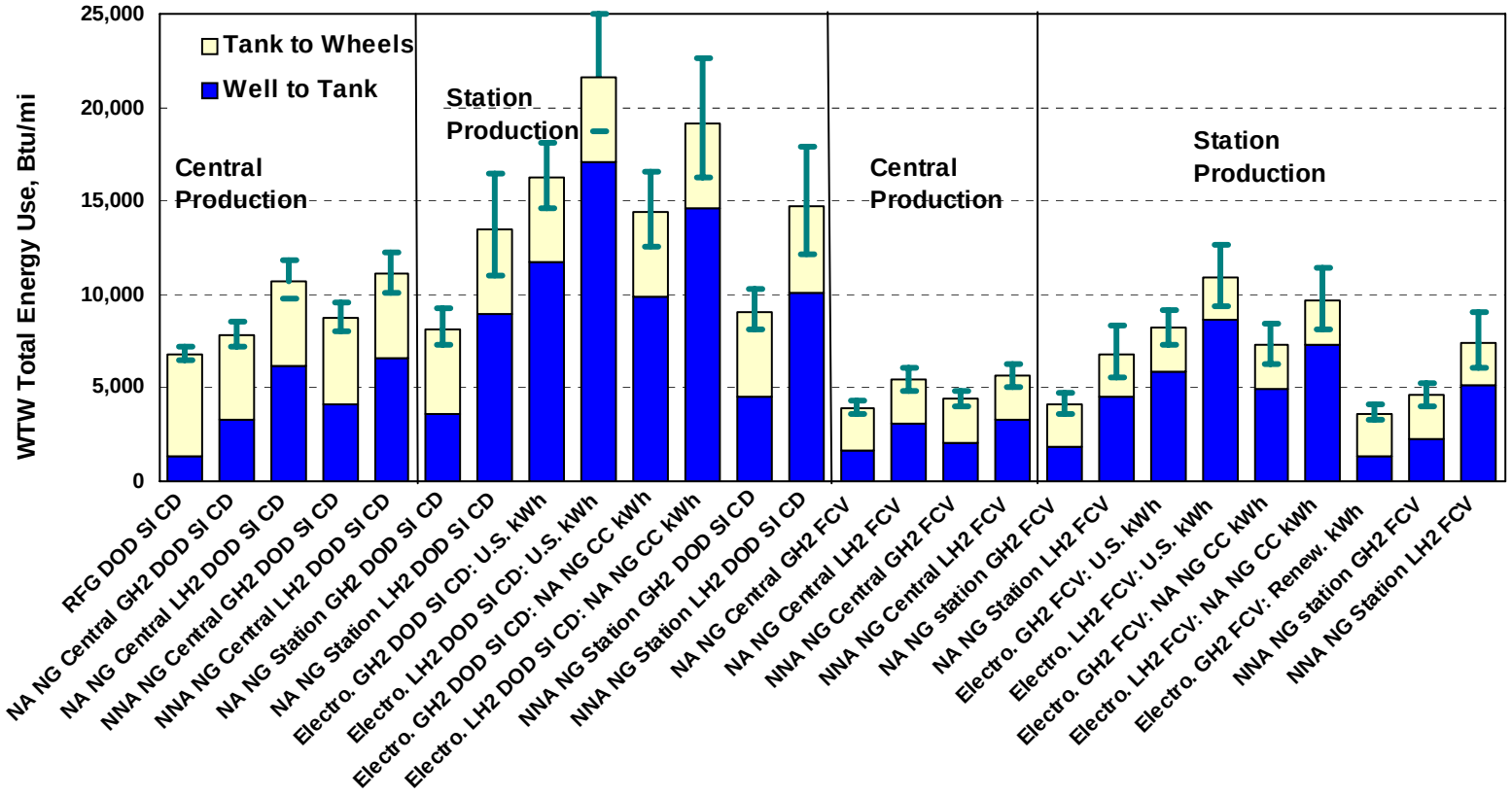

Figure 4-37 WTW Total Energy Use of Hydrogen Production Options (Btu/mi)

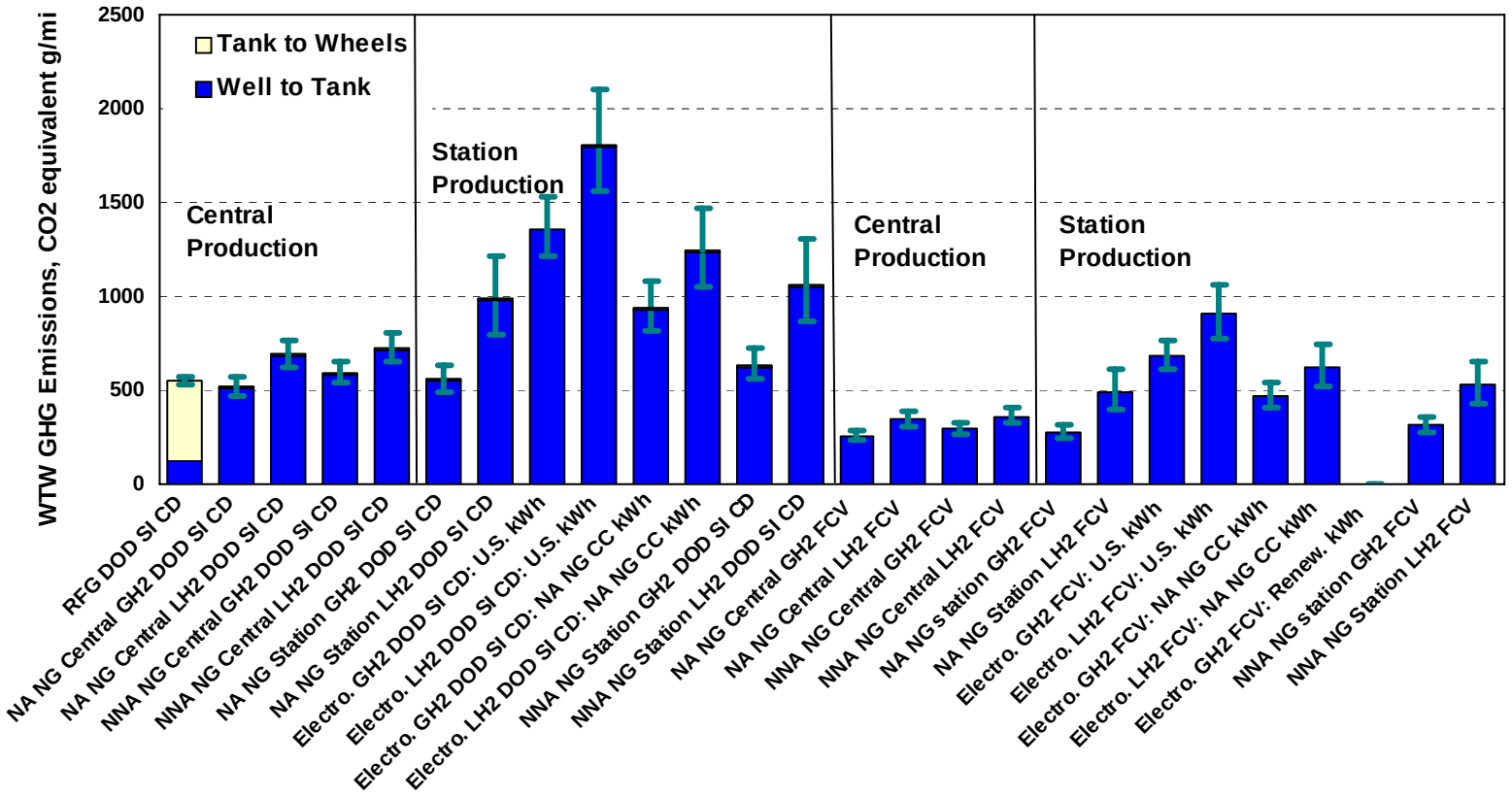

Figure 4-38 WTW GHG Emissions of Hydrogen Production Options (CO_2-equivalent g/mi)

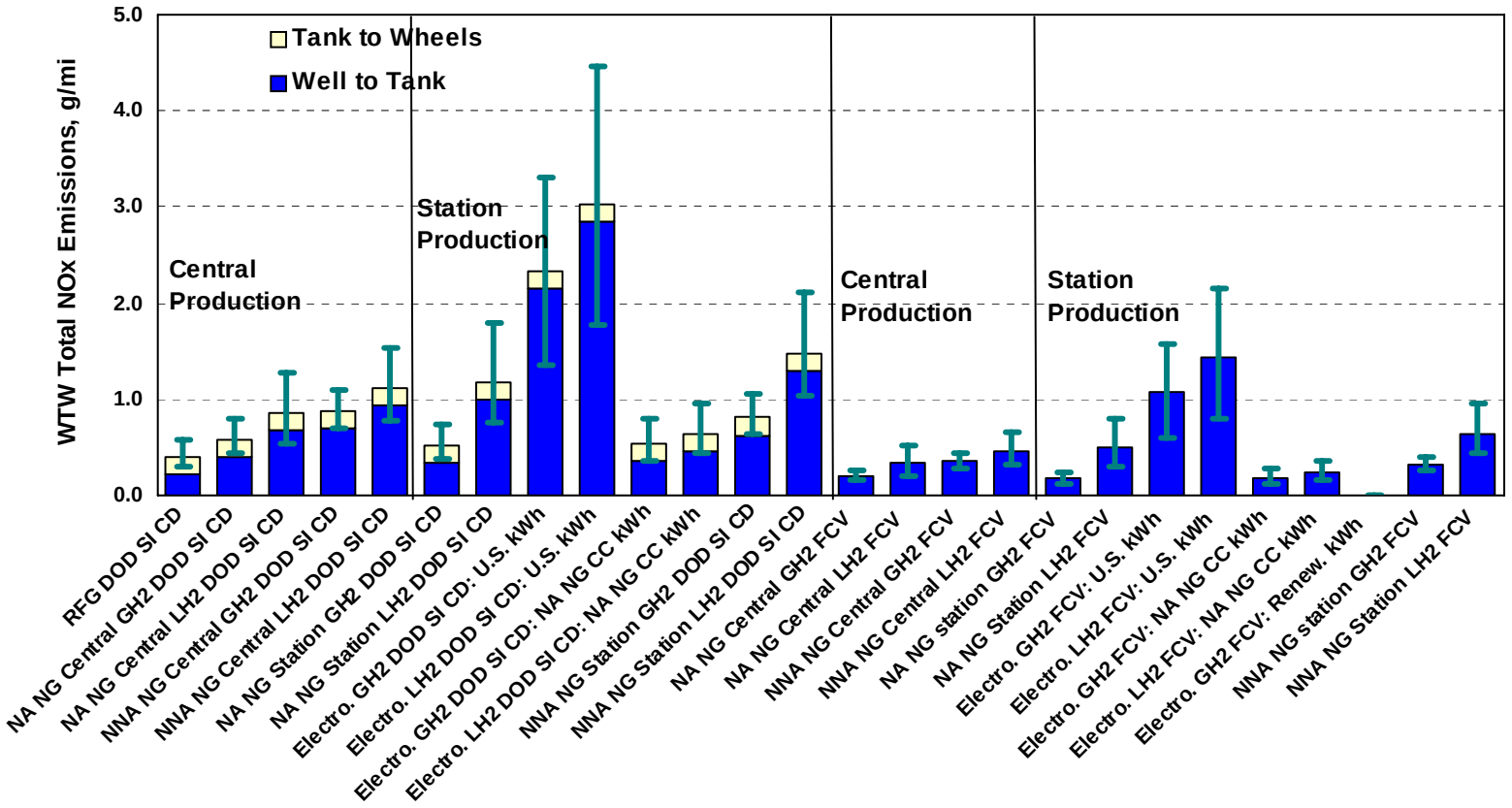

Figure 4-39 WTW Total NO_x Emissions of Hydrogen Production Options (g/mi)

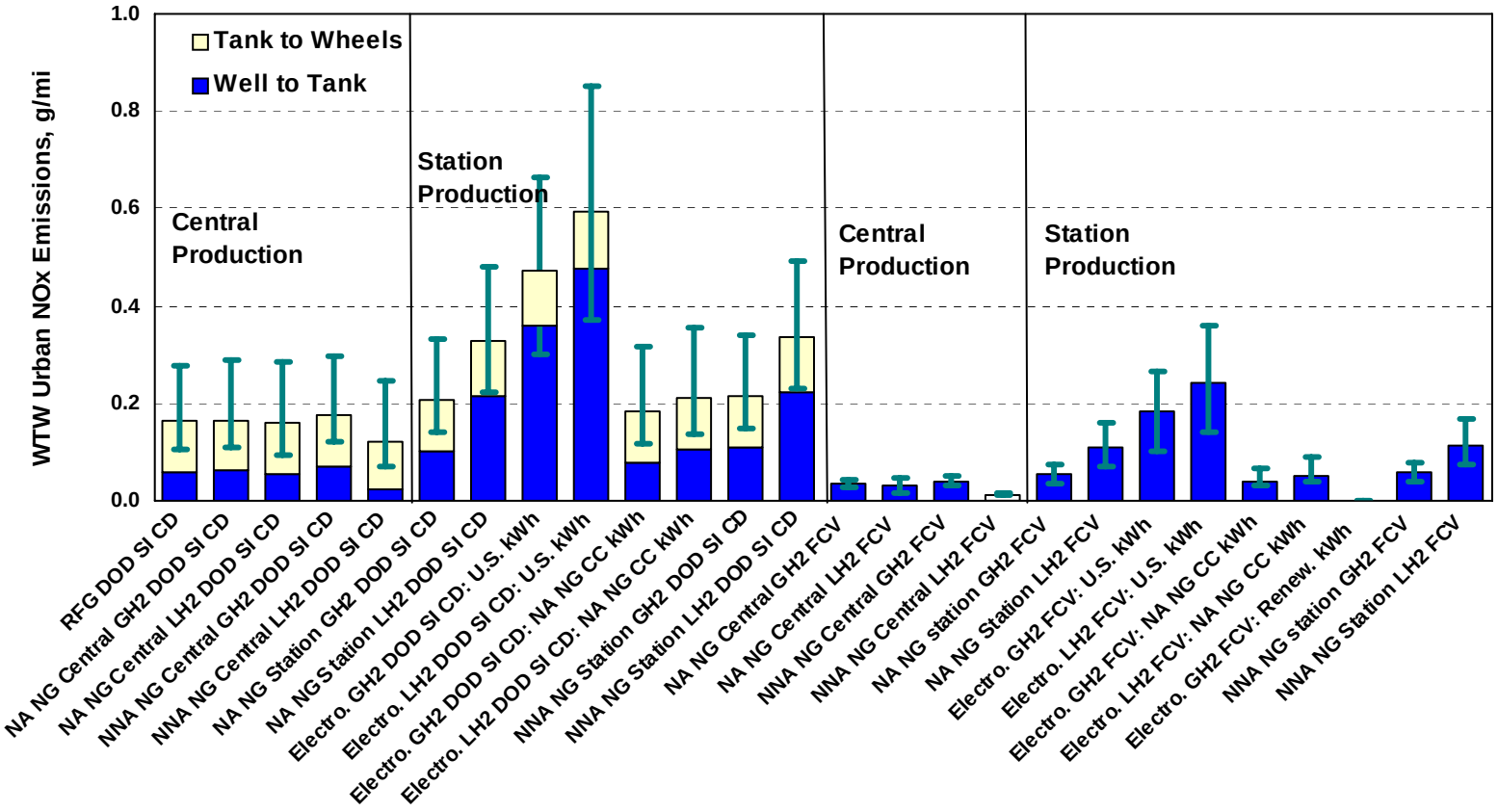

Figure 4-40 WTW Urban NO_x Emissions of Hydrogen Production Options (g/mi)

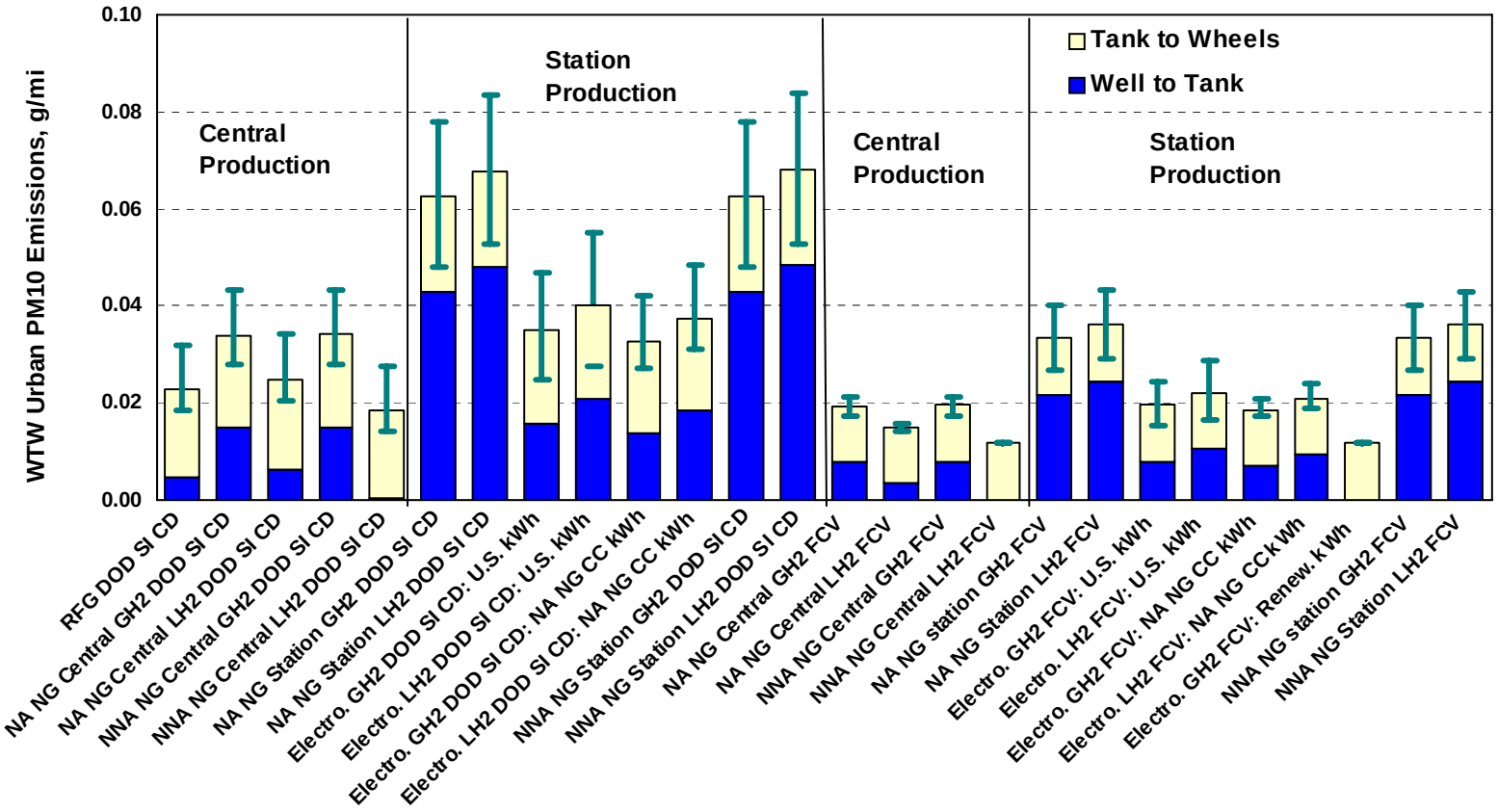

Figure 4-41 WTW Urban PM_{10} Emissions of Hydrogen Production Options (g/mi)

The results here show that LH_2 pathways are less efficient and potentially more polluting than GH_2 pathways. But the choice between GH_2 or LH_2 may be determined primarily by hydrogen storage technologies, discussion of which is beyond the scope of this study.

The increase in energy use and emissions from central production to refueling station production are small for GH_2 and moderate for LH_2. It appears that energy and emission impacts may not be a key factor in determining whether to use central or refueling station hydrogen production. The economics and availability of a hydrogen transportation and distribution infrastructure will be likely be the key factor for that decision. However, moving hydrogen production from central plants to refueling stations will move emissions of criteria pollutants closer to the population.

4.2.7 Comparisons of Renewable Fuels and Non-Renewable Fuels

Of the 124 vehicle/fuel systems analyzed in this study, eight are fueled with renewable fuels (seven with bioethanol and one with renewable electricity-based GH_2). Figures 4-42 through 4-46 present WTW energy and emission results of the eight renewable fuel-based systems, together with eight non-renewable fuel-based systems for similar vehicle technologies. Although Figure 4-42 shows that renewable fuels generally have higher WTW *total* energy use than non-renewable fuels, a significant portion of the total energy use by renewable fuel systems is indeed renewable energy. When results of WTW *fossil energy* use between renewable and non-renewable fuels are compared (such comparison is more appropriate than the comparison of total energy use), Figure 4-43 shows that renewable fuels achieve large reductions in WTW fossil energy use relative to those of non-renewable fuels.

The GHG emission results in Figure 4-44 reveal that the three systems fueled with corn ethanol achieve moderate GHG emission reductions. But the four systems fueled with cellulosic ethanol and the one renewable electricity GH_2 option achieve very substantial reductions in GHG emissions.

The WTT stage of corn and cellulosic ethanol pathways is associated with a large amount of NO_x emissions because of the NO_x emissions from farming equipment, nitrification and denitrification of nitrogen fertilizer, and ethanol production. Figure 4-45 shows large increases in WTW total NO_x emissions by the seven ethanol systems. However, most of the WTT NO_x emissions occur outside of U.S. urban areas. WTW urban NO_x emissions (Figure 4-46) from the seven ethanol systems are comparable to those of the non-renewable fuel systems.

In summary, the energy and emission benefits of renewable fuels lie in reductions in fossil energy use, petroleum energy use, and GHG emissions.

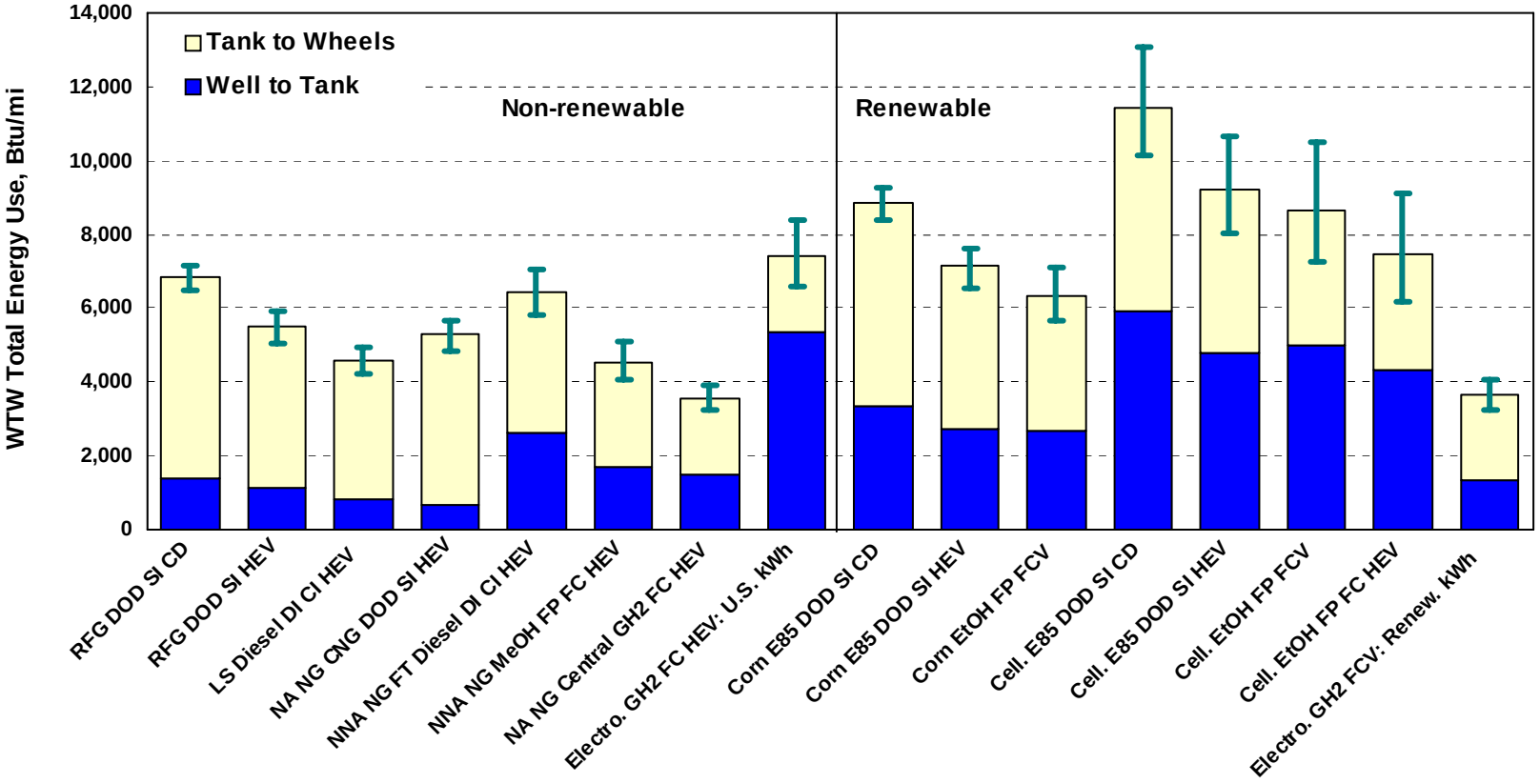

Figure 4-42 Comparison of Non-Renewable and Renewable Fuels: WTW Total Energy Use (Btu/mi)

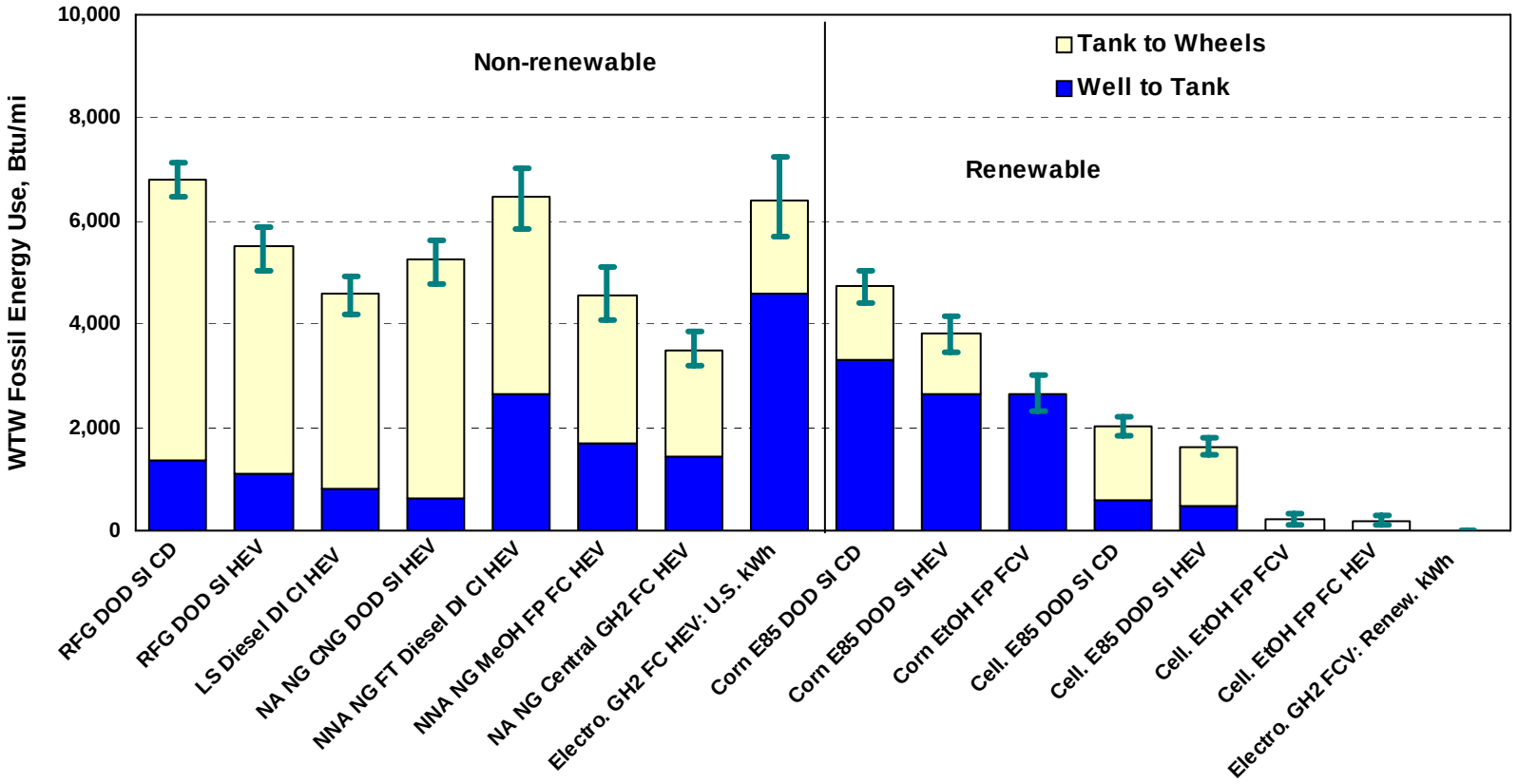

Figure 4-43 Comparison of Non-Renewable and Renewable Fuels: WTW Fossil Energy Use (Btu/mi)

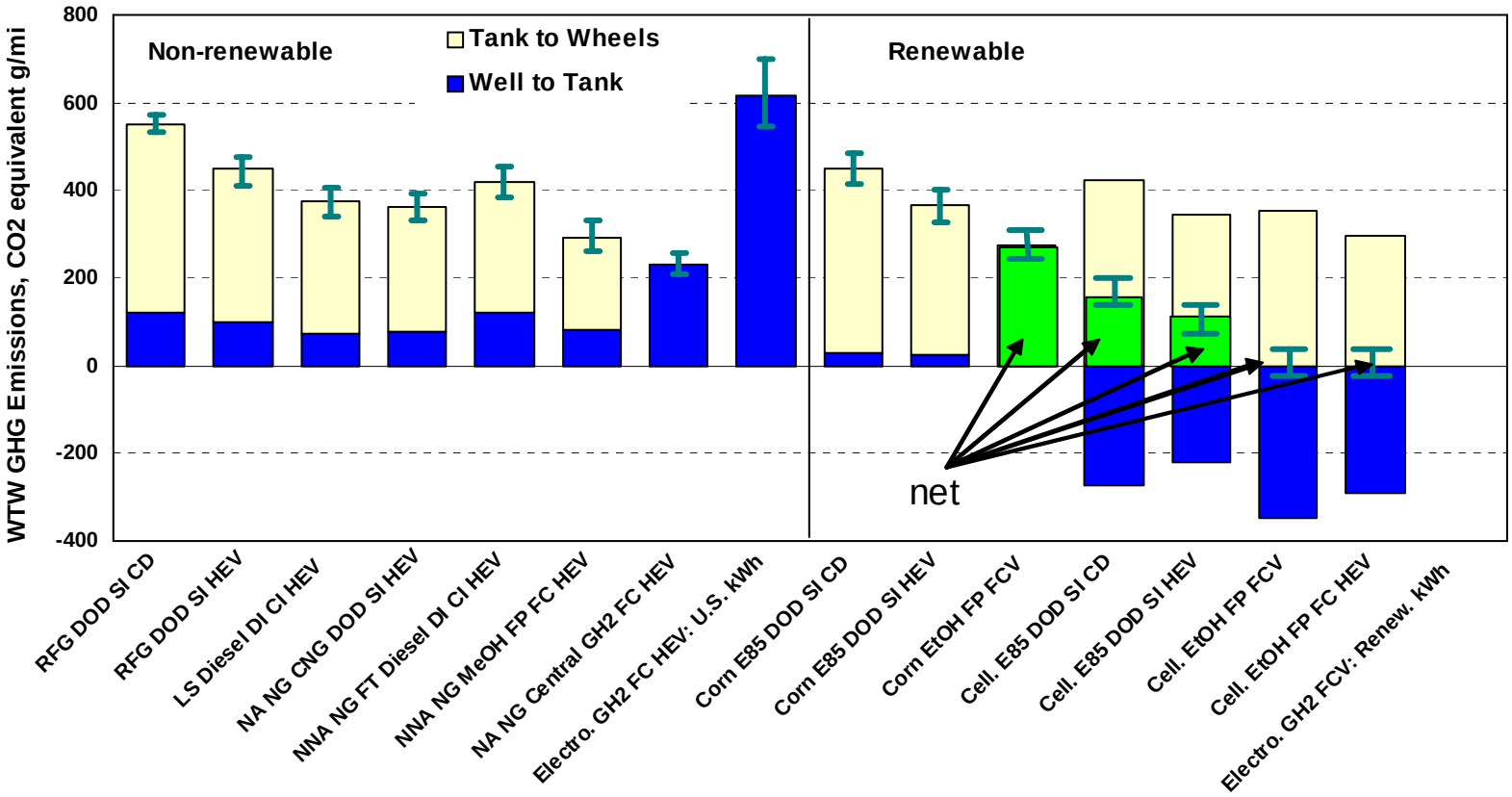

Figure 4-44 Comparison of Non-Renewable and Renewable Fuels: WTW GHG Emissions (CO_2-equivalent g/mi)

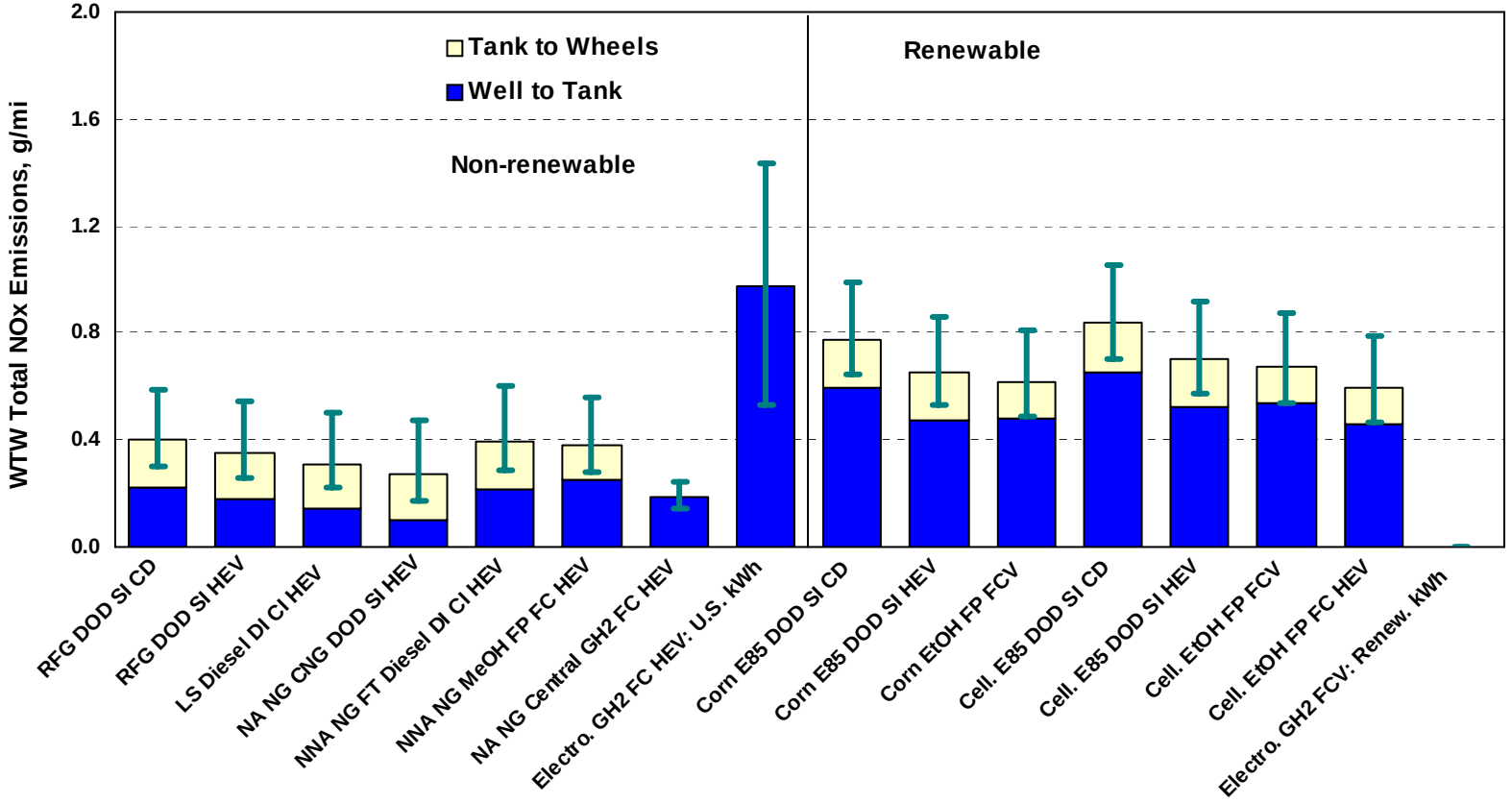

Figure 4-45 Comparison of Non-Renewable and Renewable Fuels: WTW Total NO_x Emissions (g/mi)

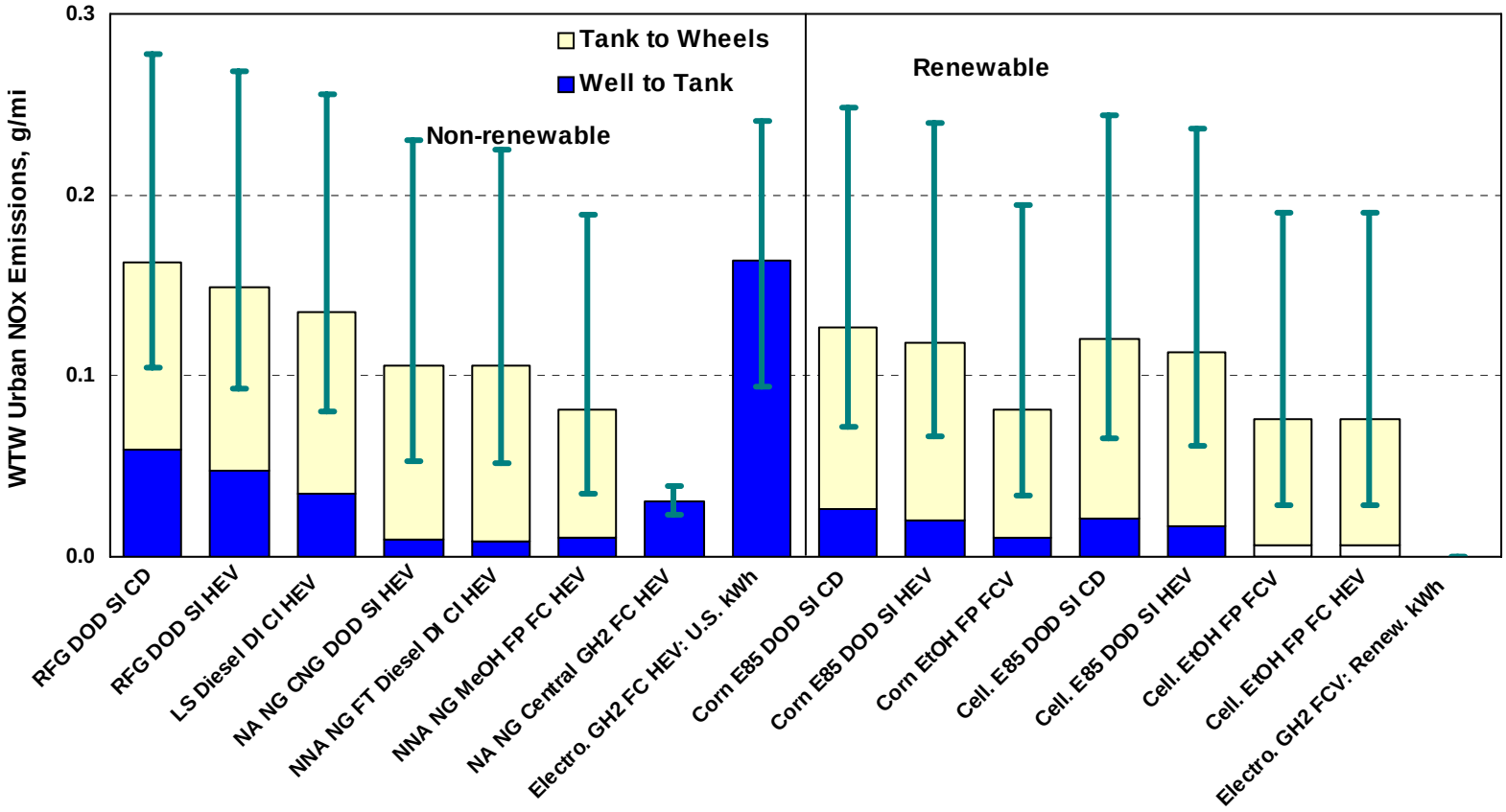

Figure 4-46 Comparison of Non-Renewable and Renewable Fuels: WTW Urban NO_x Emissions (g/mi)

4.2.8 Comparisons of Selected NG-Based Fuel Pathways

Our analysis includes many new transportation fuels that are produced from NG. NG-based transportation fuels can effectively reduce the reliance of the U.S. transportation sector on petroleum. But NG itself is a non-renewable energy source, and the NG supply in North America is and will continue to be limited. If the transportation fuels market is to be expanded to include NG-based fuels, one question is how to efficiently use NG to meet the transportation energy demand. Figures 4-47 through 4-51 present WTW energy and emission results for 22 vehicle/fuel systems fueled with NG-based fuels, together with the results for the baseline gasoline technology.

Figure 4-47 shows WTW fossil energy use for 23 vehicle/fuel systems. Relative to the baseline gasoline ICE technology, the majority of the NG-based systems reduce WTW fossil energy use. The exceptions are GH_2-fueled ICEs, standalone FCVs fueled with GH_2 and LH_2 from NG CC electricity, fuel cell HEVs fueled with LH_2 from NG CC electricity, CNG ICEs fueled with NNA NG, and FT-diesel-fueled CI ICEs. In all these cases, WTT fossil energy losses are large enough to offset potential vehicle energy efficiency gains.

Our results reveal that, of the 22 NG-based vehicle/fuel systems, the most energy-efficient ways of using NG are in GH_2-fueled FCVs, CNG HEVs, and methanol- and FT-naphtha-fueled FCVs.

Figure 4-48 shows WTW GHG emissions of the 22 NG-based systems. The patterns of WTW GHG emissions are similar to those for WTW fossil energy use.

Figure 4-49 shows WTW urban VOC emissions. Relative to the gasoline ICE technology, all NG-based systems reduce urban VOC emissions, primarily because of the low volatility of NG-based fuels. Figure 4-50 shows WTW urban NO_x emissions, which are driven largely by vehicle technologies. ICE-based systems usually have higher urban NO_x emissions than fuel-cell-based systems. The figure shows that there are large uncertainties in urban NO_x emissions for the 22 systems. Figure 4-51 shows WTW urban PM_{10} emissions. Urban PM_{10} emissions for GH_2-fueled ICEs and ICE HEVs are actually higher than those of the baseline gasoline ICE technology. This is because hydrogen production with SMR generates significant amounts of NO_x emissions (see Section 2) and because U.S. average electricity was assumed for compressing GH_2, which results in some urban NO_x emissions because some of electric power plants are located within U.S. urban areas.

While control measures can be implemented to limit the potential increases in criteria pollutants for certain NG-based fuel pathways, high fossil energy use and GHG emissions for some of the technology options (such as LH_2 from NG combined-cycle electricity) in Figures 4-47 and 4-48 are caused by high NG use during fuel production. If the purpose is to efficiently use NG resources in the transportation sector, one may argue that inefficient NG-based fuel pathways should be avoided. However, the choice of a given NG-based fuel production pathway may be determined by the availability of fuel production and distribution infrastructure and the maturity of vehicle technologies. WTW energy efficiencies and GHG emissions should not be the sole factor in determining whether to eliminate certain fuel production pathways.

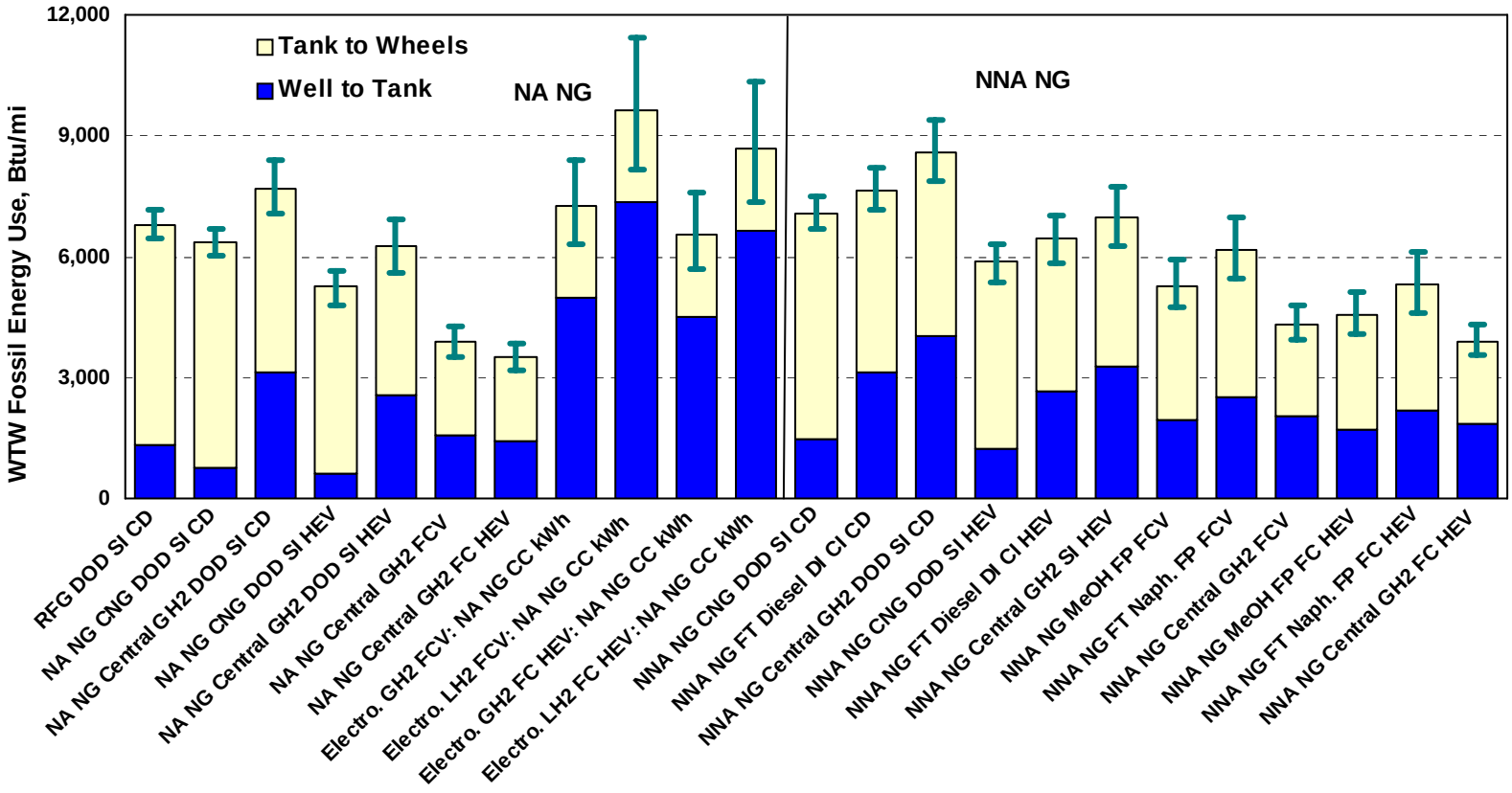

Figure 4-47 Comparison of NG-Based Systems: WTW Fossil Energy Use (Btu/mi)

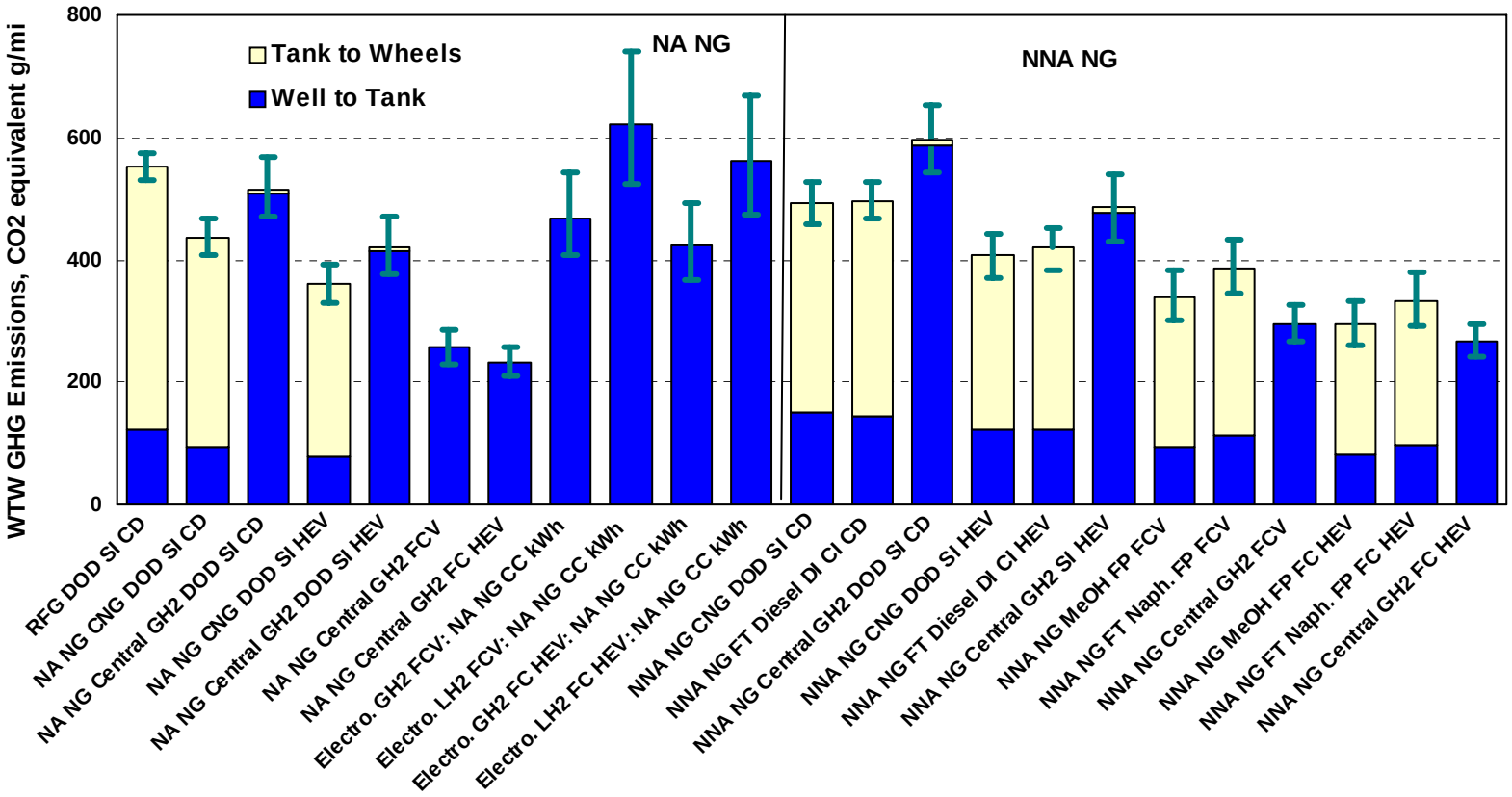

Figure 4-48 Comparison of NG-Based Systems: WTW GHG Emissions (CO_2-equivalent g/mi)

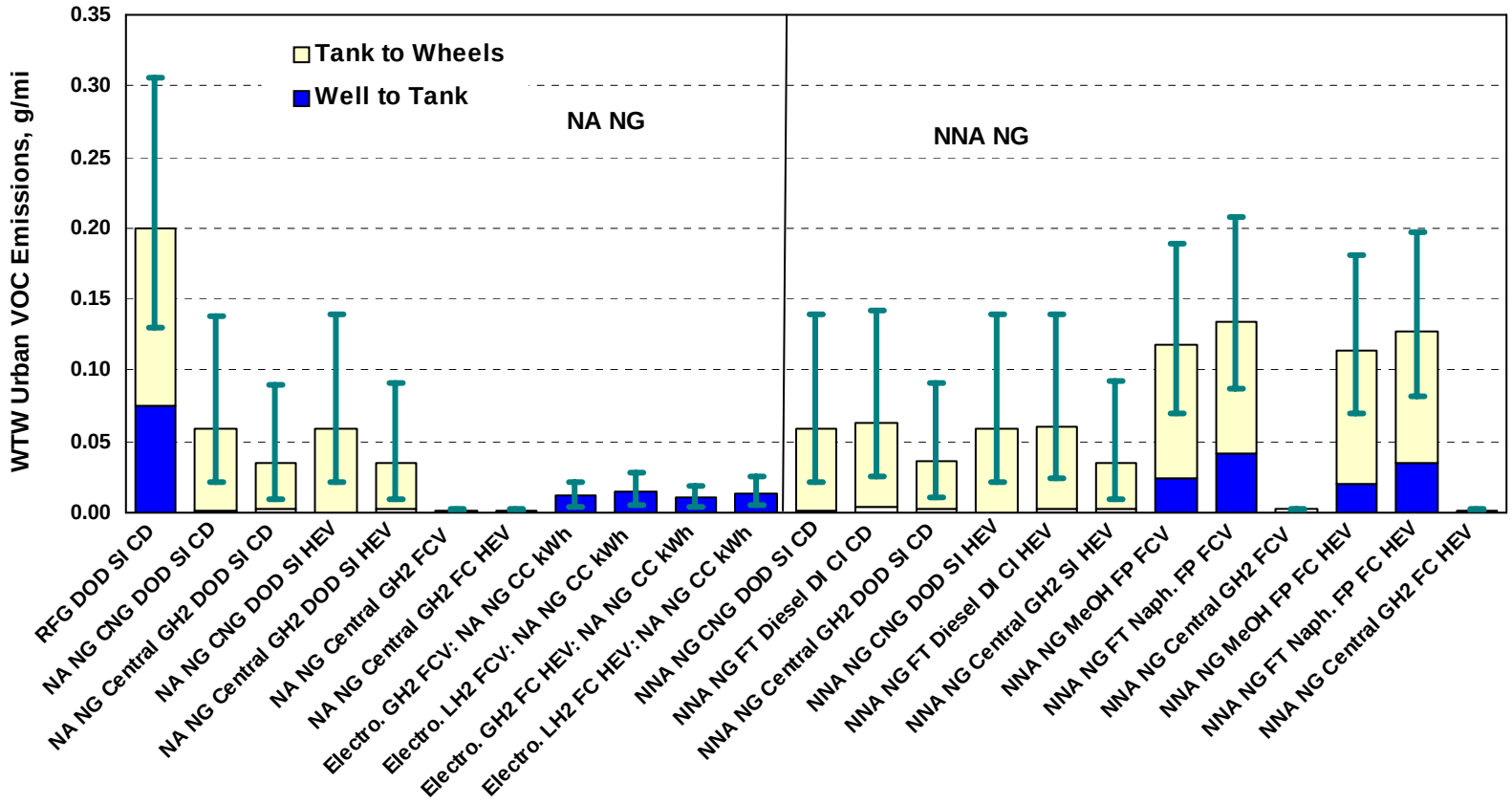

Figure 4-49 Comparison of NG-Based Systems: WTW Urban VOC Emissions (g/mi)

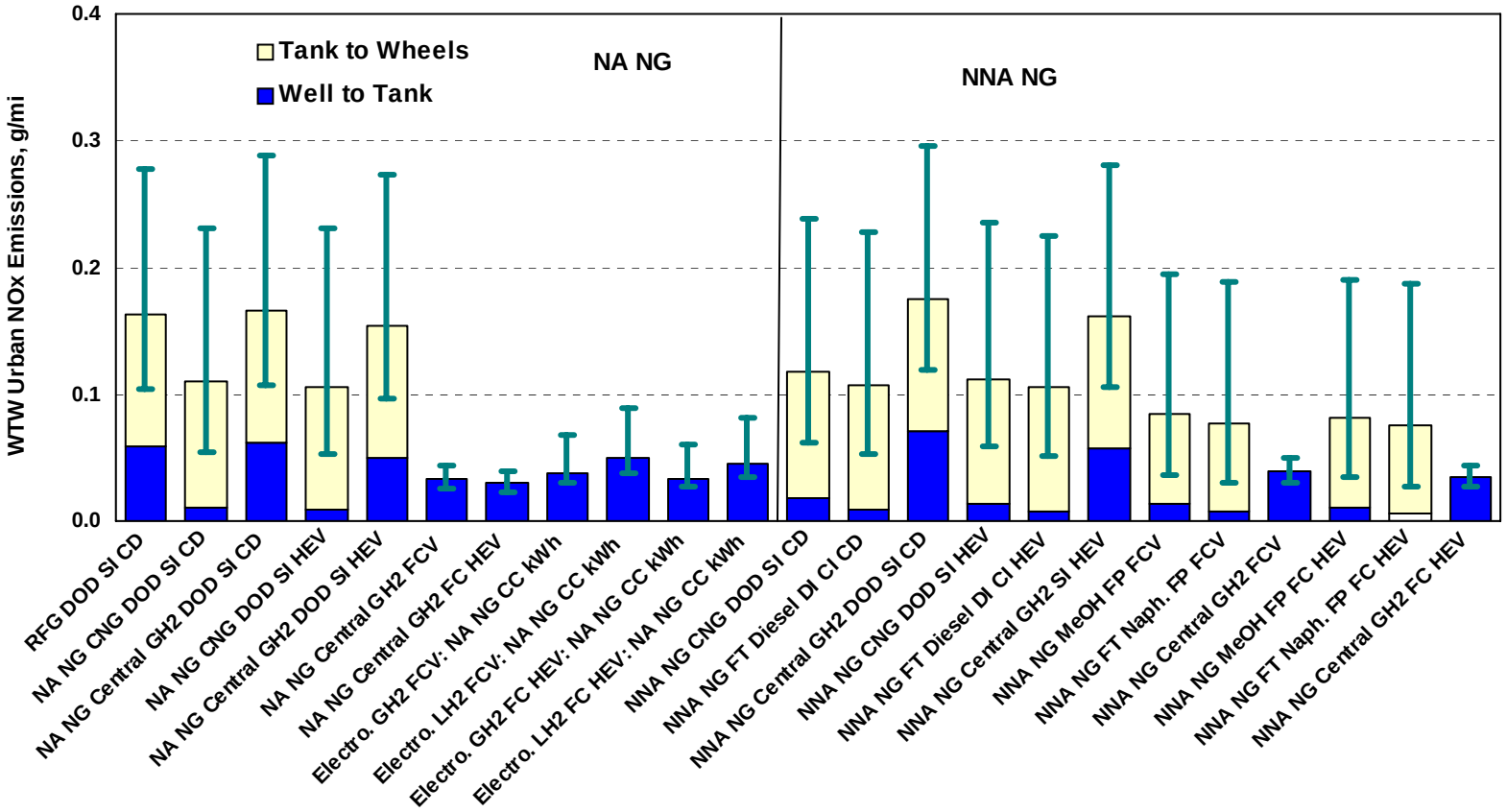

Figure 4-50 Comparison of NG-Based Systems: WTW Urban NO_x Emissions (g/mi)

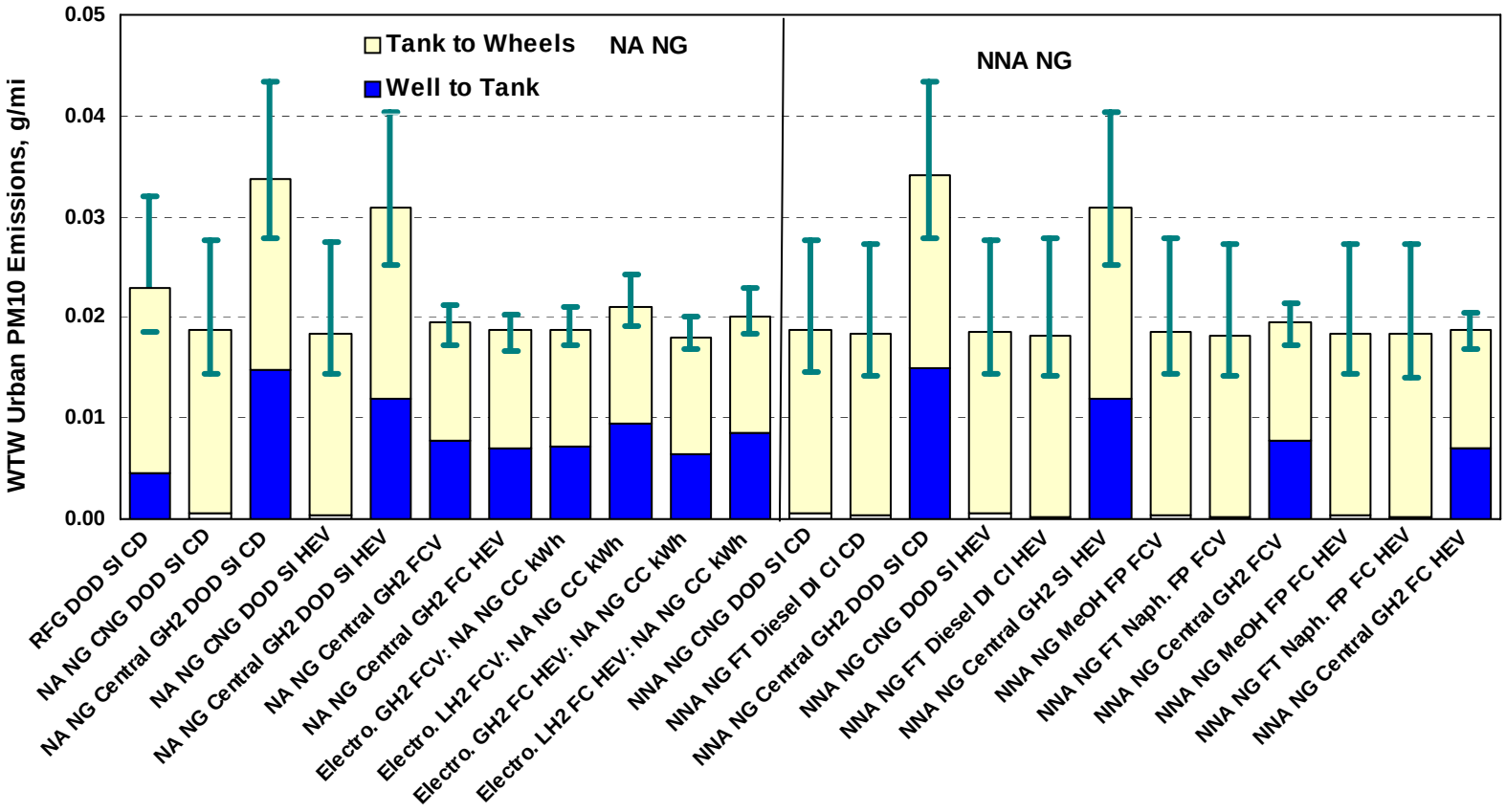

Figure 4-51 Comparison of NG-Based Systems: WTW Urban PM_{10} Emissions (g/mi)

4.2.9 Comparison of Electrolysis Hydrogen between the U.S. Electricity Generation Mix and the California Electricity Generation Mix

In previous sections, we presented the energy use and emissions results for technologies powered with electrolysis hydrogen produced by using U.S. average electricity, NG CC electricity, and renewable electricity to demonstrate the importance of electricity sources for electrolysis hydrogen production. We realize that California could deploy FCVs first. In the early stage of potential California FCV deployment, hydrogen may be produced from electricity there. Thus, besides U.S. average electric generation, we simulated electrolysis hydrogen production with the California average generation mix. Table 4-5 shows U.S. and California electricity generation mixes for 2016, our target year for analysis in this study. The U.S. generation mix is based on projections by the Energy Information Administration; the California generation mix is based on projections by the California Energy Commission. Note that the California generation mix includes out-of-state power generation for California consumption. The major difference between the U.S. and California mixes is less power from coal, more power from NG, and more power from other sources in California than in the United States.

Table 4-5 Projected U.S. and California Electricity Generation Mixes in 2016

Fuel	U.S. Generation Mix (%)	California Generation Mix (%)
Residual Oil	1	0
NG	15	33
Coal	54	21
Nuclear	18	15
Others[a]	12	31

[a] Others here include hydro, geothermal, wind, and solar power. These power sources have zero emissions (emissions associated with plant construction are not included in GREET simulations).

Figures 4-52 through 4-60 present the results of electrolysis hydrogen-based technologies with the U.S. and California electricity generation mixes. Figure 4-52 shows WTW total energy use for ICE vehicles, ICE HEVs, and FCVs powered with GH_2 and LH_2, both of which are produced from electricity. In all the cases, hydrogen produced with California average electricity results in lower total energy use than hydrogen produced with U.S. average electricity. The reduction in total energy use from U.S. to California electricity is attributable to the fact that a large share of California electricity is derived from other sources for which GREET uses 100% power plant conversion efficiency (see Figure 4-2 and related discussions there). Overall, while electrolysis-LH_2-based technology options result in increased total energy use, FCVs (both standalone and hybrid configurations) powered with GH_2 result in total energy use similar to that of baseline gasoline vehicles.

Figure 4-53 compares WTW fossil energy use for U.S. electricity-based and California electricity-based hydrogen technology options. The reductions in fossil energy use from U.S. average electricity to California average electricity for hydrogen production result from the fact that 70% of U.S. electricity is generated from fossil energy sources, while only 54% of California electricity is generated from fossil energy sources.

Figure 4-54 presents WTW GHG emissions for the U.S. and California generation mixes. The reductions in GHG emissions from U.S. electricity to California electricity for hydrogen production are attributable to the large amount of electricity that is generated from hydro, geothermal, wind, and solar power in California. In fact, with the California electricity generation mix, FCVs powered with electrolysis hydrogen could result in moderate GHG emission reductions instead of the GHG emission increases that result from the U.S. electricity generation mix. These results again demonstrate the importance of

considering the electricity sources for electrolysis hydrogen production in determining energy and emission benefits of electrolysis-hydrogen-based FCVs.

Figures 4-55 and 4-56 compare total and urban NO_x emissions for the two electricity generation mixes. For total NO_x emissions (Figure 4-55), the California generation mix results in small increases in WTW NO_x emissions relative to NO_x emissions for the baseline gasoline vehicles, while the U.S. generation mix results in large increases. For urban NO_x emissions (Figure 4-56), FCVs powered with hydrogen derived from California electricity actually result in emission reductions. However, hydrogen-ICE-based vehicle technologies still result in increased NO_x emissions because of both their tailpipe NO_x emissions and NO_x emissions associated with electricity generation.

Figures 4-57 and 4-58 show total and urban PM_{10} emissions for electrolysis-hydrogen-based technology options. In all cases, PM_{10} emissions are increased with electrolysis-based hydrogen technologies. But the increases with the California electricity generation mix are much smaller than with the U.S. generation mix. For urban PM_{10} emissions, FCVs powered with electrolysis hydrogen result in emission reductions under both the U.S. and the California generation mixes.

Figures 4-59 and 4-60 compares total and urban SO_x emissions for the two generation mixes. There are large reductions in total SO_x emissions from the U.S. electricity generation mix to the California generation mix for hydrogen production because a much smaller share of electricity is generated from coal-fired power plants in California than in the United States as a whole. In any case, SO_x emissions increase with all electrolysis-hydrogen-based technology options under both generation mixes. The results for urban SO_x emissions are similar to those for total SO_x emissions.

In summary, with the California electricity generation mix, the energy use and emissions of electrolysis-hydrogen-based technology options are reduced, relative to those with the U.S. generation mix. In the cases of GHGs and urban NO_x emissions, the differences between the two generation mixes are large enough to result in overall reductions in these emissions by FCVs powered with electrolysis hydrogen supplied by the California electricity generation mix relative to emissions associated with baseline gasoline vehicles.

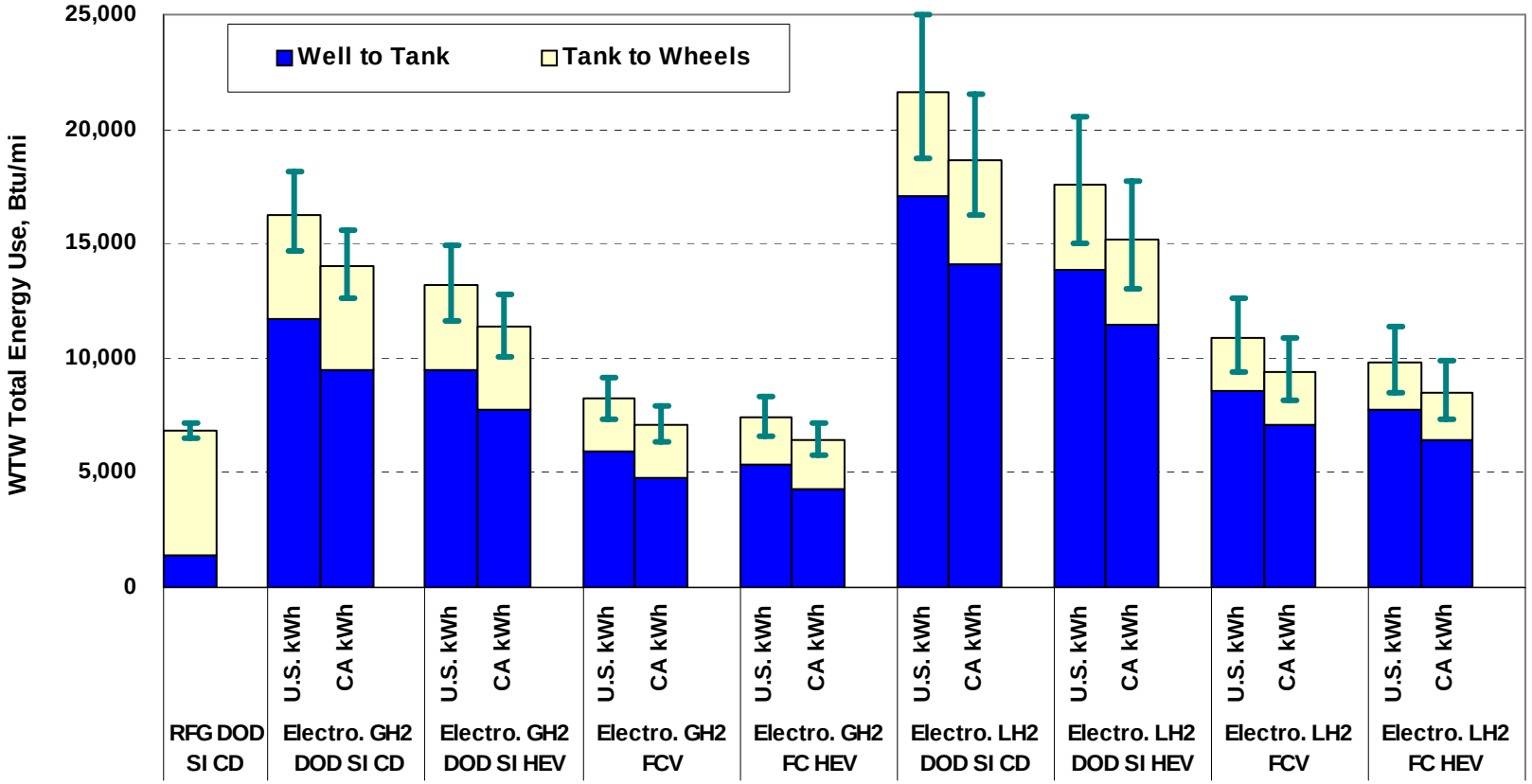

Figure 4-52 Comparison of U.S. and California Electricity Generation Mixes: WTW Total Energy Use (Btu/mi)

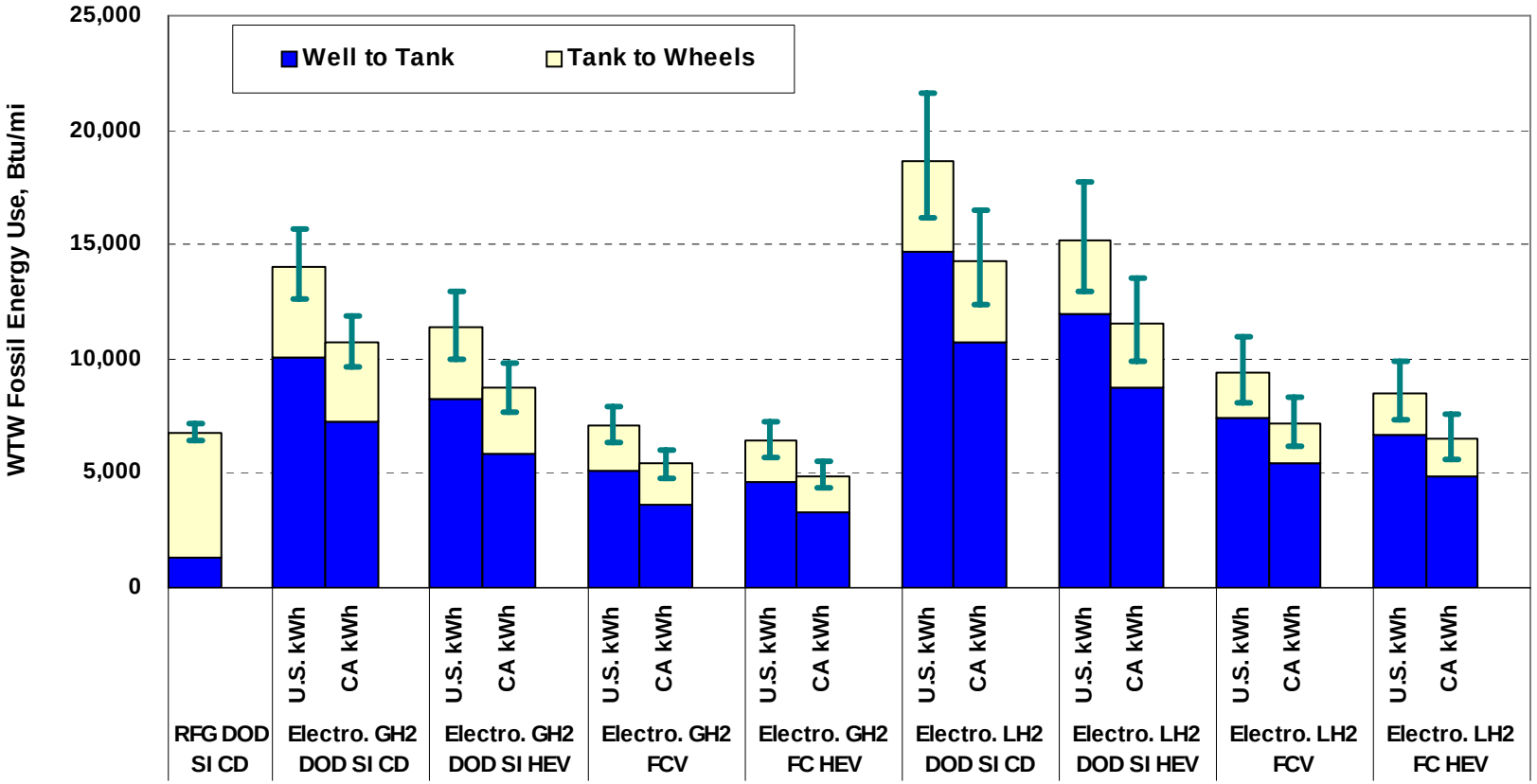

Figure 4-53 Comparison of U.S. and California Electricity Generation Mixes: WTW Fossil Energy Use (Btu/mi)

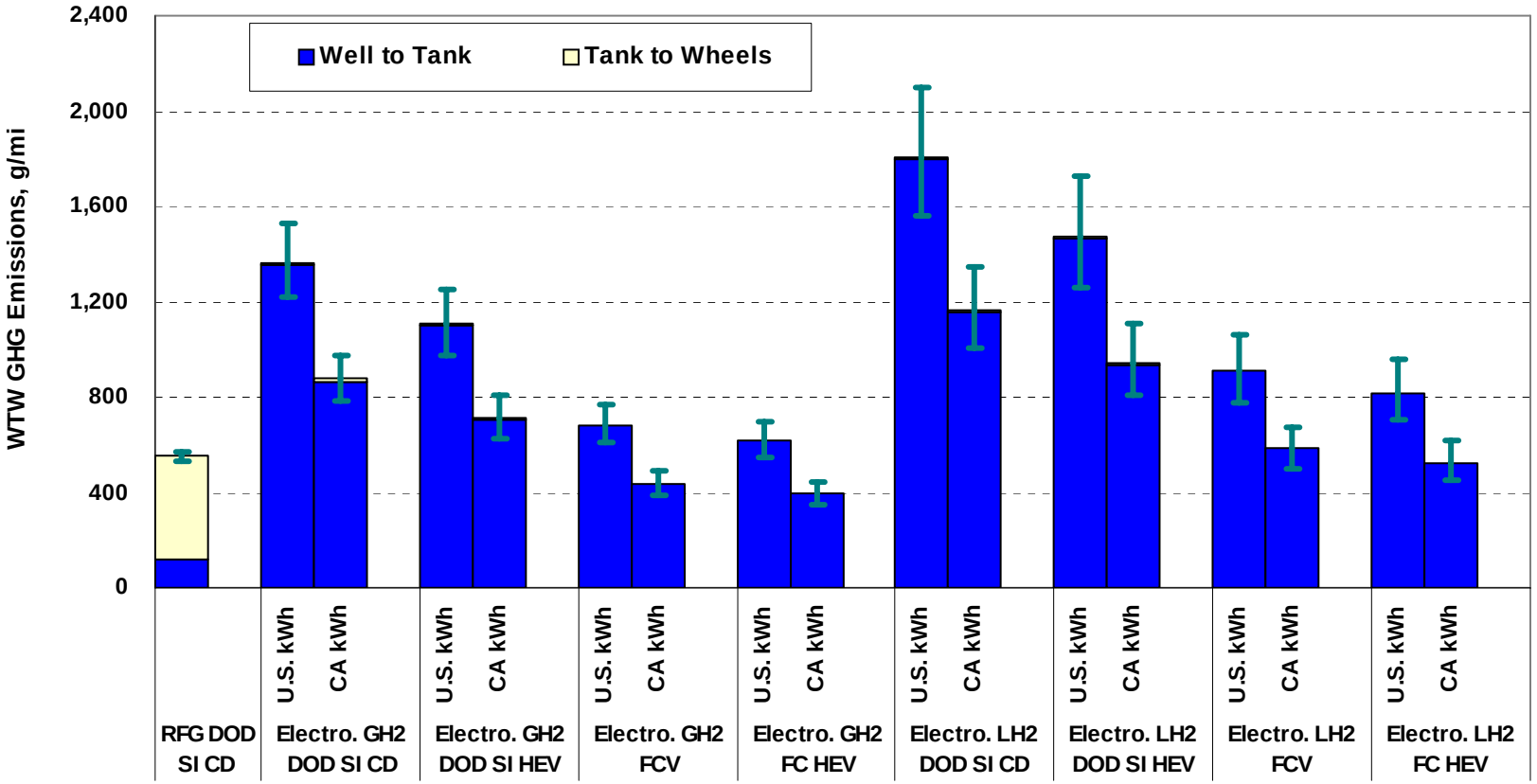

Figure 4-54 Comparison of U.S. and California Electricity Generation Mixes: WTW GHG Emissions (g/mi)

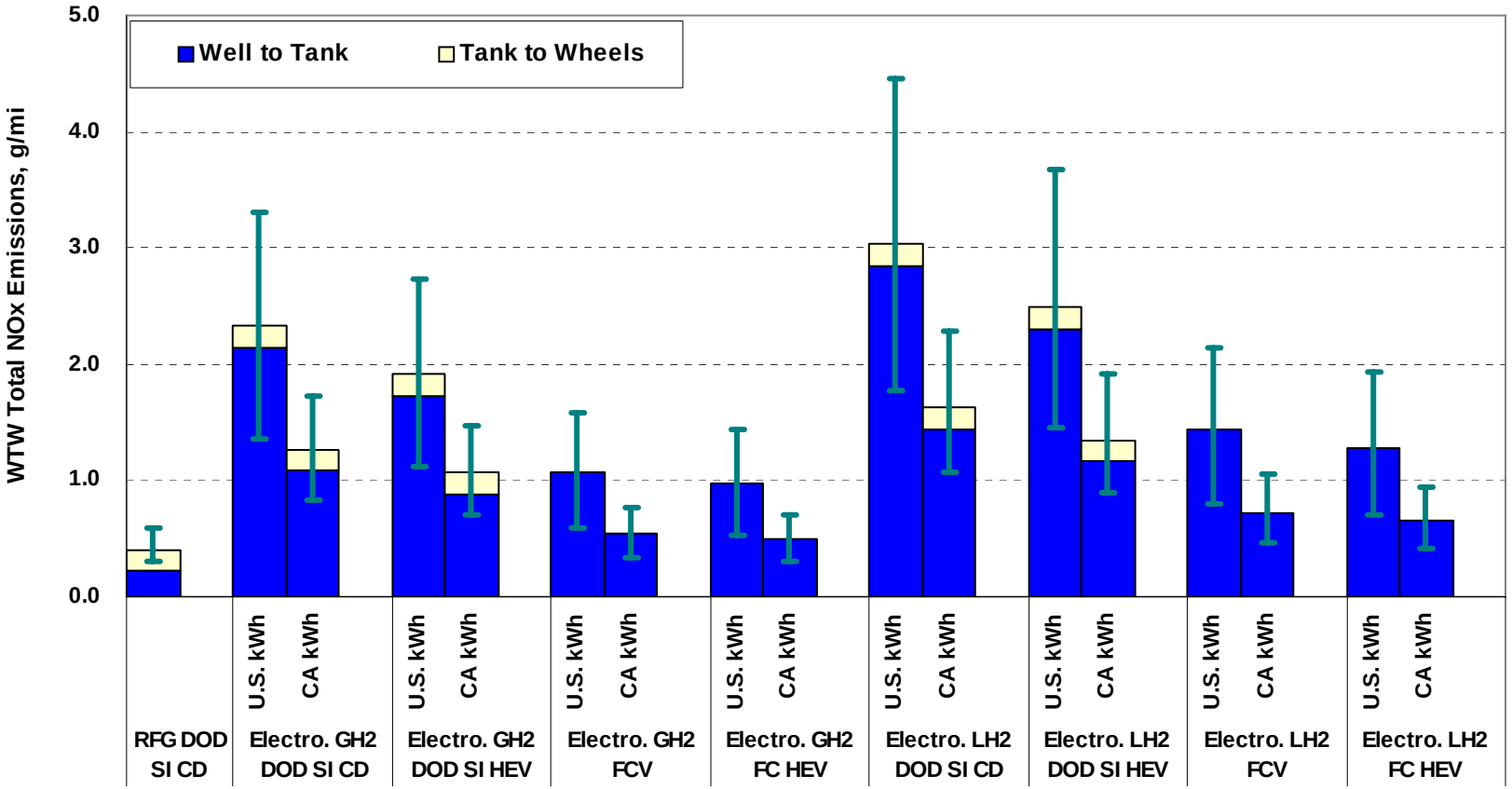

Figure 4-55 Comparison of U.S. and California Electricity Generation Mixes: WTW Total NO_x Emissions (g/mi)

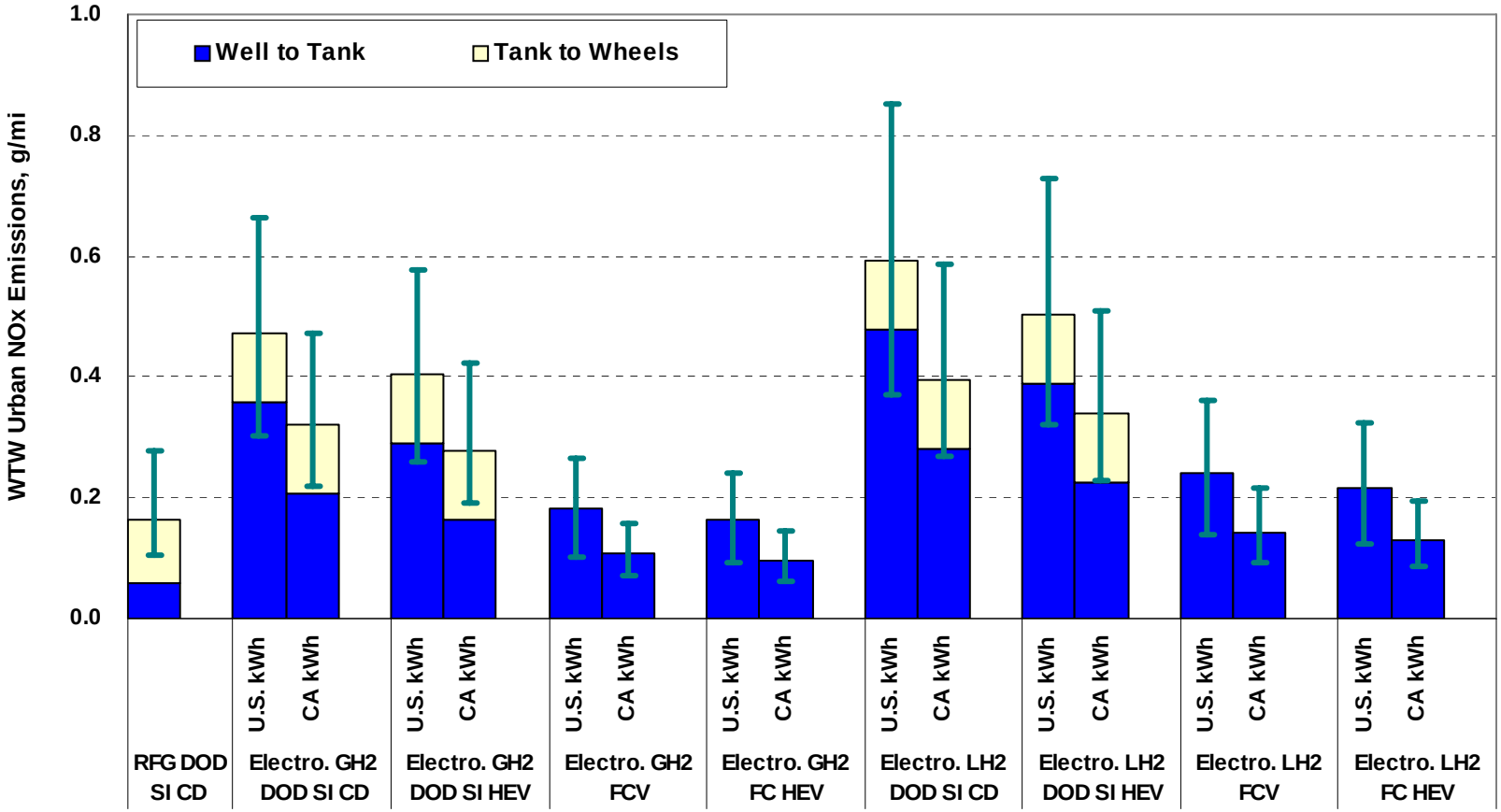

Figure 4-56 Comparison of U.S. and California Electricity Generation Mixes: WTW Urban NO_x Emissions (g/mi)

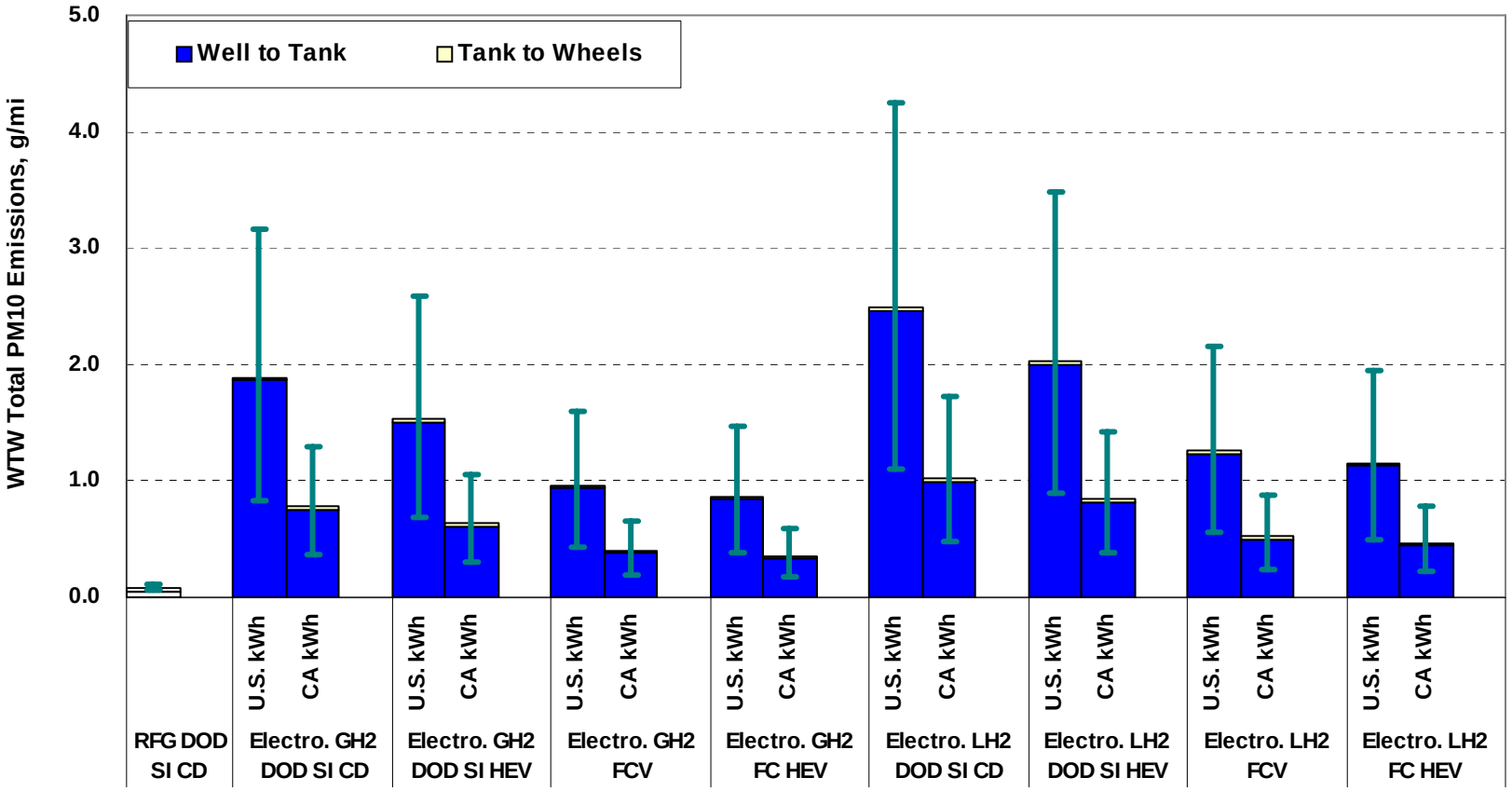

Figure 4-57 Comparison of U.S. and California Electricity Generation Mixes: WTW Total PM_{10} Emissions (g/mi)

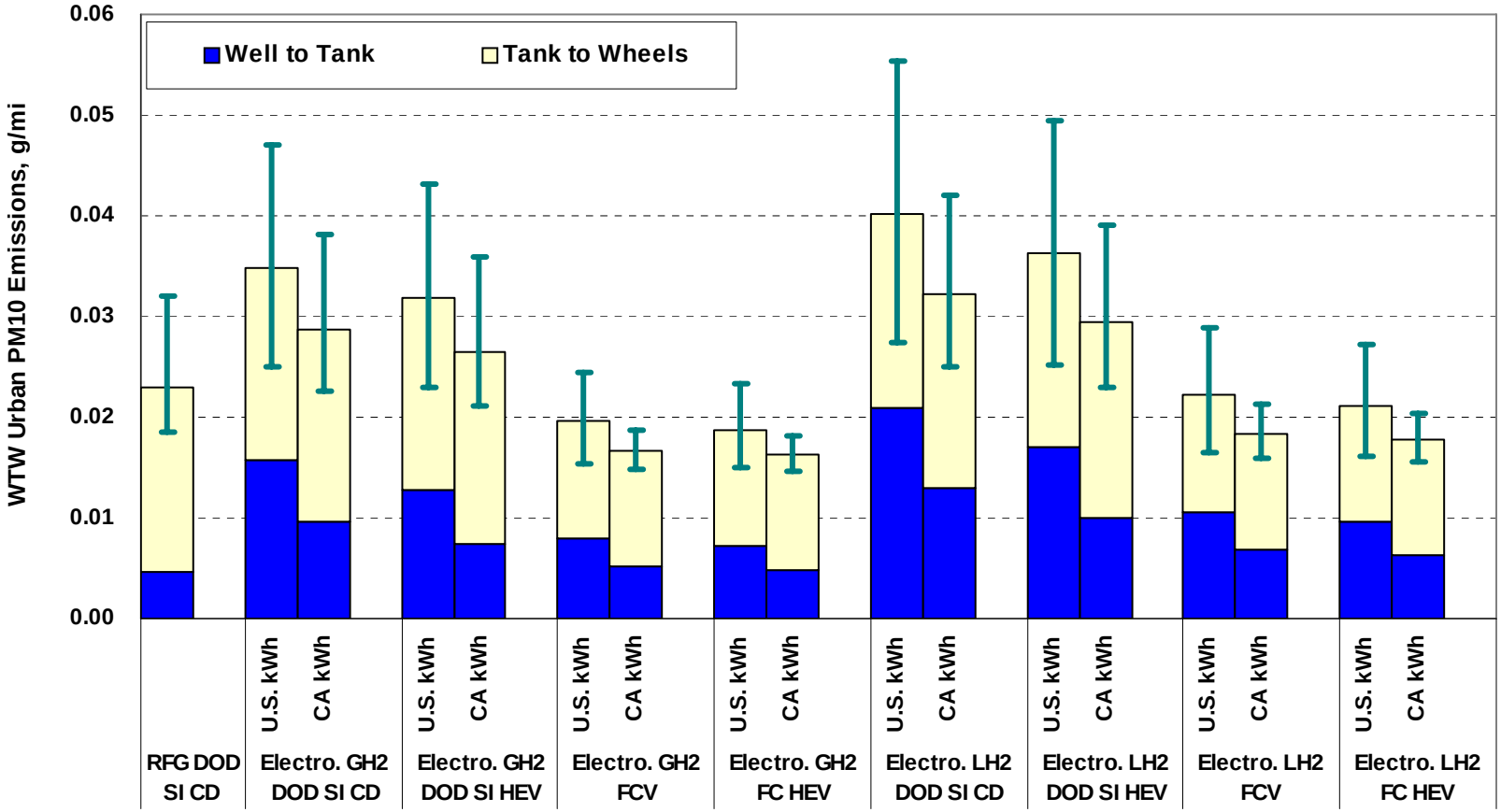

Figure 4-58 Comparison of U.S. and California Electricity Generation Mixes: WTW Urban PM_{10} Emissions (g/mi)

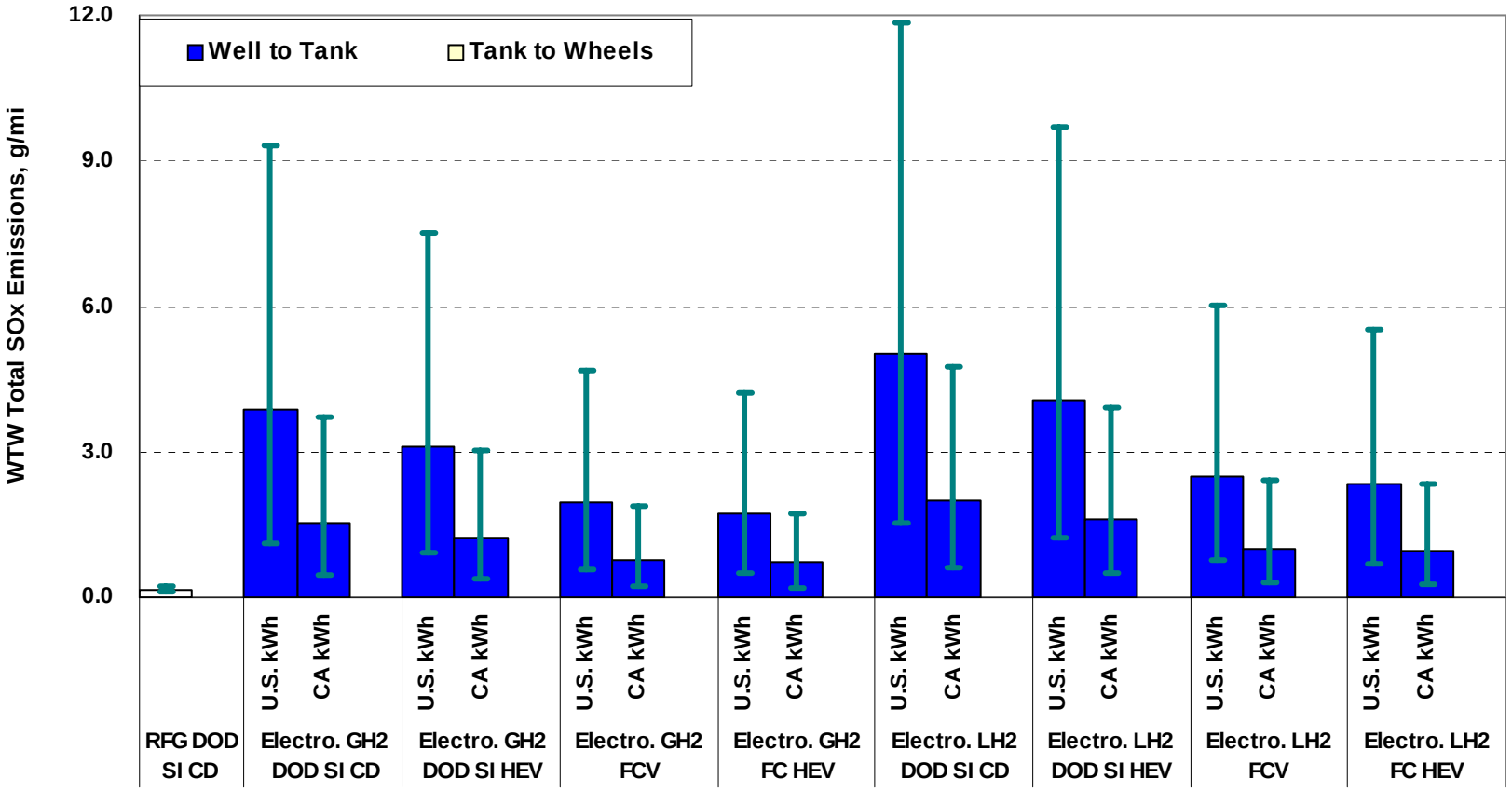

Figure 4-59 Comparison of U.S. and California Electricity Generation Mixes: WTW Total SO_x Emissions (g/mi)

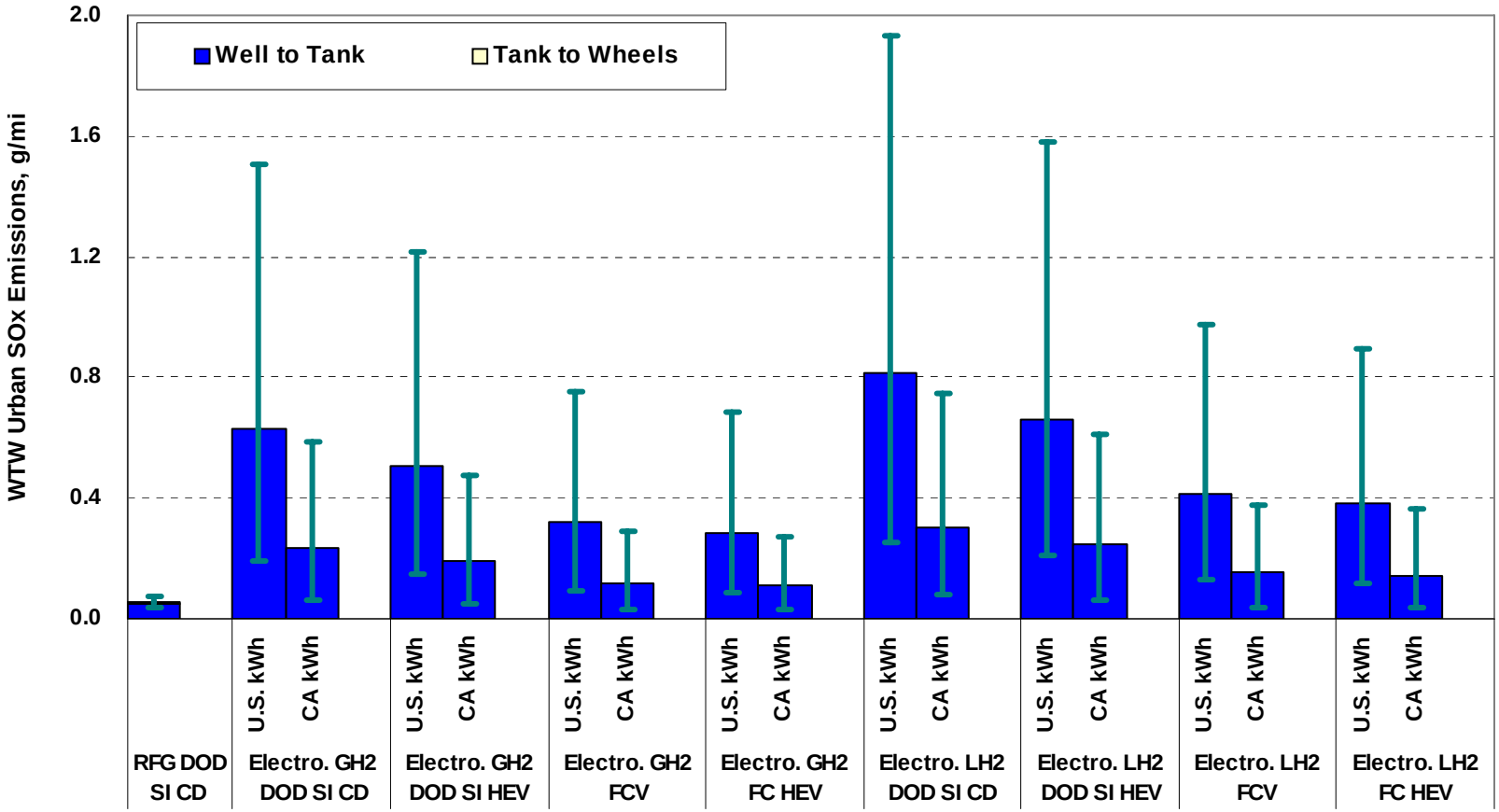

Figure 4-60 Comparison of U.S. and California Electricity Generation Mixes: WTW Urban SO_x Emissions (g/mi)

4.2.10 Effects of Power Plant Emission Reductions Resulting from the Interstate Air Quality Rule Adopted by EPA

In Section 2, we described potential reductions in NO_X and SO_X emissions from electric power plants that may result from the Interstate Air Quality Rule adopted by EPA. The adopted IAQR is intended to reduce NO_X and SO_X emissions in electric power plants in 29 Eastern U.S. states. We estimated that the IAQR rule could result in a 43% reduction in power plant NO_X emissions and a 41% reduction in power plant SO_X emissions nationwide. To test the effect of the IAQR rule, we used the GREET model to simulate the WTW NO_X and SO_X emissions of electrolysis-hydrogen-based technology options under the IAQR rule.

Figures 4-61 and 4-62 shows WTW total and urban NO_X emissions of electrolysis-hydrogen-based vehicle technologies with baseline power plant emissions projected by EPA and IAQR power plant emissions. Total NO_X emissions for electrolysis hydrogen technology options are reduced roughly by 40% from baseline power plant emissions to IAQR power plant emissions. However, the reductions are not large enough to cause overall reductions in NO_X emissions for these vehicle technologies, relative to NO_X emissions from baseline gasoline vehicles. On the other hand, the reductions in urban NO_X emissions from the baseline case to the IAQR case are large enough so that FCVs powered with electrolysis hydrogen result in urban NO_X emission reductions under the IAQR case.

Figures 4-63 and 4-64 present total and urban SO_X emissions under the two cases. Although the IAQR case results in large reductions in WTW SO_X emissions for electrolysis-hydrogen-based technologies, the reductions are not large enough to cause overall reductions in SO_X emissions by these vehicle technologies relative to baseline gasoline vehicles.

The simulations of the IAQR rule with GREET show that as power plant emissions are further controlled, FCVs powered even with U.S. average electricity mix will result in reductions in NO_X emissions.

4.2.11 Comparison of Bin 5 vs. Bin 2 Hydrogen ICE Vehicle Technologies

Our analysis assumed that hydrogen ICE technologies (both standalone and hybrid configuration) would meet EPA's Tier 2 Bin 5 NO_X emission standards. Some recent efforts have demonstrated that hydrogen ICE technologies could meet Tier 2 Bin 2 NO_X emission standards. We simulated WTW NO_X emissions of Bin 2 hydrogen ICE technologies with GREET.

Figures 4-65 and 4-66 present the WTW total and urban NO_X emissions associated with hydrogen ICE technologies meeting either Bin 5 or Bin 2 NO_X emission standards. Total NO_X emissions are reduced somewhat from Bin 5 to Bin 2 for an individual technology option. But the reductions are generally small because as vehicles meet Tier 2 standards, tailpipe NO_X emissions account for only a small share of the WTW NO_X emissions of hydrogen ICE technologies.

The reductions from Bin 5 to Bin 2 for urban NO_X emissions are larger than for total NO_X emissions. But overall, the reductions are not large enough to change the overall ranking of hydrogen ICE technologies relative to baseline gasoline vehicles. Both figures show that hydrogen ICE technologies powered with NG-based hydrogen generate an amount of NO_X emissions similar to the amount generated by baseline gasoline vehicles. However, hydrogen ICE technologies powered by electrolysis hydrogen with the U.S. average electricity generation mix produce NO_X emissions larger than those of baseline gasoline vehicles.

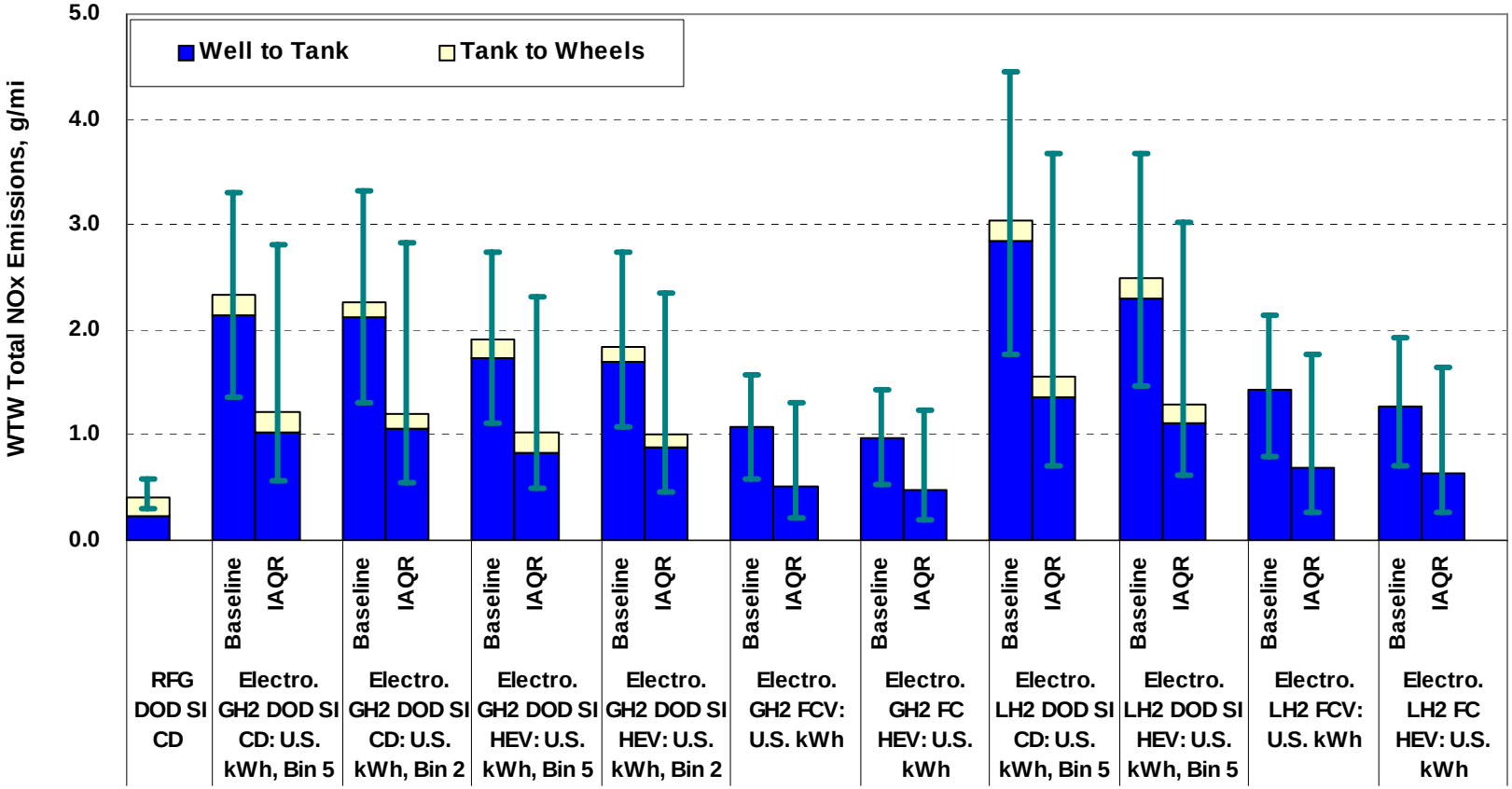

Figure 4-61 Effects of the Adopted Interstate Air Quality Rule for Power Plant Emission Control: WTW Total NO_x Emissions (g/mi)

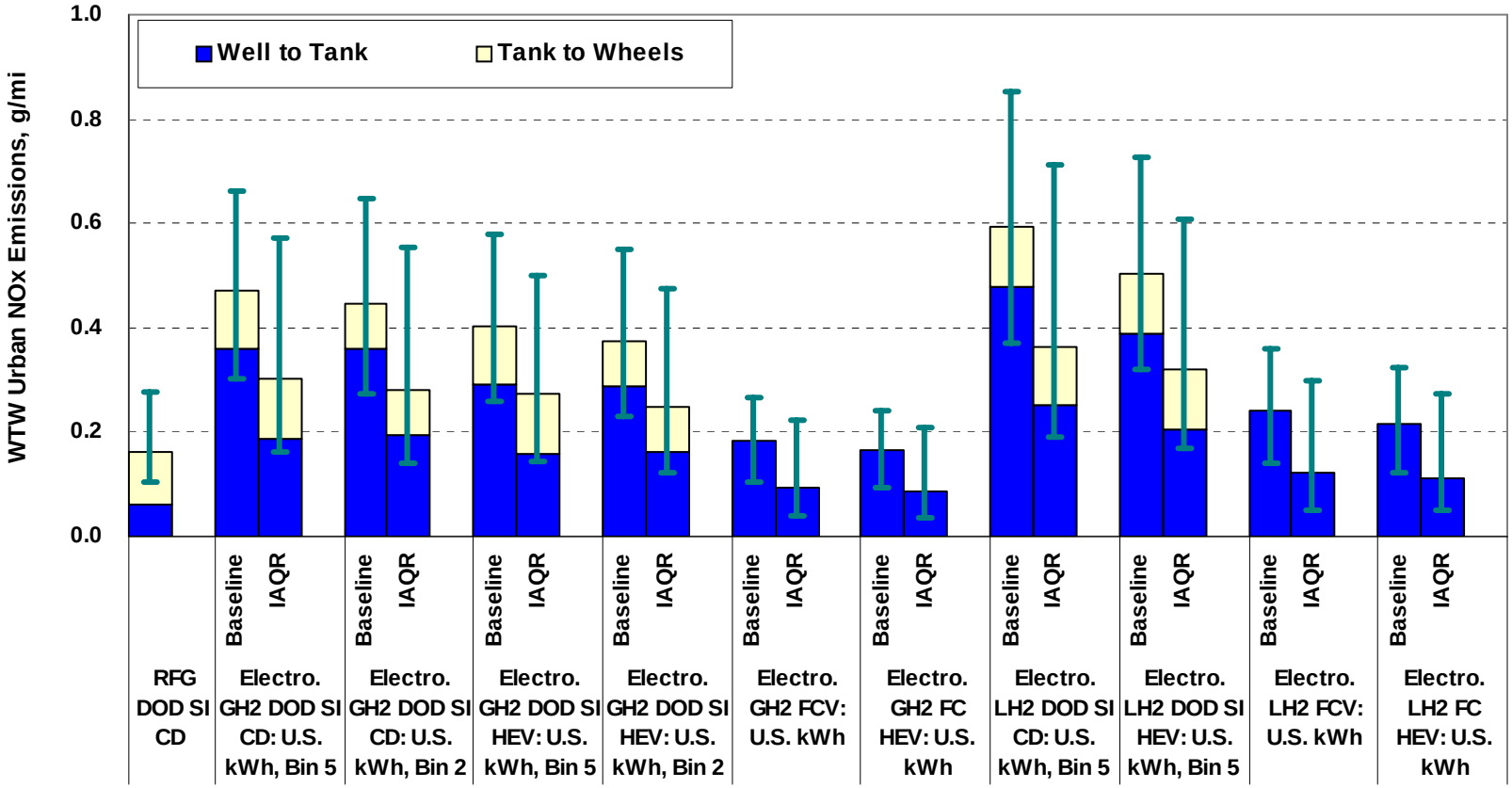

Figure 4-62 Effects of the Adopted Interstate Air Quality Rule for Power Plant Emission Control: WTW Urban NO_x Emissions (g/mi)

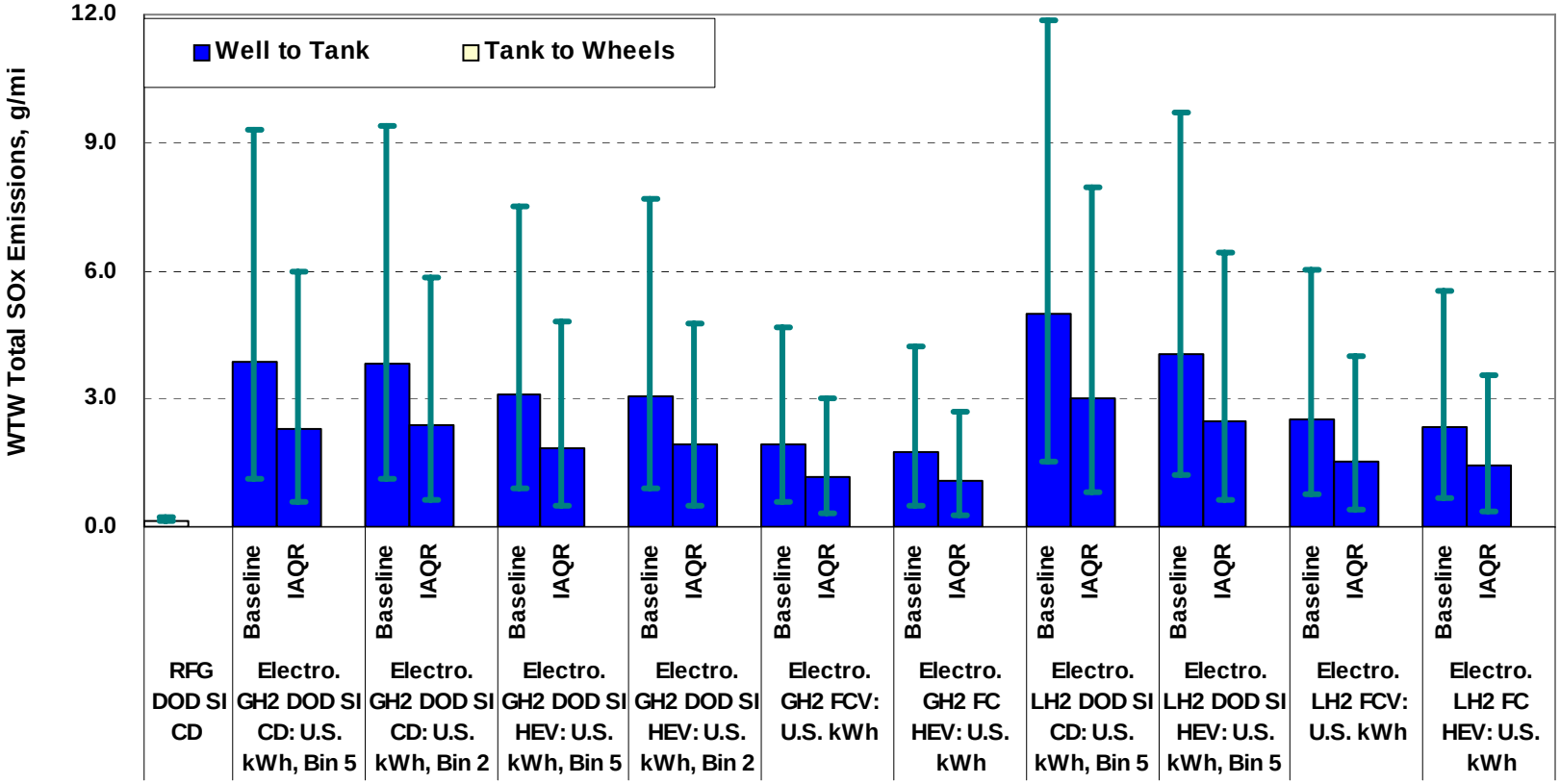

Figure 4-63 Effects of the Adopted Interstate Air Quality Rule for Power Plant Emission Control: WTW Total SO_x Emissions (g/mi)

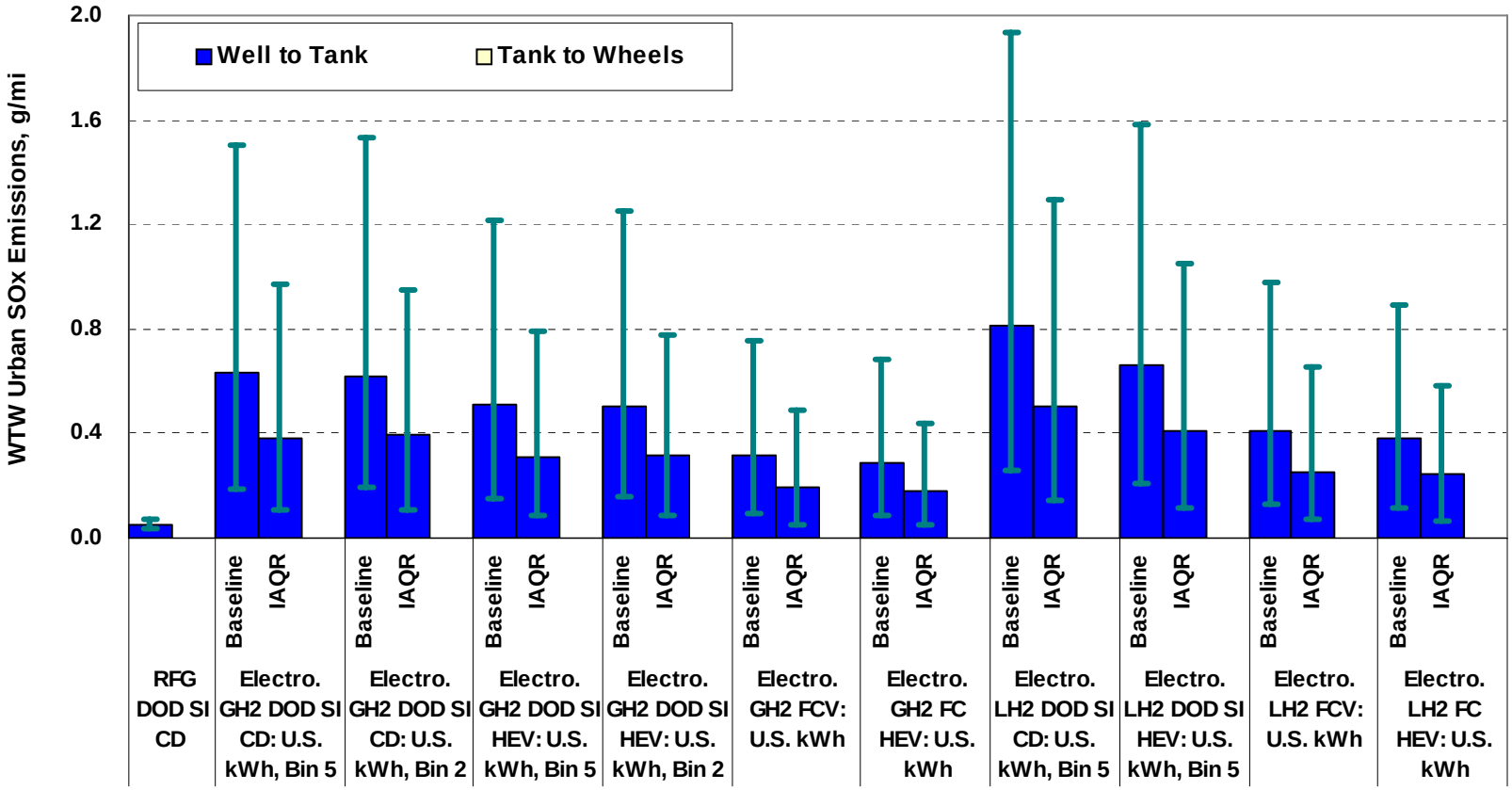

Figure 4-64 Effects of the Adopted Interstate Air Quality Rule for Power Plant Emission Control: WTW Urban SO_x Emissions (g/mi)

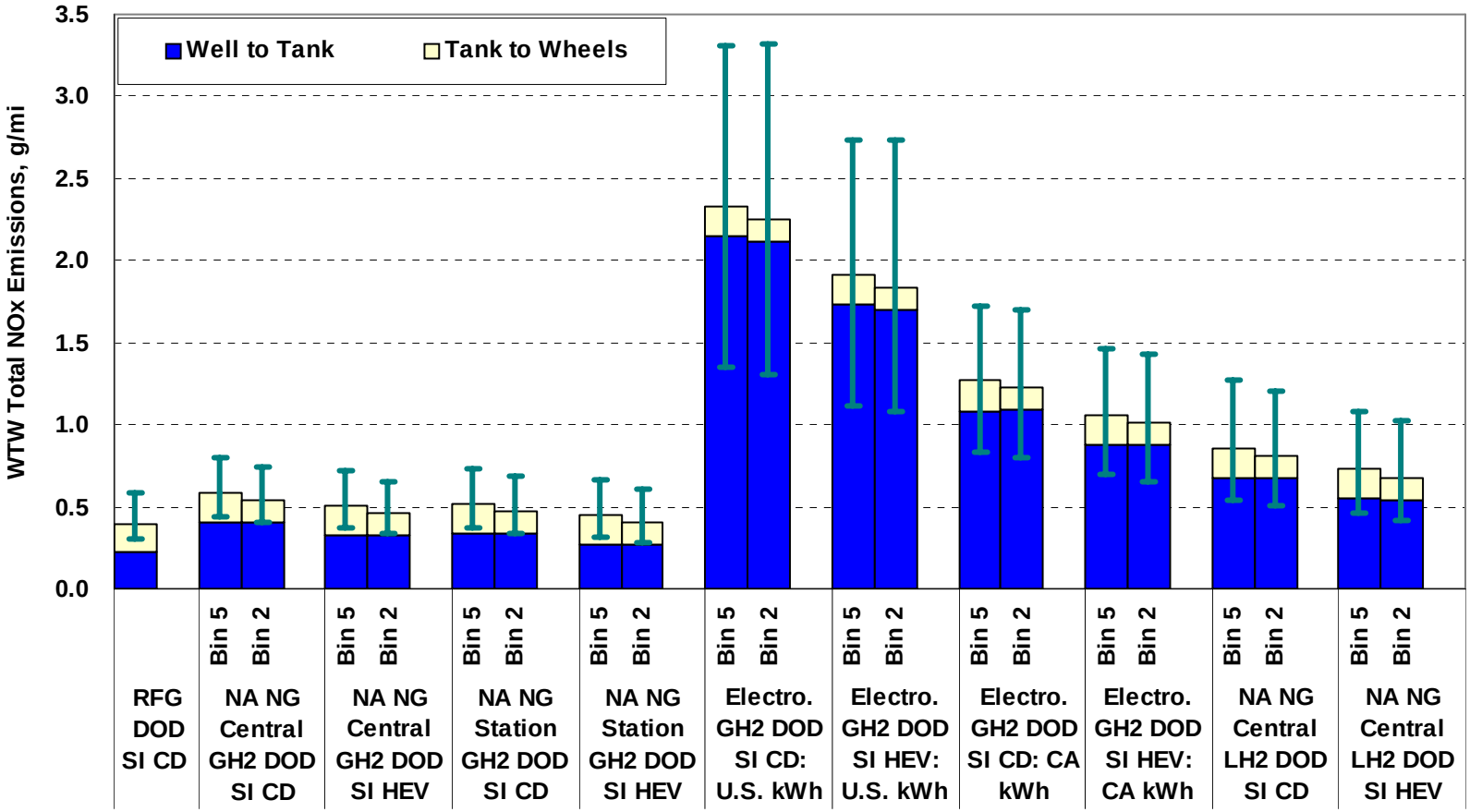

Figure 4-65 Comparison of Hydrogen ICE Technologies Meeting Bin 5 and Bin 2 NO_X Standards: WTW Total NO_X Emissions (g/mi)

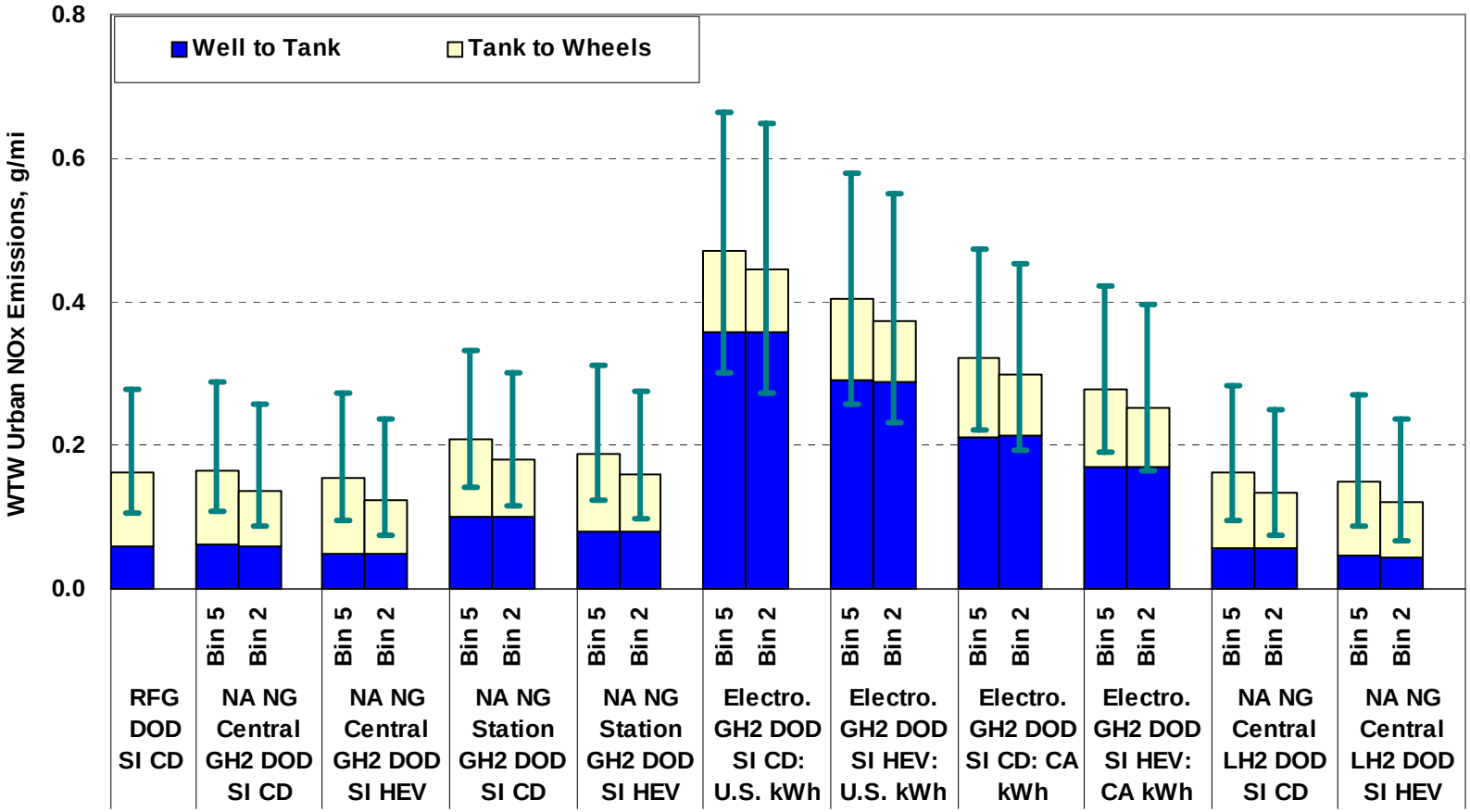

Figure 4-66 Comparison of Hydrogen ICE Technologies Meeting Bin 5 and Bin 2 NO_x Standards: WTW Urban NO_x Emissions (g/mi)

5. CONCLUSIONS

When advanced vehicle technologies are introduced together with new transportation fuels, their energy and emission effects must be evaluated on a WTW basis in order to provide an accurate assessment of their true energy and environmental benefits. The WTW results of this study show that significant shares of energy and emission burdens could occur in the WTT stages for some of the vehicle/fuel systems evaluated. This is true even for criteria pollutant emissions, as vehicle tailpipe emissions continue to decline to meet the U.S. Tier 2 vehicle emission standards.

The GREET WTW simulations completed for this study show that, in general, fuel production and vehicle operation are two key WTW stages in determining WTW energy use and emissions results. The fuel production stage usually has the largest energy-efficiency losses of all WTT stages. This is true for production of gasoline, diesel, hydrogen, FT diesel, ethanol, methanol, and electricity. Special attention must be given to the energy efficiency of each fuel production stage.

For the vehicle operation stage, the most significant factor in determining WTW results is the fuel consumption of the vehicle technologies. Fuel efficiency (or fuel energy consumption per distance driven) directly determines GHG emissions per mile during operation of vehicles fueled with carbon-containing fuels. Furthermore, fuel consumption directly affects the allocation of WTT emissions (in g/mmBtu) to WTW emission (in g/mi). Thus, simulation to determine fuel consumption values for vehicle technologies is a key activity for WTW analyses.

Vehicle simulations for this study were conducted for a full-size pickup truck. As discussed in Section 3, our simulations reveal that DI SI engine technology could achieve a gain of about 15% in fuel economy, and DI CI engine technology could achieve a gain of more than 20%. HEV technologies used with gasoline and diesel ICEs achieve 25–45% gains in fuel economy. On the other hand, FCVs employing onboard reforming offer fuel economy gains of 51–65%, and fuel cell HEVs employing onboard reforming offer gains of 70–90%. Direct-hydrogen FCVs achieve fuel economy gains of 140%, and direct-hydrogen fuel cell HEVs achieve gains of more than 160%. These fuel economy gains contribute directly to the reductions in WTW energy use and emissions by these advanced vehicle technologies. In the cases in which hydrogen is used to power vehicles, the large gains in fuel economy by fuel cell technologies far offset energy-efficiency losses during hydrogen production (except for electrolysis hydrogen production, for which fuel economy gains are not enough to offset the large energy losses of electricity generation and hydrogen production together).

Vehicle fuel economy has a smaller impact on WTW emissions of criteria pollutants (except for SO_x emissions) for ICE-based technologies, because vehicular criteria pollutant emissions are regulated on a per-mile basis, and after-combustion emission control technologies are designed to reduce per-mile emissions, resulting in a disconnection between the amount of fuel consumed and the amount of per-mile criteria pollutant emissions generated. For vehicle technologies that do not have tailpipe emissions (such as direct-hydrogen FCVs and battery-powered EVs), fuel consumption directly affects WTW criteria pollutant emissions.

Our WTW results show that advanced vehicle technologies offer great potential for reducing petroleum use, GHG emissions, and criteria pollutant emissions. Reductions in petroleum use are attributable to vehicle fuel consumption reductions by advanced vehicle technologies and the switch from petroleum to non-petroleum energy feedstocks in the case of hydrogen, electricity, CNG, FTD, methanol, and ethanol. Use of non-petroleum feedstocks for transportation fuel production essentially eliminates petroleum use.

Use of E85 in ethanol flexible-fuel vehicles reduces petroleum use by about 70% (because E85 contains about 26% gasoline, on an energy basis). On the other hand, HEVs operating on gasoline or diesel reduce petroleum use by 20–30%, exclusively because of vehicle fuel consumption reductions.

The WTW GHG emissions generated by advanced vehicle technologies are determined by the WTT energy efficiencies of fuel pathways, the vehicle fuel consumption, the carbon content of energy feedstocks for fuel production, and the renewability of those feedstocks. The use of renewable feedstocks (such as renewable electricity and cellulosic ethanol) helps eliminate (or almost eliminate) GHG emissions. Even vehicle technologies with high fuel consumption can still eliminate GHG emissions, because the fuel and its feedstock do not have carbon burdens. For example, use of renewable hydrogen in hydrogen ICE and fuel cell technologies achieves 100% reductions in GHG emissions. On the other hand, use of cellulosic E85 in ICE technologies achieves reductions of about 70% (the benefits are reduced because E85 contains 26% gasoline by energy content).

The GHG reduction results for advanced vehicles powered by carbon-containing fuels or fuels derived from carbon-containing feedstocks depend on WTT efficiencies and vehicle fuel consumption. For example, FCVs powered by NG-derived hydrogen achieve GHG reductions of about 50% because of the low fuel consumption of direct-hydrogen FCVs. If NG-derived hydrogen is used in hydrogen ICE technologies that are less efficient than hydrogen fuel cell technologies, there may be no GHG reduction benefits. In hydrogen plants, all carbon in NG ends up as CO_2. If CO_2 is captured and stored, this production pathway essentially becomes a zero-carbon pathway. Any vehicle technologies using hydrogen produced this way will eliminate GHG emissions. In our analysis, we did not assume carbon capture and storage for central hydrogen plants with NG.

Some of the vehicle technologies and fuels evaluated in this study offer moderate reductions in GHG emissions: corn-based E85 in flexible-fuel vehicles, HEVs powered by hydrocarbon fuels, and diesel-fueled vehicles. In general, these vehicle/fuel systems achieve 20–30% reductions in GHG emissions. The reduction achieved by using corn-based E85 is only moderate because (1) significant amounts of GHG emissions are generated during corn farming and in corn ethanol production plants; (2) diesel fuel, LPG, and other fossil fuels are consumed during corn farming; (3) a large amount of nitrogen fertilizer is also used for corn farming, and manufacture of nitrogen fertilizer and its nitrification and denitrification in cornfields produce a large amount of GHG emissions; and (4) usually, NG or coal is used in corn ethanol plants to generate steam. If renewable energy sources, such as corn stover or cellulosic biomass, are used in corn ethanol production plants, use of corn-based E85 could result in larger GHG emission reductions.

Hybrids fueled with CNG achieve larger GHG reductions than their fuel consumption reductions, because NG is 21% less carbon-intensive (defined as carbon content per energy unit of fuel) than gasoline (our baseline fuel). On the other hand, diesel ICEs and hybrids achieve smaller GHG reductions than their fuel consumption reductions, because diesel fuel is 7% more carbon-intensive than gasoline.

GHG results for hydrogen generated by means of electrolysis may be the most dramatic WTW results in this study. Two major efficiency losses occur during electricity generation and hydrogen production via electrolysis. Consequently, this pathway is subject to the largest WTT energy-efficiency losses. Using hydrogen (itself a non-carbon fuel) produced this way could result in dramatic increases in WTW GHG emissions. For example, if hydrogen is produced with U.S. average electricity (more than 50% of which is generated from coal-fired power plants), its use, even in efficient FCVs, can still result in increased GHG emissions; its use in less-efficient hydrogen ICEs results in far greater increases in GHG emissions. On the other hand, if a clean electricity generation mix, such as the California generation mix, is used, the use of electrolysis hydrogen in FCVs could result in moderate reductions in GHG emissions. Furthermore, if

renewable electricity, such as wind power, is used for hydrogen production, the use of hydrogen in any vehicle technology will result in elimination of GHG emissions. This case demonstrates the importance of careful examination of potential hydrogen production pathways so that the intended GHG emission reduction benefits by hydrogen-powered vehicle technologies can truly be achieved.

Ours is the first comprehensive study to address WTW emissions of criteria pollutants. The results reveal that advanced vehicle technologies help reduce WTW criteria pollutant emissions. We assumed in our study that ICE vehicle technologies will, at minimum, meet EPA's Tier 2 Bin 5 emission standards. Improvements in fuel consumption by advanced vehicle technologies will help reduce per-mile WTT criteria pollutant emissions. For example, gasoline or diesel HEVs with low fuel consumption will reduce WTW criteria pollutant emissions by 10–20%, exclusively because of their reduced WTT emissions.

Probably the most revealing results are the differences in WTW criteria pollutant emissions between ICE and fuel cell technologies. Although tailpipe criteria pollutant emissions generated by ICE technologies will be reduced significantly in the future, they will continue to be subject to on-road emission deterioration (although to a much smaller extent than past ICE technologies, thanks to OBD systems). On the other hand, FCVs, especially direct-hydrogen FCVs, generate no tailpipe emissions. Except for electrolysis hydrogen generated with U.S. average electricity, hydrogen FCVs reduce WTW emissions of criteria pollutants. For example, NG-derived hydrogen FCVs reduce WTW NO_x emissions by about 50%. FCVs also reduce the uncertainty range of criteria pollutant emissions, because they do not experience on-road deterioration of criteria pollutant emissions.

Vehicle technologies fueled with hydrogen generated via electrolysis usually result in increased criteria pollutant emissions. Power plant emissions, together with the low efficiency of electrolysis hydrogen production, cause the increases. In order to mitigate the increases, power plant emissions will have to be reduced drastically or clean power sources will have to be used for hydrogen production.

Ethanol-based technology options also result in increased total emissions for criteria pollutants, because large amounts of emissions occur during biomass farming and ethanol production. Our study estimates total and urban emissions of criteria pollutants separately. Although total emissions are increased by using ethanol, a significant amount of the total emissions occurs outside of urban areas (on farms and in ethanol plants that will be located near biomass feedstock farms). While total emission results show the importance of controlling ethanol plant emissions, urban emission estimates show that the negative effects of biofuels (such as ethanol) on criteria pollutant emissions are not as severe as total emission results imply.

Examination of GHG emissions and criteria pollutant emissions reveals tradeoffs for some vehicle/fuel technologies. For example, while diesel vehicle technologies offer the potential to reduce fuel use and, consequently, to reduce GHG emissions, they may face challenges in reducing NO_x and PM_{10} emissions. Our assumption that diesel vehicles will meet Tier 2 Bin 5 standards by no means understates the technical challenges that automakers face in achieving this goal. On the other hand, FCVs can achieve emission reductions for both GHGs and criteria pollutants — thus offering a long-term solution to emissions of both GHGs and criteria pollutants from the transportation sector.

The results of our WTW analysis of criteria pollutant emissions show that, as tailpipe emissions from motor vehicles continue to decline, WTT activities could represent an increased share of WTW emissions, especially for hydrogen, electricity, ethanol, and FT diesel. Thus, in order to achieve reductions in criteria pollutant emissions by advanced vehicle technologies, close attention should be paid to emissions associated with WTT, as well as TTW, activities.

Our study analyzed advanced vehicle technologies together with new transportation fuels, because vehicle technologies and fuels together have become increasingly important in seeking solutions to transportation energy and environmental problems. High-quality fuels are necessary to allow the introduction of advanced vehicle technologies. For example, low-sulfur gasoline and diesel are needed for gasoline lean-burn and clean-diesel engines. The energy and environmental benefits of FCVs can be guaranteed only by using hydrogen from clean feedstocks and efficient production pathways. In a way, the recent popularization of WTW analyses reflects the new reality — that vehicles and fuels must be considered together in addressing transportation energy and environmental issues.

Our study separates energy use into total energy, fossil energy, and petroleum energy. Separate results for each of the three energy types shed light on the true energy benefits of transportation fuels. For example, some other studies that developed estimates for total energy use showed large increases in energy use for biofuels. But those studies failed to differentiate among the different types of energy sources. A fuel that offers a significant reduction in petroleum use may be able to help reduce U.S. oil imports. In Section 4, we demonstrated that total energy calculations can sometimes be arbitrary. For these reasons, we maintain that the type of energy sources, as well as the amount of energy use, should be considered in evaluating the energy benefits of vehicle/fuel systems.

6. STUDY LIMITATIONS

The intent of this study was to evaluate the energy and emission effects of the vehicle/fuel systems included in the study, with the premise that they could be introduced around 2010. Like many other WTW studies, ours did not address the economics and market constraints of the vehicle/fuel systems considered. Costs and commercial readiness may eventually determine which vehicle/fuel systems are able to penetrate the vehicle market. The results of this study provide guidance to help ensure that R&D efforts are focused on the vehicle/fuel systems that will provide true energy and emission benefits. Because WTW studies generally do not address economics, consumer acceptance, and many other factors, they cannot determine the marketability of vehicle/fuel systems.

As discussed in Section 5, the fuel consumption of vehicle/fuel systems is one of the most important factors in determining WTW energy use and emissions results, especially GHG emissions. In our analysis, we based vehicle fuel consumption simulations on the full-size Silverado pickup truck. Compared with a typical passenger car, the pickup truck has higher fuel consumption and higher tailpipe emissions, resulting in higher WTW energy use and emissions per mile. Most other WTW studies were based on passenger cars. Absolute results per mile driven between this study and other completed studies cannot be compared. However, the relative changes that can be derived from per-mile results in this study and other studies can be compared to understand the differences in potential energy and emission benefits for different vehicle and fuel technologies.

Several major WTW studies have been completed in the past several years. For example, MIT conducted a WTW study in 2000 and updated it in 2003 (Weiss et al. 2000; 2003). The MIT study was based on a mid-size passenger car. The GM-sponsored European WTW study (L-B-Systemtechnik GmbH et al. 2002) was based on an Opel Zafira minivan with an engine displacement of 1.8 L. A WTW study sponsored by the Joint Research Centre of the European Commission, Concawe, and the European Council for Automotive R&D (2003) was based on a typical European compact car similar to the Volkswagen Golf. Comparison of absolute results from these studies and our study are less meaningful, mainly because different vehicle sizes were used in these studies. However, comparison of the relative change results among these studies should improve our understanding of the range of energy and emission benefits associated with advanced vehicle technologies and new transportation fuels, although such comparisons are beyond the scope of this study.

The fuel consumption improvements of HEVs directly affect their WTW energy and emission benefits. The extent of HEV fuel consumption improvements depends largely on the degree of hybridization and on designed tradeoffs between fuel consumption and vehicle performance. The HEV design simulated in this study was intended to fully meet the performance goals of the conventional Silverado truck. Furthermore, engine downsizing was not assumed here for the best-estimate HEV design. This design decision resulted in smaller fuel consumption reductions by HEVs in this study than could be achieved with downsized engines. Downsized engines were considered in the best-case HEV scenario.

Although we included many hydrogen production pathways in this study, we have certainly not covered every potential hydrogen production pathway. For instance, we included neither hydrogen production via gasification from coal and cellulosic biomass nor hydrogen production via high-temperature, gas-cooled nuclear reactors. R&D efforts are currently in progress for these hydrogen production pathways. For some of the hydrogen production pathways considered in this study (such as hydrogen from NG in central plants), we did not assume carbon capture and storage. If we had done so, those pathways might have been shown to result in huge GHG emission reductions.

Although we addressed uncertainties in our study with Monte Carlo simulations, the results of our simulations depend heavily on probability functions that we established for key WTW input parameters. Data limitations reduced the reliability of the distribution functions we built for some of the key input parameters, such as criteria pollutant emissions of key WTT and TTW stages. Nonetheless, systematic simulations of uncertainties in WTW studies could become the norm for future WTW studies.

7. ACKNOWLEDGMENTS

We appreciate the substantial contributions to this study by the individuals listed below. Without their efforts, this study would not have been possible.

	Name	**Affiliation**
WTT	Clint Burklin	Eastern Research Group, Morrisville, NC
	Amy Alexander	Eastern Research Group, Morrisville, NC
	Dennis Kahlbaum	University of Michigan
	Harry Sigworth	ChevronTexaco, Richmond, CA
	Steve Welstand	ChevronTexaco, San Ramon, CA
	Michael Milliet	ChevronTexaco, Houston, TX
	Lyman Young	ChevronTexaco, Richmond, CA
	Jean Cadu	Shell, London
	Chuck Lieder	Shell Global Solutions, Houston, TX
TTW	Moshe Miller	Advanced Development Corporation, Israel
	Rodney Rask	GM Research and Development Center, Warren, MI
	Tony Zarger	GM Fiat-GM Powertrain, Pontiac, MI
	David Masten	GM Fuel Cell Activity, Honeoye Falls, NY
	Volker Formanski	GM Fuel Cell Activity, Mainz-Kastel, Germany
WTW	Danilo Santini	Argonne National Laboratory, Argonne, IL
	Ye Wu	Argonne National Laboratory, Argonne, IL
	Greg Ruselowski	General Motors Fuel Cell Activity, Warren, MI

8. REFERENCES

American Methanol Institute, 2003, *World Methanol Plants (through December 2001)*, website of American Methanol Institute (www.methanol.org), accessed on May 20.

Burklin, C., and A. Alexander, 2002, *Technical Documentation for the Emission Factors and Trends Developed for the Transportation Fuels Industries*, July 24.

California Air Resources Board, 1999, LEV II and CAP 2000 Amendments, Final Regulation Order, Oct. 28.

California Air Resources Board, 2004, EMFAC2002 Emission Inventories Modeling Software and Documents, accessed from http://www.arb.ca.gov/msei/on-road/latest_version.htm.

CARB: See California Air Resources Board.

Eichlseder, H., et al., 2003, *The Potential of Hydrogen Internal Combustion Engines in a Future Mobility Scenario*, SAE 2003-01-2267, June.

Energy Information Administration, 2003, *Uranium Industry Annual 2002*, DOE/EIA-0478(2002), Washington, D.C., May.

EPA: See U.S. Environmental Protection Agency.

Fellini R., P. Papalambros, and T. Weber, 2000, *Application of Product Platform Design Process to Automotive Powertrains*, Proceedings of the 8th AIAA / NASA / USAF / ISSMO Symposium on Multidisciplinary Analysis and Optimization, Paper No. AIAA-2000-4849.

Fellini, R., 1998, *Derivative Free and Global Search Optimization Algorithms in an Object-Oriented Design Framework*, Master of Science Thesis, Department of Mechanical Engineering, University of Michigan, Ann Arbor, Mich.

Fellini, R., et al., 1999, *Optimal Design of Automotive Hybrid Powertrain Systems*, Proceedings of the EcoDesign '99: 1st International Symposium on Environmentally Conscious Design and Inverse Manufacturing, Tokyo, Japan, Feb.

General Motors Corporation, Argonne National Laboratory, BP, ExxonMobil, and Shell, 2001, *Well-to-Wheel Energy Use and Greenhouse Gas Emissions of Advanced Fuel/Vehicle Systems — North American Analysis*, Volumes 1–3, http://www.transportation.anl.gov/ttrdc/publications/gapc.html**,** June.

Intergovernmental Panel on Climate Change, 2001, *Technical Summary of Working Group I Report*.

IPCC: See Intergovernmental Panel on Climate Change.

The Joint Research Centre of European Commission, Concawe, and the European Council for Automotive R&D, 2003, *Well-to-Wheels Analysis of Future Automotive Fuels and Powertrains in the European Context*, Brussels, Belgium, Dec.

L-B-Systemtechnik GmbH, General Motors Corporation, BP, ExxonMobil, Shell, and TotalFinaElf, 2002, *GM Well-to-Wheel Analysis of Energy Use and Greenhouse Gas Emissions of Advanced Fuel/Vehicle Systems — A European Study*, http://www.lbst.de/gm-wtw, Ottobrunn, Germany, Sept. 27.

Lee H., M.Q. Wang, and J. Molburg, 2003, *Process Energy Allocation of Petroleum Refining Processes*, paper presented at the Spring Meeting of the American Institute of Chemical Engineers, New Orleans, La., March 31.

Michaels, H., 1998, *Emissions of Nitrous Oxide from Highway Mobile Sources*, EPA420-R-98-009, Aug.

Natkin, R., et al., 2002, *Ford Hydrogen Internal Combustion Engine Design and Vehicle Development Program*, Global Powertrain Conference.

Natkin, R., et al., 2003, *Hydrogen IC Engine Boosting Performance and NO_x Study*, SAE 2003-01-0631.

Sasena, M., 1998, *Optimization of Computer Simulations via Smoothing Splines and Kriging Metamodels*, Master of Science Thesis, Department of Mechanical Engineering, University of Michigan, Ann Arbor, Mich.

Schwieger, R., et al., 2002, "First Annual Top Plants Survey," *The Power Magazine*, Aug.

U.S. Environmental Protection Agency, 1995, *Compilation of Air Pollutant Emission Factors, Volume 1: Stationary Point and Area Sources*, AP-42 Fifth Edition, Research Triangle Park, N.C., Jan. (with updated sections from http://www.epa.gov/ttn/chief/ap42/).

U.S. Environmental Protection Agency, 1999, *Draft 1999 National Emissions Inventory Database*, http://www.epa.gov/ttn/chief/net/index.html.

U.S. Environmental Protection Agency, 2000, *Control of Air Pollution from New Motor Vehicles: Tier 2 Motor Vehicle Emissions Standards and Gasoline Sulfur Control Requirements; Final Rule*, 40 CFR Parts 80, 85, and 86, Feb. 10.

U.S. Environmental Protection Agency, 2003, MOBILE6.2 Emission Factor Modeling Software and Documents, Office of Transportation and Air Quality, accessed from http://www.epa.gov/otaq/m6.htm.

U.S. Environmental Protection Agency, 2004a, Rule to Reduce Interstate Transport of Fine Particulate Matter and Ozone (Interstate Air Quality Rule); Proposed Rule, *Federal Register*, Vol. 69, No. 20, pp. 4566-4650, Jan. 30.

U.S. Environmental Protection Agency, 2004b, EGRID – Emissions and Generation Resource Integrated Database, accessed from http://www.epa.gov/cleanenergy/egrid/index.htm, last updated by EPA on March 25.

Wang, M.Q., 1996, *Development and Use of the GREET Model to Estimate Fuel-Cycle Energy Use and Emissions of Various Transportation Technologies and Fuels*, ANL/ESD-31, Center for Transportation Research, Argonne National Laboratory, June.

Wang, M.Q., 1999, *GREET 1.5 — Transportation Fuel-Cycle Model, Volume 1: Methodology, Development, Use, and Results, Volume 1*, ANL/ESD-39, Center for Transportation Research, Argonne National Laboratory, Aug.

Wang, M.Q., 1999, *GREET 1.5 — Transportation Fuel-Cycle Model, Volume 2: Appendices of Data and Results, Volume 2*, ANL/ESD-39, Center for Transportation Research, Argonne National Laboratory, Aug.

Wang, M.Q., 2001, *Development and Use of GREET 1.6 Fuel-Cycle Model for Transportation Fuels and Vehicle Technologies*, ANL/ESD/TM-163, Center for Transportation Research, Argonne National Laboratory, June.

Wang, M.Q., and H.S. Huang, 1999, *A Full Fuel-Cycle Analysis of Energy and Emissions Impacts of Transportation Fuels Produced from Natural Gas*, ANL/ESD-40, Center for Transportation Research, Argonne National Laboratory, Dec.

Weber, T., 2003, *Vehicle System Modeling in the Automotive Industry*, University of Wisconsin, ARO/ERC Engine Modeling Symposium, Madison, Wis., June.

Weiss, M.A., et al., 2000, *On the Road in 2020 — A Life Cycle Analysis of New Automobile Technologies*, Energy Laboratory, Massachusetts Institute of Technology, Oct.

Weiss, M.A., et al., 2003, *Comparative Assessment of Fuel Cell Cars*, Energy Laboratory, Massachusetts Institute of Technology, Feb.

Wurster, R., et al., 2004, *Well-to-Wheel Analysis of Energy Use and Greenhouse Gas Emissions of Advanced Fuel/Vehicle Systems — Results from the European Study*, The 15th World Hydrogen Energy Conference, Yokohama, Japan, June.

APPENDIX A

ANALYSIS OF THE NATIONAL EMISSION INVENTORY DATABASE

TABLE A-1 Activity Data Sources Used for Process Emission Factor Calculations

Process	Activity Data Source
Bituminous coal and lignite surface mining and processing	NEI
Bituminous coal underground mining and processing	NEI
Nitrogen fertilizer production	NEI
Crude petroleum pipelines	NEI
Refined petroleum product pipelines	NEI
Petroleum bulk terminals	NEI
Gasoline and diesel service stations	NEI
Natural gas liquids production	*Oil and Gas Journal*, Vol. 97, Issue 24, June 14, 1999
Ethanol Production	BBI, International for 2001
Methanol production from natural gas	ChemExpo's Chemical Profile of Methanol for 2000
Phosphate fertilizer production	ChemExpo's Chemical Profile of Ammonium Phosphates for 1999. Applied capacity utilization factor of 78% to all facility capacities. Utilization factor from Federal Reserve Statistical Release for Industrial Production and Capacity Utilization
Petroleum Refineries	*Oil and Gas Journal*, Vol. 97, Issue 51, Dec. 20, 1999; applied utilization factor of 93%. Utilization factor from Federal Reserve Statistical Release (same as above)

TABLE A-2 Summary of Combustion Emission Factors (g/mmBtu of fuel burned)

Pollutant	Group	Count	Mean	StdDev	Min	Max	P10	Median	P90
VOC	Coal industrial boilers	6	0.809	0.203	0.682	1.220	0.686	0.739	1.173
	Coke industrial boilers	1	0.476		0.476	0.476	0.476	0.476	0.476
	Diesel industrial boilers	6	1.205	0.667	0.632	2.293	0.636	0.940	2.238
	Diesel reciprocating engines	13	157.576	156.391	18.038	649.351	40.713	156.235	264.550
	Gasoline reciprocating engines	1	1528.270		1528.270	1528.270	1528.270	1528.270	1528.270
	ICE fugitive emissions	1	989.487		989.487	989.487	989.487	989.487	989.487
	LPG industrial boilers	1	1.679		1.679	1.679	1.679	1.679	1.679
	LPG reciprocating engines	1	3.346		3.346	3.346	3.346	3.346	3.346
	NG industrial boilers	297	1.595	1.942	0.006	21.619	0.588	1.154	2.542
	NG large gas turbines	23	3.439	5.521	0.011	21.008	0.052	1.019	11.757
	NG reciprocating engines	186	55.101	61.110	0.014	435.931	3.778	37.681	138.528
	NG small industrial boilers	138	3.434	13.696	0.217	158.730	0.801	2.217	2.495
	Residual oil industrial boilers	23	2.023	2.596	0.268	12.121	0.705	0.940	5.254
	Solid waste industrial boilers	3	0.096	0.029	0.064	0.119	0.064	0.106	0.119
	Waste oil industrial boilers	3	2.508	0.068	2.458	2.586	2.458	2.479	2.586
CO	Coal industrial boilers	6	276.250	117.753	35.889	324.351	64.728	324.325	324.349
	Coke industrial boilers	1	25.463		25.463	25.463	25.463	25.463	25.463
	Diesel industrial boilers	21	16.686	3.123	12.987	24.438	12.987	16.051	21.254
	Diesel reciprocating engines	18	346.043	191.964	54.113	649.351	84.416	324.675	649.351
	Gasoline reciprocating engines	1	31167.500		31167.500	31167.500	31167.500	31167.500	31167.500
	ICE fugitive emissions	1	1772.830		1772.830	1772.830	1772.830	1772.830	1772.830
	LPG industrial boilers	2	17.227	2.992	15.111	19.342	15.111	17.227	19.342
	LPG reciprocating engines	3	1275.160	939.978	198.778	1934.240	198.778	1692.460	1934.240
	NG industrial boilers	346	16.459	11.572	0.092	57.720	7.141	14.868	36.298

TABLE A-2 Cont.

Pollutant	Group	Count	Mean	StdDev	Min	Max	P10	Median	P90
CO (Cont.)	NG large gas turbines	26	47.899	51.254	0.295	194.933	3.027	31.191	121.595
	NG reciprocating engines	211	386.314	385.661	2.562	2667.970	67.473	259.740	894.799
	NG small industrial boilers	149	23.731	16.453	0.038	129.890	8.636	17.316	36.396
	Residual oil industrial boilers	24	16.064	4.087	12.121	30.166	13.978	14.711	22.988
	Solid waste industrial boilers	3	1.787	0.018	1.772	1.808	1.772	1.783	1.808
	Waste oil industrial boilers	3	15.202	0.032	15.165	15.222	15.165	15.218	15.222
NO_x	Coal industrial boilers	6	246.110	68.047	107.209	273.896	123.877	273.889	273.896
	Coke industrial boilers	2	125.602	154.660	16.241	234.962	16.241	125.602	234.962
	Diesel industrial boilers	24	109.898	51.279	46.165	225.986	64.935	87.663	177.082
	Diesel reciprocating engines	18	1438.630	548.278	129.870	2164.500	459.957	1525.050	1952.930
	Gasoline reciprocating engines	1	782.661		782.661	782.661	782.661	782.661	782.661
	ICE fugitive emissions	1	1443.000		1443.000	1443.000	1443.000	1443.000	1443.000
	LPG commercial boiler	3	50.953	11.143	38.685	60.445	38.685	53.729	60.445
	LPG industrial boilers	4	104.286	38.364	77.369	161.186	77.369	89.294	161.186
	LPG reciprocating engines	3	1769.680	526.713	1174.600	2176.020	1174.600	1958.410	2176.020
	NG industrial boilers	356	60.546	39.870	0.110	407.648	23.092	60.529	86.580
	NG large gas turbines	26	138.627	154.770	1.879	707.410	15.105	87.310	325.113
	NG reciprocating engines	212	1060.090	868.388	6.040	3636.360	57.102	1036.680	2237.720
	NG small industrial boilers	153	41.820	18.378	1.723	173.160	16.589	43.290	60.606
	Residual oil industrial boilers	27	187.221	66.525	89.776	372.960	110.312	166.667	297.861
	Solid waste industrial boilers	3	7.079	0.057	7.018	7.130	7.018	7.088	7.130
	Waste oil industrial boilers	3	19.756	0.053	19.697	19.798	19.697	19.773	19.798
SO_2	Coal industrial boilers	6	194.677	18.539	187.086	232.520	187.087	187.112	227.981
	Coke industrial boilers	2	571.001	582.047	159.431	982.570	159.431	571.001	982.570
	Diesel industrial boilers	28	330.953	379.131	17.418	980.392	27.206	103.896	940.384
	Diesel reciprocating engines	10	140.000	73.798	18.038	259.740	49.603	146.104	250.120

TABLE A-2 Cont.

Pollutant	Group	Count	Mean	StdDev	Min	Max	P10	Median	P90
SO_2 (Cont.)	LPG reciprocating engines	1	1.673		1.673	1.673	1.673	1.673	1.673
	NG industrial boilers	287	6.108	17.387	0.212	270.134	0.713	1.480	16.971
	NG large gas turbines	16	3.535	6.583	0.248	16.832	0.251	0.315	16.818
	NG reciprocating engines	64	0.930	2.459	0.201	15.256	0.241	0.322	1.263
	NG small industrial boilers	78	6.829	27.602	0.049	219.104	0.140	0.504	14.028
	Residual oil industrial boilers	27	790.373	637.972	6.985	3214.270	225.729	775.758	1211.920
PM_{10} filterables only	Coke industrial boilers	2	4.333	5.955	0.123	8.544	0.123	4.333	8.544
	Diesel industrial boilers	6	3.026	0.689	2.239	3.820	2.241	3.117	3.798
	Diesel reciprocating engines	8	115.721	60.998	12.987	168.350	23.006	146.104	166.546
	LPG reciprocating engines	1	3.346		3.346	3.346	3.346	3.346	3.346
	NG industrial boilers	154	3.452	1.369	0.026	6.993	1.265	4.097	4.381
	NG large gas turbines	11	2.107	2.264	0.089	5.962	0.090	1.015	5.954
	NG reciprocating engines	78	6.652	5.814	0.201	19.166	0.813	4.334	18.670
	NG small industrial boilers	57	12.386	35.127	0.433	154.113	0.826	3.171	6.237
	Residual oil industrial boilers	6	55.130	47.312	1.347	140.654	3.743	52.107	132.515
	Solid waste industrial boilers	3	0.144	0.043	0.096	0.178	0.096	0.159	0.178
PM_{10} filterables + condensable	Coal industrial boilers	1	2.472		2.472	2.472	2.472	2.472	2.472
	Diesel industrial boilers	12	70.200	54.230	4.697	200.535	19.949	51.041	153.060
	Diesel reciprocating engines	3	112.782	41.437	64.935	136.705	64.935	136.705	136.705
	Gasoline reciprocating engines	1	46.311		46.311	46.311	46.311	46.311	46.311
	LPG industrial boilers	1	1.679		1.679	1.679	1.679	1.679	1.679
	NG industrial boilers	129	3.206	3.264	0.008	35.212	1.320	2.609	5.010
	NG large gas turbines	1	2.903		2.903	2.903	2.903	2.903	2.903
	NG reciprocating engines	6	5.514	1.725	3.275	8.492	3.444	5.127	8.252
	NG small industrial boilers	51	2.801	1.206	0.352	5.772	0.616	3.200	3.566
	Residual oil industrial boilers	6	44.396	17.701	24.383	66.745	24.589	46.248	65.701

TABLE A-3 Summary of Process Emission Factors (g/mmBtu of fuel throughput for all groups except fertilizers, which are in tons/1,000 tons throughput)

Pollutant	Group	Count	Mean	StdDev	Min	Max	P10	Median	P90
VOC	Crude petroleum pipelines	1	0.0000		0.0000	0.0000	0.0000	0.0000	0.0000
	Diesel service stations	6	0.0011	0.0025	0.0000	0.0062	0.0000	0.0001	0.0056
	Ethanol production	6	3.5104	1.5269	1.9667	5.9684	1.9959	3.1822	5.8219
	Gasoline service stations	22	0.0050	0.0024	0.0010	0.0065	0.0010	0.0064	0.0065
	Methanol production (from natural gas)	1	0.3719		0.3719	0.3719	0.3719	0.3719	0.3719
	Natural gas liquids production	10	0.0051	0.0049	0.0002	0.0132	0.0004	0.0026	0.0121
	Petroleum bulk terminals - crude	1	0.0002		0.0002	0.0002	0.0002	0.0002	0.0002
	Petroleum bulk terminals - diesel	6	0.0000	0.0000	0.0000	0.0000	0.0000	0.0000	0.0000
	Petroleum bulk terminals - gasoline	23	0.0009	0.0013	0.0000	0.0040	0.0000	0.0003	0.0032
	Petroleum refineries	25	0.0334	0.0324	0.0039	0.1430	0.0062	0.0291	0.0718
	Phosphate fertilizer production	6	0.0273	0.0271	0.0013	0.0707	0.0016	0.0215	0.0681
	Refined petroleum pipelines	1	0.0850		0.0850	0.0850	0.0850	0.0850	0.0850
CO	Methanol production (from natural gas)	1	0.2264		0.2264	0.2264	0.2264	0.2264	0.2264
	Natural gas liquids production	8	0.0007	0.0012	0.0000	0.0036	0.0000	0.0002	0.0028
	Petroleum refineries	22	0.0082	0.0151	0.0000	0.0682	0.0002	0.0027	0.0189
	Phosphate fertilizer production	4	0.0342	0.0361	0.0023	0.0724	0.0023	0.0310	0.0724
NO_x	Ethanol production	1	0.5560		0.5560	0.5560	0.5560	0.5560	0.5560
	Methanol production (from natural gas)	1	0.0101		0.0101	0.0101	0.0101	0.0101	0.0101
	Natural gas liquids production	8	0.0012	0.0028	0.0000	0.0081	0.0000	0.0001	0.0060
	Nitrogen fertilizer production	1	0.0200		0.0200	0.0200	0.0200	0.0200	0.0200
	Petroleum refineries	23	0.0096	0.0108	0.0000	0.0439	0.0000	0.0070	0.0225
	Phosphate fertilizer production	6	0.3484	0.2972	0.0350	0.7549	0.0371	0.3184	0.7401

TABLE A-3 Cont.

Pollutant	Group	Count	Mean	StdDev	Min	Max	P10	Median	P90
SO_2	Ethanol production	1	0.3985		0.3985	0.3985	0.3985	0.3985	0.3985
	Natural gas liquids production	6	0.0685	0.0798	0.0004	0.2046	0.0004	0.0427	0.1961
	Nitrogen fertilizer production	1	0.4987		0.4987	0.4987	0.4987	0.4987	0.4987
	Petroleum refineries	20	0.0542	0.0649	0.0000	0.2025	0.0014	0.0184	0.1582
	Phosphate fertilizer production	7	7.0935	4.1986	2.1853	13.9789	2.3881	5.8044	13.2213
PM_{10} filterables only	Bituminous coal and lignite surface mining and processing	7	0.0363	0.0416	0.0044	0.1027	0.0053	0.0144	0.1001
	Bituminous coal underground mining and processing	1	0.0279		0.0279	0.0279	0.0279	0.0279	0.0279
	Methanol production (from natural gas)	1	0.1607		0.1607	0.1607	0.1607	0.1607	0.1607
	Nitrogen fertilizer production	1	0.3319		0.3319	0.3319	0.3319	0.3319	0.3319
	Petroleum refineries	14	0.0071	0.0132	0.0000	0.0501	0.0000	0.0019	0.0180
	Phosphate fertilizer production	7	0.8913	1.2155	0.0007	3.0611	0.0084	0.2254	2.8777
PM_{10} filterables + condensable	Bituminous coal and lignite surface mining and processing	2	0.0136	0.0016	0.0125	0.0147	0.0125	0.0136	0.0147
	Bituminous coal underground mining and processing	7	0.0058	0.0045	0.0016	0.0135	0.0016	0.0044	0.0128
	Ethanol production	6	3.2478	1.0183	1.3554	4.2906	1.5354	3.4441	4.2412
	Nitrogen fertilizer production	1	0.2539		0.2539	0.2539	0.2539	0.2539	0.2539
	Petroleum refineries	6	0.0054	0.0070	0.0005	0.0193	0.0006	0.0025	0.0179

TABLE A-4 Summary of Electric Utility Emission Factors (g/kWh)

Pollutant	Group	Count	Mean	StdDev	Min	Max	P10	Median	P90
VOC	Coal+lignite	27	0.026423	0.038794	0.000126	0.176366	0.007468	0.012626	0.034197
	NG boilers	8	0.026784	0.014759	0.003807	0.045803	0.004550	0.031647	0.043446
	NG turbines	9	0.085191	0.128825	0.001641	0.367043	0.001696	0.013462	0.307075
	Oil	5	0.045430	0.015872	0.027278	0.062083	0.027278	0.042000	0.062083
CO	Coal+lignite	26	0.216240	0.446099	0.054603	2.356890	0.068703	0.097910	0.291540
	NG boilers	8	0.296644	0.167050	0.095308	0.537488	0.101764	0.287508	0.518664
	NG turbines	7	0.254231	0.360279	0.004361	1.003970	0.005347	0.103787	0.887622
	Oil	5	0.908033	1.434480	0.158361	3.467710	0.158361	0.270440	3.467710
NO_x	Coal+lignite	26	2.420490	1.314110	0.992241	6.674410	1.250440	2.007560	4.511170
	NG boilers	9	1.031530	0.800781	0.033605	2.204390	0.102272	1.019400	2.162880
	NG turbines	8	1.441160	1.766880	0.007422	4.566450	0.008809	0.849782	4.267760
	Oil	4	1.434610	0.498601	0.982138	2.012720	0.982138	1.371800	2.012720
SO_2	Coal+lignite	25	6.715010	4.371770	0.753194	18.301600	1.465620	5.715080	11.222100
	NG boilers	9	0.131082	0.346467	0.001384	1.052710	0.001895	0.006188	0.662398
	NG turbines	5	0.013368	0.022736	0.001957	0.053977	0.001957	0.003253	0.053977
	Oil	5	5.272380	4.261130	0.019976	11.812700	0.019976	5.284780	11.812700
PM_{10} filterables only	Coal+lignite	21	0.041149	0.092955	0.000054	0.428803	0.000257	0.008670	0.081956
	NG boilers	8	0.014019	0.021522	0.000593	0.059444	0.000594	0.002507	0.051728
	NG turbines	4	0.029159	0.021542	0.002432	0.053850	0.002432	0.030178	0.053850
	Oil	3	0.250416	0.373602	0.029141	0.681765	0.029141	0.040340	0.681765
PM_{10} filterables + condensable	Coal+lignite	12	0.245485	0.542284	0.001797	1.940030	0.006615	0.067251	0.768614
	Oil	2	0.015297	0.016563	0.003585	0.027009	0.003585	0.015297	0.027009

APPENDIX B

GENERATION OF EMISSION FACTOR DISTRIBUTIONS

TABLE B-1 Fuel Combustion Sources (units are g/mmBtu of fuel input)

Item	Description
NG-fired utility/industrial boilers	
VOC	Distribution fit to NEI data
CO	Distribution fit to NEI data
NO_x	Minimum changed to match that of *Power Magazine* (Schwieger et al. 2002) and the maximum matches the 98th percentile of NEI data
PM_{10}	Distribution fit to NEI data
NG-fired small industrial boilers	
VOC	Distribution fit to NEI data
CO	Minimum changed to 5. Mean is 20% reduction from AP-42.
NO_x	Minimum set to match large boiler. Distribution adjusted to make mean below average AP-42 factors.
PM_{10}	Distribution fit to NEI data
NG-fired large gas turbines, combined-cycle gas turbines, and small gas turbines	
VOC	Assumed future controls on high emitters, so maximum set to the second highest NEI data point.
CO	Assumed future controls on high emitters, so maximum set to equal AP-42 controlled. Mean close to AP-42 average.
NO_x	Assumed future controls on high emitters, so maximum set to match 2nd highest point
PM_{10}	Distribution fit to NEI data
NG-fired reciprocating engines	
VOC	Distribution fit to NEI data
CO	Minimum changed to 5
NO_x	Distribution set to match diesel engine distribution
PM_{10}	Distribution fit to NEI data
Oil-fired utility boilers, industrial boilers, and commercial boilers	
VOC	Distribution fit to NEI data
CO	Distribution fit to NEI data
NO_x	Distribution fit to NEI data
PM_{10}	Distribution fit to NEI data
SO_x	NEI data would have given emission factors higher than coal fired, so we lowered the minimum to about half that of coal (to match relative sulfur content). Distribution adjusted to make mean double the coal mean because few SO_x controls than with coal.
Diesel-fired industrial boilers and commercial boilers	
VOC	Distribution fit to NEI data
CO	Distribution fit to NEI data
NO_x	Assumed future controls on high emitters, so maximum of the distribution was set to match the maximum factor for AP-42
PM_{10}	Maximum and minimum match NEI data, but exponential function used to keep mean below the mean for residual oil

TABLE B-1 (Cont.)

Item	Description
Diesel-fired reciprocating engines	
VOC	Maximum set to 250, corresponding to the maximum in the uncontrolled heavy-duty off-road engines
CO	Maximum set to 250 and minimum set to 20. Beta distribution was adjusted to make the mean equal to 100, which corresponds to value in the heavy-duty off-road engines.
NO_x	Minimum set to match 2010 heavy-duty engine standard. Maximum set to the maximum uncontrolled AP-42 factor. Resulting distribution has a mean of about half of that for NEI data.
PM_{10}	Little data in NEI, so distribution set equivalent to controlled value for 2010 heavy-duty engine standards (0.01 g/bhph), a median consistent with 0.3 g/bhph, and a maximum near the maximum of the NEI data
Gasoline-fired reciprocating engines	
VOC	No data from NEI. Distribution function for diesel-fired reciprocating engines was adjusted with the difference of gasoline farming tractors and diesel farming tractors.
CO	No data from NEI. Distribution function for diesel-fired reciprocating engines was adjusted with the difference of gasoline farming tractors and diesel farming tractors.
NO_x	No data from NEI. Distribution function for diesel-fired reciprocating engines was adjusted with the difference of gasoline farming tractors and diesel farming tractors.
PM_{10}	No data from NEI. Distribution function for diesel-fired reciprocating engines was adjusted with the difference of gasoline farming tractors and diesel farming tractors.
LPG-fired industrial boilers[a]	
NO_x	Distribution adjusted to make mean about a 40% reduction from NEI data
LPG-fired commercial boilers[a]	
NO_x	Not enough NEI data to establish a distribution. Distribution was based on LPG industrial boilers, but mean was increased.
Coal-fired industrial boilers	
VOC	Minimum and maximum set to match AP-42 range
CO	Minimum set to match AP-42 minimum and maximum set to match AP-42 maximum
NO_x	Minimum and maximum were set to match *Power Magazine* (Schwieger et al. 2002) values. The resulting mean is 40% below NEI data.
PM_{10}	No data from NEI
SO_x	Adjusted distribution to 50% of NEI data to reflect expected controls by 2016

[a] Distribution functions were established only for NO_x emissions of LPG-fired industrial and commercial boilers. Emissions for other pollutants were point estimates.

TABLE B-2 Non-Combustion Sources (units are grams/million Btu of fuel throughput)

Item	Description
Petroleum-refinery process emissions for gasoline production[a]	
VOC	Assumed future controls on high emitters, so maximum set to match 4th highest point
CO	Assumed future controls on high emitters, so maximum set to match 2nd highest point. Skewed distribution to left to represent future controls.
NO_x	Assumed future controls on high emitters, so maximum set to match 3rd highest point
PM_{10}	Assumed future controls on high emitters, so maximum changed to the second highest NEI point. Mean consistent with mode.
SO_x	Assumed future controls on high emitters, so maximum reduced to 25. Based on future controls, distribution was skewed to the left to make a mean at 50% of the NEI data.
VOC from gasoline bulk terminals	Assumed future controls on high emitters, so maximum reduced to match 3rd highest NEI data point
VOC from gasoline refueling stations	Maximum of distribution matches current NEI data. Minimum set to match well-controlled value. Distribution based on assumption that more than half of stations will have controls by 2016.
VOC from LPG refueling stations	No data from NEI. Assumed to be 10% of gasoline station VOC evaporative emissions.
VOC from diesel bulk terminals	Distribution fit to NEI data
VOC from diesel refueling stations	Distribution fit to NEI data
VOC from naphtha bulk terminals	No data from NEI. Assumed to be the same as the gasoline bulk terminal evaporative emissions.
VOC from naphtha refueling stations	No data from NEI. Assumed to be the same as the gasoline station evaporative emissions.
Process-related emissions of NG processing plants	
VOC	NEI emission data for natural gas liquids plants were allocated to NG and LPG (85% and 15%, respectively). Set the maximum value to ERG maximum value of 11. This gives a mean value similar to independently obtained data.
CO	NEI emission data for natural gas liquids plants were allocated to NG and LPG (85% and 15%, respectively). Set the maximum value to 3, the minimum value to 0, and the mean value to 1.1, which were similar to independently obtained data.
NO_x	NEI emission data for natural gas liquids plants were allocated to NG and LPG (85% and 15%, respectively). Set the maximum value to 6.7 (which was the highest in NEI data), the minimum value to 0, and the mean value similar to independently obtained data.
PM_{10}	NEI emission data for natural gas liquids plants were allocated to NG and LPG (85% and 15%, respectively). Set the maximum value to 0.07 (which was from independently obtained data) and the minimum value to 0 (which was from the NEI data).
SO_x	NEI emission data for natural gas liquids plants were allocated to NG and LPG (85% and 15%, respectively). Set the maximum value to 50 and shifted the distribution function for the mean value to be 10 to be close to independently obtained values.
Hydrogen plant process emissions[b]	
VOC	A distribution was created with maximum, minimum, and mode consistent with non-methane VOC data received from current hydrogen manufacturers
CO	A distribution was created with maximum, minimum, and mode consistent with data received from current hydrogen manufacturers
NO_x	See text
PM_{10}	A distribution was created with maximum, minimum, and mode consistent with data received from current hydrogen manufacturers

TABLE B-2 (Cont.)

Item	Description
MeOH plant process emissions[b]	
VOC, CO, NO_x, and PM_{10}	No data were available, so distributions were based on distributions for hydrogen reforming with adjustments for relative efficiency of hydrogen and methanol production
VOC from MeOH refueling stations	
FT diesel plant process emissions[b]	
VOC, CO, NO_x, and PM_{10}	No data were available, so distributions were based on distributions for hydrogen reforming with adjustments for relative efficiency of hydrogen and Fisher Tropsch diesel production
Corn ethanol plant process emissions	
VOC	See text
PM_{10}	Assumed future controls on high emitters, so maximum set to 2nd highest NEI data point
Cellulosic ethanol process emissions	
VOC	No data from NEI. Assumed to be 50% of corn ethanol plant VOC emissions per gallon.
PM_{10}	No data from NEI. Assumed to be the same as corn ethanol plant PM_{10} emissions per gallon.
VOC from EtOH bulk terminals	No data from NEI. Assumed to be the same as gasoline bulk terminal VOC emissions.
VOC from EtOH refueling stations	No data from NEI. Assumed to be the same as gasoline station VOC emissions.
PM_{10} emissions of coal mining	
Underground mining	Future controls assumed on high emitters, so maximum set to 2nd highest NEI data point
Surface mining	Future controls assumed on high emitters, so maximum set to 2nd highest NEI data point. The high values in the distribution are likely to represent coarse particulates.

[a] Distribution functions of criteria pollutant emissions were established for gasoline production in refineries. Distribution functions for residual oil, LPG, diesel, and crude naphtha are derived from those for gasoline with adjustment of relative refining energy efficiency between gasoline and each of the other fuels.

[b] Distribution functions of criteria pollutant emissions were established for hydrogen production in SMR plants. Distribution functions for methanol and FT diesel plants are derived from those for hydrogen plants, with adjustment of relative energy efficiency between that of hydrogen and those of methanol and FT diesel.

APPENDIX C

WELL-TO-TANK ENERGY AND EMISSIONS RESULTS

TABLE C-1 Well-to-Tank Energy and Emissions Results (Btu or Grams for Each Million Btu of Fuel Available in Vehicle Tanks)

	Total Energy	WTT Efficiency (%)	Fossil Energy	Petroleum	CO_2	CH_4	N_2O	GHGs	TVOC	TCO	TNO_x	TPM_{10}	TSO_x	UVOC	UCO	UNO_x	UPM_{10}	USO_x
30 ppm S RFG without oxygenate for DOD SI engine																		
10%	215,938	77.4	212,300	101,440	16,821	105.4	0.286	19,347	13.84	9.13	37.23	5.12	19.68	7.03	2.28	8.64	0.67	6.33
50%	253,017	79.8	248,596	118,430	19,558	108.3	0.330	22,140	23.54	11.72	44.06	9.34	26.96	13.49	3.32	11.87	0.88	8.78
90%	292,024	82.2	286,977	136,527	22,357	111.3	0.376	25,027	46.02	15.90	51.91	14.69	38.18	28.71	4.72	15.81	1.16	12.56
10 ppm S RFG without oxygenate for DI SI engine																		
10%	224,340	78.1	220,599	105,790	17,461	106.2	0.296	19,989	14.04	9.12	37.57	5.07	20.00	7.15	2.31	8.83	0.68	6.41
50%	252,344	79.9	247,927	118,238	19,525	108.2	0.329	22,113	23.71	11.72	44.02	9.60	26.81	13.64	3.35	11.98	0.89	8.77
90%	280,895	81.7	275,944	130,598	21,616	110.4	0.363	24,249	46.63	15.91	51.78	14.91	37.64	28.93	4.71	15.60	1.15	12.48
5 ppm S gasoline for gasoline-powered FP FCV																		
10%	216,887	77.4	213,284	101,469	16,881	105.4	0.288	19,395	13.84	9.11	37.58	5.02	19.84	7.00	2.24	8.71	0.67	6.32
50%	252,084	79.9	247,703	118,233	19,514	108.2	0.329	22,097	23.42	11.65	44.12	9.47	26.74	13.38	3.33	11.93	0.88	8.89
90%	292,438	82.2	287,321	136,808	22,409	111.3	0.376	25,096	45.96	15.80	52.34	15.08	37.94	28.52	4.75	15.94	1.17	12.56
10 ppm low-sulfur diesel																		
10%	169,848	79.2	166,535	77,983	13,456	101.6	0.234	15,875	5.92	8.37	34.40	4.35	17.73	1.86	1.91	7.35	0.55	5.33
50%	213,987	82.4	210,090	98,930	16,658	105.1	0.286	19,157	7.59	10.87	40.75	8.07	24.40	2.88	2.92	10.12	0.76	7.80
90%	263,375	85.5	258,679	122,332	20,142	109.1	0.343	22,743	10.22	14.97	48.63	13.07	34.88	4.57	4.25	13.93	1.04	11.54
Crude naphtha																		
10%	117,081	83.3	114,704	52,468	9,607	97.4	0.171	11,893	13.14	7.52	30.35	3.33	15.12	6.77	0.48	1.90	0.05	0.62
50%	157,279	86.4	154,116	71,579	12,530	100.5	0.219	14,909	22.75	9.70	35.87	6.05	20.81	13.15	0.52	2.07	0.06	0.95
90%	201,146	89.5	197,485	92,593	15,777	104.0	0.270	18,257	45.41	13.56	43.09	9.93	29.85	28.30	0.61	2.31	0.07	1.64
NA NG to compressed NG																		
10%	115,966	83.9	106,299	2,909	9,111	236.2	0.149	14,808	3.22	4.72	16.55	4.32	13.55	0.13	0.43	1.59	0.05	1.05
50%	151,575	86.8	140,657	5,849	11,438	247.5	0.197	17,188	6.26	7.20	24.80	9.40	30.09	0.17	0.56	2.36	0.09	3.13
90%	191,971	89.6	180,428	9,519	14,106	258.7	0.251	19,985	9.76	13.71	36.35	16.03	56.73	0.21	0.73	3.24	0.14	7.28

TABLE C-1 (Cont.)

	Total Energy	WTT Efficiency (%)	Fossil Energy	Petroleum	CO_2	CH_4	$_2O$	GHGs	TVOC	TCO	TNO_x	TPM_{10}	TSO_x	UVOC	UCO	UNO_x	UPM_{10}	USO_x
						N												
NNA NG to compressed NG via liquefied NG (LNG)																		
10%	241,709	74.8	231,093	8,991	16,756	310.2	0.335	24,219	4.85	10.45	52.69	5.13	23.25	0.14	0.54	2.84	0.07	1.46
50%	286,667	77.7	274,926	12,467	19,690	324.3	0.398	27,286	8.34	14.23	67.35	10.57	41.65	0.16	0.68	3.68	0.11	3.67
90%	336,884	80.5	324,591	16,821	22,999	338.1	0.466	30,689	12.35	21.81	85.12	17.61	69.76	0.19	0.84	4.65	0.17	8.12
NNA NG to methanol																		
10%	543,710	59.9	543,022	32,442	19,983	160.6	0.392	23,863	12.67	20.87	75.68	11.71	24.40	1.65	0.94	4.49	0.12	1.43
50%	602,797	62.4	601,746	37,148	25,947	169.0	0.454	29,979	21.62	28.79	91.84	15.87	34.55	6.36	1.01	4.73	0.13	1.70
90%	669,101	64.8	667,900	42,683	31,977	177.4	0.530	36,155	44.30	39.48	112.65	19.22	51.67	21.51	1.13	5.03	0.14	2.13
NNA NG to FT diesel																		
10%	612,279	55.4	611,826	16,325	24,471	168.2	0.088	28,507	7.71	15.24	48.66	10.89	19.39	0.58	0.52	2.33	0.06	0.99
50%	705,181	58.6	704,368	21,167	27,908	179.5	0.154	32,125	12.45	23.07	61.51	15.27	30.38	0.95	0.58	2.55	0.07	1.22
90%	806,649	62.0	805,448	27,083	32,101	191.8	0.233	36,416	18.24	33.79	80.46	18.93	48.63	1.39	0.70	2.84	0.08	1.58
NNA NG to FT naphtha																		
10%	614,159	55.4	613,770	17,251	24,366	168.4	0.087	28,419	17.60	15.10	47.45	10.73	18.70	4.99	0.55	2.40	0.06	1.03
50%	703,106	58.7	702,306	21,830	27,707	179.6	0.151	31,888	28.54	23.02	60.05	15.18	29.59	11.27	0.59	2.53	0.07	1.19
90%	804,290	62.0	803,477	27,917	32,055	192.0	0.232	36,357	50.89	33.50	79.28	18.87	47.94	26.55	0.68	2.72	0.08	1.46
NA NG to GH_2 in central plants																		
10%	604,230	53.5	575,603	13,076	98,638	169.3	0.610	102,748	4.89	16.54	68.89	23.62	21.86	0.50	2.91	11.24	2.44	3.06
50%	724,223	58.0	694,017	17,231	107,552	183.3	0.697	111,981	6.72	24.74	90.13	38.94	60.04	0.78	4.52	14.75	3.42	9.14
90%	867,963	62.3	833,714	22,818	117,422	199.3	0.794	122,120	9.19	35.37	115.83	57.80	135.15	1.01	6.05	18.92	4.15	21.19
NNA NG to GH_2 in central plants via LNG																		
10%	782,568	48.1	752,905	21,744	111,168	324.2	0.881	118,954	9.53	27.48	126.21	24.99	43.96	0.63	3.28	13.58	2.49	3.77
50%	925,083	51.9	893,205	26,830	120,989	351.1	0.987	129,345	14.40	36.47	153.94	40.32	86.56	0.90	4.89	17.22	3.45	10.10
90%	1,077,818	56.1	1,043,775	33,225	131,592	380.0	1.110	140,527	20.36	48.42	186.92	60.08	164.58	1.13	6.41	21.46	4.22	22.57

TABLE C-1 (Cont.)

	Total Energy	WTT Efficiency (%)	Fossil Energy	Petroleum	CO_2	CH_4	$_2O$	GHGs	TVOC	TCO	TNO_x	TPM_{10}	TSO_x	UVOC	UCO	UNO_x	UPM_{10}	USO_x
						N												
NA NG to GH_2 in refueling stations																		
10%	611,393	49.3	584,951	6,373	99,870	336.1	0.604	107,816	7.91	18.73	54.16	24.20	27.94	1.26	6.49	16.18	6.60	2.67
50%	801,443	55.5	770,201	10,819	112,650	376.2	0.712	121,499	12.47	28.43	75.96	38.86	69.14	2.08	11.69	23.32	9.51	8.70
90%	1,028,722	62.1	995,044	16,894	127,445	424.5	0.837	137,419	18.12	43.18	102.39	57.41	144.29	2.95	18.73	32.97	12.32	20.64
NNA NG to GH_2 in refueling stations via LNG																		
10%	800,275	44.2	771,892	15,575	111,383	493.3	0.882	123,097	10.64	28.72	111.00	25.45	42.81	1.27	6.60	17.78	6.57	3.42
50%	1,004,730	49.9	974,433	20,977	124,914	551.0	1.015	137,856	15.86	39.68	140.00	40.83	86.48	2.10	11.70	24.81	9.52	9.65
90%	1,262,081	55.5	1,226,008	28,138	141,879	622.7	1.183	156,376	22.30	56.16	177.45	59.83	165.77	2.95	18.92	34.71	12.32	22.23
NA NG to LH_2 in central plants																		
10%	1,169,772	38.6	1,168,861	10,139	131,450	204.0	1.413	136,592	7.61	16.82	85.00	11.78	9.22	0.50	1.30	7.34	1.09	0.68
50%	1,366,426	42.3	1,364,957	16,647	144,798	221.4	1.641	150,370	14.41	25.93	147.09	16.09	24.99	0.79	2.03	13.10	1.50	1.42
90%	1,590,068	46.1	1,588,399	24,841	160,106	241.9	1.909	166,194	22.42	40.90	229.57	19.51	50.90	1.14	2.85	21.12	1.82	2.56
NNA NG to LH_2 in central plants																		
10%	1,249,477	37.3	1,248,295	17,522	138,098	213.3	1.492	143,446	8.69	20.64	139.14	12.68	20.16	0.17	0.46	5.33	0.07	1.37
50%	1,451,060	40.8	1,450,010	24,556	152,222	232.7	1.729	158,042	15.69	30.19	203.16	17.24	36.43	0.22	0.53	5.82	0.08	1.63
90%	1,680,645	44.5	1,679,094	33,322	167,768	253.1	2.010	174,094	24.23	46.05	290.57	21.27	63.13	0.29	0.65	6.37	0.09	2.06
NA NG to LH_2 in refueling stations																		
10%	1,448,828	27.6	1,318,791	25,983	162,718	433.3	1.618	173,314	14.37	34.99	132.78	73.96	102.48	1.65	10.48	31.62	7.64	14.86
50%	1,978,881	33.6	1,792,112	38,489	203,360	504.0	2.273	215,662	20.69	52.14	220.20	161.34	311.28	2.52	16.50	47.99	10.75	48.81
90%	2,625,644	40.8	2,359,753	54,200	251,564	584.9	3.115	266,030	28.17	75.81	348.56	296.22	789.48	3.42	24.79	70.60	13.71	125.90
NNA NG to LH_2 in refueling stations via LNG																		
10%	1,696,182	25.3	1,566,510	36,268	174,717	598.6	1.918	189,406	17.32	45.21	192.50	74.02	116.24	1.63	10.57	32.88	7.66	15.53
50%	2,249,451	30.8	2,054,256	49,648	215,155	682.0	2.575	231,564	23.98	63.24	283.08	162.14	330.16	2.53	16.73	49.70	10.81	49.99
90%	2,946,637	37.1	2,678,820	66,031	267,120	781.7	3.458	286,077	32.46	88.18	415.90	309.16	814.72	3.46	24.42	72.81	13.74	128.56

TABLE C-1 (Cont.)

	Total Energy	WTT Efficiency (%)	Fossil Energy	Petroleum	CO_2	CH_4	$_2O$	GHGs	TVOC	TCO	TNO_x	TPM_{10}	TSO_x	UVOC	UCO	UNO_x	UPM_{10}	USO_x
							N											
Corn to ethanol																		
10%	692,783	55.3	678,691	73,694	-23,578	102.9	37.677	-7,573	28.67	42.42	117.51	38.58	48.28	4.80	0.22	2.08	0.06	1.42
50%	748,694	57.2	732,839	81,469	-19,397	111.6	55.312	-221	40.92	52.90	135.57	58.22	76.60	10.97	0.41	3.18	0.12	4.34
90%	807,904	59.1	790,231	99,970	-14,881	121.2	75.933	7,679	64.20	67.15	156.78	82.80	118.48	26.19	0.63	4.47	0.20	10.23
Cellulosic biomass to ethanol																		
10%	1,090,660	35.8	33,454	72,596	-89,076	2.2	22.287	-80,559	34.34	80.94	130.62	7.70	-32.32	5.12	0.38	0.91	-0.01	-5.96
50%	1,390,238	41.8	60,561	84,793	-83,190	5.1	30.903	-73,864	44.21	92.78	150.29	16.84	-7.73	11.26	0.56	1.88	0.04	-2.02
90%	1,790,295	47.8	91,655	99,724	-77,779	8.4	41.669	-67,239	67.01	108.27	174.95	25.58	3.97	26.34	0.72	2.68	0.09	-0.13
U.S. average electricity to GH_2 in refueling stations																		
10%	2,256,709	25.2	1,944,546	53,256	259,773	359.9	4.570	269,390	22.06	44.25	260.29	177.92	246.33	0.93	9.38	45.38	1.64	41.72
50%	2,585,834	27.9	2,234,268	60,808	287,982	396.5	5.038	298,546	25.36	73.50	471.36	409.98	850.16	1.35	14.68	79.57	3.46	139.19
90%	2,966,213	30.7	2,571,193	69,651	321,115	439.8	5.574	332,849	29.19	103.76	693.65	689.22	2,050	1.86	20.54	115.18	5.63	331.31
U.S. average electricity to LH_2 in refueling stations																		
10%	3,152,411	18.2	2,716,193	74,409	332,253	459.2	5.820	344,601	28.55	58.80	351.41	236.10	332.23	1.21	12.36	61.00	2.12	56.42
50%	3,765,527	21.0	3,256,416	88,698	382,727	526.7	6.683	396,787	33.76	97.28	628.03	542.28	1,102	1.78	19.52	106.12	4.63	180.40
90%	4,483,130	24.1	3,881,597	105,521	442,871	607.6	7.720	458,972	39.95	140.87	942.33	930.18	2,616	2.45	27.76	156.66	7.58	424.71
CA average electricity to GH_2 in refueling stations																		
10%	1,818,967	29.3	1,382,296	9,841	164,891	315.4	3.266	173,171	13.81	40.50	149.05	73.55	99.53	0.96	10.32	30.87	1.40	13.02
50%	2,092,202	32.3	1,595,492	12,934	182,134	347.6	3.589	191,186	18.44	58.75	237.71	166.16	338.92	1.67	15.82	46.74	2.20	51.49
90%	2,409,212	35.5	1,843,703	16,986	202,489	385.7	3.961	212,425	23.67	83.57	335.02	278.20	823.24	2.64	24.80	68.95	3.10	129.36
CA average electricity to LH_2 in refueling stations																		
10%	2,601,979	21.2	1,979,681	14,639	211,062	404.0	4.171	221,648	18.15	53.83	200.92	97.31	135.29	1.25	13.62	40.63	1.84	17.54
50%	3,108,612	24.3	2,376,100	19,380	242,649	462.2	4.773	254,705	24.41	79.04	316.87	220.26	443.72	2.18	21.16	62.05	2.92	67.22
90%	3,712,411	27.8	2,846,676	25,784	279,025	530.7	5.495	292,800	31.91	114.41	457.40	375.74	1,049	3.42	34.08	93.87	4.17	164.44

TABLE C-1 (Cont.)

	Total Energy	WTT Efficiency (%)	Fossil Energy	Petroleum	CO_2	CH_4	$_2O$	GHGs	TVOC	TCO	TNO_x	TPM_{10}	TSO_x	UVOC	UCO	UNO_x	UPM_{10}	USO_x
							N											
NGCC electricity to GH_2 in refueling stations																		
10%	1,796,970	27.5	1,796,106	3,356	167,398	467.7	4.143	179,976	16.26	54.21	53.11	7.44	11.61	2.04	16.48	13.14	2.50	0.70
50%	2,182,025	31.4	2,180,806	12,294	191,441	534.7	4.714	205,251	27.86	105.51	78.04	9.32	32.28	5.12	37.28	16.50	3.07	1.12
90%	2,633,822	35.8	2,631,497	23,442	219,989	612.3	5.379	235,272	41.75	197.81	123.01	12.20	68.23	9.24	76.70	29.76	4.06	1.85
NGCC electricity to LH_2 in refueling stations																		
10%	2,604,835	20.1	2,603,641	4,595	215,560	604.6	5.345	231,318	20.48	69.50	67.35	9.57	14.93	2.49	21.81	16.91	3.27	0.90
50%	3,226,203	23.7	3,224,036	15,776	253,664	708.9	6.272	271,791	36.78	138.26	100.77	12.34	42.07	6.67	49.60	21.58	4.09	1.45
90%	3,973,823	27.7	3,972,334	30,959	299,591	837.1	7.331	320,971	55.09	272.21	160.92	16.28	89.54	12.25	106.30	38.41	5.45	2.37
Renewable electricity to GH_2 in refueling stations																		
10%	458,965	57.0	0	0	0	0.0	0.000	0	0.00	0.00	0.00	0.00	0.00	0.00	0.00	0.00	0.00	0.00
50%	592,616	62.8	0	0	0	0.0	0.000	0	0.00	0.00	0.00	0.00	0.00	0.00	0.00	0.00	0.00	0.00
90%	755,041	68.5	0	0	0	0.0	0.000	0	0.00	0.00	0.00	0.00	0.00	0.00	0.00	0.00	0.00	0.00
U.S. average electricity to GH_2 in refueling stations with proposed IAQR																		
10%											90.31		132.84			17.29		23.73
50%											225.56		504.68			40.18		84.39
90%											577.61		1,325			96.96		214.24
U.S. average electricity to LH_2 in refueling stations with proposed IAQR																		
10%											118.98		173.83			22.70		31.35
50%											303.40		673.02			53.93		112.40
90%											772.12		1,752			130.00		285.38

APPENDIX D

WELL-TO-WHEELS RESULTS

TABLE D-1 Well-to-Wheels Results (Btu or Grams per Mile Driven)

	Total Energy	Fossil Energy	Petroleum	CO_2	CH_4	$_2O$	GHGs	TVOC	TCO	TNO_x	TPM_{10}	TSO_x	UVOC	UCO	UNO_x	UPM_{10}	USO_x
					N												
RFG DOD SI CD																	
10%	6,489	6,469	5,831	507	0.627	0.030	531	0.223	1.314	0.301	0.056	0.115	0.131	0.795	0.104	0.019	0.039
50%	6,823	6,800	6,092	528	0.654	0.030	552	0.330	4.001	0.399	0.082	0.155	0.199	2.466	0.162	0.023	0.053
90%	7,170	7,145	6,361	549	0.684	0.030	573	0.495	9.049	0.586	0.115	0.216	0.306	5.606	0.278	0.032	0.074
RFG DI SI CD																	
10%	5,733	5,713	5,142	449	0.562	0.029	471	0.212	1.315	0.275	0.053	0.098	0.125	0.799	0.099	0.018	0.032
50%	6,005	5,984	5,365	465	0.584	0.030	487	0.316	3.974	0.367	0.077	0.131	0.192	2.453	0.153	0.022	0.044
90%	6,292	6,269	5,594	482	0.608	0.030	504	0.474	9.139	0.568	0.105	0.184	0.293	5.667	0.279	0.032	0.061
NA NG CNG DOD SI CD																	
10%	6,071	6,016	16	365	1.615	0.015	407	0.067	1.350	0.197	0.053	0.077	0.022	0.816	0.055	0.014	0.007
50%	6,409	6,348	32	392	1.701	0.015	436	0.131	4.073	0.303	0.083	0.168	0.059	2.506	0.111	0.019	0.018
90%	6,759	6,693	53	421	1.785	0.015	466	0.259	9.233	0.500	0.121	0.318	0.139	5.712	0.231	0.028	0.041
NNA NG CNG DOD SI CD																	
10%	6,770	6,709	50	407	2.019	0.016	459	0.078	1.384	0.413	0.058	0.131	0.022	0.816	0.062	0.015	0.009
50%	7,154	7,089	69	438	2.127	0.016	492	0.142	4.116	0.542	0.090	0.232	0.059	2.509	0.118	0.019	0.021
90%	7,574	7,506	94	471	2.236	0.017	527	0.271	9.269	0.747	0.130	0.391	0.139	5.711	0.238	0.028	0.046
Corn E85 DOD SI CD																	
10%	8,399	4,418	1,801	337	0.658	0.179	416	0.286	1.546	0.645	0.192	0.230	0.122	0.819	0.071	0.016	0.018
50%	8,835	4,734	1,932	359	0.702	0.251	451	0.398	4.120	0.774	0.280	0.349	0.189	2.422	0.127	0.020	0.032
90%	9,262	5,051	2,067	382	0.747	0.334	486	0.568	9.479	0.989	0.386	0.529	0.296	5.762	0.249	0.029	0.059
Cellulosic E85 DOD SI CD																	
10%	10,150	1,849	1,807	78	0.256	0.118	127	0.306	1.713	0.703	0.078	-0.077	0.123	0.822	0.066	0.015	-0.008
50%	11,411	2,023	1,936	102	0.272	0.153	154	0.410	4.278	0.837	0.113	0.010	0.190	2.424	0.120	0.019	0.007
90%	13,062	2,211	2,068	124	0.290	0.197	181	0.579	9.650	1.053	0.147	0.051	0.296	5.771	0.244	0.029	0.015

TABLE D-1 (Cont.)

	Total Energy	Fossil Energy	Petroleum	CO_2	CH_4	$_2O$	GHGs	TVOC	TCO	TNO_x	TPM_{10}	TSO_x	UVOC	UCO	UNO_x	UPM_{10}	USO_x
					N												
NA NG Central GH_2 DOD SI CD (Bin 5 NO_x Standard)																	
10%	7,194	7,062	59	443	0.767	0.031	470	0.040	0.628	0.434	0.137	0.099	0.010	0.332	0.108	0.028	0.014
50%	7,815	7,675	78	488	0.838	0.031	516	0.082	2.429	0.583	0.208	0.272	0.035	1.459	0.166	0.034	0.041
90%	8,533	8,382	103	536	0.918	0.032	566	0.171	6.116	0.799	0.296	0.614	0.089	3.757	0.289	0.043	0.097
NA NG Central GH_2 DOD SI CD (Bin 2 NO_x Standard)																	
10%										0.401					0.086		
50%										0.539					0.137		
90%										0.744					0.256		
NNA NG Central GH_2 DOD SI CD (Bin 5 NO_x Standard)																	
10%	8,011	7,872	98	498	1.461	0.032	541	0.071	0.697	0.701	0.144	0.199	0.010	0.351	0.119	0.028	0.017
50%	8,733	8,583	121	548	1.597	0.032	595	0.121	2.402	0.874	0.213	0.394	0.036	1.409	0.175	0.034	0.046
90%	9,538	9,381	151	602	1.747	0.033	652	0.210	6.095	1.103	0.305	0.744	0.091	3.715	0.296	0.043	0.102
NNA NG Central GH_2 DOD SI CD (Bin 2 NO_x Standard)																	
10%										0.663					0.097		
50%										0.828					0.147		
90%										1.061					0.267		
NA NG Station GH_2 DOD SI CD (Bin 5 NO_x Standard)																	
10%	7,259	7,135	29	451	1.520	0.031	495	0.063	0.672	0.370	0.140	0.126	0.016	0.387	0.141	0.048	0.012
50%	8,170	8,027	49	510	1.711	0.031	558	0.112	2.369	0.517	0.207	0.313	0.042	1.440	0.208	0.062	0.039
90%	9,271	9,109	76	583	1.945	0.032	637	0.201	6.048	0.730	0.294	0.652	0.097	3.734	0.333	0.078	0.093
NA NG Station GH_2 DOD SI CD (Bin 2 NO_x Standard)																	
10%										0.334					0.117		
50%										0.470					0.181		
90%										0.686					0.300		

TABLE D-1 (Cont.)

	Total Energy	Fossil Energy	Petroleum	CO_2	CH_4	$_2O$	GHGs	TVOC	TCO	TNO_x	TPM_{10}	TSO_x	UVOC	UCO	UNO_x	UPM_{10}	USO_x
					N												
NNA NG Station GH_2 DOD SI CD (Bin 5 NO_x Standard)																	
10%	8,106	7,978	70	502	2.231	0.032	563	0.076	0.710	0.631	0.145	0.195	0.016	0.387	0.148	0.048	0.015
50%	9,083	8,944	95	567	2.502	0.033	634	0.128	2.414	0.814	0.217	0.393	0.042	1.441	0.216	0.062	0.044
90%	10,299	10,136	129	647	2.845	0.033	723	0.217	6.108	1.051	0.305	0.750	0.097	3.736	0.340	0.078	0.101
NNA NG Station GH_2 DOD SI CD (Bin 2 NO_x Standard)																	
10%										0.587					0.124		
50%										0.771					0.188		
90%										1.009					0.310		
Electrolysis U.S. Electricity GH_2 DOD SI CD (Bin 5 NO_x Standard)																	
10%	14,656	12,632	345	1,168	1.625	0.049	1,219	0.124	0.876	1.356	0.833	1.102	0.013	0.401	0.302	0.025	0.189
50%	16,242	14,027	383	1,304	1.801	0.051	1,361	0.168	2.571	2.330	1.892	3.854	0.038	1.458	0.472	0.035	0.632
90%	18,116	15,697	426	1,465	2.014	0.053	1,527	0.256	6.269	3.308	3.155	9.299	0.093	3.753	0.662	0.047	1.506
Electrolysis U.S. Electricity GH_2 DOD SI CD (Bin 2 NO_x Standard)																	
10%										1.308					0.274		
50%										2.254					0.444		
90%										3.322					0.649		
Electrolysis CA Electricity GH_2 DOD SI CD (Bin 5 NO_x Standard)																	
10%	12,651	9,629	68	741	1.422	0.043	787	0.090	0.808	0.838	0.362	0.450	0.014	0.409	0.221	0.023	0.059
50%	14,020	10,695	87	826	1.584	0.044	876	0.138	2.500	1.269	0.786	1.544	0.040	1.465	0.321	0.029	0.234
90%	15,577	11,921	111	923	1.767	0.046	977	0.227	6.202	1.723	1.292	3.735	0.094	3.760	0.473	0.038	0.584
Electrolysis CA Electricity GH_2 DOD SI CD (Bin 2 NO_x Standard)																	
10%										0.800					0.194		
50%										1.228					0.299		
90%										1.705					0.453		

TABLE D-1 (Cont.)

	Total Energy	Fossil Energy	Petroleum	CO_2	CH_4	$_2O$	GHGs	TVOC	TCO	TNO_x	TPM_{10}	TSO_x	UVOC	UCO	UNO_x	UPM_{10}	USO_x
					N												
Electrolysis NGCC Electricity GH_2 DOD SI CD (Bin 5 NO_x Standard)																	
10%	12,574	12,567	15	754	2.111	0.047	820	0.112	1.078	0.366	0.061	0.053	0.026	0.540	0.116	0.027	0.003
50%	14,379	14,373	56	867	2.429	0.049	938	0.186	2.915	0.539	0.073	0.146	0.057	1.664	0.185	0.033	0.005
90%	16,574	16,563	106	1,002	2.807	0.053	1,080	0.287	6.634	0.802	0.091	0.309	0.114	3.981	0.318	0.042	0.008
Electrolysis NGCC Electricity GH_2 DOD SI CD (Bin 2 NO_x Standard)																	
10%										0.327					0.094		
50%										0.484					0.155		
90%										0.749					0.286		
NA NG Central LH_2 DOD SI CD (Bin 5 NO_x Standard)																	
10%	9,748	9,743	46	592	0.922	0.034	624	0.064	0.644	0.538	0.082	0.042	0.010	0.336	0.095	0.020	0.003
50%	10,712	10,706	75	657	1.012	0.035	690	0.119	2.387	0.852	0.103	0.113	0.034	1.412	0.161	0.025	0.006
90%	11,839	11,832	113	731	1.113	0.037	767	0.211	6.152	1.266	0.124	0.230	0.089	3.762	0.283	0.034	0.012
NA NG Central LH_2 DOD SI CD (Bin 2 NO_x Standard)																	
10%										0.502					0.074		
50%										0.811					0.134		
90%										1.207					0.249		
NNA NG Central LH_2 DOD SI CD (Bin 5 NO_x Standard)																	
10%	10,089	10,084	79	620	0.965	0.035	653	0.070	0.669	0.772	0.086	0.091	0.007	0.327	0.069	0.014	0.006
50%	11,113	11,106	111	689	1.061	0.036	724	0.126	2.402	1.114	0.109	0.165	0.031	1.405	0.123	0.018	0.007
90%	12,259	12,252	152	767	1.165	0.037	805	0.218	6.169	1.533	0.131	0.286	0.086	3.752	0.246	0.027	0.009
NNA NG Central LH_2 DOD SI CD (Bin 2 NO_x Standard)																	
10%										0.735					0.047		
50%										1.065					0.095		
90%										1.469					0.210		

TABLE D-1 (Cont.)

	Total Energy	Fossil Energy	Petroleum	CO_2	CH_4	$_2O$	GHGs	TVOC	TCO	TNO_x	TPM_{10}	TSO_x	UVOC	UCO	UNO_x	UPM_{10}	USO_x
					N												
NA NG Station LH_2 DOD SI CD (Bin 5 NO_x Standard)																	
10%	11,045	10,466	118	736	1.956	0.035	793	0.095	0.755	0.752	0.364	0.466	0.018	0.399	0.222	0.053	0.067
50%	13,488	12,638	175	921	2.293	0.038	985	0.148	2.508	1.173	0.765	1.410	0.042	1.484	0.327	0.068	0.221
90%	16,435	15,245	246	1,146	2.664	0.042	1,218	0.239	6.276	1.796	1.381	3.604	0.097	3.833	0.482	0.083	0.574
NA NG Station LH_2 DOD SI CD (Bin 2 NO_x Standard)																	
10%										0.725					0.203		
50%										1.131					0.301		
90%										1.733					0.446		
NNA NG Station LH_2 DOD SI CD (Bin 5 NO_x Standard)																	
10%	12,167	11,562	164	789	2.703	0.037	862	0.107	0.803	1.031	0.368	0.526	0.018	0.401	0.229	0.053	0.071
50%	14,700	13,849	225	975	3.096	0.040	1,058	0.164	2.555	1.475	0.767	1.496	0.042	1.478	0.335	0.068	0.226
90%	17,941	16,748	302	1,217	3.564	0.044	1,311	0.258	6.321	2.111	1.425	3.701	0.098	3.838	0.493	0.084	0.582
NNA NG Station LH_2 DOD SI CD (Bin 2 NO_x Standard)																	
10%										1.004					0.210		
50%										1.424					0.308		
90%										2.030					0.451		
Electrolysis U.S. Electricity LH_2 DOD SI CD (Bin 5 NO_x Standard)																	
10%	18,744	16,174	442	1,495	2.076	0.054	1,560	0.156	0.969	1.766	1.105	1.517	0.014	0.412	0.371	0.027	0.256
50%	21,635	18,670	508	1,737	2.396	0.058	1,809	0.206	2.712	3.032	2.490	5.004	0.039	1.492	0.592	0.040	0.814
90%	24,982	21,650	589	2,019	2.773	0.063	2,101	0.296	6.496	4.455	4.248	11.847	0.094	3.840	0.853	0.055	1.933
Electrolysis U.S. Electricity LH_2 DOD SI CD (Bin 2 NO_x Standard)																	
10%										1.752					0.356		
50%										2.956					0.563		
90%										4.348					0.817		

TABLE D-1 (Cont.)

	Total Energy	Fossil Energy	Petroleum	CO_2	CH_4	$_2O$	GHGs	TVOC	TCO	TNO_x	TPM_{10}	TSO_x	UVOC	UCO	UNO_x	UPM_{10}	USO_x
					N												
Electrolysis CA Electricity LH_2 DOD SI CD (Bin 5 NO_x Standard)																	
10%	16,231	12,349	90	951	1.824	0.047	1,007	0.112	0.883	1.069	0.473	0.613	0.016	0.426	0.269	0.025	0.079
50%	18,645	14,249	116	1,099	2.104	0.050	1,162	0.164	2.634	1.627	1.029	2.010	0.041	1.505	0.395	0.032	0.305
90%	21,509	16,471	151	1,273	2.425	0.053	1,345	0.257	6.389	2.290	1.733	4.743	0.096	3.854	0.585	0.042	0.746
Electrolysis CA Electricity LH_2 DOD SI CD (Bin 2 NO_x Standard)																	
10%										1.038					0.249		
50%										1.571					0.365		
90%										2.225					0.558		
Electrolysis NGCC Electricity LH_2 DOD SI CD (Bin 5 NO_x Standard)																	
10%	16,237	16,233	21	974	2.737	0.052	1,053	0.135	1.179	0.437	0.071	0.068	0.030	0.576	0.137	0.031	0.004
50%	19,114	19,109	72	1,150	3.224	0.056	1,240	0.227	2.969	0.644	0.087	0.191	0.066	1.675	0.211	0.037	0.007
90%	22,625	22,616	141	1,366	3.816	0.061	1,472	0.341	6.735	0.958	0.109	0.405	0.121	4.011	0.354	0.048	0.011
Electrolysis NGCC Electricity LH_2 DOD SI CD (Bin 2 NO_x Standard)																	
10%										0.412					0.117		
50%										0.603					0.182		
90%										0.926					0.325		
LS Diesel DI CI CD																	
10%	5,174	5,159	4,726	398	0.460	0.017	414	0.069	1.321	0.247	0.048	0.082	0.035	0.804	0.087	0.017	0.025
50%	5,454	5,437	4,939	426	0.483	0.017	442	0.132	3.937	0.339	0.068	0.112	0.074	2.431	0.142	0.022	0.037
90%	5,768	5,748	5,158	458	0.509	0.018	474	0.262	9.177	0.531	0.094	0.160	0.155	5.691	0.261	0.031	0.053
NNA NG FT Diesel DI CI CD																	
10%	7,150	7,148	73	445	0.758	0.016	468	0.087	1.391	0.325	0.077	0.087	0.025	0.797	0.052	0.014	0.004
50%	7,662	7,658	95	472	0.816	0.017	496	0.153	3.974	0.444	0.099	0.136	0.063	2.409	0.107	0.018	0.005
90%	8,206	8,203	122	501	0.881	0.017	526	0.280	9.239	0.648	0.121	0.218	0.142	5.695	0.227	0.027	0.007

TABLE D-1 (Cont.)

	Total Energy	Fossil Energy	Petroleum	CO_2	CH_4	$_2O$	GHGs	TVOC	TCO	TNO_x	TPM_{10}	TSO_x	UVOC	UCO	UNO_x	UPM_{10}	USO_x
					N												
RFG DOD SI HEV																	
10%	5,042	5,025	4,519	392	0.501	0.029	412	0.202	1.338	0.256	0.050	0.092	0.119	0.816	0.093	0.018	0.031
50%	5,529	5,510	4,935	428	0.542	0.029	449	0.302	3.975	0.350	0.072	0.123	0.183	2.456	0.149	0.022	0.043
90%	5,911	5,890	5,246	453	0.575	0.030	475	0.451	9.116	0.542	0.099	0.175	0.278	5.655	0.268	0.031	0.059
RFG DI SI HEV																	
10%	4,679	4,663	4,192	366	0.470	0.029	385	0.198	1.365	0.238	0.049	0.081	0.118	0.834	0.087	0.017	0.026
50%	4,992	4,974	4,458	386	0.496	0.029	406	0.291	3.998	0.334	0.069	0.109	0.177	2.465	0.146	0.022	0.036
90%	5,276	5,255	4,688	405	0.520	0.029	425	0.442	9.056	0.531	0.094	0.153	0.273	5.618	0.269	0.031	0.051
NA NG CNG DOD SI HEV																	
10%	4,841	4,797	13	293	1.360	0.015	329	0.060	1.332	0.174	0.049	0.062	0.022	0.805	0.053	0.014	0.006
50%	5,303	5,252	27	324	1.462	0.015	362	0.123	3.931	0.275	0.074	0.139	0.059	2.422	0.106	0.018	0.015
90%	5,680	5,624	44	353	1.552	0.015	392	0.255	8.924	0.475	0.107	0.259	0.139	5.533	0.230	0.028	0.034
NNA NG CNG DOD SI HEV																	
10%	5,399	5,351	40	327	1.681	0.016	370	0.069	1.365	0.351	0.053	0.107	0.022	0.805	0.059	0.014	0.007
50%	5,928	5,873	57	362	1.815	0.016	408	0.133	3.976	0.474	0.079	0.192	0.059	2.426	0.112	0.019	0.018
90%	6,360	6,302	78	394	1.928	0.016	443	0.264	8.957	0.683	0.114	0.323	0.139	5.537	0.236	0.028	0.038
Corn E85 DOD SI HEV																	
10%	6,534	3,455	1,413	263	0.536	0.149	328	0.252	1.433	0.531	0.161	0.184	0.111	0.778	0.066	0.015	0.015
50%	7,148	3,824	1,558	290	0.586	0.208	365	0.361	4.152	0.653	0.230	0.281	0.177	2.466	0.118	0.020	0.026
90%	7,611	4,140	1,691	313	0.630	0.275	400	0.515	9.372	0.858	0.317	0.424	0.275	5.729	0.240	0.028	0.047
Cellulosic E85 DOD SI HEV																	
10%	8,019	1,458	1,415	62	0.222	0.100	102	0.267	1.551	0.574	0.068	-0.061	0.112	0.778	0.061	0.015	-0.006
50%	9,193	1,629	1,562	81	0.238	0.128	125	0.371	4.282	0.704	0.096	0.008	0.178	2.467	0.113	0.019	0.005
90%	10,641	1,804	1,697	100	0.255	0.165	149	0.526	9.495	0.914	0.126	0.041	0.276	5.727	0.237	0.028	0.012

TABLE D-1 (Cont.)

	Total Energy	Fossil Energy	Petroleum	CO_2	CH_4	$_2O$	GHGs	TVOC	TCO	TNO_x	TPM_{10}	TSO_x	UVOC	UCO	UNO_x	UPM_{10}	USO_x
					N												
NA NG Central GH_2 DOD SI HEV (Bin 5 NO_x Standard)																	
10%	5,714	5,610	48	352	0.610	0.030	375	0.036	0.634	0.369	0.117	0.081	0.009	0.353	0.096	0.025	0.011
50%	6,376	6,259	63	397	0.683	0.031	422	0.078	2.447	0.502	0.175	0.220	0.035	1.478	0.153	0.031	0.034
90%	7,063	6,942	85	443	0.761	0.031	470	0.170	6.110	0.715	0.246	0.497	0.092	3.755	0.273	0.040	0.078
NA NG Central GH_2 DOD SI HEV (Bin 2 NO_x Standard)																	
10%										0.337					0.075		
50%										0.457					0.124		
90%										0.658					0.235		
NNA NG Central GH_2 DOD SI HEV (Bin 5 NO_x Standard)																	
10%	6,351	6,246	79	395	1.161	0.031	431	0.060	0.681	0.587	0.122	0.160	0.009	0.361	0.106	0.025	0.014
50%	7,102	6,983	99	446	1.301	0.032	486	0.107	2.473	0.738	0.180	0.319	0.035	1.472	0.162	0.031	0.037
90%	7,863	7,731	123	496	1.444	0.032	538	0.200	6.157	0.954	0.254	0.602	0.092	3.768	0.281	0.040	0.083
NNA NG Central GH_2 DOD SI HEV (Bin 2 NO_x Standard)																	
10%										0.549					0.084		
50%										0.695					0.133		
90%										0.912					0.244		
NA NG Station GH_2 DOD SI HEV (Bin 5 NO_x Standard)																	
10%	5,783	5,685	23	360	1.211	0.030	397	0.053	0.648	0.320	0.118	0.102	0.014	0.383	0.124	0.042	0.010
50%	6,643	6,531	40	415	1.394	0.031	456	0.100	2.452	0.446	0.174	0.253	0.040	1.499	0.187	0.054	0.032
90%	7,603	7,472	63	479	1.600	0.031	525	0.192	6.134	0.660	0.246	0.528	0.097	3.789	0.312	0.067	0.076
NA NG Station GH_2 DOD SI HEV (Bin 2 NO_x Standard)																	
10%										0.279					0.099		
50%										0.403					0.159		
90%										0.606					0.274		

TABLE D-1 (Cont.)

	Total Energy	Fossil Energy	Petroleum	CO_2	CH_4	$_2O$	GHGs	TVOC	TCO	TNO_x	TPM_{10}	TSO_x	UVOC	UCO	UNO_x	UPM_{10}	USO_x
					N												
NNA NG Station GH_2 DOD SI HEV (Bin 5 NO_x Standard)																	
10%	6,463	6,356	56	400	1.778	0.031	450	0.064	0.688	0.531	0.124	0.157	0.014	0.384	0.129	0.042	0.013
50%	7,390	7,274	77	461	2.042	0.032	517	0.113	2.498	0.690	0.182	0.320	0.040	1.499	0.194	0.054	0.035
90%	8,453	8,317	105	529	2.327	0.032	592	0.206	6.168	0.920	0.255	0.605	0.097	3.791	0.316	0.067	0.081
NNA NG Station GH_2 DOD SI HEV (Bin 2 NO_x Standard)																	
10%										0.490					0.106		
50%										0.644					0.166		
90%										0.872					0.279		
Electrolysis U.S. Electricity GH_2 DOD SI HEV (Bin 5 NO_x Standard)																	
10%	11,626	10,016	274	930	1.293	0.044	972	0.101	0.824	1.116	0.686	0.901	0.011	0.397	0.258	0.023	0.151
50%	13,227	11,424	312	1,060	1.471	0.047	1,107	0.147	2.622	1.916	1.538	3.098	0.037	1.509	0.404	0.032	0.509
90%	14,919	12,920	351	1,203	1.659	0.049	1,255	0.238	6.327	2.736	2.583	7.525	0.094	3.812	0.578	0.043	1.216
Electrolysis U.S. Electricity GH_2 DOD SI HEV (Bin 2 NO_x Standard)																	
10%										1.084					0.231		
50%										1.839					0.373		
90%										2.740					0.551		
Electrolysis CA Electricity GH_2 DOD SI HEV (Bin 5 NO_x Standard)																	
10%	10,063	7,644	54	590	1.136	0.040	628	0.074	0.773	0.700	0.302	0.368	0.012	0.405	0.190	0.021	0.048
50%	11,416	8,708	70	673	1.291	0.041	714	0.122	2.573	1.063	0.642	1.243	0.039	1.519	0.279	0.027	0.189
90%	12,824	9,812	91	760	1.454	0.043	805	0.213	6.258	1.464	1.060	3.018	0.096	3.820	0.422	0.036	0.473
Electrolysis CA Electricity GH_2 DOD SI HEV (Bin 2 NO_x Standard)																	
10%										0.656					0.165		
50%										1.010					0.251		
90%										1.429					0.397		

TABLE D-1 (Cont.)

	Total Energy	Fossil Energy	Petroleum	CO_2	CH_4	$_2O$	GHGs	TVOC	TCO	TNO_x	TPM_{10}	TSO_x	UVOC	UCO	UNO_x	UPM_{10}	USO_x
						N											
Electrolysis NGCC Electricity GH_2 DOD SI HEV (Bin 5 NO_x Standard)																	
10%	10,019	10,015	12	604	1.688	0.043	657	0.095	0.973	0.307	0.054	0.043	0.023	0.505	0.104	0.025	0.003
50%	11,704	11,700	45	704	1.974	0.045	764	0.161	2.770	0.468	0.065	0.119	0.053	1.608	0.166	0.030	0.004
90%	13,650	13,641	86	823	2.299	0.048	888	0.259	6.490	0.707	0.082	0.251	0.110	3.913	0.292	0.040	0.007
Electrolysis NGCC Electricity GH_2 DOD SI HEV (Bin 2 NO_x Standard)																	
10%										0.278					0.081		
50%										0.419					0.140		
90%										0.655					0.264		
NA NG Central LH_2 DOD SI HEV (Bin 5 NO_x Standard)																	
10%	7,748	7,745	37	472	0.735	0.033	498	0.056	0.634	0.458	0.071	0.034	0.009	0.336	0.088	0.019	0.002
50%	8,713	8,709	61	534	0.825	0.034	563	0.107	2.397	0.729	0.089	0.092	0.034	1.440	0.149	0.023	0.005
90%	9,771	9,764	92	604	0.919	0.035	635	0.205	6.279	1.083	0.109	0.187	0.095	3.851	0.270	0.033	0.009
NA NG Central LH_2 DOD SI HEV (Bin 2 NO_x Standard)																	
10%										0.419					0.066		
50%										0.681					0.120		
90%										1.025					0.236		
NNA NG Central LH_2 DOD SI HEV (Bin 5 NO_x Standard)																	
10%	8,017	8,013	64	492	0.767	0.033	520	0.060	0.648	0.656	0.075	0.074	0.007	0.332	0.064	0.014	0.005
50%	9,059	9,055	90	561	0.865	0.034	591	0.113	2.416	0.937	0.094	0.134	0.032	1.435	0.118	0.018	0.006
90%	10,123	10,117	123	633	0.963	0.036	665	0.210	6.291	1.305	0.115	0.234	0.093	3.845	0.239	0.028	0.008
NNA NG Central LH_2 DOD SI HEV (Bin 2 NO_x Standard)																	
10%										0.615					0.043		
50%										0.889					0.091		
90%										1.233					0.202		

TABLE D-1 (Cont.)

	Total Energy	Fossil Energy	Petroleum	CO_2	CH_4	$_2O$	GHGs	TVOC	TCO	TNO_x	TPM_{10}	TSO_x	UVOC	UCO	UNO_x	UPM_{10}	USO_x
					N												
NA NG Station LH_2 DOD SI HEV (Bin 5 NO_x Standard)																	
10%	8,889	8,414	95	592	1.576	0.034	639	0.080	0.722	0.638	0.302	0.376	0.015	0.388	0.193	0.046	0.055
50%	10,965	10,293	141	747	1.865	0.036	800	0.131	2.503	0.994	0.625	1.150	0.041	1.492	0.284	0.058	0.178
90%	13,524	12,525	202	944	2.191	0.040	1,005	0.226	6.363	1.506	1.127	2.954	0.101	3.901	0.430	0.073	0.470
NA NG Station LH_2 DOD SI HEV (Bin 2 NO_x Standard)																	
10%										0.605					0.168		
50%										0.948					0.258		
90%										1.447					0.397		
NNA NG Station LH_2 DOD SI HEV (Bin 5 NO_x Standard)																	
10%	9,831	9,322	132	636	2.157	0.035	699	0.091	0.762	0.861	0.300	0.428	0.015	0.389	0.198	0.046	0.057
50%	11,965	11,262	182	793	2.520	0.037	862	0.144	2.531	1.234	0.628	1.213	0.041	1.492	0.293	0.058	0.184
90%	14,723	13,707	246	997	2.932	0.041	1,075	0.243	6.411	1.769	1.161	3.014	0.101	3.908	0.433	0.073	0.471
NNA NG Station LH_2 DOD SI HEV (Bin 2 NO_x Standard)																	
10%										0.828					0.176		
50%										1.192					0.265		
90%										1.699					0.400		
Electrolysis U.S. Electricity LH_2 DOD SI HEV (Bin 5 NO_x Standard)																	
10%	15,018	12,933	354	1,203	1.664	0.049	1,257	0.130	0.877	1.461	0.899	1.229	0.013	0.400	0.320	0.025	0.209
50%	17,568	15,167	413	1,410	1.945	0.053	1,471	0.178	2.651	2.488	2.028	4.048	0.038	1.503	0.504	0.036	0.663
90%	20,547	17,768	483	1,658	2.280	0.057	1,727	0.274	6.533	3.676	3.477	9.695	0.098	3.911	0.727	0.049	1.581
Electrolysis U.S. Electricity LH_2 DOD SI HEV (Bin 2 NO_x Standard)																	
10%										1.435					0.299		
50%										2.447					0.475		
90%										3.553					0.689		

TABLE D-1 (Cont.)

	Total Energy	Fossil Energy	Petroleum	CO_2	CH_4	$_2O$	GHGs	TVOC	TCO	TNO_x	TPM_{10}	TSO_x	UVOC	UCO	UNO_x	UPM_{10}	USO_x
						N											
Electrolysis CA Electricity LH_2 DOD SI HEV (Bin 5 NO_x Standard)																	
10%	13,024	9,895	73	764	1.462	0.043	810	0.093	0.831	0.902	0.390	0.492	0.014	0.414	0.228	0.023	0.064
50%	15,153	11,556	94	892	1.707	0.046	945	0.145	2.598	1.350	0.840	1.625	0.040	1.515	0.340	0.029	0.247
90%	17,717	13,543	124	1,046	1.996	0.049	1,105	0.241	6.459	1.924	1.422	3.894	0.100	3.915	0.509	0.039	0.609
Electrolysis CA Electricity LH_2 DOD SI HEV (Bin 2 NO_x Standard)																	
10%										0.861					0.209		
50%										1.310					0.312		
90%										1.845					0.477		
Electrolysis NGCC Electricity LH_2 DOD SI HEV (Bin 5 NO_x Standard)																	
10%	13,054	13,048	17	782	2.198	0.047	846	0.114	1.096	0.377	0.062	0.055	0.027	0.546	0.122	0.028	0.003
50%	15,558	15,552	58	933	2.616	0.051	1,009	0.196	2.885	0.555	0.076	0.156	0.059	1.645	0.190	0.034	0.005
90%	18,573	18,566	115	1,126	3.144	0.056	1,214	0.305	6.716	0.840	0.096	0.328	0.119	4.031	0.326	0.044	0.009
Electrolysis NGCC Electricity LH_2 DOD SI HEV (Bin 2 NO_x Standard)																	
10%										0.346					0.101		
50%										0.518					0.162		
90%										0.802					0.295		
LS Diesel DI CI HEV																	
10%	4,197	4,184	3,816	324	0.375	0.017	338	0.063	1.331	0.219	0.044	0.069	0.032	0.810	0.081	0.017	0.021
50%	4,602	4,587	4,172	359	0.410	0.017	373	0.124	3.905	0.309	0.062	0.093	0.070	2.413	0.135	0.021	0.031
90%	4,958	4,940	4,451	392	0.439	0.017	407	0.253	9.101	0.504	0.084	0.134	0.151	5.645	0.255	0.030	0.045
NNA NG FT Diesel DI CI HEV																	
10%	5,839	5,837	61	362	0.622	0.016	382	0.079	1.412	0.286	0.069	0.072	0.025	0.827	0.052	0.014	0.004
50%	6,457	6,454	79	398	0.691	0.017	419	0.141	4.037	0.395	0.088	0.115	0.061	2.455	0.106	0.018	0.005
90%	7,027	7,023	102	430	0.754	0.017	452	0.269	9.406	0.599	0.108	0.185	0.140	5.797	0.225	0.028	0.006

TABLE D-1 (Cont.)

	Total Energy	Fossil Energy	Petroleum	CO_2	CH_4	$_2O$	GHGs	TVOC	TCO	TNO_x	TPM_{10}	TSO_x	UVOC	UCO	UNO_x	UPM_{10}	USO_x
					N												
5-ppm S Gasoline FP FCV																	
10%	4,057	4,043	3,631	314	0.383	0.015	328	0.160	0.567	0.191	0.047	0.071	0.094	0.337	0.065	0.017	0.023
50%	4,519	4,503	4,035	350	0.423	0.015	364	0.233	2.415	0.271	0.066	0.096	0.141	1.487	0.112	0.021	0.032
90%	5,067	5,050	4,515	390	0.470	0.015	405	0.350	6.068	0.447	0.089	0.139	0.216	3.762	0.219	0.030	0.046
Crude Naphtha FP FCV																	
10%	3,743	3,733	3,482	273	0.358	0.015	286	0.156	0.546	0.160	0.039	0.054	0.093	0.319	0.028	0.014	0.002
50%	4,174	4,162	3,861	307	0.395	0.015	320	0.233	2.333	0.243	0.053	0.075	0.142	1.428	0.074	0.018	0.003
90%	4,702	4,687	4,333	347	0.440	0.015	362	0.345	6.213	0.419	0.072	0.110	0.213	3.842	0.185	0.027	0.006
NNA NG FT Naphtha FP FCV																	
10%	5,464	5,462	61	327	0.606	0.014	346	0.176	0.591	0.236	0.067	0.067	0.087	0.318	0.030	0.014	0.004
50%	6,169	6,166	79	366	0.681	0.015	386	0.252	2.334	0.343	0.085	0.107	0.135	1.395	0.078	0.018	0.004
90%	6,965	6,961	103	410	0.769	0.015	432	0.369	6.208	0.525	0.105	0.175	0.208	3.803	0.189	0.027	0.005
NNA NG MeOH FP FCV																	
10%	4,751	4,749	104	285	0.529	0.015	302	0.149	0.640	0.317	0.066	0.080	0.070	0.340	0.036	0.014	0.005
50%	5,289	5,285	123	322	0.591	0.016	340	0.224	2.362	0.426	0.082	0.115	0.118	1.410	0.084	0.019	0.006
90%	5,942	5,938	146	364	0.660	0.016	384	0.340	6.061	0.614	0.102	0.172	0.189	3.713	0.195	0.028	0.007
Corn EtOH FP FCV																	
10%	5,658	2,325	255	174	0.386	0.150	236	0.219	0.706	0.489	0.168	0.175	0.087	0.319	0.034	0.015	0.006
50%	6,313	2,648	298	198	0.436	0.216	273	0.299	2.477	0.614	0.241	0.279	0.136	1.420	0.082	0.019	0.018
90%	7,079	3,017	369	227	0.495	0.296	315	0.421	6.262	0.808	0.335	0.435	0.209	3.757	0.194	0.028	0.042
Cellulosic EtOH FP FCV																	
10%	7,272	118	253	-54	0.040	0.092	-17	0.236	0.853	0.539	0.057	-0.120	0.088	0.320	0.029	0.014	-0.025
50%	8,661	219	307	-32	0.051	0.125	6	0.312	2.612	0.673	0.092	-0.030	0.137	1.420	0.076	0.018	-0.008
90%	10,501	337	372	-13	0.064	0.168	31	0.429	6.391	0.873	0.127	0.015	0.209	3.757	0.190	0.027	-0.001

TABLE D-1 (Cont.)

	Total Energy	Fossil Energy	Petroleum	CO_2	CH_4	$_2O$	GHGs	TVOC	TCO	TNO_x	TPM_{10}	TSO_x	UVOC	UCO	UNO_x	UPM_{10}	USO_x
					N												
5-ppm S Gasoline FP FC HEV																	
10%	3,416	3,403	3,057	265	0.328	0.015	277	0.151	0.570	0.170	0.044	0.060	0.089	0.344	0.059	0.017	0.019
50%	3,896	3,883	3,479	302	0.369	0.015	315	0.221	2.442	0.249	0.061	0.083	0.134	1.504	0.106	0.021	0.027
90%	4,439	4,424	3,958	342	0.417	0.015	356	0.333	6.079	0.425	0.082	0.121	0.206	3.770	0.213	0.030	0.040
Crude Naphtha FP FC HEV																	
10%	3,158	3,151	2,934	231	0.307	0.015	242	0.147	0.547	0.142	0.037	0.046	0.088	0.322	0.026	0.014	0.002
50%	3,599	3,588	3,336	265	0.345	0.015	277	0.220	2.337	0.224	0.050	0.065	0.134	1.437	0.074	0.018	0.003
90%	4,126	4,115	3,800	304	0.390	0.015	317	0.327	6.075	0.404	0.068	0.096	0.203	3.759	0.185	0.027	0.005
NNA NG FT Naphtha FP FC HEV																	
10%	4,619	4,618	52	276	0.517	0.014	292	0.162	0.585	0.208	0.061	0.058	0.082	0.322	0.028	0.014	0.003
50%	5,320	5,318	68	316	0.591	0.014	334	0.236	2.383	0.310	0.078	0.092	0.128	1.437	0.075	0.018	0.004
90%	6,128	6,125	90	361	0.676	0.015	381	0.344	6.115	0.495	0.097	0.150	0.196	3.759	0.187	0.027	0.005
NNA NG MeOH FP FC HEV																	
10%	4,085	4,083	89	246	0.460	0.015	261	0.142	0.631	0.279	0.060	0.068	0.070	0.345	0.034	0.014	0.004
50%	4,555	4,551	105	277	0.513	0.015	294	0.213	2.411	0.381	0.075	0.099	0.113	1.449	0.081	0.018	0.005
90%	5,119	5,115	126	314	0.575	0.016	332	0.321	6.220	0.563	0.093	0.149	0.181	3.820	0.190	0.027	0.006
Cellulosic EtOH FP FC HEV																	
10%	6,159	101	215	-46	0.039	0.081	-14	0.216	0.807	0.468	0.053	-0.104	0.084	0.320	0.029	0.014	-0.025
50%	7,450	189	263	-28	0.049	0.110	6	0.289	2.566	0.596	0.083	-0.026	0.130	1.420	0.076	0.018	-0.008
90%	9,134	292	325	-11	0.059	0.147	27	0.400	6.348	0.791	0.115	0.013	0.199	3.757	0.190	0.027	-0.001
NA NG Central GH_2 FCV																	
10%	3,574	3,511	30	221	0.378	0.001	230	0.011	0.038	0.156	0.073	0.050	0.001	0.007	0.025	0.017	0.007
50%	3,950	3,880	39	246	0.420	0.002	256	0.015	0.057	0.206	0.107	0.137	0.002	0.010	0.034	0.019	0.021
90%	4,343	4,270	52	273	0.463	0.002	284	0.021	0.081	0.266	0.151	0.308	0.002	0.014	0.044	0.021	0.048

TABLE D-1 (Cont.)

	Total Energy	Fossil Energy	Petroleum	CO_2	CH_4	$_2O$	GHGs	TVOC	TCO	TNO_x	TPM_{10}	TSO_x	UVOC	UCO	UNO_x	UPM_{10}	USO_x
					N												
NNA NG Central GH_2 FCV																	
10%	3,996	3,929	49	249	0.727	0.002	267	0.022	0.063	0.286	0.076	0.100	0.001	0.007	0.031	0.017	0.009
50%	4,407	4,333	61	277	0.803	0.002	296	0.033	0.083	0.352	0.111	0.199	0.002	0.011	0.039	0.020	0.023
90%	4,845	4,768	77	306	0.886	0.003	328	0.047	0.112	0.430	0.156	0.377	0.003	0.015	0.049	0.021	0.051
NA NG Station GH_2 FCV																	
10%	3,634	3,572	14	226	0.758	0.001	244	0.018	0.042	0.123	0.074	0.064	0.003	0.015	0.037	0.027	0.006
50%	4,121	4,052	25	258	0.862	0.002	278	0.028	0.065	0.174	0.108	0.157	0.005	0.027	0.053	0.033	0.020
90%	4,690	4,613	39	295	0.982	0.002	318	0.041	0.100	0.235	0.150	0.330	0.007	0.043	0.076	0.040	0.047
NNA NG Station GH_2 FCV																	
10%	4,054	3,992	35	251	1.109	0.002	277	0.024	0.065	0.252	0.077	0.098	0.003	0.015	0.040	0.027	0.008
50%	4,587	4,515	48	286	1.262	0.002	316	0.036	0.091	0.321	0.112	0.198	0.005	0.027	0.057	0.033	0.022
90%	5,231	5,145	65	328	1.439	0.003	361	0.051	0.129	0.406	0.156	0.379	0.007	0.044	0.080	0.040	0.050
Electrolysis U.S. Electricity GH_2 FCV																	
10%	7,341	6,324	173	586	0.810	0.010	608	0.050	0.101	0.589	0.424	0.563	0.002	0.021	0.103	0.015	0.095
50%	8,210	7,091	194	659	0.909	0.012	683	0.058	0.168	1.074	0.957	1.940	0.003	0.033	0.182	0.020	0.318
90%	9,192	7,955	216	743	1.020	0.013	770	0.067	0.238	1.581	1.591	4.661	0.004	0.047	0.266	0.025	0.753
Electrolysis CA Electricity GH_2 FCV																	
10%	6,337	4,820	34	371	0.709	0.007	390	0.031	0.092	0.340	0.186	0.227	0.002	0.023	0.070	0.015	0.030
50%	7,094	5,407	44	418	0.797	0.008	438	0.042	0.135	0.545	0.399	0.778	0.004	0.036	0.107	0.017	0.118
90%	7,896	6,039	56	469	0.894	0.009	492	0.054	0.192	0.769	0.652	1.869	0.006	0.057	0.158	0.019	0.293
Electrolysis NGCC Electricity GH_2 FCV																	
10%	6,305	6,300	8	378	1.055	0.009	406	0.037	0.123	0.121	0.035	0.027	0.005	0.038	0.030	0.017	0.002
50%	7,269	7,266	28	437	1.223	0.011	469	0.064	0.241	0.178	0.040	0.074	0.012	0.085	0.038	0.019	0.003
90%	8,413	8,411	54	509	1.416	0.012	544	0.096	0.455	0.281	0.047	0.156	0.021	0.176	0.068	0.021	0.004

TABLE D-1 (Cont.)

	Total Energy	Fossil Energy	Petroleum	CO_2	CH_4	$_2O$	GHGs	TVOC	TCO	TNO_x	TPM_{10}	TSO_x	UVOC	UCO	UNO_x	UPM_{10}	USO_x
					N												
Electrolysis Renewable Electricity GH_2 FCV																	
10%	3,266	0	0	0	0.000	0.000	0	0.000	0.000	0.000	0.019	0.000	0.000	0.000	0.000	0.012	0.000
50%	3,642	0	0	0	0.000	0.000	0	0.000	0.000	0.000	0.019	0.000	0.000	0.000	0.000	0.012	0.000
90%	4,072	0	0	0	0.000	0.000	0	0.000	0.000	0.000	0.019	0.000	0.000	0.000	0.000	0.012	0.000
NA NG Central LH_2 FCV																	
10%	4,863	4,860	23	296	0.457	0.003	308	0.017	0.038	0.193	0.046	0.021	0.001	0.003	0.017	0.014	0.002
50%	5,406	5,403	38	331	0.507	0.004	344	0.033	0.059	0.333	0.055	0.057	0.002	0.005	0.030	0.015	0.003
90%	6,020	6,017	57	372	0.561	0.004	386	0.051	0.093	0.527	0.064	0.116	0.003	0.007	0.048	0.016	0.006
NNA NG Central LH_2 FCV																	
10%	5,041	5,038	40	310	0.479	0.003	322	0.020	0.047	0.315	0.048	0.046	0.000	0.001	0.012	0.012	0.003
50%	5,609	5,607	56	348	0.532	0.004	361	0.036	0.069	0.465	0.058	0.083	0.001	0.001	0.013	0.012	0.004
90%	6,233	6,229	76	390	0.589	0.005	404	0.055	0.106	0.665	0.068	0.144	0.001	0.001	0.015	0.012	0.005
NA NG Station LH_2 FCV																	
10%	5,537	5,255	59	371	0.982	0.004	395	0.033	0.079	0.301	0.186	0.236	0.004	0.024	0.072	0.029	0.034
50%	6,811	6,393	88	464	1.150	0.005	492	0.047	0.119	0.503	0.388	0.713	0.006	0.038	0.110	0.036	0.112
90%	8,308	7,716	124	579	1.344	0.007	612	0.064	0.174	0.798	0.698	1.826	0.008	0.057	0.162	0.043	0.290
NNA NG Station LH_2 FCV																	
10%	6,097	5,793	82	396	1.348	0.004	428	0.039	0.102	0.436	0.187	0.264	0.004	0.024	0.074	0.029	0.035
50%	7,414	6,985	113	492	1.561	0.006	529	0.055	0.145	0.647	0.389	0.748	0.006	0.038	0.113	0.036	0.114
90%	9,088	8,471	152	615	1.800	0.008	657	0.075	0.202	0.964	0.723	1.863	0.008	0.056	0.167	0.043	0.293
Electrolysis U.S. Electricity LH_2 FCV																	
10%	9,387	8,098	221	750	1.037	0.013	778	0.064	0.134	0.803	0.559	0.750	0.003	0.028	0.139	0.017	0.128
50%	10,921	9,438	256	878	1.206	0.015	910	0.077	0.224	1.433	1.255	2.509	0.004	0.045	0.242	0.022	0.412
90%	12,664	10,963	298	1,024	1.400	0.018	1,061	0.092	0.323	2.146	2.150	6.016	0.006	0.064	0.360	0.029	0.977

TABLE D-1 (Cont.)

	Total Energy	Fossil Energy	Petroleum	CO_2	CH_4	$_2O$	GHGs	TVOC	TCO	TNO_x	TPM_{10}	TSO_x	UVOC	UCO	UNO_x	UPM_{10}	USO_x
					N												
Electrolysis CA Electricity LH_2 FCV																	
10%	8,128	6,188	45	477	0.908	0.009	500	0.041	0.122	0.458	0.241	0.308	0.003	0.031	0.093	0.016	0.040
50%	9,409	7,179	58	555	1.057	0.011	582	0.056	0.180	0.724	0.521	1.008	0.005	0.048	0.142	0.018	0.153
90%	10,911	8,343	77	645	1.227	0.013	677	0.073	0.261	1.050	0.878	2.401	0.008	0.077	0.215	0.021	0.377
Electrolysis NGCC Electricity LH_2 FCV																	
10%	8,153	8,150	10	488	1.368	0.012	524	0.046	0.158	0.153	0.040	0.035	0.006	0.050	0.038	0.019	0.002
50%	9,646	9,643	36	580	1.621	0.014	621	0.084	0.317	0.230	0.047	0.097	0.015	0.113	0.049	0.021	0.003
90%	11,441	11,436	71	692	1.928	0.017	741	0.127	0.624	0.366	0.056	0.205	0.028	0.243	0.088	0.024	0.005
NA NG Central GH_2 FC HEV																	
10%	3,251	3,194	27	201	0.344	0.001	209	0.010	0.035	0.145	0.068	0.046	0.001	0.006	0.023	0.017	0.006
50%	3,574	3,510	36	223	0.380	0.001	232	0.014	0.051	0.188	0.099	0.122	0.002	0.009	0.031	0.019	0.018
90%	3,923	3,853	47	246	0.418	0.002	256	0.019	0.073	0.242	0.139	0.277	0.002	0.012	0.040	0.020	0.044
NNA NG Central GH_2 FC HEV																	
10%	3,621	3,558	45	225	0.656	0.002	240	0.019	0.057	0.259	0.070	0.092	0.001	0.007	0.028	0.017	0.008
50%	3,978	3,912	55	250	0.724	0.002	267	0.030	0.075	0.317	0.102	0.178	0.002	0.010	0.035	0.019	0.020
90%	4,385	4,311	69	277	0.801	0.002	296	0.042	0.100	0.392	0.144	0.339	0.002	0.013	0.044	0.020	0.046
NA NG Station GH_2 FC HEV																	
10%	3,281	3,228	14	203	0.683	0.001	219	0.016	0.039	0.113	0.068	0.060	0.003	0.013	0.033	0.025	0.006
50%	3,722	3,658	23	232	0.774	0.001	250	0.026	0.059	0.158	0.100	0.140	0.004	0.024	0.048	0.031	0.018
90%	4,251	4,178	35	267	0.887	0.002	288	0.038	0.091	0.213	0.140	0.296	0.006	0.039	0.068	0.037	0.043
NNA NG Station GH_2 FC HEV																	
10%	3,667	3,609	32	227	1.006	0.002	251	0.022	0.059	0.227	0.071	0.089	0.003	0.014	0.036	0.025	0.007
50%	4,153	4,088	43	258	1.140	0.002	285	0.033	0.082	0.291	0.103	0.175	0.004	0.024	0.051	0.031	0.020
90%	4,749	4,673	58	298	1.307	0.002	328	0.047	0.116	0.372	0.146	0.338	0.006	0.039	0.073	0.037	0.045

TABLE D-1 (Cont.)

	Total Energy	Fossil Energy	Petroleum	CO_2	CH_4	$_2O$	GHGs	TVOC	TCO	TNO_x	TPM_{10}	TSO_x	UVOC	UCO	UNO_x	UPM_{10}	USO_x
					N												
Electrolysis U.S. Electricity GH_2 FC HEV																	
10%	6,608	5,694	155	527	0.730	0.009	547	0.045	0.091	0.533	0.389	0.509	0.002	0.019	0.094	0.015	0.087
50%	7,411	6,401	175	594	0.819	0.010	616	0.052	0.151	0.974	0.865	1.738	0.003	0.030	0.164	0.019	0.285
90%	8,365	7,242	197	676	0.927	0.012	701	0.061	0.215	1.432	1.465	4.218	0.004	0.043	0.240	0.023	0.683
Electrolysis CA Electricity GH_2 FC HEV																	
10%	5,736	4,361	31	335	0.641	0.007	352	0.028	0.084	0.305	0.175	0.207	0.002	0.021	0.062	0.015	0.029
50%	6,397	4,883	39	377	0.720	0.007	396	0.038	0.123	0.494	0.357	0.710	0.003	0.033	0.097	0.016	0.108
90%	7,190	5,501	51	426	0.813	0.008	447	0.049	0.174	0.703	0.597	1.713	0.005	0.051	0.146	0.018	0.269
Electrolysis NGCC Electricity GH_2 FC HEV																	
10%	5,707	5,704	7	342	0.958	0.008	367	0.033	0.111	0.108	0.034	0.025	0.004	0.035	0.027	0.017	0.001
50%	6,571	6,568	25	396	1.106	0.010	424	0.058	0.216	0.162	0.038	0.065	0.011	0.077	0.034	0.018	0.002
90%	7,602	7,599	49	461	1.278	0.011	494	0.087	0.421	0.251	0.044	0.137	0.019	0.165	0.060	0.020	0.004
NA NG Central LH_2 FC HEV																	
10%	4,403	4,401	21	267	0.414	0.003	277	0.016	0.034	0.177	0.043	0.020	0.001	0.003	0.015	0.014	0.001
50%	4,881	4,878	34	299	0.458	0.003	311	0.030	0.054	0.304	0.052	0.050	0.002	0.004	0.027	0.015	0.003
90%	5,441	5,438	52	335	0.507	0.004	348	0.046	0.084	0.476	0.059	0.104	0.002	0.006	0.044	0.015	0.005
NNA NG Central LH_2 FC HEV																	
10%	4,578	4,576	36	281	0.435	0.003	292	0.018	0.043	0.287	0.045	0.043	0.000	0.001	0.011	0.012	0.003
50%	5,068	5,065	51	314	0.481	0.004	326	0.033	0.062	0.422	0.054	0.074	0.000	0.001	0.012	0.012	0.003
90%	5,633	5,629	69	352	0.532	0.004	366	0.050	0.095	0.601	0.063	0.130	0.001	0.001	0.013	0.012	0.004
NA NG Station LH_2 FC HEV																	
10%	4,994	4,739	54	334	0.887	0.003	356	0.030	0.072	0.267	0.169	0.216	0.003	0.021	0.065	0.027	0.031
50%	6,155	5,774	80	419	1.039	0.005	444	0.043	0.108	0.450	0.353	0.657	0.005	0.034	0.099	0.034	0.103
90%	7,526	6,978	112	524	1.219	0.006	553	0.059	0.157	0.717	0.637	1.646	0.007	0.051	0.146	0.040	0.261

TABLE D-1 (Cont.)

	Total Energy	Fossil Energy	Petroleum	CO_2	CH_4	$_2O$	GHGs	TVOC	TCO	TNO_x	TPM_{10}	TSO_x	UVOC	UCO	UNO_x	UPM_{10}	USO_x
					N												
NNA NG Station LH_2 FC HEV																	
10%	5,512	5,237	74	357	1.218	0.004	387	0.035	0.092	0.394	0.170	0.238	0.003	0.022	0.067	0.027	0.032
50%	6,703	6,308	102	445	1.408	0.005	479	0.050	0.131	0.582	0.352	0.690	0.005	0.034	0.102	0.034	0.105
90%	8,221	7,655	137	556	1.632	0.007	595	0.068	0.183	0.860	0.651	1.728	0.007	0.051	0.150	0.040	0.272
Electrolysis U.S. Electricity LH_2 FC HEV																	
10%	8,497	7,327	200	678	0.937	0.012	704	0.058	0.121	0.709	0.494	0.683	0.003	0.025	0.122	0.016	0.116
50%	9,852	8,516	232	790	1.089	0.014	819	0.070	0.201	1.277	1.145	2.330	0.004	0.040	0.215	0.021	0.381
90%	11,405	9,888	270	923	1.263	0.016	957	0.083	0.289	1.932	1.945	5.536	0.005	0.057	0.323	0.027	0.895
Electrolysis CA Electricity LH_2 FC HEV																	
10%	7,357	5,591	41	431	0.822	0.009	452	0.038	0.111	0.416	0.216	0.268	0.003	0.028	0.085	0.016	0.035
50%	8,509	6,489	53	501	0.954	0.010	526	0.051	0.164	0.653	0.468	0.945	0.005	0.044	0.129	0.018	0.143
90%	9,904	7,577	70	586	1.119	0.012	615	0.066	0.235	0.946	0.788	2.325	0.007	0.069	0.196	0.020	0.366
Electrolysis NGCC Electricity LH_2 FC HEV																	
10%	7,374	7,372	9	442	1.234	0.011	474	0.043	0.145	0.142	0.039	0.032	0.005	0.046	0.035	0.018	0.002
50%	8,708	8,703	33	524	1.463	0.013	561	0.076	0.287	0.212	0.044	0.085	0.014	0.102	0.045	0.020	0.003
90%	10,339	10,334	65	625	1.741	0.015	669	0.116	0.566	0.336	0.053	0.184	0.026	0.221	0.081	0.023	0.005
Electrolysis U.S. Electricity GH_2 DOD SI CD (Bin 5 NO_x Standard, Proposed IAQR)																	
10%	14,603	12,593	344	1,167	1.616	0.048	1,219	0.122	0.885	0.574	0.835	0.602	0.013	0.412	0.161	0.025	0.107
50%	16,258	14,047	382	1,305	1.802	0.051	1,361	0.168	2.656	1.212	1.914	2.302	0.037	1.508	0.301	0.035	0.380
90%	18,149	15,736	428	1,465	2.014	0.054	1,527	0.258	6.440	2.808	3.164	5.995	0.094	3.862	0.573	0.047	0.972
Electrolysis U.S. Electricity GH_2 DOD SI CD (Bin 2 NO_x Standard, Proposed IAQR)																	
10%										0.545					0.141		
50%										1.199					0.281		
90%										2.832					0.555		

TABLE D-1 (Cont.)

	Total Energy	Fossil Energy	Petroleum	CO_2	CH_4	$_2O$	GHGs	TVOC	TCO	TNO_x	TPM_{10}	TSO_x	UVOC	UCO	UNO_x	UPM_{10}	USO_x
						N											
Electrolysis U.S. Electricity LH_2 DOD SI CD (Bin 5 NO_x Standard, Proposed IAQR)																	
10%	18,762	16,173	441	1,500	2.076	0.054	1,565	0.156	0.992	0.714	1.094	0.788	0.015	0.433	0.191	0.027	0.142
50%	21,575	18,632	508	1,726	2.386	0.058	1,799	0.207	2.770	1.547	2.525	3.028	0.039	1.528	0.365	0.040	0.507
90%	24,914	21,555	588	2,009	2.762	0.063	2,091	0.299	6.540	3.677	4.186	7.974	0.096	3.892	0.713	0.055	1.297
Electrolysis U.S. Electricity LH_2 DOD SI CD (Bin 2 NO_x Standard, Proposed IAQR)																	
10%										0.683					0.172		
50%										1.552					0.343		
90%										3.763					0.705		
Electrolysis U.S. Electricity GH_2 DOD SI HEV (Bin 5 NO_x Standard, Proposed IAQR)																	
10%	11,660	10,052	273	929	1.294	0.044	972	0.102	0.783	0.500	0.690	0.487	0.011	0.383	0.145	0.023	0.086
50%	13,217	11,419	311	1,060	1.468	0.047	1,107	0.147	2.557	1.023	1.563	1.851	0.038	1.470	0.272	0.032	0.307
90%	14,978	12,964	352	1,207	1.662	0.049	1,259	0.236	6.325	2.323	2.583	4.830	0.093	3.842	0.501	0.043	0.790
Electrolysis U.S. Electricity GH_2 DOD SI HEV (Bin 2 NO_x Standard, Proposed IAQR)																	
10%										0.464					0.122		
50%										1.015					0.247		
90%										2.351					0.474		
Electrolysis U.S. Electricity LH_2 DOD SI HEV (Bin 5 NO_x Standard, Proposed IAQR)																	
10%	15,007	12,942	352	1,197	1.662	0.049	1,251	0.130	0.869	0.614	0.898	0.639	0.013	0.400	0.168	0.025	0.114
50%	17,507	15,119	413	1,403	1.939	0.053	1,463	0.179	2.654	1.293	2.056	2.464	0.039	1.490	0.321	0.037	0.411
90%	20,504	17,711	484	1,651	2.271	0.057	1,721	0.268	6.426	3.029	3.425	6.419	0.095	3.859	0.607	0.050	1.049
Electrolysis U.S. Electricity LH_2 DOD SI HEV (Bin 2 NO_x Standard, Proposed IAQR)																	
10%										0.580					0.146		
50%										1.291					0.298		
90%										3.066					0.598		

TABLE D-1 (Cont.)

	Total Energy	Fossil Energy	Petroleum	CO_2	CH_4	$_2O$	GHGs	TVOC	TCO	TNO_x	TPM_{10}	TSO_x	UVOC	UCO	UNO_x	UPM_{10}	USO_x
					N												
Electrolysis U.S. Electricity GH_2 FCV (Proposed IAQR)																	
10%	7,265	6,264	171	581	0.803	0.010	602	0.050	0.102	0.207	0.426	0.302	0.002	0.022	0.039	0.015	0.054
50%	8,197	7,080	193	658	0.907	0.012	682	0.058	0.167	0.517	0.968	1.159	0.003	0.033	0.092	0.020	0.191
90%	9,223	7,988	217	745	1.020	0.013	772	0.068	0.238	1.315	1.597	3.006	0.004	0.047	0.221	0.024	0.486
Electrolysis U.S. Electricity LH_2 FCV (Proposed IAQR)																	
10%	9,399	8,094	220	750	1.036	0.013	778	0.064	0.134	0.271	0.554	0.396	0.003	0.028	0.052	0.017	0.072
50%	10,879	9,391	256	872	1.201	0.015	904	0.077	0.221	0.692	1.276	1.531	0.004	0.044	0.123	0.022	0.254
90%	12,635	10,932	298	1,017	1.394	0.018	1,054	0.093	0.321	1.766	2.120	3.999	0.006	0.064	0.297	0.029	0.652
Electrolysis U.S. Electricity GH_2 FC HEV (Proposed IAQR)																	
10%	6,633	5,713	156	530	0.733	0.009	549	0.045	0.091	0.193	0.385	0.280	0.002	0.019	0.037	0.015	0.050
50%	7,425	6,415	175	596	0.821	0.010	618	0.053	0.151	0.483	0.866	1.089	0.003	0.030	0.086	0.019	0.181
90%	8,342	7,217	196	672	0.923	0.012	697	0.061	0.214	1.245	1.437	2.697	0.004	0.043	0.208	0.023	0.438
Electrolysis U.S. Electricity LH_2 FC HEV (Proposed IAQR)																	
10%	8,484	7,316	200	680	0.936	0.012	705	0.058	0.119	0.257	0.504	0.371	0.002	0.025	0.049	0.016	0.066
50%	9,835	8,495	231	788	1.087	0.014	817	0.069	0.200	0.637	1.138	1.451	0.004	0.040	0.113	0.021	0.242
90%	11,453	9,912	269	922	1.265	0.016	956	0.083	0.288	1.638	1.920	3.560	0.005	0.058	0.275	0.027	0.581